UNIVERSITY OF SOUTHAMPTON

FACULTY OF NATURAL AND ENVIRONMENTAL SCIENCES

Centre for Biological Sciences

Influence Of Low-Dose Nitric Oxide on Mono- and Mixed-Species Biofilms Formed by Bacteria Isolated From Cystic Fibrosis Patients

by

Caroline Marie Duignan
BSc (Hons), MSc

Thesis for the degree of Doctor of Philosophy

July 2016

Abstract

UNIVERSITY OF SOUTHAMPTON

<u>**ABSTRACT**</u>

FACULTY OF NATURAL AND ENVIRONMENTAL SCIENCES

Centre for Biological Sciences

<u>Doctor of Philosophy</u>

INFLUENCE OF LOW-DOSE NITRIC OXIDE ON MONO- AND MIXED-SPECIES BIOFILMS FORMED BY BACTERIA ISOLATED FROM CYSTIC FIBROSIS PATIENTS

by Caroline Marie Duignan BSc (Hons), MSc

Cystic fibrosis (CF) is an autosomal recessive disorder. One of the characteristic hallmarks of the disease is infection of the lung. Over the life time of a CF patient, a number of pulmonary exacerbations occur which result in irreversible lung damage. Despite continuous treatment with antimicrobials, microorganisms continue to persist in the CF lung due to the formation of biofilms. The biofilm mode of growth can display up to a 1000x greater tolerance to antimicrobial treatments than their free living planktonic counterparts. Hence, anti-biofilm therapy strategies are required to break up these tolerant microbial communities.

Nitric oxide (NO) is one of the proposed anti-biofilm therapies, which has been shown to successfully initiate biofilm dispersal of one of the most widely recognized CF pathogens, *P. aeruginosa*. The work in this thesis was undertaken to investigate the use of NO as a potential biofilm dispersing agent for the monospecies biofilms formed by other commonly identified CF microorganisms. The second chapter outlines the isolation of these microorganisms from CF sputum samples and describes the culture profiling results for the CF patient cohort sampled. The third results chapter examines the effect of NO on the monospecies biofilms formed the CF microorganisms isolated in chapter 2. A biofilm dispersal effect was not observed across a range of NO concentrations; however intriguingly there was an effect on biofilm cell viability for NO concentrations ≥ 100 pM. Chapter 4 outlines a mixed species biofilm model composed of CF isolates for *P. aeruginosa* and *S. aureus* and a method to recover and analyse genomic DNA from biofilms. Biofilm dispersal for this mixed species biofilm was not observed however a reduction in the *S. aureus* population fraction was noted. The work in Chapter 5 was undertaken to adapt a new fluorescence *in situ* hybridisation method CLASI-FISH for the identification of microorganisms within CF sputum.

LIST OF CONTENTS

LIST OF TABLES

LIST OF FIGURES

LIST OF FIGURES

LIST OF FIGURES

LIST OF FIGURES

LIST OF FIGURES

DECLARATION OF AUTHORSHIP

I, Caroline Marie Duignan

declare that the thesis entitled

'Influence Of Low-Dose Nitric Oxide on Mono- and Mixed-Species Biofilms Formed by Bacteria Isolated From Cystic Fibrosis Patients'

and the work presented in the thesis are both my own, and have been generated by me as the result of my own original research. I confirm that:

- this work was done wholly or mainly while in candidature for a research degree at this University;

- where any part of this thesis has previously been submitted for a degree or any other qualification at this University or any other institution, this has been clearly stated;

- where I have consulted the published work of others, this is always clearly attributed;

- where I have quoted from the work of others, the source is always given. With the exception of such quotations, this thesis is entirely my own work;

- I have acknowledged all main sources of help;

- where the thesis is based on work done by myself jointly with others, I have made clear exactly what was done by others and what I have contributed myself;

- none of this work has been published before submission, or [delete as appropriate] parts of this work have been published as: [please list references]

Signed: ....

Date:...

ACKNOWLEDGEMENTS

You learn and gain so much throughout the course of doing a PhD. But to me the biggest reward was that of true friendships. When you move to another country you realize quickly how important these friendships really are!!

Judith, I am so grateful that we both started in Southampton at the same time. You were the first real friend I made in Southampton and I have truly enjoyed our friendship. There has never been a dull moment between our exploration of what Southampton has to offer or your extremely quick wit; it is a friendship I truly treasure.

Salomé, you are one of the most kind-hearted people I know and I am truly glad I can call you a great friend. Thank you for your constant support throughout the PhD and for the countless house moves you helped me with and for ensuring I wasn't homeless at any stage! You truly are an amazing friend. Thank you also for including me in social events with others.

Thank you to you, Susie, for the fun lab chats, discussions on microbiology related topics, stats, proof reading the thesis and for always looking out for adventures- be it sailing or canoeing.
Thank you to you, Natalya for all the coffee breaks where we'd wonder why on earth we were doing PhDs and complain about the bacteria we worked with, fun times! Now the discussions no longer revolve around PhD stuff just life, we made it out alive! Thank you to Dawei Ren, for your friendship and a fun 2012 summer in the lab. Thank you also to Stefania, for your humour.
Thank you to Verena Sauer for your friendship.

And now, last but not least! I owe everything I have accomplished, to two of the hardest working people I know, my parents. Thank you Dad and Mum for your constant love and encouragement throughout the years! Thank you to my brothers Shane and Ronan for your support and for cheering me up when I was feeling down via skype. Thank you to wee Méabh for the funny and detailed conversations "Go raibh maith agat" agus "Merci", they brought a smile to my face each time. Thank you to all those people I have had the pleasure of working with or met over the years as a result of doing this project.

"The eye by long use comes to see even in the darkest cavern: and there is no subject so obscure but we may discern some glimpse of truth by long poring on it."   George Berkeley

xx

LIST OF ABBREVIATIONS AND SYMBOLS

ASL	Airway surface liquid
ATCC	American Type Culture Collection
ATP	Adenosine triphosphate
BHI	Brain Heart Infusion
CAMHB	Mueller Hinton Broth 2, Cation-Adjusted
c-di-GMP	bis-(3'⇒5') cyclic dimeric guanosine monophosphate
CF	Cystic Fibrosis
CFTR	Cystic fibrosis transmembrane conductive regulator
CFU	Colony forming unit
CLASI-FISH	Combinatorial Labelling and Spectral Imagining Fluorescence *in situ* Hybridisation
CLSM	Confocal laser scanning microscope
CO_2	Carbon dioxide
cont'd	Continued
CTAB	Cetyl trimethylammonium bromide
DMSO	Dimethyl sulfoxide
EPS	Exopolymeric substance
FEV_1	Forced expiratory volume
FISH	Fluorescence *in situ* hybridisation
FITC	Fluorescein isothiocyanate
gDNA	Genomic DNA

LIST OF ABBREVIATIONS AND SYMBOLS

HPA	Health Protection Agency
IRT	Immunoreactive trypsinogen
ITS	Internal transcribed spacer
MALDI-TOF MS	Matrix Assisted Laser Desorption/Ionization Time of Flight Mass Spectrometry
MRSA	Methicillin resistant *Staphylococcus aureus*
MSSA	Methicillin susceptible *S. aureus*
NA	Numerical aperture
NAD	Nicotinamide adenine dinucleotide
NBS	Newborn screening
NO	Nitric Oxide
O_2	Oxygen
OD	Optical density
PBS	Phosphate buffer saline
PCR	Polymerase Chain Reaction
PDEs	Phosphodiesterases
PEP	Positive expiratory pressure
PF	Potassium ferricyanide
PFA	Paraformaldehyde
PI	Propidium Iodide
PMA	Propidium monoazide

LIST OF ABBREVIATIONS AND SYMBOLS

PMNs	Polymorphonuclear leukocytes
PNA	Peptide nucleic acid
PTIO	2-Phenyl-4, 4, 5, 5-tetramethylimidazoline-1-oxyl-3-oxide
PVP	Polyvinylpyrrolidinone
qPCR	Quantitative real-time Polymerase Chain Reaction
QS	Quorum sensing
RNA	Ribonucleic acid
rRNA	Ribosomal ribonucleic acid
RU	Relative unit
RT	Room temperature
sBHI	Supplemented BHI with hemin and NAD
sCAMHB	Supplemented Cation-Adjusted Mueller Hinton Broth 2, with hemin and NAD
SDS	Sodium dodecyl sulphate
SNP	Sodium nitroprusside dihydrate
STD	Standard deviation
TRITC	Tetramethylrhodamine isothiocyanate
TSA	Tryptic soy agar
TSB	Tryptic soy broth
U.K.	United Kingdom
UV	Ultraviolet
v/v	volume/volume

LIST OF ABBREVIATIONS AND SYMBOLS

VBNC	Viable but non cultivable
∞	Infinity

Chapter 1

An Introduction to Cystic Fibrosis, Biofilm Development and Nitric Oxide

1.0 Overview of Cystic Fibrosis

Cystic fibrosis (CF) is the most common autosomal recessive disorder within Caucasian populations worldwide. CF is caused by a mutation in the transmembrane conductance regulator gene (CFTR) causing abnormal epithelial ion transport in secretory cells. This mutation leads to an imbalance within the epithelial layer which results in thicker mucus secretions within the pulmonary tract, gastrointestinal tract, reproductive tract, liver and pancreas. Due to these complications individuals with this mutation have a reduced life span (Davies, 2007).

The earliest reference to the symptoms of cystic fibrosis can be found as far back as the 1600s. In 1606 Alonso y de Los Ruyzes de Fontecha J. Diez made reference to the widely held belief that a child whose skin tasted salty when kissed was said to foretell untimely death (Quinton, 1999). Fanconi and colleagues in 1936 made the first clinical distinction between the features presented by celiac disease as separate from those presented in a condition referred to as "cystic fibromatosis with bronchiectasis" (Fanconi *et al.*, 1936). In 1938 Dr Dorothy Andersen, a pathologist at Columbia Presbyterian's Babies and Children's Hospital in New York City, compiled the first set of clinical symptoms affecting both the intestinal and respiratory tracts by observing paediatric patients who presented with these complications. This work recognised CF as a distinct clinical disease for the first time.

The classification of cystic fibrosis as a separate clinical disease enabled clinicians and scientists to uncover key features of the disease which could be used in diagnosis. Historically, the diagnosis of CF was primarily based on family history and clinical features, thereby making an accurate and timely diagnosis of patients exhibiting a milder set of symptoms difficult (Farrell *et al.*, 2008). The greatest and most important contribution in the advancement of the diagnosis of cystic fibrosis came in 1953 when Dr Paul di Sant'Agnese published a paper describing how measurements of the salt concentration in sweat could be used as a tool in the diagnosis of cystic fibrosis. This first tool was referred to as the sweat test and has remained as the gold standard in the diagnosis of CF; improvements have occurred throughout the decades to allow for more standardized results for clinical laboratories worldwide. Gibson and Cooke, 1959, were the first to introduce a standard methodology for the

measurement of the electrolyte levels in a sweat sample. The discovery of chloride as the principal electrolyte affected in CF was firstly elucidated by Quinton, (1983). Today in practice the sweat test measures the concentration of the chloride ion, and a level of >60 mmol/L on more than one occasion is taken as a positive result (LeGrys, 1996).

The defective gene responsible for cystic fibrosis, the cystic fibrosis transmembrane conductance regulator was discovered by three separate groups concurrently (Kerem *et al.*, 1989; Riordan *et al.*, 1989; Rommens *et al.*, 1989). These discoveries lead to the development of molecular panels which can be used to screen for mutations within this region to aid in the diagnosis of CF (Bobadilla *et al.*, 2002).

Importantly, to date there are currently 1,971 known mutations affecting the CFTR gene (http://www.genet.sickkids.on.ca/StatisticsPage.html). Due to this vast number of mutations, coupled with the difference in the frequency and distribution of these mutations among ethnic groups, requires that careful consideration is needed in choosing the appropriate molecular screening panel by CF clinicians and molecular testing laboratories for the regional population (Bobadilla *et al.*, 2002).

Routine screening for cystic fibrosis was implemented as part of the newborn screening (NBS) test panel carried out on the blood spot taken from the heel prick within the first week of life. The level of immunoreactive trypsinogen (IRT) is measured, with levels > 60-80 ng/ml being indicative of CF (Crossley, Elliott and Smith, 1979). However the measurement of IRT within the NBS test has been shown not be a specific method, as it can be affected by factors such as the weight of the newborn, the season and reagent lot used (Kloosterboer *et al.*, 2009). In many countries including the U.K. analysis of the IRT levels from a second sample which is typically taken during the 2nd -4th week of life is preferred (Southern, 2012). The preferred strategy in screening for CF is the 2-tier system involving the measurement of the IRT levels and molecular testing for CF mutations. Currently four mutations are screened for in the initial molecular screening panel used to detect CF within the U.K. population. The following four mutations were chosen based on their frequency within the U.K. population, ΔF508, G551D, G542X and 621+1G>T. Finally, referral to a CF centre for a sweat test and further observation is undertaken if: (1) two CF

mutations are noted, (2) one CF mutation and high IRT levels or (3) two high levels of IRT are reported (Public Health England, 2014). The diagnosis of CF requires both clinical observation and laboratory tests, which together offer a robust checklist to diagnose a patient with CF, Refer to Figure 1.1 for an outline of the disease traits associated with CF.

International meetings held with both clinicians and scientists within the cystic fibrosis field have led to a consensus on the appropriate consultative panel to aid in the diagnosis and treatment of CF.
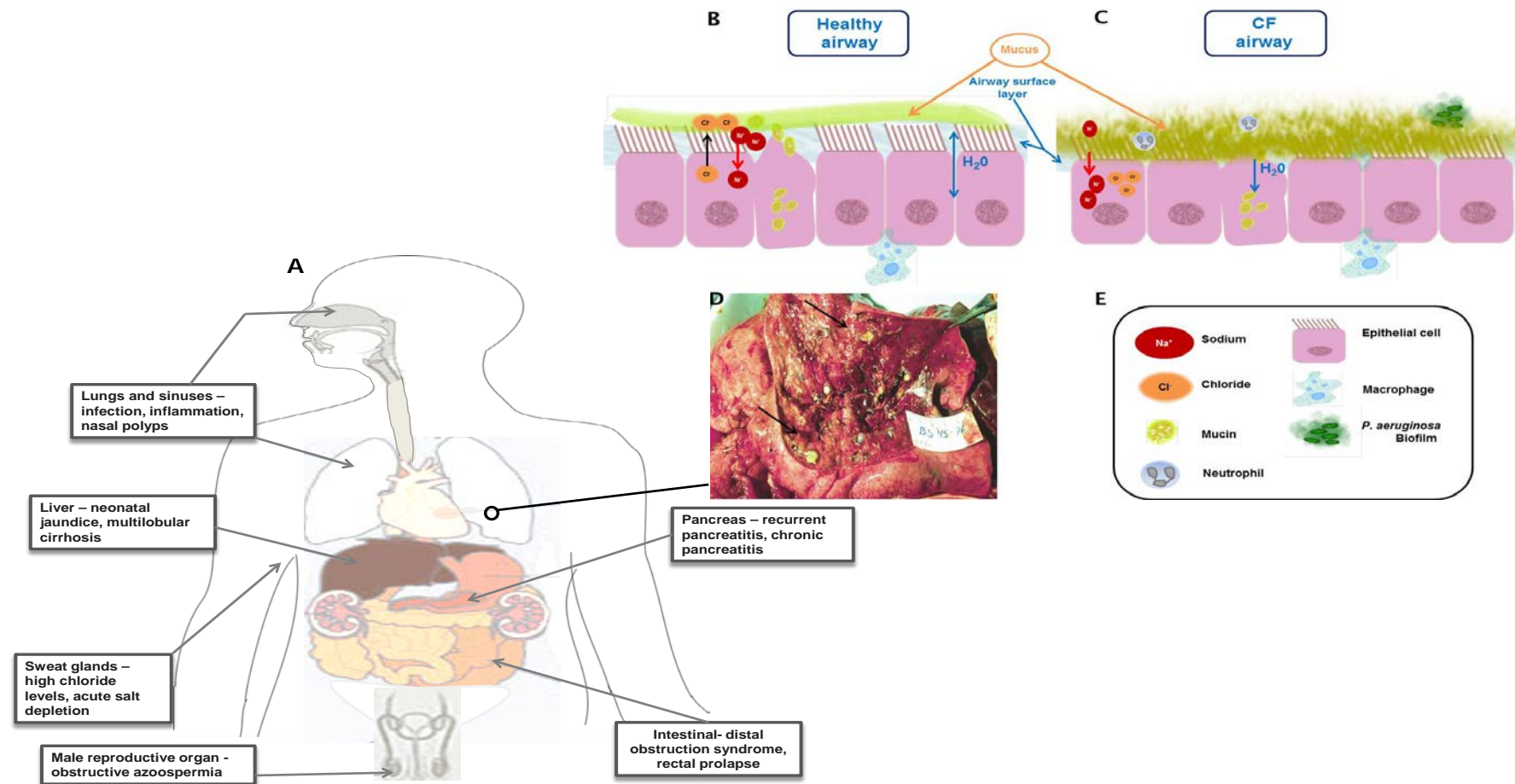
Figure 1.1　　　Diagram for the phenotypic features of CF. Diagnosis made based on sweat chloride levels of > 60 mol / L and on observations as outlined in **A**) organs of the body effected, **B**) normal airway, **C**) CF airway, **D**) post mortem lung image obtained by Høiby *et al.* (2010) black arrows point to mucus plugs within airways, **E**) figure legend for figure **B** and C. Figures A, B, C and E: Illustrated by Caroline M. Duignan.

1.0.1 Genetics

CF was first noted to be due to an autosomal recessive disorder in 1946 by Andersen and Hodges. However, it was not until 1989 that the defective gene on chromosome 7 which encodes the cystic fibrosis transmembrane conductance regulator (CFTR) protein was identified by three separate studies (Kerem *et al.*, 1989; Riordan *et al.*, 1989; Rommens *et al.*, 1989). The gene expands over 250 kb which is translated to produce a 14800 amino acid protein belonging to the ATP-binding cassette superfamily of transporters. Functionally, the protein acts as an integral membrane protein regulating the chloride channel in epithelial cells (Riordan *et al.*, 1989; Zielenski *et al.*, 1991). There are currently 1,971 mutations which have been submitted to the CF Genetic Analysis Consortium database (http://www.genet.sickkids.on.ca/cftr/) affecting the CFTR. Mainly these mutations are point mutations or the result of a deletion range from 1- 84 bp causing missense, frameshift, sequence variation and splicing mutational types in order of frequency (http://www.genet.sickkids.on.ca/cftr/). The most common mutation as mentioned previously is the ΔF508 which is caused by the deletion of a 3 bp resulting in the omission of the amino acid phenylalanine at 508 for the CFTR protein.

CF is found within all ethnic groups however each ethnic group have mutations which are more prevalent and/ rare when compared against another ethnic group. Therefore the detection rate between countries vary, Refer to Figure 1.2. CF remains the most common autosomal recessive disorder within Caucasian populations. Currently 1 in 2,381 babies are diagnosed with CF every year in the United Kingdom (Dodge *et al.*, 2007) with a median life expectancy of 41 years. Due to the higher frequency of diagnosis of CF within the Caucasian population, CF was thought to have originated within the European population. However, the disorder is not purely confined to Caucasian populations or due solely to admixture with Caucasians. Through the use of microsatellites, which are genetic markers used to quantify genetic variation within and between populations of a species, the most prevalent mutation ΔF508 when compared to the unaffected chromosome produced haplotypes which were genetically distant. Therefore these data showed that

the European population was not the origin of this mutation (Morral *et al.*, 1994). This group also estimated the possible age of ΔF508 to be dated at approximately 52,000 years ago. Given this date a more likely location for the emergence of CF may be within the Middle East (Dawson and Frossard, 2000). This date lead to a hypothesis stating that the Baluchi people may very well provide the closest link to the earliest carriers of this mutation. This explanation is compelling given all sufferers of CF possess a homozygous state for ΔF508 primarily due to the cultural practice of arranged marriages within this group which results in narrowing the gene pool (Frossard *et al.*, 1998). Further work would need to be carried out to prove these descendants are the source of the ΔF508. CF is thought to have prevailed due to the advantage a heterozygous mutation offers to an individual; the defect prevents a carrier from dehydration during infection by pathogens such as *Salmonella enterica* Typhi (Pier *et al.*, 1998). Such an advantage could also offer protection during infection by *Vibrio cholerae* (Romeo *et al.*, 1989; Gabriel *et al.*, 1994). In vivo laboratory work carried out in mice demonstrated that ΔF508 heterozygous mice infected with *S. enterica* Typhi to elicit typhoid fever were found to have fewer numbers of *S.* Typhi cells internalized by the epithelial cells in the intestine compared to wild type mice (Pier *et al.*, 1998). *S.* Typhi use their type IVB pili to bind to the first extracellular domain of the CFTR channel for translocation to the intestinal tract, possibly explaining the considerable advantage a heterozygous individual with the ΔF508 allele would possess (Pier *et al.*, 1998). The higher frequency of this allele within Caucasians is very likely due to such selection pressure exerted by the co-existence of *S.* typhi. To further support the theory of selective pressure, molecular evidence was uncovered that typhoid fever was responsible for the mass graves in Kerameikos which date back to 426 - 430 BC (Papagrigorakis *et al.*, 2007). Historically these deaths were thought to have been due the plague caused by the bacterium *Yersinia pestis*. This group showed that dental pulp from the remains within the mass grave contained DNA with a 93 - 96% homology to that of the current *S. enterica* Typhi.

This study therefore provides a link to the possible role this bacterium has played in the frequency of the ΔF508 allele within the Caucasian population.
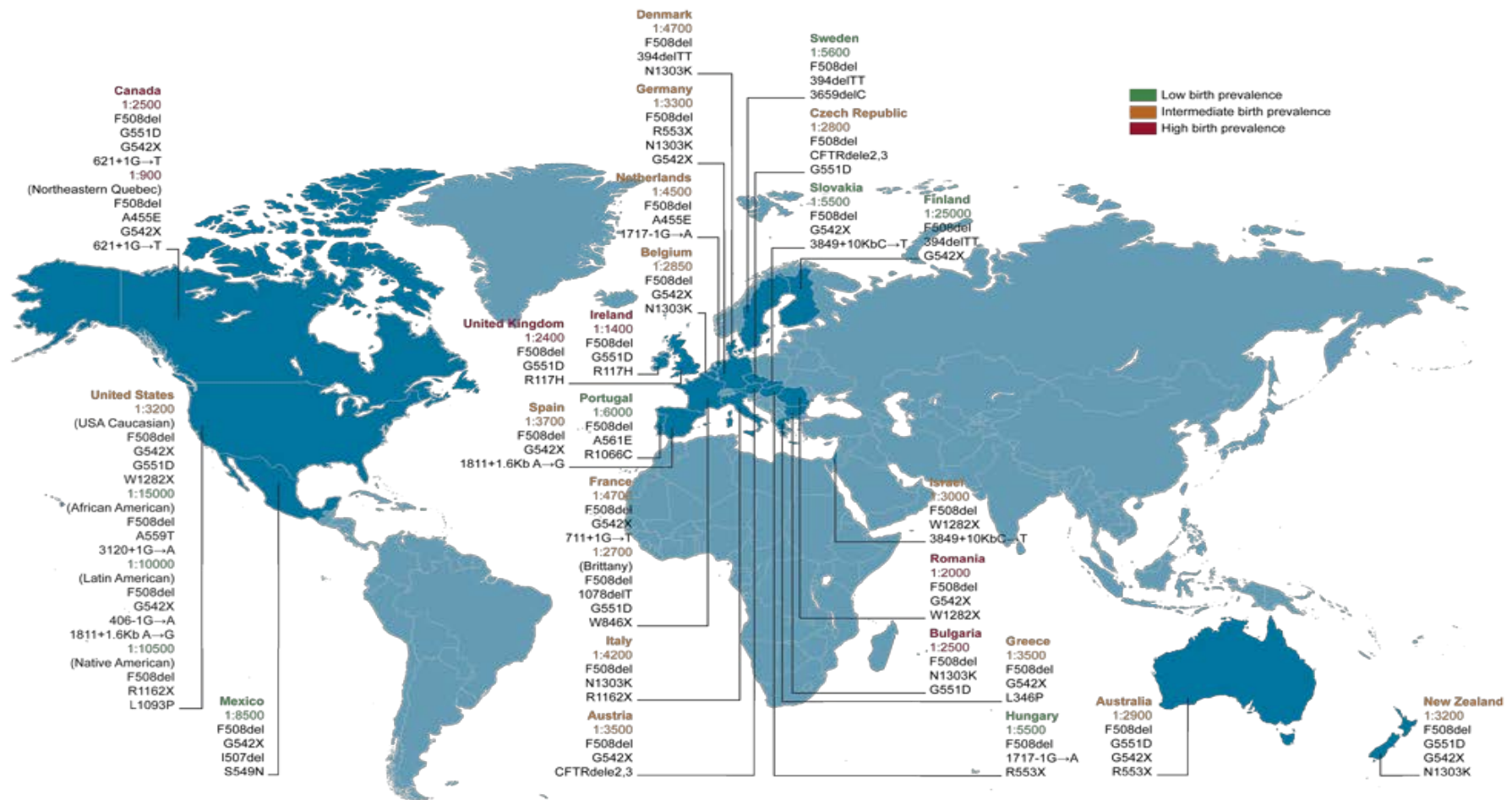
Figure 1.2   Map outlining the most common CFTR mutations. Adapted figure (CFTR Science 2015; O'Sullivan and Freedman, 2009).

1.0.2 Cystic fibrosis pathogenesis

The normal surface of the human lung comprises a mucus layer plus a layer of cilia (~7 μm) covered by a periciliary liquid which is maintained at a low-viscosity to aid ciliary beating (Matsui *et al.*, 1998). There are hypotheses for the effect the defective CF-causing gene has on the composition of the airway surface liquid (ASL). The first is coined the "low volume" hypothesis which suggests that the ASL volume is adjusted by epithelia cells ensuring an equilibrium by water permeability adjustment to ensure sufficient ciliary beating. Therefore this theory is suggesting that there is a similar salt concentration between the ASL and the plasma for both CF and non CF patients (Matsui *et al.*, 1998).The second theory is termed the "compositional" hypothesis which proposes that ASL salt concentration is controlled by the epithelia cells which implies that within CF patients there is a higher salt concentration to those without the defective gene (Smith *et al.*, 1996). A tight regulation of the periciliary layer is required in order to clear the airways of particles, aiding our innate defence. In CF mucins or low volume content in the periciliary layer are responsible for drastically slower clearance rate of particles. Studies have estimated that the clearance rate of particulates can be up to 6 h slower (Knowles and Boucher, 2002) which can significantly increase the time microorganisms have to colonize the lungs.

1.0.3 Monitoring and treatment

Regular visits to CF clinics allow assessment of disease progression and for assessment of the microbial composition of expectorated sputum which can inform decisions regarding appropriate antibiotic choices where treatment with empirical regimes has failed. Lung function is analysed via spirometry with forced expiratory volume (FEV1). The daily treatment of CF requires both chemical and physical means. Physical treatments which can be carried out at home involve (1) the use of manual chest physiotherapy (CPT), (2) hand held positive expiratory pressure (PEP) devices such as a PEP value, flutter and acapella and (3) vests which vibrate the chest. All of these treatments can be carried out at CF centres and at home. Although the latter therapy involves purchasing an expensive kit for use at home, in the last few years CF patients

within the US are purchasing devices such as the inCourage® System airway clearance vest from RespirTech for use at home.

The use of bronchodilators such as albuterol are used to relax the airways in order to facilitate the clearance of thick mucus, the use of albuterol prior to CPT is commonly practised (Moffett, 2010). Adjunctive therapies such as the use of 3% and 7% hypertonic saline, HyperSal® given via a nebulizer machine has been shown to increase hydration and aid in the break-up of thick mucus in the lower airways for ease of clearance (Donaldson *et al.*, 2006). Pulmozyme®/dornase alfa is another form of airway clearance treatment which can be nebulized and is used for its mucolytic properties for patients with mild to severe lower airway obstruction. Pulmozyme® has been shown to reduce two critical properties of CF sputum; 1) viscosity and 2) adhesion through the depolymerisation of DNA which is secreted into the ASL as a result of epithelial and neutrophil cell necrosis (Shak *et al.*, 1990; van der Giessen, 2009). In addition to the release of DNA, other eukaryotic intracellular components are released such as F-actin. Unfortunately, these two polyanionic polymers have been shown to form an effective cobweb/mesh which can bind to anti-microbial agents rendering them inactive (Bucki *et al.*, 2007). Collectively, the goal of the adjunctive therapies is to reduce the adhesiveness and thin the sputum to make it easier for the patient to expectorate. Furthermore, this prevents the accumulation polymers which can hamper the activity of the anti-microbial agents administered (Drew *et al.*, 2009). The above treatments can be prescribed for daily usage but can then be increased during exacerbation periods (Wood and Ramsey, 1996)

Antimicrobial treatment of CF can involve antibiotics taken (1) orally, (2) through a nebuliser or (3) parenterally. The antibiotics used in treatment are patient specific and chosen based on culture results obtained from the laboratory. The most commonly prescribed antibiotics used in CF are colistin and tobramycin.

1.1 The polymicrobial nature of infection in the CF lung

Early understanding of the bacteria associated with respiratory infection in CF have been shaped by culture dependent techniques (Thomson, 1999). These early studies investigating the CF microbiome suggested only a handful of bacterial species to be consistently identified across CF patients, namely *Pseudomonas aeruginosa* (Laraya-Cuasay, Cundy and Huang, 1976; Doggett *et al.*, 1964), *Staphylococcus aureus* (Szaff and Høiby, 1982), *Haemophilus influenzae* (Bilton *et al.*, 1995) and *Burkholderia cepacia* (LiPuma *et al.*, 1988). However in the last decade there have been major advances in molecular approaches to characterizing microbial community composition and this revolution has revealed that the diversity of microorganisms has been greatly underappreciated for the CF lung (Rogers *et al.*, 2004; Sibley *et al.*, 2009) and for other human and environmental niches harbouring microbial life (Sogin *et al.*, 2006; Flores *et al.*, 2012). Such techniques include sequence analysis of cloned 16S ribosomal RNA genes (Harris *et al.*, 2007; Bittar *et al.*, 2008), terminal restriction fragment length polymorphism analysis (Rogers *et al.*, 2006; Sibley *et al.*, 2008), a high-density phylogenetic microarray PhyloChip analysis (Cox *et al.*, 2010) and pyrosequencing (Armougom *et al.*, 2009; Guss *et al.*, 2011). Data from studies involving these methods have demonstrated that the level of microbial diversity within the CF lung was completely at odds with the dogma of only a handful of bacterial species. The level of bacterial diversity also showed the presence of both aerobic and anaerobic bacteria within the lung. Bacteria belonging to the following phyla have been commonly identified across a number of studies: Proteobacteria, Firmicutes, Fusobacteria, Actinobacteria, Bacteroidetes, Tenerictues and Spirochaetes (Guss *et al.*, 2011; Bittar *et al.*, 2008; van der Gast *et al.*, 2011). This wealth of information has come with the dilemma of figuring out exactly which microorganisms can colonize the CF airways versus transient colonizers and species which maybe non-viable/redundant within the CF airways. This vast microbial diversity of the CF airway has proven that within these airways there is a polymicrobial infection similar to other infections such as those found in burn wounds (Metcalf and Bowler, 2013) or central venous catheters (Downes *et al.*, 2008), and which must be understood in order to properly inform clinical treatment.

Ultimately the benefit of the knowledge provided by the above molecular techniques can better inform researchers to develop methodologies to investigate biofilm formation and the inter- and intra-species interactions within this polymicrobial niche. However despite the benefit molecular studies offer, microorganisms need to first be isolated from CF samples in order to study biofilm formation and inter species interactions. Despite the pitfalls in culturing (refer to section 1.2.1), over the last number of decades a few bacterial species have been consistently identified across CF patients which has been supported by molecular studies (Sibley *et al.*, 2006; Harris *et al.*, 2007). The most prevalent CF pathogens are *P. aeruginosa*, *S. aureus*, *H. influenzae*, *Achromobacter xylosoxidans*, *Stenotrophomonas maltophilia*, *B. cepacia* complex, *Candida albicans* and *Streptococcus pneumoniae* (Burns *et al.*, 1998; Gibson *et al.*, 2003; Davies and Bilton, 2009; Delhaes *et al.*, 2012). As these microorganisms are the most prevalent microorganisms identified in CF pathogens a brief overview in the following section will be given for each, as the work within this thesis will primarily focus on these microbes of interest.
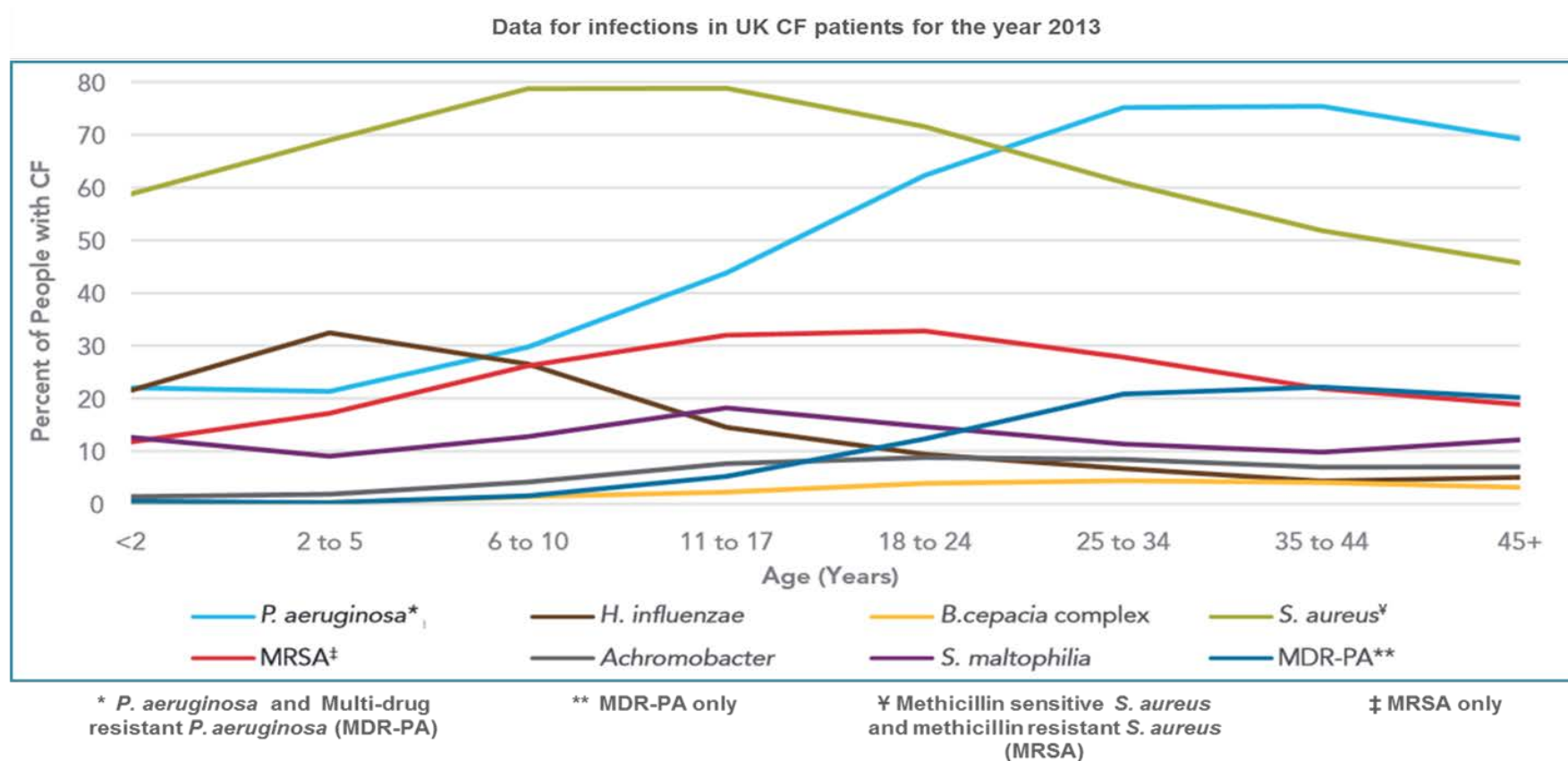
Figure 1.3 Figure outlining the prevalence of the most commonly identified pathogens over the lifetime of CF patients within the U.K. Figure adapted from the Cystic Fibrosis Foundation Patient Registry, 2012.

1.1.1 *S. aureus*

The CF lung becomes colonised from an early age with *H. influenzae* and *S. aureus* becoming the first two most common bacterial species to colonize the CF airways (Armstrong *et al.*, 1997), refer to Figure 1.3 for an outline of the microorganisms commonly identified during the lifetime of a CF patient. *S. aureus* is a commensal microorganism commonly found on human skin, within the gastrointestinal tract and in the nasal cavity of healthy humans. It is known that approximately one-third of people are persistent carries of *S. aureus* while one-third of the population are transient carriers and the remainder of the population do not pertain any association with this bacterium (Wertheim *et al.*, 2005). Due to this high community reservoir, it is understandable that CF patients from an early age are colonized by *S. aureus*. Interestingly, a study has shown that members which reside in the same house as a CF patient carried both methicillin-sensitive *S. aureus* (MSSA) and methicillin-resistant *S. aureus* (MRSA) strains which were subsequently identified from samples obtained from the CF patient's lung (Stone *et al.*, 2009). With the risk of both the household members and the community posing as carriers of this pathogen, the continual occurrence of *S. aureus* throughout the lifetime of the patient makes its eradication extremely difficult without the added factor of multidrug resistance. Both U.K. and USA databases show an increase for MRSA within CF patients with the USA harbouring a higher prevalence for this bacterium (Anonymous, 2012, 2013). Also an increasing amount of researchers are identifying small colony variants (SCV) of *S. aureus* from the CF lung particularly during co-infection with *P. aeruginosa* (Besier *et al.*, 2007). This work involved a temporal study on the isolation of SCVs of *S. aureus* from CF patients over the course of a year. They found that the SCV were more resistant to antibiotics, isolated consistently from older patients and from patients which were always colonized with *P. aeruginosa*. Due to these combined factors, patients colonized with SCVs of *S. aureus* showed a decline in lung functioning and overall clinical status (Besier *et al.*, 2007). More research is required to further unravel the relationship between the initial and continual colonization of *S. aureus* with that of the clinical status of a CF patient and subsequent co-colonization of other CF pathogens. Also there is lack of research into whether *S. aureus* forms biofilms within the CF lung. Another clear microbe co-colonization dynamic is that between *S. aureus* and

H. influenzae. Which does prompt the question - does early colonization of the CF lung by *S. aureus* promote or affect the co-colonization of other microorganisms?

1.1.2 *H. influenzae*

H. influenzae similar to *S. aureus* colonizes the nasal cavity, approximately 50% of children by the age of six are positive for the bacterium which rises to 75% by adolescence (Spinola *et al.*, 1986). *H. influenzae* can be split into two categories, typeable and non-typeable. Typeable strains – possess a capsule with six recognised serotypes and the non-typeable *H. influenzae* strains (NTHI) are not encapsulated. It is the non-encapsulated strains which are identified in respiratory diseases and found within the CF lung (Möller *et al.*, 1992). Although there is a paucity of work carried out on the importance of the early and in some cases transient colonization of the CF lung with *H. influenzae*, there is important work which highlights resistance among NTHI CF isolates (Möller *et al.*, 1995). In the latter study, *H. influenzae* strains resistant to β-lactam antibiotics were continually isolated over a period of two years from patients undergoing antibiotic treatment. This observation is the key to the continual isolation of *H. influenzae* throughout the lifetime of certain CF patients as shown in Figure 1.3.

1.1.3 *P. aeruginosa*

No other bacterial species can rival the ability of the Gram-negative bacterium *P. aeruginosa* in colonizing the CF airways from an early age right through till the end. *P. aeruginosa* is a highly adaptive microbe and important environmental sources where it is found are water and soil; important built environmental sources are sanitary systems (Greenwood *et al.*, 1997). Over 50% of CF patients by the age of twenty are colonized by this bacterium, refer to Figure 1.3. Once colonized by *P. aeruginosa*, patients show an overall poorer prognosis due to continual deterioration of the lungs which ultimately results in a shorter life expectancy (Moffett, 2010). There are two notable phenotypes which *P. aeruginosa* displays over the course of infection in CF

patients. The first is the non-mucoid phenotype, which if identified early and the patient is placed on an aggressive antibiotic regimen of oral ciprofloxacin or intravenous agents and nebulized treatments such as tobramycin and colistin, can result in the removal of the bacterium (Høiby, 2011). However, the second phenotype which is called the mucoid phenotype occurs due to the overproduction of alginate. This phenotype cannot be eradicated from the CF lung once identified (Henry *et al.*, 1992).

Apart from the mucoid phenotype allowing prolonged infection, the main cause for persistence of *P. aeruginosa* is due to its ability to establish biofilms within the CF lung (Lam *et al.*, 1980; Bjarnsholt *et al.*, 2009; Høiby, 2011). Growth in a biofilm allows *P. aeruginosa* to evade the host's innate immunity. Additionally, the production of rhamnolipids by *P. aeruginosa* cells within biofilms is governed by quorum sensing to effectively act as a further defence against the innate immune defence cells, polymorphonuclear neutrophilic leukocytes (PMNs) (Alhede *et al.*, 2009). Rhamnolipids have been shown to induce necrosis of PMNs on contact (Jensen *et al.*, 2007). Other virulence factors which enable *P. aeruginosa* to evade the host defences are elastases and proteases both of which are capable of disabling the activity of immunoglobulins and cytokines by breaking their structure (Kharazmi *et al.*, 1984). Apart from evading the host defences *P. aeruginosa* can prevent the effectiveness of antibiotics through the use of enzymes such as β lactamases and membrane efflux pumps (Hancock and Speert, 2000). However the biofilm mode of growth allows cells within the matrix to become tolerant to the constant onslaught of antibiotics given to CF patients. This is the primary reason why infection persists allowing the bacterium to evolve within the CF lung. Yang and colleagues found that *P. aeruginosa* had undergone up to 200,000 generations within CF patients sampled over the course of thirty five years (Yang *et al.*, 2011). Unfortunately, constant antibiotic regimens apply selective pressure whereby various phenotypes of *P. aeruginosa* (Boles *et al.*, 2004) are tested and weeded out (Bagge *et al.*, 2004). One of the typical characteristics of late stage infection with *P. aeruginosa* is the presence of a mutator phenotype which is resistant to antibiotics (Oliver *et al.*, 2000; Ciofu *et al.*, 2005). But the main hurdle in treating chronic CF infections is attempting to clear biofilm growth of *P. aeruginosa* which is capable of growing

aerobically in the lung and within anaerobic pockets such as damaged sections of the lung or mucus plugs (Høiby, 2011). It is now well established that *P. aeruginosa* biofilms are capable of growing anaerobically which therefore allows the bacterium to survive deep in the lung within mucus plugs (Yoon *et al.*, 2002; Hill *et al.*, 2005). Collectively all of these above traits need to be taken into account when treating patients with chronic lung infections as there are a diminishing number of effective antibiotics to utilize once resistance occurs. Importantly, other researchers have pointed to the need to explore the use of other therapies such as (1) quinolones, aztreonam, amikacin within liposomes (Bakker-Woudenberg *et al.*, 2002), (2) 2-bromohexanoic acid to inhibit rhamnolipid production (Gutierrez *et al.*, 2013), (3) QS antagonists-AHL-lactonase enzymes (Migiyama *et al.*, 2013) and (4) bacteriophage therapy (Morello *et al.*, 2011). All of these different therapies highlight the current various efforts being explored to combat chronic infections.

Although *P. aeruginosa* can colonize the lungs quite early and over the course of a patient's lifetime other important Gram-negative bacterial species such as *S. maltophilia*, *A. xylosoxidans* can also both be transient or permanent inhabitants of the CF lung.

1.1.4 *S. maltophilia*

S. maltophilia has found to in habitat a multitude of environments such as soil, plant rhizosphere, rivers and distribution systems (Denton and Kerr, 1998). This bacterium is clinically recognized as capable of causing nosocomial pneumonia (Nseir *et al.*, 2006). It was first isolated from a CF patient by Blessing *et al.* (1979). *S. maltophilia* is of clinical importance as it has a wide range of drug resistance and has also been implicated in the induction of pulmonary exacerbations (Saiman and Siegel, 2004). However, the role *S. maltophilia* plays in disease progression in CF lung infections is not clear, but researchers are suggesting that CF patients which are colonized by *S. maltophilia* are more likely to undergo pulmonary exacerbations and are at greater risk for the need of a lung transplant (Waters *et al.*, 2013). These are important points which require further work, to understand the role *S. maltophilia* plays in the polymicrobial infection and disease progression of the CF lung.

1.1.5 *A. xylosoxidans*

A. xylosoxidans, similar to the other Gram-negative microorganisms infecting the CF lung, has been identified in a wide number of environments (Amoureux *et al.*, 2013). This bacterium is an opportunistic pathogen and this has been nicely demonstrated through work showing that infections have been caused through contaminated disinfectants and dialysis fluids (Molina-Cabrillana *et al.*, 2007). *A. xylosoxidans* is now being more widely identified in CF lung samples with some studies showing some patients can be chronically infected with this bacterium while others are transiently infected for a number of years (Tan *et al.*, 2002). Like *S. maltophilia* this bacterium has a wide range of antibiotic resistance (Saiman and Siegel, 2004), but research into the importance of this bacterium in CF infection is still in the early days.

1.1.6 *S. pneumoniae*

S. pneumoniae is a known respiratory pathogen involved in bacterial pneumonia, chronic otitis media and acute bacterial sinusitis (Gomez *et al.*, 1999). The isolation of *S. pneumoniae* has previously been associated with paediatric CF patients (García-Castillo *et al.*, 2007) and has been identified in patients undergoing pulmonary exacerbation (del Campo *et al.*, 2005). However this bacterium can also be isolated from adult CF patients (Maeda *et al.*, 2011). Although work regarding *S. pneumoniae* infection in the CF lung is in the early stages, An important study demonstrated that *S. pneumoniae* isolates from the CF lung readily formed biofilms with minimum biofilm inhibitory (MBIC) concentrations that were greater than the minimum planktonic inhibitory concentration to penicillin and tetracycline (García-Castillo *et al.*, 2007). A recent study to determine the impact of *S. pneumoniae* infection on the disease progression of CF patients could not find any correlation between colonization of this species and a decline in the health of CF patients (Thornton *et al.*, 2015). However its role in the polymicrobial infection in CF has not yet been explored and nor has the ability of this bacterium to undergo horizontal gene transfer been explored, which previously has been shown to be of clinical importance during infection (Hiller *et al.*, 2010).

1.1.7 *B. cepacia* complex

In addition to *P. aeruginosa*, isolation and identification of *B. cepacia* complex is also associated with poor patient prognosis. *B. cepacia* complex is composed of 18 closely related Gram-negative bacteria (Sousa *et al.*, 2010; Peeters *et al.*, 2013). These microorganisms are used as an indicator of poor prognosis in CF, and can lead to the more severe condition called *B. cepacia* syndrome, whereby instead of solely colonizing the lungs the infection spreads throughout the body. This is extremely difficult to treat and can result in the death of the patient within a short period of time (Zuckerman and Seder, 2007).

1.1.8 Fungi

Although the literature regarding the microbiome of the CF lung is predominated by bacterial species, fungi from the *Aspergillus* sp. namely *A. fumigatus*, *Candida albicans* and *C. dubliniensis* are notably being more routinely identified from CF airway samples (Verweij *et al.*, 1996; Wahab *et al.*, 2014). The main problem caused by *A. fumigatus* is the elicitation of an immune response on exposure to spores in the air which can result in a range of symptoms: from the onset of a mild cough with wheezing to serious damage such as pulmonary fibrosis (Moss, 2002). Biofilm growth for some of these isolates has been carried out, however an overall understanding of the interactions between these species during their biofilm mode of growth needs to be investigated (Spasenovski *et al.*, 2010). A recent excellent review on the increasing frequency of *C. albicans* isolation in CF samples by Chotirmall and colleagues draws attention to the overwhelming lack of work in this area (Chotirmall *et al.*, 2010). Moreover, a study by Wahab and collegaues has provided further cause for the need of more focused studies to understand the role *Candida* spp. play in the polymicrobial infection with an increasing number of patients presenting with *C. dubliniensis*, a close relative of *C. albicans* (Wahab *et al.*, 2014). Especially considering that *C. albicans* and *C. dubliniensis* have previously been shown to be pivotal agents in increasing the adhesion and colonization of other microorganisms within the oral cavity (Lamont and Jenkinson, 2000). The CF microbiome is now known to be highly diverse, with important work suggesting that despite intensive antibiotic

treatment, the pre and post exacerbation community composition is not altered significantly (Tunney *et al.*, 2011). Also the diversity of the CF lung tends to lower towards the latter stages of infection with paediatrics and young adults typically showing a more diverse range of microorganisms (Zhao, Schloss, *et al.*, 2012). The role of the various inter and intra species interactions along with how this impacts on biofilm formation needs to be addressed, to collectively piece together a clearer picture of how these factors contribute to a decline in the overall health of the patient.

Throughout this brief introduction to the CF microbiome in section 1.1, the importance of understanding the role of any one microorganism found in the CF lung should not be untethered from association with any other microorganism. Future work exploring mixed species interactions will provide results which more closely mirror that of the CF lung (Lopes *et al.*, 2012; Tavernier and Coenye, 2015). Work within this thesis will explore ways of accessing mixed species communities within the CF microbiome and explore new techniques to visually inspect the spatial organization of these communities.

1.2 Methodologies to study the polymicrobial nature of the CF lung

As described in section 1.0.3, CF patients routinely attend a CF clinic for assessment and treatment. During these visits a sample of sputum can be obtained from a patient during a chest physiotherapy session or induced by using inhaled hypertonic saline or spontaneously expectorated. The sputum sample is then analyzed in a clinical laboratory using a range of techniques. All clinical laboratories utilize the fundamental microbiological techniques such as selective and differential plating and Gram staining. But additionally laboratories can employ biochemical profiling applications such as those offered by BIOLOG® or API® kits and utilize molecular analysis such as Polymerase Chain Reaction (PCR) assays to identify the microorganisms present within the sputum. All of these approaches serve to identify the microorganisms present within the sputum sample to aid in tailoring the antibiotic treatment of the individual. However these approaches alone are not sufficient methodologies to gain an understanding of whether the microorganisms (1) exist as sessile or planktonic cells (Singh *et al.*, 2000) (2) are part of a monospecies or multispecies biofilm (Burmølle *et al.*, 2010) (3) are viable but non-cultivable state (VBNC) (Xu *et al.*, 1982; Bogosian and Bourneuf, 2001) or (4) their spatial structuring within a multispecies biofilm .

In this section, an overview of the current methodologies used to address the issues highlighted above for research purposes but not limited to, will be discussed. These focal points will include methodologies used for studies carried out within this thesis, with the aim of elucidating the biofilm dynamics of microorganism isolated from CF sputum at the foreground.

1.2.1 Culture methods

It is now widely accepted that the CF airways harbor a vast diversity of microorganisms than was previously appreciated (Andersen and Hodges, 1946; Pier, 1985) and therefore CF infections are polymicrobial (Sibley *et al.*, 2006). In order to identify or study the microorganisms present in a sputum sample they must be either grown on agars or visualized using microscopy, refer to section 1.4.2 for a review of this area. CF sputum is viscous and must first be liquefied before analysis, dithiothreitol (DTT) (Wooten and Dulfano, 1978) or *N*-acetylcysteine are commonly used for this purpose and act by breaking disulphide bonds, see Figure 1.4. The liquefied sputum is serially

diluted and plated onto enriched or selective and differential agars; see Table 1.1 for a list of agars and the microorganisms they recover.
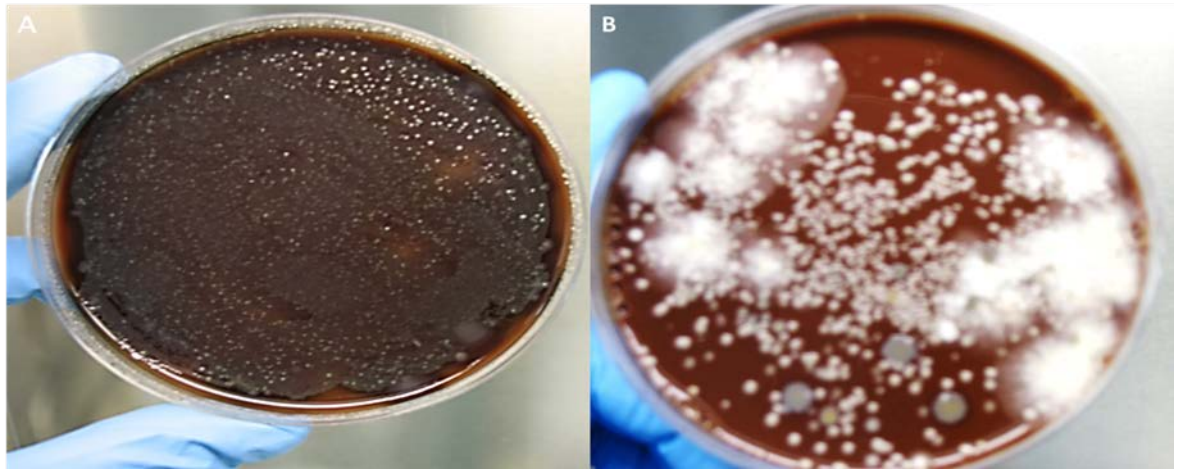
Figure 1.4   Liquefied sputum from two CF patients, 100 μl of the neat suspension spread onto chocolate agar. **A**) One bacterial species produces a lawn of growth over two bacterial species; **B**) A fungal species grows over four bacterial species (refer to Chapter 2).

Pure isolates are processed for Gram staining to determine both the cell morphology and classification. Using this information, a range of biochemical tests along with observing colony morphology such as mucoidy or small colony variants, presence of haemolysis on blood agar and pigment production can collectively be utilized to build up a profile of the microorganism. Biochemical tests can range from the simple enzyme based tests such as the catalase (Taylor and Achanzar, 1972) and oxidase tests (Steel, 1961), to commercial kits by BIOLOG®, RapID (Remel) and API®(bioMérieux) or to more complex systems such as the Phoenix (Becton-Dickinson) and VITEK (bioMérieux) systems can be employed to identify a microorganism to the species level based on the range of substrates the microorganism can utilize. The technique coined, matrix-assisted laser desorption/ionization time-of-flight mass spectrometry (MALDI-TOF MS) which determines the mass of proteins in a sample and provides effectively a fingerprinting account of a specimen are being more routinely utilized in microbiology labs. The use of MALDI-TOF MS has proved useful in the rapid identification of microorganisms from isolated from CF specimens, especially

strains which are closely related such as *B. cepacia* complex members (Vanlaere *et al.*, 2008).

Table 1.1   List of media used to isolate microorganisms present in CF sputum.

Media	Classification	Microorganisms Isolated
Pseudomonas Isolation Agar	Selective and differential	*P. aeruginosa* and *Pseudomonas* spp.
Cetrimide agar	Selective and differential	*P. aeruginosa* and *Pseudomonas* spp.
Mac Conkey	Selective and differential	Gram negative bacteria
Blood Agar	Enriched and differential	Most Gram-positive and gram-negative bacteria. Differential use in identifying haemolytic bacteria such as *Streptococcus* spp.
Chocolate Agar	Enriched	*H. influenzae* and fastidious microorganisms
Tryptic Soy Agar	General purpose media	Most Gram-positive and gram-negative bacteria and fungi but not fastidious bacteria
Baird-Parker Agar	Selective and differential	*S. aureus*
Mannitol Salt Agar	Selective and differential	*Staphylococcus* spp.
Burkholderia cepacia Agar *	Selective	*B. cepacia* and *B. cepacia* complex spp.
Sabouraud Dextrose Agar	Selective	Fungi

*Supplement added which contains: polymixin B, gentamicin and ticarcillin. (Doern and Brogden-Torres, 1992; Burns and Rolain, 2014).

Although culture based techniques have played a large role in microbiology, it is important to highlight the main pitfall with this methodology, which is referred to as "the great plate anomaly" (Staley and Konopka, 1985). This term is used to describe the evident discrepancies between microscopy and culture counts of microorganisms, with the former revealing a greater number and diversity (Jennison, 1937; Handelsman, 2004). This issue becomes clearly evident when dealing with clinical and environmental samples (Eckburg *et al.*, 2005; Venter *et al.*, 2004). A number of hypotheses exist to account for these

striking differences: (1) inadequate medium to support growth (Moore *et al.*, 2007) (2) insufficient environmental parameters i.e. temperature, pH, air conditions (Moore *et al.*, 2007) (3) VBNC (Oliver, 2010) (4) inhibiting effect of by-products as a result of sterilizing the agar (Tanaka *et al.*, 2014) (5) lack of co-culture counterpart (Kaeberlein *et al.*, 2002) and (6) length of incubation (Davis *et al.*, 2005). Therefore, the adequate recovery of the vast diversity of bacteria from CF sputum can be hindered by one or more of these factors. This contributed to the early shortcomings of research into the dynamics of the polymicrobial nature of the CF lung. Consequently, work to explore which microorganisms grow as biofilms and if any of microorganisms form multispecies biofilms within the CF lung has only began to be researched in later years.

Recently, this challenge is being tackled with research groups beginning to devise methodologies to study the importance of multi-species biofilms formed by bacterial species isolated from the CF lung; such as work by Bragonzi *et al.* (2012) and Tavernier and Coenye, (2015). This thesis will also explore methods to study multi-species biofilms formed by bacteria isolated from sputum samples collected from CF patients attending clinic at Southampton University Hospital.

Finally, the isolation and identification of microorganisms within a CF sputum specimen is necessary for (1) antibiotic susceptibility testing, (2) to test biofilm formation, (3) phenotypic characteristics (colony morphology, mucoidy, small colony variants) (Bittar and Rolain, 2010), (4) to test anti biofilm strategies (5) to aid in the developmental of better identification techniques for atypical bacteria and (6) to begin to unravel the interactions of the multitude of bacteria present in the CF lung; thereby identifying the dynamics which lead to a negative impact on the patient's health and aid in developing strategies to dismantle biofilm development.

1.2.2 Molecular methodologies

Culture independent analysis of CF sputum revolutionized the study of the microbiota of the CF lung and confirmed the CF lung infection as a polymicrobial infection (Sibley *et al.*, 2006; Rogers *et al.*, 2010; Zhao, Schloss, *et al.*, 2012). A number of molecular methodologies have been used to date

to identify members of the CF microbiome ranging from the relatively simple but powerful technique of PCR to the more complex methodologies such as next generation sequencing. Firstly, although PCR is used routinely to confirm identification of a microorganism or as part of more complex methodologies, it can also be employed quantitatively which is known as real-time quantitative PCR (qPCR). This technique has proven to be both a rapid and useful tool in CF studies investigating the abundance of important CF microorganisms such as *P. aeruginosa* during both stable and pulmonary exacerbation periods in CF patients or in estimating the bacterial load of a number of CF pathogens (Zemanick *et al.*, 2010; Deschaght *et al.*, 2013).

Molecular taxonomy of organisms by using the ribosomal RNA (rRNA) gene to separate organisms based on the sequence similarity of particular regions of this gene, has proven to be extremely useful particularly in microbiology (Woese, 1987; Woese *et al.*, 1990; Janda and Abbott, 2007). The use of 16S rRNA as a marker for the identification of bacteria is due to its presence in almost all bacteria and that there are highly conserved regions within the 16S rRNA gene. Given there are a number of databases which house sequence information for thousands of microbial species, some noteworthy ones are the European Molecular Biology Laboratory Nucleotide Sequence Database (Stoesser *et al.*, 1999), the Ribosomal Database Project (Cole *et al.*, 2005) and Greengenes (DeSantis *et al.*, 2006), using 16S rRNA to decipher the microbial species present makes it an extremely powerful tool in microbial ecology. The first use of the 16S rRNA gene sequence as a tool to distinguish between the different microbial members in a sample was described by Pace *et al.*, (1986). The development of PCR lead to the ability of researchers to routinely amplify the 16S rRNA region or another region of the genome such as the recA gene which are known to exist in bacterial species and thereby allow identification down to the taxonomic level (Lynch and Bruce, 2013). The first studies involving the application of 16S rRNA for the identification of bacteria found in CF infection were described by Karpati and Jonasson, 1996 for *Pseudomonas aeruginosa*; by Whitby *et al.* (1998) for *Burkholderia cepacia* complex members and by Whitby *et al.* (2000) for *Stenotrophomonas maltophilia*. Importantly, the first molecular work by Rogers *et al.* (2003) which begin to reveal a greater microbial diversity of the CF lung than was previously appreciated involved the use of a technique called terminal

restriction fragment length polymorphism (T-RFLP) (Liu *et al.*, 1997). Briefly this method involves amplification of the 16S rRNA gene using fluorescently-labelled primers of DNA extracted from sputum which undergoes restriction digestion followed by separation of the digested products using electrophoresis in an automated DNA analyzer; a profile/fingerprint is generated which allow for the level of microbial diversity to be estimated. This study prompted other researchers to further investigate the diversity of the CF microbiome using molecular approaches (LiPuma, 2010). The vast advances made in the field of genomics for the identification of microorganisms allowed a number of sequencing methodologies to be applied to study the CF microbiome. As demonstrated by the use of Sanger chemistry sequencing by Harris *et al.* (2007), pyrosequecing by Armougom *et al.* (2009) and finally to the most comprehensive genomic technique whole-genome sequencing (WGS). Whole genome sequencing was utilized by Winstanley *et al.* (2009) on the Liverpool epidemic strain of *P. aeruginosa*, by Rolain *et al.* (2009) on a multi-resistant CF strain of *S. aureus* and by Holden *et al.* (2009) on *B. cenocepacia*.

Collectively, all of the above molecular methodologies are powerful tools in the study of both the CF microbiome and the genetic content of individual CF microorganisms, important points regarding DNA extraction protocols and viable versus dead cells have been highlighted (Rogers *et al.*, 2009). The first concern is related to the various DNA extraction protocols which can be employed, evaluation of the protocol used will ensure no bias occurs (Zhao, Carmody, *et al.*, 2012a). Secondly, DNA extracted from sputum will contain an unknown amount of DNA from dead cells, extracellular DNA and from species which may never contribute to disease progression (Rogers *et al.*, 2009; Deschaght *et al.*, 2013). Currently two methods to circumvent the latter issue have been utilized in CF studies; the first is to use reverse transcription so only metabolically active cells will be sampled in assays as carried out by Rogers *et al.* (2009) and the second requires the use of a chemical called propidium monoazide (PMA), which was used in a study by Deschaght *et al.* (2013). Both of these important points will be explored as part of the work carried out in Chapter 4.

1.2.3 Microscopy methods

The study of microorganisms, Microbiology began with the invention of the microscope. It was Anton van Leeuwenhoek in the 17th century who produced the first simple microscope containing one powerful lens. The microscopes he created were capable of a magnification up to 270x, which enabled him to view microorganisms in dental scrapings which he referred to as "wee animalcules". Anton van Leeuwenhoek is today considered "the Father of Microscopy and Microbiology" (Zuylen, 1981).

The field of microscopy has produced a wealth of developments which have in turn greatly enhanced the field of Microbiology. Numerous microscopic approaches have been used as a tool to analyze samples of sputum and tissue from the lungs of CF patients. A brief overview of the current microscopy approaches used in the study of *in vivo* and *in vitro* planktonic and sessile microorganisms will be explored.

The use of Gram staining with brightfield microscopy can be used for the analysis of CF sputum (Sadeghi *et al.*, 1994) as it is a low cost method. However crucially, the method used to obtain the CF sputum is of additional importance. Expectorated CF sputum samples can be highly contaminated with saliva. The level of cross contamination can be determined by using the Q score system which involves counting the number of polymorphonuclear leukocytes and squamous epithelial cells to identify the quality of sputum obtained from the patient. However work by Nair *et al.* (2002) showed that when using criteria such as the Q score for evaluating Gram staining results of sputum samples in order to determine if culturing should be carried out, was shown to be a considerably weaker tool when compared against the subjective observations made by an experienced bacteriologist.

The most widely used method of staining involves the use of fluorescent dyes and fluorophores, this approach is referred to as fluorescence microscopy. Fluorescence involves the ability of a molecule to absorb energy from an ultraviolet or visible light source at a certain wavelength which causes an electron to move into a higher energy orbit/energy state, referred to as the excited state. After a number of picoseconds the electrons return to their original lower energy state which results in a longer wavelength photon to be emitted during this process as some energy is lost, referred to as the

emission state. This difference between the emission wavelength and the excitation wavelength is known as Stokes Shift. Once the emission and excitation wavelength of a fluorophore or fluorochrome are measured, the use of optical filters which permits only the emission spectra through can be selected to visualize the fluorescence of the specimen, see figure 1.5.
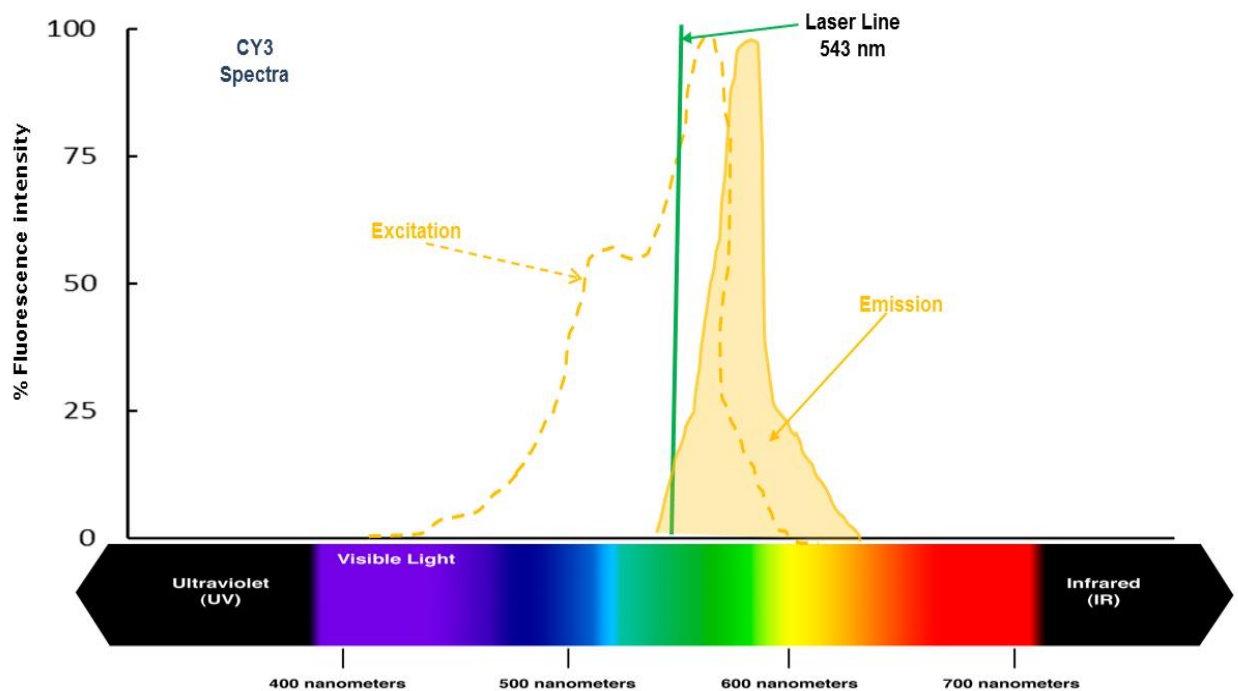
Figure 1.5   Diagram showing the excitation curve for Cy3 and the emission spectra of the fluorophore using the Helium-neon (HeNe) laser line 543 nm. In confocal microscopy the emission filter can be set up to allow the detection of wavelengths between 553 – 570 nm by the photomultiplier tube. Illustrated by Caroline M. Duignan.

Due to these properties three-four fluorophores/fluorochromes can be used to visualize several components in a specimen (Carlsson *et al.*, 1985). Today, there are numerous fluorescent stains; with some capable of distinguishing between viable and dead cells such as *Bac*Light™ and to assess the physiological state of a cell, such as 5-cyano-2, 3 ditolyl tetrazolium chloride (CTC). Fluorescent stains such as *Bac*Light™ which consists of two components, the first component is SYTO 9 which is a low molecular weight

fluorescent dye that can pass through a cell membrane to intercalate with DNA. The second component is propidium iodide (PI) which can only enter cells with a compromised cell membrane due to its higher molecular weight. Therefore *Bac*light™ can be used to determine the number of viable versus dead cells. Typically this fluorescent stain has been used in analyzing *in vitro* biofilms formed by bacterial isolates acquired from the CF lung in (a) antibiotic susceptibility testing (Ciofu *et al.*, 2012), (b) in the study of biofilm formation and structure (Novotny *et al.*, 2013). The use of *Bac*light™ as a stain to distinguish between viable and dead cells must first be validated prior to use (Gião *et al.*, 2009).

Alternatively, fluorescent molecules can be attached to a DNA and RNA molecules or protein. The first application of this in biology commenced with dye-conjugated antibodies and was referred to as immunofluorescence. Immunofluorescence was used by Baltimore *et al.* (1989) to detect the location of mucoid strains of *P. aeruginosa* within sections of a preserved CF lung. This work by Baltimore and colleagues revealed that the majority of bacteria observed within the conductive zones. Both Worlitzsch *et al.* (2002) and Bjarnsholt *et al.* (2009) also used immunofluorescence to detect the alginate produced by mucoid strains of *P. aeruginosa* and demonstrated the presence of mucoid strains in both the conductive and respiratory zone of the CF lung.

The molecular breakthrough highlighting the use of the 16S rRNA as a tool to detect the microorganisms in a given sample lead to the development of a technique called fluorescence *in situ* hybridization (FISH) (Edward F DeLong *et al.*, 1989; Amann *et al.*, 1995). FISH involves the design of an rRNA-targeted oligonucleotide probe to either a complementary sequence detecting a microorganism at the genus or species level. Numerous probes have been published on databases such as Slivia and probeBase, which contain just fewer than 2,800 probe entries. Additionally there are two kinds of probes, DNA based probes and peptide nucleic acid probes (PNA). DNA based probes are negatively charged and consist of a sugar phosphate backbone, while PNA probes are uncharged with a polyamide backbone.

Oligonucleotide probes can be designed to be genus specific or species specific. The probes can range from 15 - 25 nucleotides and are labelled on

the 5' end with a fluorophore such as Cy3. FISH is typically broken down into five stages: (1) Fixation- using paraformaldehyde, to stabilize any protein through covalent bonds often referred to as a cross-linking fixative, (2) Permeabilization - the cell walls of typically Gram-positive bacteria with lysozyme or lysostaphin to allow the probe to enter the cell, (3) Hybridization- the probe is added to the sample in a buffer and the reaction is carried out at an optimal temperature to allow specific binding of the probe to its sequence, (4) Washing- unbound probe is removed during washes at a slightly higher temperature than that used during hybridization and finally (5) Imagining- using epifluorescent microscope or confocal laser scanning microscopy (CLSM), refer to Figure 1.6 for an overview of the use of FISH in the detection of bacteria. Recently, the FISH methodology has been adapted by Valm *et al.*, (2011) to combine a binary labelling system for identifying microorganisms at the genus/species specific level and spectral imaging; called Combinatorial Labelling and Spectral Imagining FISH (CLASI-FISH). This modification has greatly increased the number of microbial species which can be identified within a sample. This technique will be further discussed in section 5.1.

The value of FISH as a rapid and diagnostic tool to identify CF pathogens of interest in sputum was first demonstrated by Hogardt *et al.* (2000). Subsequently, a number of studies have since utilized FISH to demonstrate the presence of *P. aeruginosa* biofilms in both sputum sample, in tissue obtained from the conductive zones of the CF lung and in tissue taken from the respiratory zone in patients who are in the late stage of infection (Worlitzsch *et al.*, 2002; Bjarnsholt *et al.*, 2009). Refer to Figure 1.7 for FISH images of CF sputum.
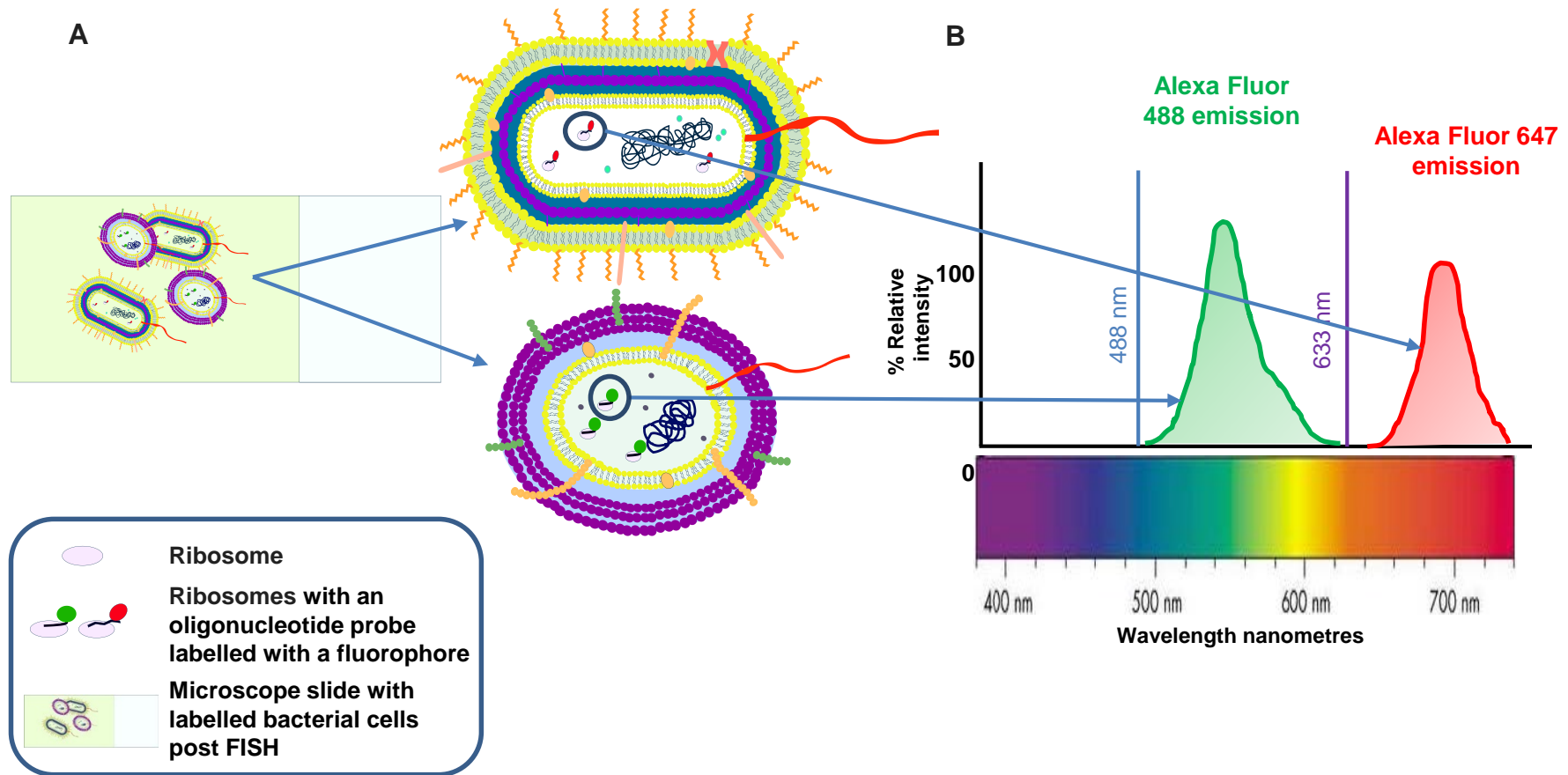
Figure 1.6 Combining compatible fluorophores for imaging. **A**) Using FISH to identify two different bacterial species using two types of fluorophores; Alexa Fluor (AF) 488 (green fluorophore) and AF 647 (red fluorophore) and **B**) emission spectra for the fluorophores, no overlap allows for the simultaneous imaging of both bacterial species using a 488 nm and 633 nm laser lines. Illustrated by Caroline M. Duignan.

Typically visualization of FISH is carried out using an episcopic microscope which makes use of Stokes shift by using a dichroic mirror to allow excitation of the fluorochrome/fluorophore and detection of the emission wavelength (Rost, 1991). Alternatively CLSM is increasingly being utilized in studies to visualize both biofilms and FISH assays. By using CLSM, users are able to acquire 3D images of a specimen which is thick such as biofilms. In CLSM, the laser line used is focused using a aperture through to the objective lens to excite the specimen and the emission wavelength is focused through a beam-splitter with only wavelengths selected for being detected by a photomultiplier tube. An image is built up by scanning one or more of the focused beams of light and also allows for scanning a specimen in the x, y and z plane. The difference between confocal and epifluorescent microscopes is the use of a pinhole in the system right before the photomultiplier tube (Sheppard and Matthews, 1987), see Figure 1.8 for a schematic for CLSM.
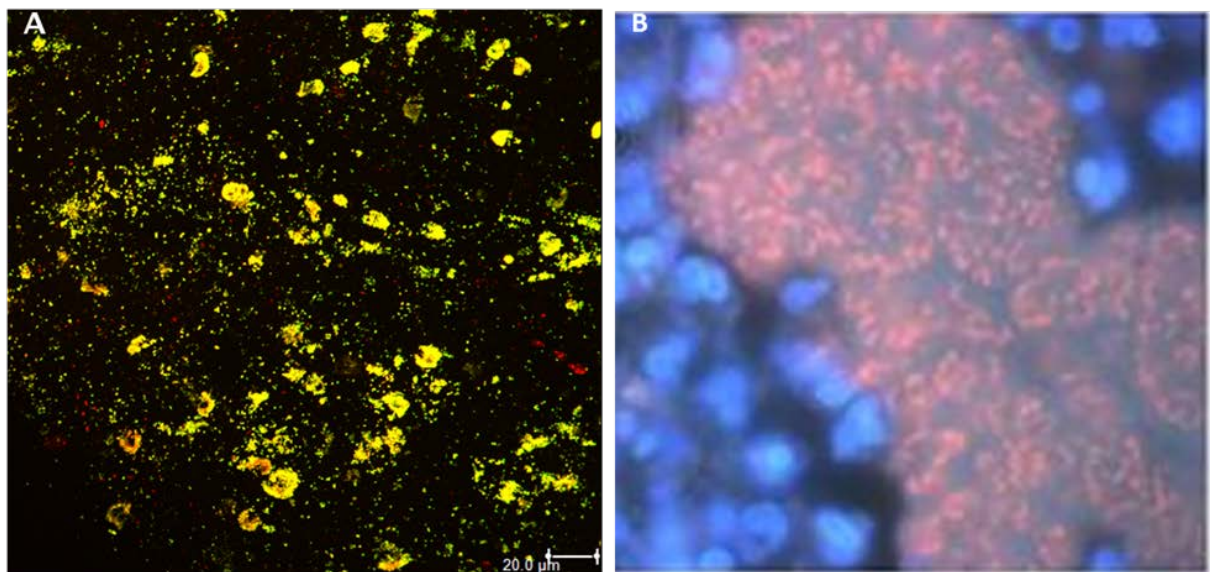
Figure 1.7   Images for FISH carried out on CF sputum samples with probes targeting *P. aeruginosa*. (**A**) DNA probes for Eubacteria tagged with Cy5 and *P. aeruginosa* species specific probe tagged with Cy3; yellow and green fluorescence represent probes labelling *P. aeruginosa* cells (Image acquired by Caroline M. Duignan). (**B**) PNA probe: cells with red fluorescence represent *P. aeruginosa* cells and cells with blue fluorescence represents DAPI bound to DNA (PNA probe image source - Bjarnsholt *et al.*, 2009).

A high resolution microscopic technique called transmission electron microscopy (TEM) provides a 2D black and white image. Lighter sections of an image are due to a greater number of electrons passing through the specimen in a vacuum chamber versus the darker areas of an image resulting from fewer electrons passing through a particular section of the specimen. TEM is capable of giving detailed images of cell structures, to as low as one nanometer in size. The first proof that *P. aeruginosa* was capable of forming microcolonies within the CF lung was remarkably demonstrated using TEM by Lam *et al.* (1980). This work provided proof that microorganisms were capable of forming biofilms within the CF lung. Subsequently, these observations lead to the need for studies to understand infections caused by biofilms instead of solely relying on data from studies using planktonic bacteria.

The following section (1.2.4) will give an overview of the most commonly used techniques to grow and analyze biofilms formed by isolated microorganisms.
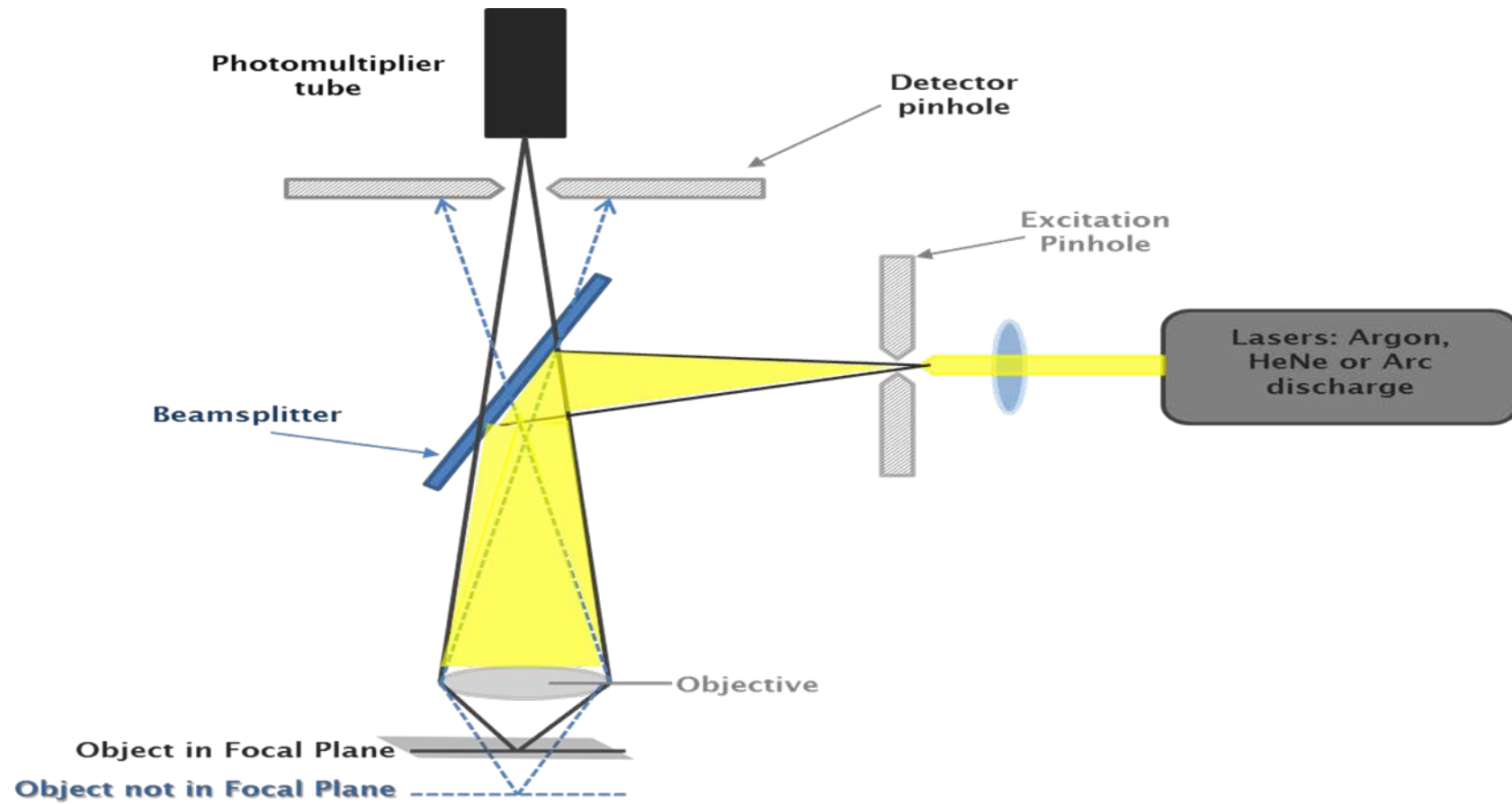
Figure 1.8 Schematic diagram of a confocal laser scanning microscope. Only fluorescence from the focal plane is allowed through the pinhole to the detector. Illustrated by Caroline M. Duignan.

35

1.2.4 Approaches for studying biofilms

Numerous studies have now shown that *P. aeruginosa* does form biofilms in the CF lung (Lam *et al.*, 1980; Baltimore *et al.*, 1989; Worlitzsch *et al.*, 2002; Bjarnsholt *et al.*, 2009). Initial studies investigating *P. aeruginosa* infections in the CF lung used rats as models, wherein they inoculated non-CF rats with *P. aeruginosa* contained on seaweed alginate or agar beads (Johansen, 1996). The purpose of these studies was to understand the host's response to infection in the lung. Moreover, these studies were not focused on biofilm formation but served to help decipher what host and pathogen factors contribute the most to the deterioration of the lung (Tam *et al.*, 1999). The need for work focusing on biofilm formation was prompted by studies such as those by Singh *et al.* (2000) and Favre-Bonté *et al.* (2002), wherein they detect quorum sensing signals in both the sputum and tissue from the lungs of CF patients. However the study of biofilms formed within the lungs of a human or animal is extremely difficult and currently limited. Therefore, approaches to study biofilm formation must be carried out using *in vitro* assays.

The formation of biofilms by microorganism isolated from the lungs of CF patients have previously been grown in the lab using polystyrene plates (1) 96-well microtiter plates (Deligianni *et al.*, 2010), (2) Calgary Biofilm Device (Lopes *et al.*, 2014a) or (3) 6 or 24-well tissue culture plates (Anderson *et al.*, 2008). These plates can be then incubated using static or non-static conditions with fresh media applied at regular intervals. Also these plates can be placed in various air conditions to analyze biofilms formed under aerobic (Lopes *et al.*, 2012), anaerobic (Yoon *et al.*, 2002) and microaerophilic (Moskowitz *et al.*, 2005; Lopes *et al.*, 2014a) conditions, to mirror conditions within the lung as described in the associated papers. Alternatively, biofilms of *P. aeruginosa* CF isolates have been grown in constant flow systems such as the flow cell (Lee *et al.*, 2005; Deligianni *et al.*, 2010). Flow cells are systems which allow biofilms to form in channels under a controlled rate of flow of fresh media.

There have been two separately developed protocols for making artificial sputum which closely resemble the composition of that found in CF patients. Both do not require the use of sputum within their medium as has been

previously been described (Palmer *et al.*, 2005). The first developed was ASM (Sriramulu *et al.*, 2005) and the second is referred to as a modified artificial-sputum medium (ASMDM) (Fung *et al.*, 2010). Although a greater number of biofilm studies should utilize artificial sputum medium in their *in vitro* biofilm assays in order to study biofilms in conditions which are a lot closer to the *in vivo* conditions there are important points to be raised. Firstly, the ASM medium protocol advocates filtering which results in a greater deal of the components being trapped within a filtration device, as these components do not dissolve into solution. This results in a medium which clearly contains an altered concentration of components as shown in protocol demonstrated online (Diraviam Dinesh, 2010). The second medium AMDM requires the use of antibiotics in order to sterilize the solution which therefore makes it a poorer substitute than routinely used media used in a lab such as LB. The use of antibiotics would therefore not lend its use as a medium for multispecies biofilm assays in the study of the polymicrobial nature if the CF lung.

Finally, biofilm growth can be analyzed using culture techniques, crystal violet assessment (O'Toole and Kolter, 1998), molecular techniques and microscopic analysis to give the number of viable cells, surface coverage and biofilm thickness. Software programs such as Comstat (Heydorn *et al.*, 2000) and PHLIP-ML (Merod *et al.*, 2007) have been developed, both can analyze CLSM data to give information on the percentage of cells containing a stain, biofilm biomass and biofilm thickness among other biofilm parameters. Visualization of the 3D structure of a biofilm can be obtained through the use of the associated CLSM package or through commercial software packages such as IMARIS (Bitplane).

Collectively all these current approaches in section 1.2 which are available for the analysis of both planktonic and sessile microorganisms, allow researchers to closely mirror and assess *in vivo* conditions to develop strategies to circumvent the negative effects of infection in CF patients.

1.3 Biofilm Development

Biofilms are sessile communities of microbial cells which can colonize surfaces and liquid to air interfaces which are encased in a matrix consisting of polysaccharides, lipids, proteins and extracellular DNA (Ellwood *et al.*, 1982; Costerton *et al.*, 1987; Flemming *et al.*, 2007). Within the medical arena, biofilms are increasingly being implicated in various medical conditions from CF to chronic wounds and infections resulting from indwelling medical devices, which can cause chronic infections and lead to poor therapeutic outcomes in patients (Donlan, 2001; Bjarnsholt *et al.*, 2008; Hall-Stoodley and Stoodley, 2009). The biofilm mode of growth enables bacteria to withstand immune attacks as well as anti-microbial agents, with bacterial cells within biofilms possessing up to x1000 more resistance than their planktonic counterparts to these agents (Nickel *et al.*, 1985; Olson *et al.*, 2002).

The accepted biofilm model is defined as the development of a heterogeneous structure with bacterial cells forming aggregates that are encased in exopolymers with water channels or void spaces running throughout (Siebel and Characklis, 1991; Keevil *et al.*, 1993; Wimpenny and Colasanti, 2006; Wilking *et al.*, 2013), refer to Figure 1.9 for a figure outlining biofilm development. These channels can be thought of as analogous to a primitive circulating system by acting as carriers for the removal of metabolic waste products and allowing the flow of nutrients and cell-cell signalling molecule throughout the structure to neighbouring cells. This architectural framework for biofilms is evident in both pure mono-species and multi-species microbial biofilms (Jurcisek and Bakaletz, 2007; Zijnge *et al.*, 2010). Akin to the preserved formation steps in the ordered production of any multi-cellular organism, there are multiple developmental stages in microbial biofilms (Nikolaev and Plakunov, 2007). Both monospecies and multi-species biofilm can be thought of as an ecosystem in which there exist numerous different niches.
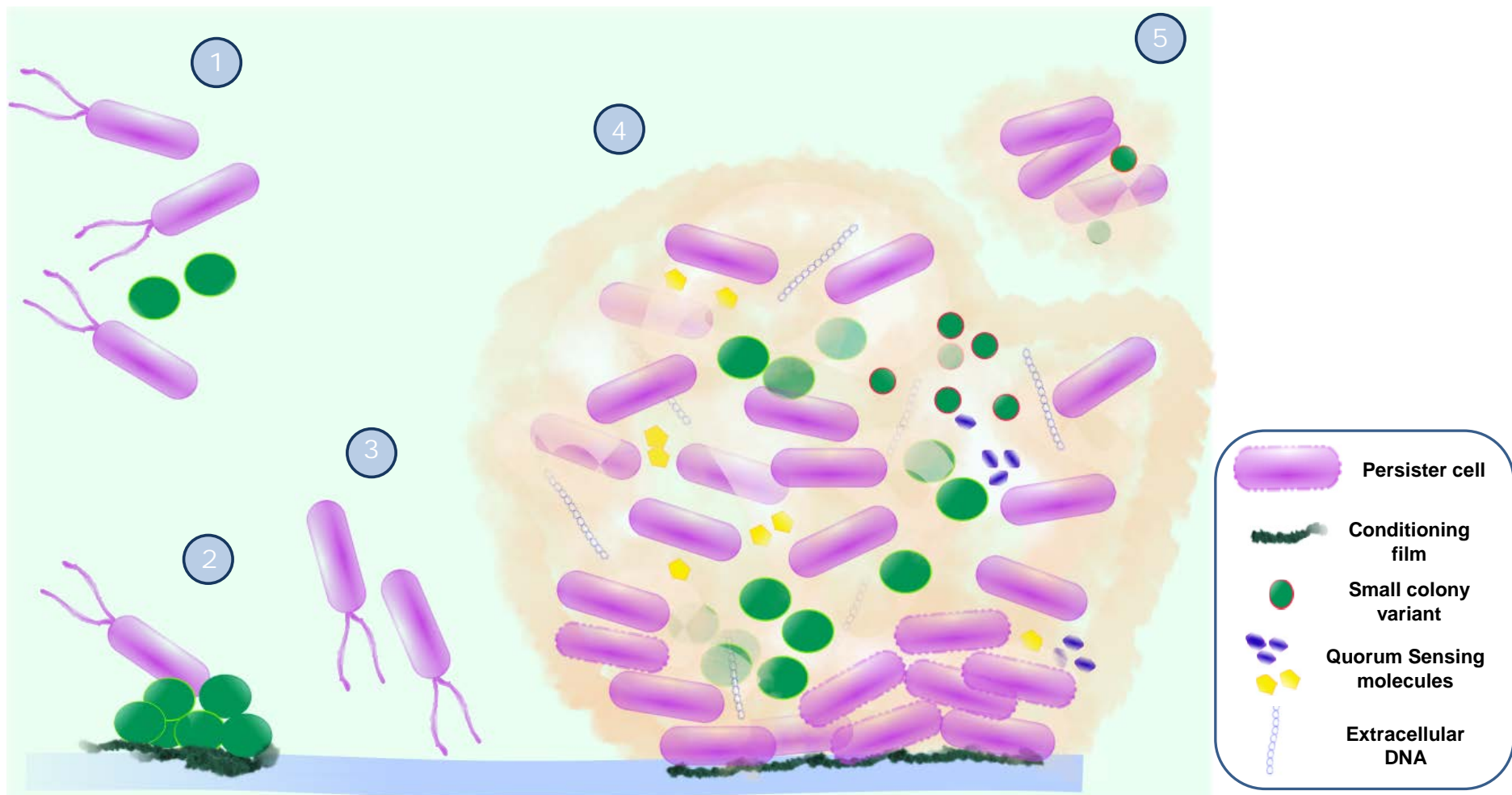
Figure 1.9 Schematic diagram of biofilm development: 1) Planktonic cells, 2) Cell adsorption, 3) Desorption, 4) Mature Biofilm and 5) Dispersal, erosion and sloughing. Illustrated by Caroline M. Duignan.

1.3.1 Initial cell attachment

Bacterial cell attachment to a surface can be due to a combination of both physicochemical forces and cellular driven forces. Physicochemical forces consist of Brownian motion, van der Waals forces, surface charge, hydrophobicity and environmental conditions (Hermansson, 1999; Palmer *et al.*, 2007). Cellular driven forces are dependent on the external components of the bacterial cell wall and its structures such as capsules (Adamou *et al.*, 1998), pili and fimbriae collectively referred to as adhesins (Kline *et al.*, 2009). The properties of a surface are key in the initial stage of attachment such as the surface roughness (Mitik-Dineva *et al.*, 2009; Truong *et al.*, 2010), surface conditioning (Gómez-Suárez *et al.*, 2001), surface charge and the surface micro-topography (Edwards and Rutenberg, 2001).

The properties of the outermost layer of a surface will determine the interactions which can aid or prevent attachment of bacterial cells. The accumulation of substances on a surface provide a conditioning layer to buffer the surface charge and surface free energy which would otherwise cause repulsion of an approaching microbe (Dickson and Koohmaraie, 1989). A conditioning film on a surface can also act as a substrate source for a microbe that adheres (Palmer *et al.*, 2001; Ma *et al.*, 2006). The conditioning film on a surface can be attributed to a macromolecular enriched environment due to the remnants of other organisms or as a result of a currently active organism. A relevant new study has revealed that the driving force behind a single microbial cell opting to initiate adhesion resembles that of a classic chemotactic response. This was based on the analysis that a single cell of *P. aeruginosa* opting for adhesion to other cells or to sites was driven by the presence of a polymer previously secreted by an explorer cell (Zhao *et al.*, 2013). This group showed a direct relationship between the depositing of the exopolysaccharide Psl from *P. aeruginosa* cells with an increased number of visits, length of stay and bacterial cell attachment at these sites on the surface of a flow cell versus sites lacking Psl. The authors showed that *P. aeruginosa* cells used type IV pili to explore the surface, leaving a trail of Psl which in turn acts as an attractant for others cells thereby resulting in a larger portion of the surface being unexplored. This revealed a non-random behaviour pattern

intertwined with Psl deposition; the mutant Δ*pilA* showed a marked decrease in the level of surface exploration (Zhao *et al.*, 2013).

Various studies focused on food industry practices have linked surface conditioning with enhanced bacterial adhesion (Speers and Gilmour, 1985; Whitehead and Verran, 2006). This has been aptly demonstrated in a study which uncovered more bacterial cells left adhered to a surface conditioned with bovine serum albumin (BSA) versus an unconditioned surface post cleaning (Whitehead and Verran, 2006). Others studies have observed a higher number of cells of the most commonly known milk microorganisms attached to both stainless steel and rubber surfaces in the presence of lactose and whey proteins (Speers and Gilmour, 1985). However it is important to note that although there are studies linking a positive correlation between surface conditioning and bacterial cell attachment others offer conflicting results (Cunliffe *et al.*, 1999; van der Mei *et al.*, 1991). In the former study they show a reduced number of *Escherichia coli* and *Listeria monocytogenes* cells attaching to surfaces pre-treated with BSA and in the latter study a reduction in the number of vegetative cells and spores of thermophilic bacilli attached to stainless steel surfaces treated with skim milk. Nevertheless all these studies demonstrate that a multitude of intricate factors interplay between the bacterial cell, surface and the surrounding environment which all act on a temporal scale.

Planktonic bacteria can come into contact with a surface through (1) Brownian motion, (2) sedimentation which is dependent on the liquid content, (3) convective transport which is controlled by the flagellar activity of the microbe and flow of the system (Van Loosdrecht *et al.*, 1990). The initial attachment is thought to be based more on electrostatic attraction than on physical structures such as fimbriae. This attraction is based on stepwise process of adjective transport, reversible adsorption, desorption before finally irreversible adsorption occurs.

The level of hydrophobicity of a surface can have a direct effect on the number of cells which attach, with more hydrophobic surfaces supporting a greater number of cell attachments (Fletcher and Loeb, 1979; Bendinger *et al.*, 1993). The hydrophobicity of microbial cell surface structures can be measured using contact angle measurements (Van der Mei *et al.*, 1998), hydrophobic interaction chromatography (Smyth *et al.*, 1978) or by the microbial adherence to hydrocarbons test more commonly known as the MATH test (Rosenberg *et al.*, 1980; van der Mei *et al.*, 1991). Measuring the hydrophobicity of the cell surface and understanding the surface chemistries to which the cells will come in contact with allows for an understanding of the initial factors which may promote cell attachment or elucidate ways the cell overcomes these hurdles. Water contact angle measurements can vary widely between different strains of the same species. Experiments outlining hydrophobicity measurements of bacterial cells obtained through water contact angle measurements in order to observe the attachment of *Staphylococcus epidermis* to di-acteate and four different polymeric materials used in indwelling devices has been investigated (Oliveira *et al.*, 2001; Fonseca *et al.*, 2001). Three strains RP62A and M187 polysaccharide/adhesin (+) capsules and an isogenic mutant M187-Sn-3-mutant of M187 with a polysaccharide/adhesion (-) capsule were used. The mutant strain was less capable of attachment than of any of the other strains used and also exhibited the least hydrophobicity compared to all the other strains. This study showed that there was a direct correlation between the rate of cell adhesion and the hydrophobicity of the cell, which is increased when cellular structures such as fibrils and fimbriae are present.

Attachment to abiotic and biotic surfaces is enhanced by extracellular polymeric substances which can offer a wider variety of molecules with differing physio-chemical properties such as hydrophobic and hydrophilic regions. This has been investigated by a group who tested the difference between high, medium and low gellan secreting mutants of *Sphingomonas paucimobilis* in order to establish the effect on the microbe's ability to attach to a glass slide when grown in conjunction with extracts of exploymers (Azeredo and Oliveira, 2000). Cell adhesion was lower without the addition of exploymer in allowing for better attachment of microbes to a surface by also acting as a conditioning layer.

1.3.2 Matrix – function and composition

Once irreversible cell attachment has taken place and the cells begin to multiply, extracellular polymeric substances (EPS) are secreted continually. EPS consists of a collection of biopolymers - polysaccharides, lipids, glycoproteins, glycolipids, extracellular DNA and lipoproteins which altogether make up the matrix in which the cells are encased. EPS production is not solely confined to prokaryotes, both archaeal and eukaryotic microorganisms secrete these biopolymers which form what is referred to as the matrix, this acts as the scaffold for biofilm cells. These biopolymers were first discovered to be involved in microbes adhering to surfaces when "footprints" were left behind after the removal of bacterial cells from surfaces via shear force in studies (Marshall, Stout and Mitchell, 1971; Paul and Jeffrey, 1985; Neu and Marshall, 1991). The formation of the matrix aids in the arrangement of the bacterial species within the biofilm structure which allows the progression from the formation of a monolayer to a mature biofilm structure (Costerton *et al.*, 1994). Extracellular DNA (eDNA) was shown to be found in a high concentration within the EPS of *P. aeruginosa* biofilms (Steinberger and Holden, 2005). eDNA was thought to be in the matrix as a result of bacterial cell lysis which occurs as part of the natural developmental process within biofilms (Webb *et al.*, 2003). Interestingly it was discovered that membrane vesicles which are actively excreted from *P. aeruginosa* contained DNA which is incorporated into the matrix of a biofilm (Kadurugamuwa and Beveridge, 1995; Schooling and Beveridge, 2006). eDNA was first shown as a structural component of the matrix using an aquatic bacterium strain F8 (Böckelmann *et al.*, 2006). This group showed that it was the eDNA that formed a meshwork in which the bacterial cells were supported on the threads of eDNA. This group also highlighted that although eDNA had similarities to genomic DNA through the use of random amplification of polymorphic DNA (RAPD) banding profiles there also were clear differences between them. Based on this work they proposed that the eDNA may differ from the genomic DNA by way of CpG methylation because the restriction enzyme NotI is sensitive to CpG methylation which was prevented from cleaving the DNA within the assay. The differences between genomic DNA and eDNA may occur through modifications by the addition of proteins or in structuring of the DNA molecule i.e. linear DNA (Steinberger and Holden, 2005).

Cells within a biofilm are markedly resilient towards antimicrobial attack and phagocytosis within a host. This is due in part to the protective barrier the matrix components pose by reducing diffusion of molecules and the ability of these components to interact with the antimicrobial agents thereby rendering them ineffective. The mucoid phenotype exhibited by *P. aeruginosa* isolates from the CF lung is typically associated with a decline in the patient's condition. This mucoidy phenotype is a result of excessive amounts of alginate production which has been shown to prevent phagocytosis by polymorphonuclear leukocyte (PMNs) and prevent the diffusion of aminoglycosides (Bayer *et al.*, 1991). Another important exoproduct which interferes directly with PMNs are the glycolipid biosurfactants called rhamnolipids. These glycolipids were first discovered as exoproducts of *P. aeruginosa* by Bergström *et al.* (1946) and Jarvis and Johnson, (1949). A number of both pathogenic and nonpathogenic bacteria have been identified as producers of rhamnolipids, *Burkholderia pseudomallei* (Häussler et al., 1998) and *P. chlororaphis* (Gunther *et al.*, 2005) respectively. Rhamnolipids have been shown to cause necrosis of PMNs on contact, allowing rhamnolipids to essentially act as protective shield against phagocytosis thereby rendering the most direct clearance mechanism of the innate immunity ineffective (Watt *et al.*, 2005; Jensen *et al.*, 2007).

Matrix structure and composition can be influenced by environmental factors such as flow conditions, concentration of nutrients and surface structures (Purevdorj and Stoodley, 2003). A wide range of techniques have been applied to uncover both the chemical and physical structure of biofilms. The organization of microcolonies into pillar-like/mushroom structures separated by fluid channels covered by EPS (Davey and O'Toole, 2000) was uncovered by the use of pH and dissolved oxygen microsensors, fluorescent labelled antibodies and confocal microscopy with GFP (Sutherland, 2001). Additionally, the use of methods such as immunofluorescence, specifically immunogold labelling and differential interference contrast microscopy were employed to detect the presence of *Legionella pneumophilia* in biofilms and the biofilm structures present on pipes within a water system have been nicely demonstrated by Rogers and Keevil, 1992.

In experiments carried out using *P. aeruginosa* PA01 fluid channel formation was shown to be due to the action of secreted rhamnolipids, which are biosurfactants composed of a glycolipid with one to two rhamnose molecules (Davey *et al.*, 2003; Espinosa-Urgel, 2003). These studies revealed the spatial heterogeneity which exists in these multicellular communities; both chemical and gaseous gradients are evident which can affect the metabolic activity of the cells which allows for creation of niches at the micrometer scale.

Additionally, though it is important to be aware that the classic structure of the mushroom shape which is often used to describe biofilm structure, rarely holds true for both environmental and clinical biofilms. Biofilm structures typically consist of a more fluid structure which can contain "fronds" and "streamers" amongst the structure, along with water channels running through the biofilm mass (Keevil, 2001; Simões *et al.*, 2006).

1.3.3 Cell-cell interactions: physical (cell proximity) and Quorum sensing

1.3.3.1 Physical

Two important types of cell-cell interaction within the biofilm are (1) co-aggregation and (2) co-adhesion. Co-aggregation involves the adhesion between unrelated species which is well characterized for oral bacteria between *Streptococcus gordonii* and *Actinomyces naeslundii* (Egland and Greenberg, 2001). Co- adhesion involves one cell attaching to another via adhesion and receptors on the cell surface cells. Antigen 43 is an autotransporter protein which is produced by *E. coli* and is a self-recognizing adhesin (Hasman *et al.*, 1999). Antigen 43 dramatically improved biofilm formation in *E. coli* and *P. fluorescens* (Kjærgaard *et al.*, 2000). Secondary colonizers are also important in the biofilm structure as they are attracted to the matrix and they can carry out important roles such as the removal of waste products from the primary colonizers therefore both commensal and mutualistic interactions can operate in a biofilm.

1.3.3.2 Quorum sensing

Quorum sensing (QS) is the term given to the cell-cell signalling which is defined as cell-density dependent bacterial intercellular signalling that enables bacteria to direct the expression of certain genes to coordinate the group behaviour (Purevdorj-Gage and Stoodley, 2004). Gram-negative and Gram-positive bacteria are both capable of QS, however their mechanisms differ. Gram-negative bacteria use acylated homoserine lactones (AHLS) (Fuqua *et al.*, 2001; Schuster *et al.*, 2013) and Gram-positive use oligo-peptides (Kleerebezem *et al.*, 1997; Rutherford and Bassler, 2012). Focusing on *P. aeruginosa* as an example for QS due to it being the most predominant microorganism in the CF lung; studies have shown that the LuxIR- type QS systems, with the signal synthases LasR-LasI and RhlR-RhlI, which interact with quinolone signal and a host of other regulators and sigma factors (Latifi *et al.*, 1995; Miller and Bassler, 2001; Girard and Bloemberg, 2008). The LasI protein produces N-(3-oxododecanoyl)-L-homoserine lactone (3OC12- HSL) which is responsible for the activation of a transcriptional regulator of the RhlR-RhlI system, designated LasR, when the concentration of LasI reaches a threshold (Pesci and Iglewski, 1997; Diggle *et al.*, 2006). The *rhlI* proteins produce N-buytirly-L-homoserine lactone signals that causes RhlR to switch on the *rpoS* and the stationary phase σ factor (Pesci and Iglewski, 1997; Diggle *et al.*, 2006). *P. aeruginosa* possesses a third QS system called the PQS system whose signals are alkyl quinolones; this system is positively regulated by LasR protein (Pesci *et al.*, 1999; Heeb *et al.*, 2011).

QS plays a role in biofilm maturation as it is dependent on concentration which would be low during the early stages of biofilm formation but increase with a high cell density. Studies with *Streptococcus gordonii* (Loo *et al.*, 2003) and *Aeromonas hydrophila* (Lynch *et al.*, 2002) proved that QS was involved in the maturation of biofilm structure and not in the early stages of biofilm development. Both the adherence and proliferation of the wild-type (WT) *P. aeruginosa* PA01 biofilm was shown to be considerably higher with a thickness difference of 80% when compared to a *lasI-rhl-I* mutant and a *lasI* mutant. Both mutants formed continuous sheets lacking microcolonies separated by fluid channels, these results highlight the importance of QS in biofilm development (Davies *et al.*, 1998). The biofilm forming capabilities were recovered on the

addition of 3OC12-HSL into the reaction chamber of the *lasI* mutant, a thicker biofilm with clusters of relatively loosely packed cell were observed.

1.3.4 Quorum sensing and the CF lung

Since the late 1980s, a number of authors have begun to investigate the impact QS controlled components referred to as virulence factors how they could impact on the disease progression in the CF lung (Wilson *et al.*, 1988; Lau *et al.*, 2004; Hammond *et al.*, 2015). The virulence factors controlled by the QS system in *P. aeruginosa* and how they affect: 1) the inflammatory response, 2) evade the immune system, 3) other microorganisms and 4) neutralize ROS and antimicrobial agents is summarized in Figure 1.10, adapted from a review by Winstanley and Fothergill, 2009. Although it is recognised that the QS system in *P. aeruginosa* is a highly regulated and complicated signalling cascade triggering the production of virulence factors which can negatively impact on lung functioning. These observations are further perplexed by the higher frequency in the isolation of *LasR* mutants from the sputum of chronically infected CF patients compared to the isolates obtained in the early stages of infection (Hoffman *et al.*, 2009). This opens up a number of questions, as the QS system is linked to the expression of virulence factors yet chronic infections have a higher frequency of QS mutants (Smith *et al.*, 2006): a) why are *LasR* mutants selected for in chronic infections, b) what are these selective pressures, c) do these bacterial cells live within the same biofilm cooperative/fill a niche within the same biofilm, d) is this observed with other microorganisms which are important in CF lung infection?

There is an important gap in the knowledge of how the interaction between established microorganisms impacts the disease progression in the CF lung, as it is now widely recognised to be polymicrobial infection. However, *in vitro* work by Riedel *et al.*, 2001 showed that interspecies QS signal-responses was demonstrated to occur in a dual-species biofilm containing *B. cepacia* and *P. aeruginosa*; whereby *P. aeruginosa* AHLs were sensed by *B. cepacia* under the conditions used. Additionally, an important CF related study by the authors of Bragonzi *et al.*, 2012b showed that the co-existence of biofilms of both *B. cenocepacia* and *P. aeruginosa* grown in a murine model leads to increasing lung damage through triggering the host inflammatory responses more so

than either species' biofilm alone. These studies aptly highlight the need for further investigation into the effect of inter- signalling responses between the co-existing microorganisms within an infection have on each other and the implication of this in the disease context.
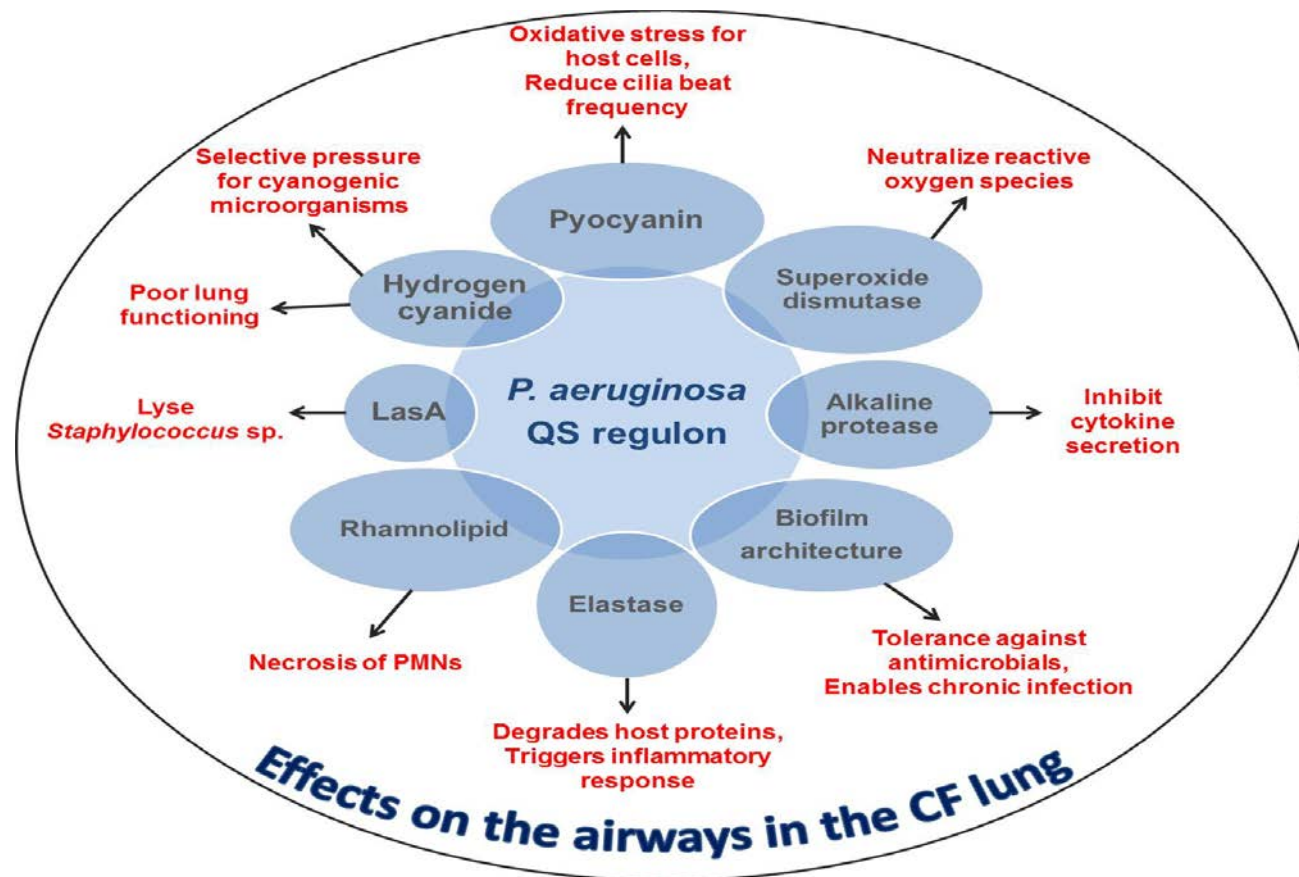
Figure 1.10   Quorum sensing in *P. aeruginosa* and its role in the production of virulence components which have a direct impact on the functioning of the CF lung. Adapted from Winstanley and Fothergill, 2009.

1.3.5 Gene expression in biofilm cells versus planktonic cells

Studies investigating the differences in gene expression between planktonic cells versus biofilm cells are continually shedding light on important differences between these two bacterial modes of growth (Resch *et al.*, 2005; He and Ahn, 2011; Dötsch *et al.*, 2012). Gene expression differs significantly in the planktonic mode versus the biofilm mode. There is an up-regulation of genes producing adhesion structures such as type IV pili and OmpR/Env2 occurring in cells within a biofilm (Espinosa-Urgel, 2003). DNA arrays to uncover the differences at the transcriptional level between the planktonic cells and sessile populations of *P. aeruginosa* (Whiteley *et al.*, 2001). This study revealed a difference of 1% between the two different modes of bacterial growth. This same result was observed when subtractive cDNA analysis was carried out on extracted mRNA from planktonic and biofilm cells of *P. putida* (Sauer and Camper, 2001). The latter study showed that there was 40 differentially expressed mRNA species. PilA, a type IV pili was expressed in the biofilm mode but FliC, a flagellar protein, was not expressed and was shown to be expressed only in the planktonic mode. Phenotypically, this may be a consequence of flagella being no longer required during biofilm growth (Espinosa-Urgel, 2003).

Gene expression within a biofilm structure can be driven by environmental signals. For example in *E. coli* the osmotic sensing system OmpR/Env2 results in curli production promoting cell attachment upon sensing osmolarity (Prigent-Combaret *et al.*, 2001). Nutrient concentrations affect *Aeromonas hydrophila* biofilm formation, as mutants formed which are defective in phosphorus uptake and lacking a Mg transporter have been shown to be incapable of matrix formation when (Monds *et al.*, 2001; Merino *et al.*, 2001).

Up-regulation of *ica* genes in *S. aureus*, which are involved in the production of a cell-adhesion polymer called glucosamine occurred in biofilms cells for 16 h compared to planktonic cells. Also clues into why biofilm cells are so resilient were provided by this study, wherein it was found that *S. aureus* cells in a biofilm show up-regulation of shock proteins, antioxidants and cell-envelope associated proteins when compared against planktonic cells (Resch *et al.*, 2005). Studies are revealing that within the biofilm phase of growth virulence systems like the Type III secretion system (T3SS) are down-regulated which

would point towards collective behaviour acting to prevent a host immune response (Dötsch *et al.*, 2012). Conversely metabolic processes, cell membrane components, proteins involved in the inactivation of reactive oxygen species and pathways to neutralize organic radicals are all upregulated several fold in biofilm cells compared against their planktonic counterparts (Resch *et al.*, 2005; He and Ahn, 2011; Dötsch *et al.*, 2012). Based on these studies biofilm development within a host is primarily focused on persistence instead of mounting an intracellular attack by way of producing toxins. Further understanding on the delicate balancing of the homeostasis within a biofilm could provide avenues to exploit and disrupt its development.

1.3.6 Biofilm dispersal

Biofilm formation is a dynamic process with distinct development stages, including attachment, microcolony formation, maturation and dispersal of the cells back into the planktonic stage. Genomic and proteomic research has shown that specific genes and proteins are expressed at these different stages clearing outlining that biofilm formation is a developmental process. Studies aimed at controlling biofilms have focused mainly on agents targeting the initial stages of biofilm formation to prevent the establishment of a biofilm infection or presence on a surface. Approaches that are capable of disrupting or dispersing an existing biofilm are more likely to be effective in treating robust biofilm infections. The environmental cues and signalling mechanisms involved in biofilm dispersal are currently the subject of much research interest but remain to be fully understood. It has long been recognised that factors including low nutrient concentration and a high density of microbial cells can cause the detachment of cells from both *P. aeruginosa* biofilms and *P. putida* biofilms as outlined by Sauer *et al.*, 2004; Gjermansen *et al.*, 2010, respectively.

One study revealed the use of an enzyme by the bacterium *S. mutans* to release bacterial cells from their encased community into the surrounding planktonic phase (Lee *et al.*, 1996). Conversely, high nutrient conditions has been shown to cause biofilm dispersal in *Acinetobacter* sp. (James *et al.*, 1995).

The biofilm detachment process whereby EPS reduction occurs and detachment of *P. fluorescens* cells occurs has been outlined (Allison *et al.*, 1998). Detachment may serve to allow the microbe to search for an environment which has more nutrients than the one in which it is situated in and has already exhausted (O'Toole *et al.*, 2000).

Investigations into the mechanisms responsible for virulence within *Xanthomonas campestris* pathovar *campestris* lead to the discovery of the diffusible signal factor (DSF) (Barber *et al.*, 1997). This group found that this molecule was linked to the production of extracellular enzyme proteases, endoglucanase, polygalacturonate lyase and polysaccharides and virulence factors. Later Dow *et al.* (2003) described this molecule to be an α, β unsaturated fatty acid cis-11-methyl-2-dodecenoic acid that is capable of initiating dispersal. This group showed that DSF was responsible for dispersal as rpfF mutant strains dispersed on the addition of DSF to the media however the other mutants which were deficient in the signalling components of the RpFfG/C system did not disperse. Another short chain fatty acid cis-2-decenoic acid, similar to the DSF produced by *X. campestris* pathovar *campestris*, was found to be produced and secreted by *P. aeruginosa*. This fatty acid was shown to disperse biofilms formed by a selected few species as representatives for both prokaryotic and eukaryotic microorganisms.

Dispersal of *P. aeruginosa* and a range of other biofilm forming bacteria have been linked to the endogenous production of nitric oxide (NO) (Barraud *et al.*, 2006; Barraud *et al.*, 2009). NO production and dispersal are regulated by the nitrite reductase NirS and mutants of the *nirS* gene are unable to generate NO and fail to undergo cell death and dispersal. In contrast mutants that cannot express the genes that encode nitric oxide reductase (an enzyme that removes NO) undergo exaggerated dispersal. It has further been shown that perception of the NO signal leads to changes in the intracellular concentration of the ubiquitous second messenger nucleotide cyclic-di-GMP (c-di-GMP) (Barraud *et al.*, 2009). NO has now been implicated in biofilm dispersal in a range of bacteria, indicating that this pathway may be highly conserved and impacts on the c-di-GMP signalling pathway. These studies clearly demonstrate that

modulation of NO levels with the biofilm community is a powerful tool for controlling the biofilm life-cycle and that adding small molecules which generate NO generically termed (NO) donors, could be used to induce biofilm bacteria to disperse into free-living planktonic cells. Refer to sections 1.4.3 and 1.4.4 for a review of the current work outlining the role of NO signalling in prokaryotes.

1.3.7 The resilient nature of microorganisms: Biofilm tolerance and Bacterial resistance

Microorganisms have numerous mechanisms of defending themselves against physical and chemical attack. The most widely known mechanism is the ability to produce antimicrobial compounds with the purpose of offering the competitive edge against other microorganisms within the same niche.

1.3.7.1 Bacterial resistance

Antibiotics can be loosely split into two groups based on their action: 1) Bactericidal – if > 99.9% of the cells are killed versus 2) Bacteriostatic – which are responsible for killing of cells anywhere from 90-99% thereby causing cellular stasis in a time kill-curve assay (Clinical and Laboratory Standards Institute, 2006). This loose definition is due to the fact that the bactericidal antibiotics never result in the complete killing of all bacterial cells and bacteriostatic antibiotics do kill cells but do not result in a killing of > 99.9% and act more to inhibit cell proliferation. The discovery of the antibiotic penicillin produced by certain *Penicillium* sp. by Fleming in 1928 led to the antibiotic era (Fleming, 1929). Although the discovery of antibiotics has undoubtedly positively shaped the practice of medicine and saved countless lives, they have been exploited. Three of the main avenues which led us down this path have been 1) antibiotics being too readily prescribed for viral infections, 2) use of multiple antibiotics, trial and error approach and 3) inadequate antimicrobial doses. Collectively, these errors have led us to the point where bacteria have developed intrinsic genetic resistance to antibiotics which has worrying implications in the healthcare setting (Nathan and Cars, 2014).

This intrinsic genetic resistance can occur through genetic mutation selected

for, due to the selective pressure exerted on the bacteria (Kohanski *et al.*, 2010) or they acquire resistance via horizontal gene transfer (Redfield, 1993; Barlow, 2009; Hsu *et al.*, 2014).

1.3.7.2 Bacterial tolerance

In brief, bacterial tolerance is the ability of a group of cells to withstand antimicrobial challenge despite lacking the necessary genetic resistance to confer this ability to survive the antimicrobial agent. Herein lies the issue, biofilms were first noted to offer this tolerance by being capable of withstanding a 1000 fold great concentration of tobramycin compared to their planktonic counterparts (Nickel *et al.*, 1985). This observation has led to numerous studies which have been reviewed to explore the properties of a biofilm which influence this protection (Hall-Stoodley and Stoodley, 2009; Sadekuzzaman *et al.*, 2015). Bacterial tolerance in biofilms can be attributed to four main properties: 1) the extracellular matrix, 2) spatial heterogeneity - microniches with gaseous and chemical gradients, 3) persister cells. The extracellular matrix is composed of a range of polymers, refer to section 1.3.2, the ability of eDNA to bind to vancomycin in *S. epidermidis* biofilms thereby causing the antimicrobial activity to be redundant has been outlined (Doroshenko *et al.*, 2014). Similar observations for have been made for the eDNA in *P. aeruginosa* biofilms binding to tobramycin (Mulcahy *et al.*, 2008). Spatial heterogeneity can confer bacterial tolerance due to creation of micro-niches within the biofilm which will differ in oxygen levels (Williamson *et al.*, 2012), nutrient levels (Proia *et al.*, 2012), pH levels and metabolite waste products which in turn have a direct effect on the bacteria's metabolic activity (Kindaichi *et al.*, 2007; Dige *et al.*, 2016). Additionally, antibiotics which are active against metabolically active cells will be ineffective against cells within microniches which have triggered a slowdown in metabolic activity (Walters *et al.*, 2003).

Lastly but equally important, the existence of bacterial cells termed persister cells, truly demonstrate the resilient nature of microorganisms. The term persister cells was first described by Bigger, 1944, who keenly observed that despite treating *S. aureus* with penicillin there was always a small fraction of bacterial cells which survived and were capable of replicating after a period of

time. This phenomenon has since been observed in numerous microorganisms (Lewis, 2010; Jermy, 2013). Essentially, persister cells are bacterial cells within a biofilm which have entered a dormant state during repeated antimicrobial challenge, which thereby further complicate the issue of bacterial tolerance (Lewis, 2010). Persister cells are phenotypic variants of the wild type strain which harbour the same level of antimicrobial tolerance as the originator cell and although dormant they can revert once the antimicrobial challenge has been removed (Lewis, 2010). After these cells have begun to replicate they can re-establish a biofilm and once again this biofilm will contain a small fraction of persister cells, and the cycle continues (Keren *et al.*, 2004). Currently, there are two possible mechanisms proposed to be responsible for the formation of persister cells, 1) toxin/antitoxin modules (Keren *et al.*, 2004) and 2) SOS response (Dörr *et al.*, 2009) but further work is required to understood this phenomenon. Specifically, the importance of persister cells in CF has been investigated for *P. aeruginosa* and remarkably a greater number of persister cells were found later into infection with a phenotype termed high-persister cells/*hip* mutants which have a higher tolerance to antimicrobials compared to their originator strain (Mulcahy *et al.*, 2010).

Collectively, all of the combined traits discussed above in section 1.3 outlines the recalcitrant nature of biofilms and highlights the need for strategies to combat and structurally dismantle these tightly packed and protected communities. The following sections 1.4.3 to 1.4.4 will explore the possible use of nitric oxide as a biofilm dispersion agent, which can lead to dismantling of the biofilm structure and thereby cause the bacterial cells to succumb to antimicrobial attack.

1.4 Nitric Oxide

1.4.1 Overview and Chemistry of the molecule

Nitric oxide (NO) was first discovered by Joseph Priestley in 1772. The production of NO as an intermediate in the reduction of NO_3^- by *Pseudomonas perfectomarinus* during denitrification was the first biological reference to its production (Barbaree and Payne, 1967). The first highlighted application of NO in eukaryotes was its use as a muscle relaxant in an experiment using contracted bovine coronary artery strips (Gruetter *et al.*, 1978). However it was not until 1980s that Furchgott and Ignarro independently presented evidence that the endothelium derived relaxing factor produced by endothelial cells was in fact NO (Furchgott and Zawadzki, 1980; Ignarro *et al.*, 1987). NO was named "Molecule of the Year" in 1992 *Science* (Koshland, 1992). In 1998 Robert Furchgott, Louis Ignarro and Ferid Murad were awarded the Nobel Prize in Physiology and Medicine for their contribution to uncovering the role of NO as a signalling molecule.

NO is a gaseous hydrophobic molecule and is a diatomic free radical which can interact with oxygen. The products formed are dependent on whether the reaction occurs under the gaseous or aqueous phase. Within the gaseous phase nitric oxide and oxygen form nitrogen dioxide which is in a constant equilibrium between its dimeric form dinitrogen tetroxide under room temperature conditions. Nitric oxide and oxygen react under aqueous conditions to produce nitrite (NO^-) and protons. NO half-life can be anywhere from seconds to minutes, this range is due to the dependence on the concentration of oxygen in the aqueous state and the presence of hemoglobin (Beckman and Koppenol, 1996; Eich *et al.*, 1996; Liu *et al.*, 1998; Rassaf *et al.*, 2002). NO and NO2 chemical production can occur after the decomposition of nitrous acid (HNO2) under acidic conditions when NO2 reacts with the readily available protons (Park and Lee, 1988).

Globally, inhaled NO is used as a therapeutic treatment to improve intrapulmonary air flow and the dilation of the pulmonary vasculature system in the treatment of pulmonary hypertension in newborns (Ichinose *et al.*, 2004; Bloch *et al.*, 2007). Although the use of NO as a therapeutic agent has focused on the possible benefits for the pulmonary system (Bloch *et al.*, 2007), a

number of studies have been investigating the use of inhaled NO for treating ischemia-reperfusion injury (Hataishi *et al.*, 2006; Fox-Robichaud *et al.*, 1998).

1.4.2 Nitric oxide signalling in eukaryotes

Nitric oxide acts as a biological signalling molecule in eukaryotic systems and has been implicated in the neural, cardiovascular and immune systems which all undergo reactions in aqueous phase. NO is manufactured by cells using the enzyme NO synthase (NOS) to catalyze the conversion of L-arginine along with O_2 and NADPH to L-citrulline and NO, refer to Figure 1.11 for a schematic representation of this reaction.
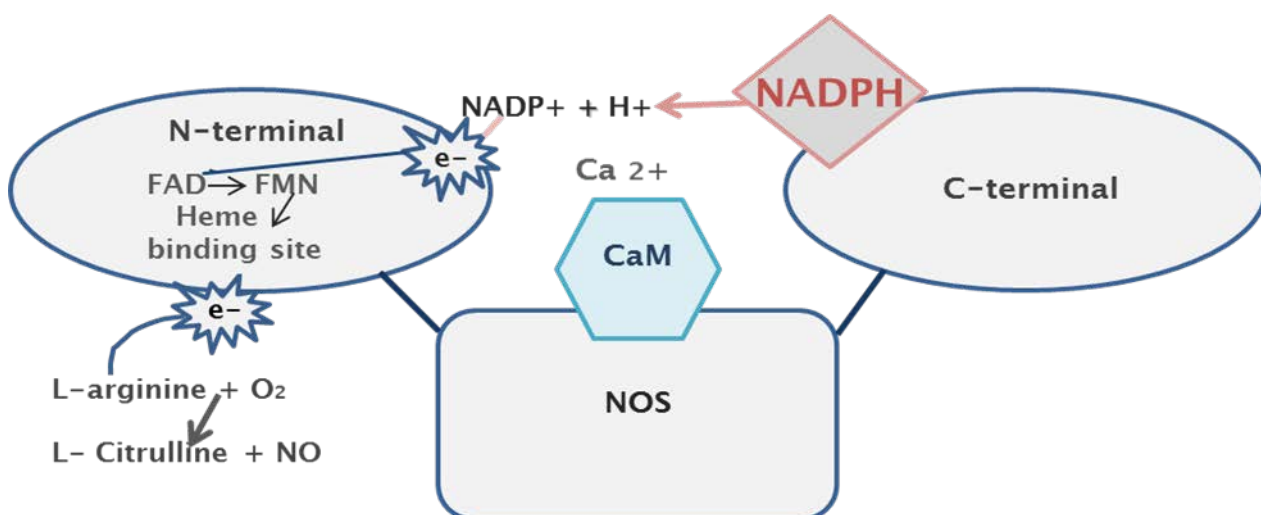
Figure 1.11 Representation of NOS activity in the reduction of L-arginine to L-citrulline and NO. Illustrated by Caroline M. Duignan.

Three isoforms of NOS synthase exist in mammals, neuronal NOS (nNOS), inducible NOS (iNOS or NOS II) and endothelia NOS (eNOS or NOS III) (Alderton *et al.*, 2001; Förstermann and Sessa, 2012). Briefly nNOS is produced in neurons within the central (CNS) and peripheral nervous (PNS) system for the control of blood pressure and synaptic plasticity through the CNS and vasodilation within the PNS (Förstermann and Sessa, 2012). Within the vasculature system eNOS is primarily produced by endothelial cells for the control of vasodilation and in the maintenance of unobstructed blood flow throughout the blood vessel networks (Förstermann et al., 1994). Lastly

iNOS is produced by cells in the innate immune system as part of a non-specific defense mechanism (Förstermann et al., 1994). Cells such as macrophages, PMNs and hepatocytes have been shown to produce iNOS (Facchetti et al., 1999; Förstermann and Sessa, 2012; Mannick et al., 1996). The detection of unrecognized structures such as the LPS of Gram-negative bacteria by the Toll-like receptors of the innate immune system result in a signalling cascade causing the production of iNOS, this immune response has been linked with septic shock and in the initiation of inflammation (Förstermann and Sessa, 2012; Lowenstein and Padalko, 2004).

Alternatively NO can be produced from nitrite under acidic and hypoxic conditions to form NO as oxygen is required for the conversion of L- arginine via the enzymatic reaction of NOS synthase. The oxidation of NO produced from NOS synthase activity results in the production of nitrite which can also be produced through bacteria reducing nitrate which can occur within the oral cavity. NO signalling is a result of protein modifications within the metal segments via S-nitrosylation of cysteine thiols and iron-nitrosylation (Stamler *et al.*, 2001). NO signalling in mammalian systems using the human cardiovascular system as an example involves NO binding to the heme group of soluble guanylate cyclase (sGC) in turn converting guanosine 5´ triphosphate (GTP) to cyclic guanosine 3´, 5´ monophosphate (cGMP) which results in muscle relaxation. The end product of the last reaction, cGMP functions as a second messenger and is responsible for controlling transmembrane ion channels, the activation of protein kinases and mediating phosphodiesterases (Gomelsky and Galperin, 2013). As NO production has an effect within each system in mammals this molecule also has to be removed quite rapidly to prevent adverse effects. Therefore it is important to note that NO is quickly sequestered by reacting with oxygen radicals, iron or in the thiol centers in specific proteins such as albumin to form S-nitrosothiols (Stamler *et al.*, 1992). NO is one of the smallest signalling molecules within mammals (Förstermann and Sessa, 2012). Additionally NO is also a hydrophobic molecule which makes it an ideal messenger as it can readily diffuse through the lipid membranes in cells. Collectively these aspects including its short half-life make NO an excellent messenger within any biological system.

1.4.3 Nitric oxide signalling in prokaryotes

The first discovery that nitrogen oxides were liberated as a result of fermenting plant material along with the isolation of two bacterial strains referred to as denitrifying bacteria was uncovered by Gayon and Dupetit, (1886). These authors were the first to describe the process of denitrification carried out by a bacterium. A better understanding of the biochemical pathway lacking the requirement of oxygen was not understood until Kluyver and Donker, (1926) described the use of nitrate as an electron acceptor in place of oxygen for anaerobic bacterial respiration (Woese, 2008). Later, NO was described as an intermediate in the conversion of nitrate in the denitrification process as shown in Figure 1.12 (Miyata *et al.,* 1969).
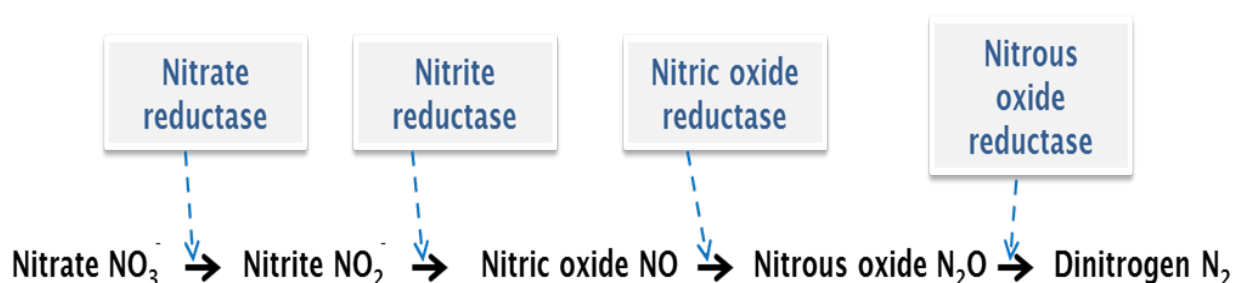
Figure 1.12 Denitrification. The enzyme which catalyzes each conversion is above the reaction step.

Until the early 90s an appreciation for the complex role that NO signalling has in prokaryotes lagged behind the wealth of data amassed on the role of NO signalling within eukaryotic cells (Römling *et al.,* 2013; Spiro, 2007; Wink, 2000). Studies prior to this, were highlighting the role of NO as a cytotoxic agent (Hibbs *et al.,* 1987; Hibbs *et al.,* 1988) or responsible for the activation of signalling cascades within prokaryotes to protect against macrophage attack. A study revealed that NO could activate the stress system SoxR in *E. coli* which protects against external oxidative stresses (Nunoshiba *et al.,* 1993). Although to date the involvement of NO has been identified in a number of prokaryotic signalling pathways, an understanding of the exact mechanisms involved is still unclear (Spiro, 2007; Sudhamsu and Crane, 2015). This thesis will investigate the use of NO as a biofilm dispersing agent and therefore the following review will concentrate on this area of ongoing research.

It is known that NOSs amino acid sequences similar to that found in mammalian cells has been identified in bacteria (Adak *et al.,* 2002) such as those identified in *Bacillus subtilis*, *S. aureus* and *Geobacillus stearothermophilus* (Crane, 2008).

Interestingly work has shown conserved domains exist for soluble guanylyl cyclases between animal and microbial organisms. They are referred to as the HNOB (Heme NO Binding) and HNOBA (Heme NO Binding associated) domains as they serve as receptors for NO and other gaseous molecules resulting in the activation of signalling cascades similar to cGMP signalling observed in mammalian cells (Iyer *at al.,* 2003).

Within the last decade it has emerged that NO is involved in regulating the level of cyclic dimeric GMP (c-di-GMP) within bacteria (Barraud *et al.,* 2009), this molecule will be discussed in 1.4.4. The work which prompted this finding was the due to the observations that the hollowing of mature microcolonies coincided with the detection of reactive oxygen species (ROS) (Webb *et al.,* 2003). Further testing revealed that reactive oxygen and nitrogen species were detected during biofilm dispersal events, with the gaseous free radical NO being highlighted as the causative agent in the dispersal of *P. aeruginosa* biofilms (Barraud *et al.,* 2006; Kirov *et al.,* 2007; Webb *et al.,* 2003). Barraud *et al.* (2006) revealed that dispersal could be triggered with low concentrations of NO administered to firstly *P. aeruginosa* biofilm but later went on to show that similar concentrations of NO were capable of inducing biofilm dispersal in monospecies biofilms formed by *Serratia marcescens*, *Vibrio cholerae*, *E. coli*, *Fusobacterium nucleatum*, *Bacillus licheniformis*, *S. epidermidis*, *Candida albicans* and in a multi-species water system biofilm (Barraud *et al.,* 2009).

These above experiments provide a promising means of controlling biofilm development which would be of great importance in the clinical setting. Especially for CF patients who are chronically infected with *P. aeruginosa*, which forms biofilms within the CF lung (Bjarnsholt *et al.,* 2009) and although patients are constantly treated with antimicrobials, all efforts fail to eradicate this species due to the sheltering of bacterial cells within a biofilm. Based on the above research, NO offers a means to circumvent this issue by its ability to initiate dispersal by influencing c-di-GMP, a key molecule in the

maintenance of a biofilm structure (Galperin, 2004; Jenal, 2004; Römling *et al.*, 2005). The role c-di-GMP plays in the maintenance of a biofilm structure and how NO impacts its role will be discussed in the next section 1.4.4.

1.4.4 The role of cyclic-di-GMP in the biofilm cycle and its link with NO

Cyclic-di-GMP, bis-(3′- 5′)-cyclic dimeric guanosine monophosphate was first discovered in a study in the 1980s, the purpose of which was to identify the processes regulating the formation of cellulose in *Gluconacetobacter xylinum* (Ross *et al.*, 1987). This cyclic dinucleotide second messenger plays a role in an array of key processes such as motility, production of exopolysaccharides, cell progression, adhesins and maintenance of a biofilm within bacteria (Hengge, 2009), as shown in Figure 1.13.

The level of c-di-GMP within a bacterial cell is governed by two enzymes, diguanylate cyclase (DGC) which has a GGDEF domain and phosphodiesterase (PDE) which can contain either an EAL or HD-GYP domain (Römling *et al.*, 2013; Tal *et al.*, 1998). DGC enzyme catalyzes the conversion of two GTP to c-di-GMP while the PDE enzyme catalyzes the hydrolysis of c-di-GMP (Römling *et al.*, 2013) (Figure1.13). The absence of sequences encoding for GGDEF and EAL domains within the Eukarya and Archaea domains reveals that c-di-GMP signalling is solely a bacterial activity (Römling *et al.*, 2005). Although important to note, sequences encoding for the synthesis of GGDEF and EAL domain have not been identified in the following classes of bacteria; Bacteroidetes, Chlamydiales and Fusobacteria. Additionally, the number of sequences encoding for these regulatory domains varies considerably among bacterial species (Römling *et al.*, 2005). Although c-di-GMP is involved in a variety of bacterial cell processes, its role in the modulation of biofilm formation is of great importance to microbiologists. Therefore research focused on teasing apart the c-di-GMP signalling cascade can provide methods of exploiting it, in order to trigger dispersal of a biofilm.
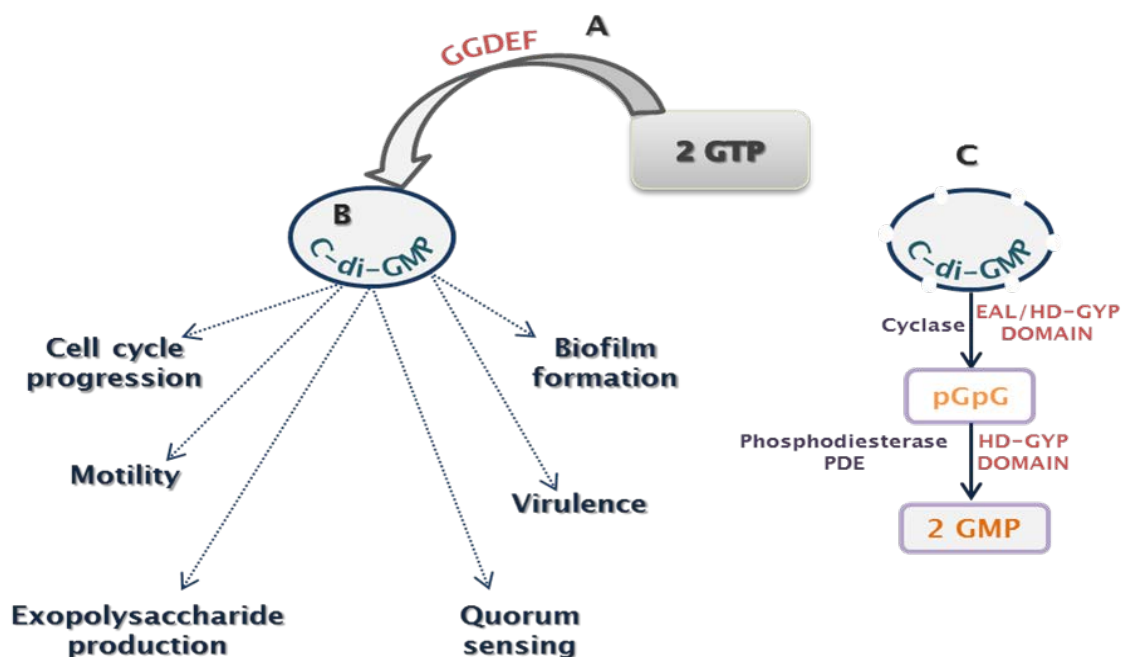
Figure 1.13 Outline of **A**) the synthesis, **B**) the role and **C**) the breakdown of cyclic-di-GMP in bacteria. Adapted from (Ryan, 2013 and Römling *et al.*, 2005).

It is now known that when levels of c-di-GMP are high/maintained gene expression for regions relating to biofilm formation are continually expressed. Whereas when hydrolysis of c-di-GMP occurs ultimately lowering the level of c-di-GMP within bacterial cells, results in converse behavior and an up-regulation of genes related to motility/the planktonic state are identified, (Figure 1.13 and Figure 1.14) (Römling *et al.*, 2013; Ryan, 2013). However, not all bacterial species exhibit regulation of biofilm formation/dispersal via c-di-GMP concentrations such *S. aureus* (Holland *et al.*, 2008).

The discovery that introducing low concentrations of NO into pre-established biofilms of *P. aeruginosa* caused the sessile cells to become planktonic prompted further work (Barraud *et al.*, 2006) . This group later linked the biofilm dispersal locus *bdlA* which contains two PAS domains thereby permitting it to react with NO, with the induction of biofilm dispersal occurring via a decrease in c-di-GMP (Barraud *et al.*, 2009). The up-regulation of *bdlA* in the presence of NO resulted in an increase in phosphodiesterase which lowers c-di-GMP and results in the dispersal of *P. aeruginosa* biofilms (Barraud *et al.*,

2009). The exact mechanism by which BdlA binding with NO regulates an increase in phosphodiesterase is as of yet unknown. This study uncovered a means of inducing dispersal of biofilms via modulation of c-di-GMP concentration by using NO thereby proposing the search for proteins which are capable of binding to NO through an intermediate step to induce the decrease of c-di-GMP resulting in biofilm dispersal.
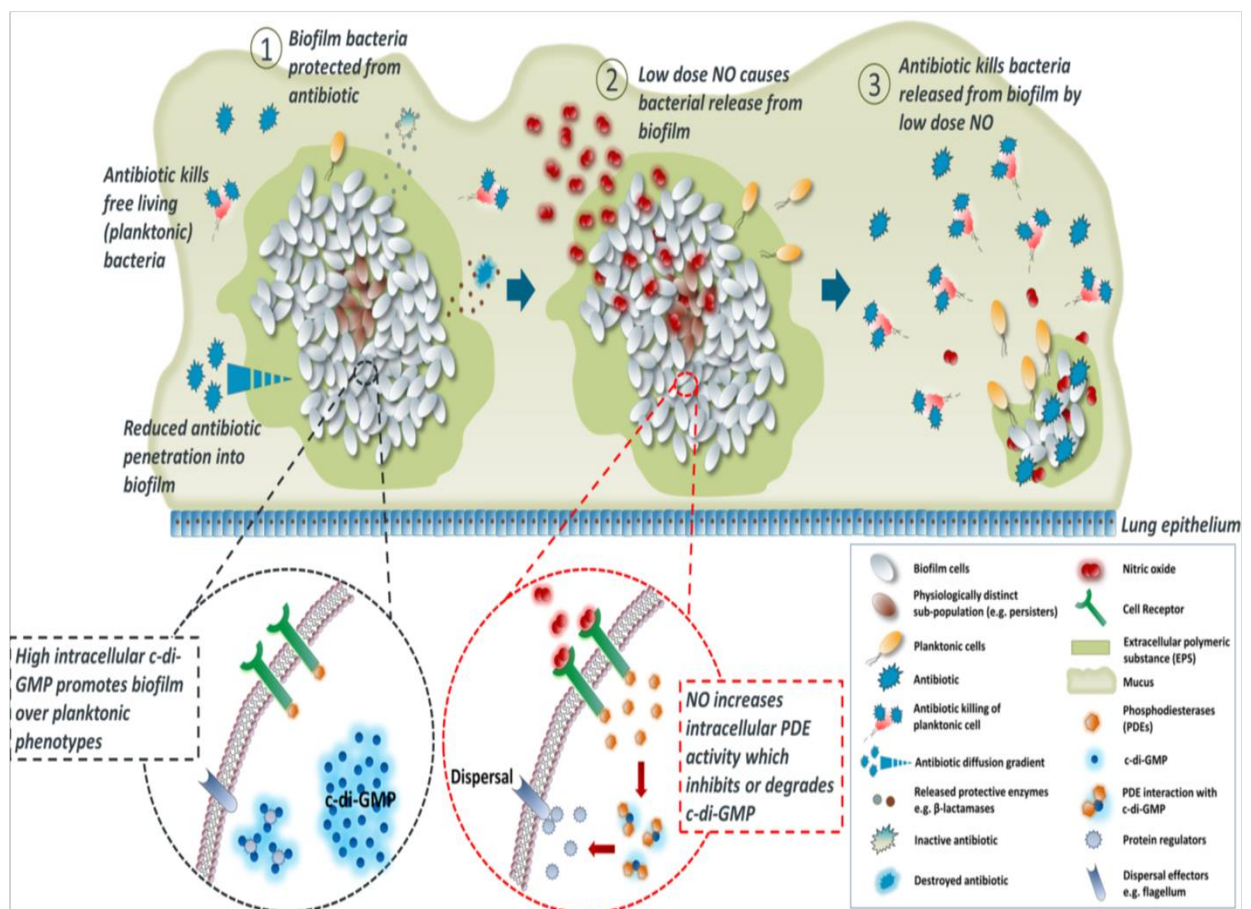
Figure 1.14   A representation of the impact of the concentration levels of c-di-GMP within bacteria cells in biofilm dynamics. Permission for use obtained from Dr Robert P. Howlin, University of Southampton, UK.

Additionally, there are a number of studies which have shown a reduction in biofilm cell viability through the use of nitric oxide releasing nanoparticles (Hetrick *et al.*, 2009), gaseous nitric oxide (Ghaffari *et al.*, 2007), NO probiotic patches (Jones *et al.*, 2010) and NO loaded zeolites (Fox *et al.*, 2010). Moreover, the use of a compound termed DEA NONOate-Cephalosporin Prodrug (DEACP) which consists of cephalsporin-3'-diazeniumdiolate structure which resembles *ß*- lactam but contains a NONOate donor, this structure releases NO on contact with the *ß*- lactamase and has been shown to successfully mediate biofilm dispersal of *P. aeruginosa* biofilms (Barraud *et al.*, 2012).

Work within our research group by Howlin, Cathie, Hall-Stoodley, Cornelius, Duignan *et al.*, 2017) has provided further evidence for the use of NO as a biofilm dispersing agent (Appendix 4). In the aforementioned study, *in vitro* biofilms formed by *P. aeruginosa* isolates from the CF lung were dispersed using the NO donor SNP. This work prompted the research for this thesis, to investigate the use of NO as a biofilm dispersal agent against *in vitro* biofilms formed by some of the other key CF microbiome members.

1.5 Overall Aims and Objectives of The Thesis

The above sections outlined the rich diversity of the CF microbiome and that biofilm formation allows microorganisms to persist within the CF lung. Consequently this leads to persistent chronic infection and deterioration of lung functioning, with respiratory failure the leading cause of approximately 85% of deaths in CF patients according to the Cystic Fibrosis Foundation, 2008.

Previous work has shown that NO can lead to disruption and enhanced antimicrobial susceptibility of *P. aeruginosa* biofilms, further work is needed to understand whether NO can mediate the dispersal of other clinically dominant microorganisms within the CF microbiome. Additionally, a visual representation of the spatial arrangement of this polymicrobial community would aid in the development of more targeted treatments. The aim of the work within this thesis is to investigate these issues, via these four core routes of investigation:

(1)   Isolate and identify the predominant cultivable microorganisms from sputum samples obtained from CF patients recruited in the Adult Cystic Fibrosis Clinic at Southampton General Hospital, United Kingdom.

(2)   Develop mono-species biofilm assays for the CF microorganisms isolated in Chapter 1 to investigate their response to NO treatment.

(3)   Develop a dual-species biofilm assay for two of the most prevalent CF pathogens, *P. aeruginosa* and *S. aureus*. Use quantitative molecular techniques to investigate the response of the dual-species biofilm to NO treatment.

(4)   Investigate the use of CLASI-FISH as a diagnostic tool and its use as a method to study the spatial structuring of microbial species within CF sputum samples.

Chapter 2

Culture Profiling CF Sputum Samples for the Isolation of the Predominant Microorganisms Commonly Identified as Members of the Cystic Fibrosis Microbiome

2.1 Introduction

One of the earliest publications highlighting infection within the respiratory tract in CF was described by Andersen, (1938). Culture based isolation techniques have remained central to the successful identification of the microorganisms from expectorated sputum, oropharyngeal swabbing (Farrell *et al.*, 1997) or bronchoscopy (Lam *et al.*, 1980) samples from CF patients. However due to the properties of the mucus in CF patients it was noted that the bacterial load was not evenly distributed (May, 1953; May *et al.*, 1972), making the quantification of bacteria inaccurate. The methodology for the liquefaction of a sputum sample, subsequent serial dilution and plating onto selective media resolved this issue (Kilbourn *et al.*, 1968). This method not only allowed the quantification of the bacterial species present within the sputum but it also allowed for the separation of the more abundant/faster growing species from those which are slower growing/fastidious microorganisms. Today this methodology is still applied in all studies dealing with expectorated CF sputum samples (Rogers *et al.*, 2004; Cox *et al.*, 2010; Guss *et al.*, 2011).

Based on a vast number of studies the microorganisms most commonly isolated across all CF patients are *P. aeruginosa*, *S. aureus*, *H. influenzae*, *A. xylosoxidans*, *S. maltophilia*, *B. cepacia* complex and *S. pneumoniae* (Bittar *et al.*, 2008; Guss *et al.*, 2011; Lam *et al.*, 1980; Renders *et al.*, 2001; Sibley *et al.*, 2006). The aforementioned microorganisms were selected based on the literature published wherein they highlight the colonisation pattern of these microorganisms over the life span of CF patients (Harris *et al.*, 2007; Sibley *et al.*, 2006; Rajan and Saiman, 2002).

The isolation of pure culture stocks of these most commonly isolated microorganisms from the CF microbiome was required for this PhD study in order to focus on the biofilm structures they form within the CF lung. In doing so this can help shape of our understanding of the polymicrobial community dynamics within the CF lung to enhance our knowledge of how this affects the patient's wellbeing and potentially help in the tailoring of CF treatments.

The aim of this chapter was to isolate the above most commonly identified microorganisms within the CF microbiome. These species would then be used to (1) establish systems for the study of biofilms formed by CF microorganisms in single and mixed species biofilms and (2) investigate if dispersal events could be triggered in the biofilms formed in the presence of nitric oxide.

2.2. Sputum collection and processing methodology

2.2.1 Ethics Statement

The study was approved by NHS Research Ethics Committee 08/H0502/126 in Southampton, U.K. CF patients were recruited in the Adult Cystic Fibrosis Clinic at Southampton General Hospital, United Kingdom. Expectorated sputum samples were collected (January 2011 to July 2011) from teenagers and adults with cystic fibrosis (mean age at informed consent: 28, range: 19-65). A total of 31 sputum samples obtained from 16 different patients were used for the work carried out within this section. All microorganisms isolated from patients were assigned the patient's identification number after consenting i.e. A57 *Burkholderia cepacia* complex isolate was obtained from patient A57.

2.2.2 Isolation and identification of the predominant microorganisms of interest from CF sputum samples

Expectorated sputum samples were collected in a sterile container from in-patients and patients attending routine clinical visits. Each sample was stored in a fridge and processed in the laboratory within five hours of the sample being obtained from a patient. Sputum samples were liquefied using 1:1 volume of mucolyse (Pro-Lab Diagnostics), vortexed to homogenise and placed in an incubator at 37°C for 15 - 30 min with shaking at 200 rpm (Stuart SI500). Once the sputum was liquefied, the sample was vortexed for 1 min. Dilution series were prepared in phosphate-buffered saline (PBS) pH 7.4 (Sigma-Aldrich). The spread-plate method was employed whereby 100 µl aliquots from neat to 10^{-8} were plated onto the agar plates listed in Table 2.1. All agars were prepared by following the manufacturer's guidelines and sterilized by autoclaving at 121°C for 15 min. All plates were incubated in a microaerophilic environment at 37°C with 5% CO_2 - 95% air for 24 – 48 h depending on the growth rate or for up to 5 days, plates were observed daily. Microorganisms were identified based on colony morphology relative to the agar and subcultured onto a fresh agar plate to ensure purity. One pure colony for each isolated microorganism was grown overnight in the appropriate broth refer to Table 2.1, till turbidity reached the range of 0.5 - 1.0 Mc Farland standard. For each strain two cryovials were labelled with the patient number and 1 ml of the overnight cultures was added to the cryovial. To each cryovial 330 µl of 60% (v/v) glycerol (Sigma-Aldrich) was added, the cryovials were vortexed for 1 min and stored at – 80°C.

Table 2.1   Culture profiling of the microbiome of CF sputum samples.

Microorganism	Agar	Supplements added	Media used for isolates growth prior to storage at -80 ˚C
S. aureus *S. maltophilia* *A. xylosoxidans*	Trytone soy agar (TSA) (Fluka, UK)	n/a	Tryptone soy broth (TSB) (Oxoid, UK)
S. pneumoniae *H.* influenzae	Chocolate agar – Blood agar base (CHOC) (Oxoid, UK)	7% (v/v) defibrinated horse blood (Oxoid, UK)	§ Brain Heart Infusion (Oxoid, UK) ‡ sMueller Hinton Broth 2 (Oxoid, UK)
B. cepacia complex	*Burkholderia cepacia* agar (Oxoid, UK)	Polymixin B, gentamicin and ticarcillin (Oxoid, UK)	Luria-Bertani broth (LB) (Oxoid, UK)
S. pneumoniae	Columbia agar plates (Oxoid, UK)	n/a	As above for CHOC
Yeast	Maltose agar (Oxoid, UK)	n/a	YPD
Yeast	Sabouraud Dextrose Agar (SDA) (Oxoid, UK)	n/a	YPD
S. aureus	¥ Baird-Parker agar (Oxoid, UK)	5% (v/v) egg tellurite emulsion (Sigma, UK)	n/a
S. aureus	¥ DNase agar (Oxoid, UK)	n/a	n/a

¥ Used for biochemical tests

§ All isolates except *H. influenzae*

‡ All presumptive *H. influenzae*, media supplemented with 10 μg/ml NAD and 10 μg/ml hemin

2.2.3 Gram staining, biochemical tests and colony morphology

Gram staining for isolates excluding mould isolates was carried out on smears prepared by taking an isolated colony and mixing it with a drop of DNase, RNase free H_2O (Molecular grade water) (Sigma-Aldrich) on a microscope slide. The smear was left to dry and heat fixed. A standard Gram staining protocol was followed (Gerhardt, 1994). *P. aeruginosa* PA01and *S. aureus* ATCC 25923 were used as controls for Gram staining. The Gram stained smears where observed using an Olympus BX51 microscope at a magnification of x1000. The biochemical test known as the catalase test named after the enzyme it detects was carried out on a microscope slide using 3% (v/v) hydrogen peroxide as outlined in a widely used protocol (Mac Faddin, 2000). Coagulase disc (Fluka, U.K.) test was used according to

the manufacturer's instructions for Gram-positive cocci. Presumptive *S. aureus* and *S. maltophilia* isolates were streaked onto a DNase agar plate (Oxoid, U.K.) and incubated overnight as outlined in section 2.2.2. After 24 h the DNase agar plates were flooded with a 0.1% (w/v) toluidine blue (Sigma-Aldrich, U.K.) solution prepared in sterile dH_2O. Presumptive *B. cepacia* complex isolates were identified based on colony morphology. *S. pneumoniae* isolates were presumptively identified based on colony morphology on blood and chocolate agar based on the presence of alpha haemolysis. Yeast and mould isolates were identified by the colony morphology observed on malt agar. All bacterial isolates were catalase tested. Refer to Figure 2.1 for images of the various methods used to identify microorganisms using the type strain as a comparison prior to molecular confirmation.

2.2.4 Type strains

Type strains used for the validation of both the biochemical and molecular work were obtained from the LGC Standards (U.K.). Isolates following the American Type Culture Collection (ATCC) numbering system were acquired for *B. cepacia* complex ATCC 25416, *S. aureus* ATCC 25923, *H. influenzae* ATCC 49766, *S. maltophilia* ATCC 13637, *A. xylosoxidans* ATCC 9220 and *C. albicans* ATCC 10231. An isolate following the National Collection of Type Culture (NCTC) for MRSA NCTC 13143 was generously donated by Dr Sarah Warnes. Clinical isolates of *S. pneumoniae* Serotypes 14 and 22F which were biochemically and molecularly confirmed by the Public Health England Laboratory (SouthEast, U.K.) were generously donated by Dr Nick Churton.

2.3   Molecular identification of isolates

2.3.1 Extraction of genomic DNA from bacteria

Bacterial type strains and CF sputum isolates were removed from -80 °C storage and streaked onto the appropriate agar as outlined in Table 2.1. All plates were incubated for 16-24 h at 37°C with 5% CO_2 to ensure purity prior to DNA extraction. One colony was inoculated into the appropriate medium as outlined in Table 2.1and incubated at 37°C with 5% CO_2 until the exponential phase was reached for DNA extraction. Genomic DNA was isolated from bacterial type strains and CF sputum isolates using the DNeasy Blood & Tissue Kit (Qiagen, Hilden, Germany). The

manufacturer's instructions were followed for extracting DNA from both Gram-positive and Gram-negative bacteria. Extracted DNA concentrations were assessed by measurement of 2 µl sample using the Nanodrop ND-1000 spectrophotometer. DNA concentrations were diluted to within the range of 20 to 100 ng / µl; using the AE kit elution buffer, prior to use in PCR assays.

2.3.2 Extraction of genomic DNA from yeast

The type strain for *C. albicans* ATCC 10231 and the yeast isolates from CF sputum were removed from -80°C storage and streaked on malt agar to inspect culture purity. Plates were incubated as outlined above. A single colony was inoculated into YPD (Sigma-Aldrich) and incubated overnight as above. Genomic DNA extraction was carried out using a protocol outlined by Philippsen *et al.* (1991) with modifications as follows. Five ml of the overnight cultures were transferred to a fresh 15 ml Falcon tube and centrifuged at 4000 rpm for 2 min using the Heraeus Instruments Megafuge 1.0. The supernatant was removed and a 5 ml wash of RNase, DNase free molecular grade water (Sigma-Aldrich) was applied and the Falcon was vortexed for 1min. The Falcon tube was centrifuged as stated above. The supernatant was removed. Five hundred µl of a lysis buffer containing 200 µl of 1M Tris pH 8.0 (Sigma-Aldrich), 200 µl of 0.5 M EDTA (Sigma-Aldrich), 200 µl of 10% (v/v) SDS and 1.4 ml of molecular grade water was applied to the cell pellet and the Falcon tube was vortexed for 1 min to resuspend the pellet. Acid-washed glass beads 425 - 500 µm (Sigma-Aldrich) were added to the Falcon tube to 2 mm below the meniscus. The Falcon tube was vortexed for 30 s, 25 µl of 5M of NaCl was pipetted in and the Falcon tube was vortexed for 30 s. The Falcon tube was centrifuged at 4000 rpm for 2 min using the Heraeus Instruments Megafuge 1.0. The lysed cells in the liquid at the bottom of the Falcon were removed and transferred into a 1.5 ml centrifuge tube. A total volume of 400 µl of phenol (Sigma-Aldrich) was added to the centrifuge tube and the vortexed for 30 s. The centrifuge tube was centrifuged at 10000 g for 2 min using the Thermo Scientific Heraeus Fresco 21 centrifuge. Four hundred microliters of TE-saturated phenol was added to the centrifuge tube and vortexed briefly for ~ 15 s. The centrifuge tube was centrifuged at 10000g for 4 min. The upper phase was transferred to a fresh 1 ml centrifuge tube and 400 µl of phenol:chloroform (4:1) (Sigma-Aldrich) was added. The centrifuge tube was vortexed for 30 s and centrifuged at 10000 g for 4 min as above. The upper phase was transferred to a fresh centrifuge tube and 1 ml of 95% (v/v) ice-cold EtOH was added and the centrifuge tube was

gently inverted 3 times. The centrifuge tube was centrifuged at 10000 g for 6 min as above and the supernatant was poured off. A 1 ml wash of 70% EtOH was pipetted in and the centrifuge tube was gently inverted 3 times. The centrifuge tube was centrifuged at 10,000 g for 8 min and the supernatant was poured off. The DNA pellet was air-dried in a biological safety cabinet. The dry pellet was resuspended in 50 µl of TE buffer (500 µl of 1 M Tris pH 7.5, 100 µl of 0.5 M EDTA pH 8.0, 49.5 ml of RNase, DNase free water). The concentration of the DNA extracts were measured using 2 µl of sample on the Nanodrop ND-1000 spectrophotometer. After observing the 260/280 and 260/230 values using the Nanodrop; the above protocol was repeated commencing from the phenol:chloroform step to remove the remnants of the DNA extraction process with the phenol:chloroform:isoamyl alcohol 25:24:1 (Sigma-Aldrich) used instead of phenol:chloroform. The DNA extracts were visualized by running a 1% (w / v) agarose gel in 0.5X TBE, refer to section 2.3.5 for an outline of this procedure.

2.3.3 Amplification of the ITS1–ITS2 region of rDNA for each yeast isolate

A total of 3 yeast isolates were identified based on colony morphology and Gram staining as shown in Figure 2.2. Two panfungal primers known as the internal transcribed spacer 1 (ITS1) and ITS4 are routinely used in the identification of fungal species (White *et al.*, 1990; Fujita *et al.*, 2001). Refer to Table 2.2 for the primer sequences, oligonucleotides were obtained from Eurogentec (Hamsphire, U.K.). The ITS1-ITS4 primer pair amplify the 5.8S gene and the ITS regions 1 and 2, which flank the 5.8S gene in the fungal ribosomal gene cluster, see the schematic outlined in Figure 2.1.
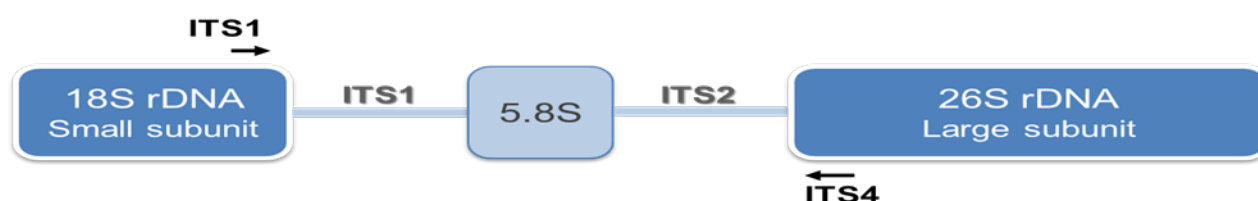
Figure 2.1   Schematic representation of the yeast nuclear ribosomal RNA detailing the location of the primer pair (ITS1 and ITS2) annealing sites. Forward primer is above in the diagram and the reverse primer is below. Internal transcribed spacer regions (ITS) and a Svedberg unit (S).

PCR assays were performed in 25 µl reaction volumes containing 2 µl of the DNA template at a concentration of 40 - 50 ng/µl and 23 µl master mix. The final concentration of components in the master mix was as follows: 5 µM for each oligonucleotide, 1X GoTaq® Green Master Mix (Promega). The amplification reaction was carried using the MJ Mini Thermocycler (Bio-rad,U.K.) under the following conditions: initial denaturation at 95°C for 5 min, followed by 35 cycles at 95°C for 30 s, 52°C for 60 s, 72°C for 60 s; a final extension at 72 °C for 8 min after which a hold cycle at 4°C for ∞. The amplicons were visualized using 1% (w/v) agarose gel; refer to section 2.3.6 for this procedure. The PCR product was prepped for sequencing as outline in section 2.3.6.

2.3.4 PCR assays for molecular confirmation of the bacterial isolates obtained from CF sputum

The primers used in this study are shown in Table 2.2; all were synthesized by Eurogentec (Hampshire, U.K.). The primer sets used to molecularly confirm isolates obtained where chosen based on the specificity testing used within the studies which published their sequences and have also been used by numerous other studies, refer to Table 2.2.

For identification of *B. cepacia* complex, the BCR primer set (Mahenthiralingam *et al*., 2000;Table 2.2) designed to target a region of the *recA* gene which is involved in DNA recombination was used. Concentrations of the reagents were consistent with previously published methodology with the exception of the oligonucleotide concentration; in this assay a lower concentration of 0.5 µM provided a greater yield and quality of PCR product. DNA amplification cycles consisted of an initial denaturation of 94°C for 3min, 30 cycles of 94°C for 30 s, 60°C for 40 s, 72°C for 1 min and a final extension at 72°C for 10 min.

PCR-based identification of *S. aureus* utilised the NUC primer set targeting species-specific section of the nuclease gene *nuc* (Brakstad *et al*., 1992; Table 2.2). The reaction mixture contained 1x GoTaq Green MasterMix (Promega, U.K.), 4% (v/v) DMSO, 1µM oligonucleotides and 1µl DNA template and was prepared to a final volume of 20 µl with molecular grade water. The PCR cycle consisted of denaturation at 94°C for 3 min followed by 35 cycles of 94°C for 60 s, 59°C for 30 s, 72°C for 90 s with a final extension time of 4 min 30 s at 72°C. The PCR mastermix for PCR-based

identification of MRSA utilised the MEC primer set (Murakami *et al*., 1991; Table 2.2) targeting a penicillin-binding protein section of the *mecA* gene. The experimental set up was similar to that for the NUC primer set reaction although 250 nM oligonucleotides, 2 µl DNA template and the exclusion of 4% (v/v) DMSO were used. The cycle parameters consisted of an initial denaturation of 94°C for 2 min followed by 40 cycles of 94°C for 60 s, 55°C for 30 s, 72°C for 90 s with a final extension of 4 min 30 s.

The primer set STR1and DG74 a universal primer target, were used to identify a region of the 16S rRNA gene in *S. pneumoniae* (Matar *et al*., 1998; Greisen *et al*., 1994 respectively; Table 2.2). The PCR reaction mixture for *S. pneumoniae* used an oligonucleotide concentration of 200 nM. DNA amplification consisted of an initial denaturation at 96°C for 4 min, 39 cycles of 95°C for 50 s, 55°C for 45 s, 72°C for 1 min 40 s with a final extension cycle of 72°C for 4 min.

All PCR reactions were performed using the MJ Mini Thermocycler (Bio-Rad, U.K.) for both optimization and confirmatory assays. However the PCR assay for *S. pneumoniae* was performed by the Sprint Thermal cycler (Hybaid, U.K.). PCR runs for each assay consisted of a negative control (mastermix without template or molecular grade water). In addition, type strains referenced in section 2.2.4 for each of the bacterial species were used a positive control for the PCR reaction. For each PCR assay, the annealing conditions and primer concentrations were optimized. Assays with the lowest primer concentrations which produced no amplification artefacts, reduced primer dimer and bright amplicons were used for the molecular confirmation of bacterial isolates from CF sputum.

Table 2.2　　　　List of the primers used in this study for the molecular characterisation of the CF sputum isolates.

Species	Primer	Target region	Sequence (5'　3')	Amplicon size	Reference
B. cepacia complex	BCR For	*recA*	TGA CCG CCG AGA AGA GCA A	~ 1,040 bp	(Mahenthiralingam *et al.*, 2000)
	BCR Rev		CTC TTC TTC GTC CAT CGC CTC		
S. aureus MSSA	NUC For	*nuc*	GCG ATT GAT GGT GAT ACG GTT	~ 270 bp	(Brakstad *et al.*, 1992)
	NUC Rev		AGC CAA GCC TTG ACG AAC TAA AGC		
MRSA	MEC For	*mecA*	AAA ATC GAT GGT AAA GGT TGG C	533 bp	(Murakami *et al.*, 1991)
	MEC Rev		AGT TCT GGC ACT ACC GGA TTT GC		
S. pneumoniae	STR1 For	16S rDNA	AGT CGG TGA GGT AAC CGT AAG	105 bp	(Matar *et al.*, 1998)
	DG74 Rev		AGG AGG TGA TCC AAC CGC A		
Fungi *	ITS1	18S rDNA - 28S rDNA	TCC GTA GGT GAA CCT GCG G	350 – 900 bp	(White *et al.*, 1990)
	ITS4		TCC TCC GCT TAT TGA TAT GC		

* Yeast isolates for analysis only

2.3.5 Agarose gel electrophoresis

The PCR products from all reactions in section 2.3.4 were separated in 1.5% (w/v) Ultrapure agarose (Invitrogen, U.K.) added to 0.5x Tris-Borate-EDTA (TBE) (Sigma-Aldrich). This agarose was heated in a microwave to boiling point and on cooling stained with 0.1 μl/ml of SYBR® Safe DNA Gel (Life technologies) stain. The agarose gel was then poured into a sealed gel slab and a well comb was inserted. All agarose gel electrophoresis assays in this chapter were run using 0.5x TBE buffer as the running buffer. All PCR products were loaded with the 5x Loading buffer red (Bioline); 1x as the final concentration. For each agarose gel electrophoresis assay a DNA ladder was also loaded; either the Easyladder™ I (Bioline) was used or the peqGold 50 bp DNA ladder (Peqlab, U.K.) was used; for a reference image refer to Appendix 2. The aforementioned PCR products were run using a power supply (Fisher Scientific LABOSI Power 300) set at 80V for 50 min with the exception of the PCR amplicons from the *mecA* and STR1-DG74 primer set which had a total run time of 1 h. Gels were visualized using the UV transilluminator G:box (Syngene, U.K.). The PCR products obtained in section 2.3.3 were run on a 1% (w/v) agarose gel prepared using 0.5x TBE buffer, as described above. The gel was set to run at 80 V for 40 min. For this agarose gel electrophoresis assay, Easyladder™ I (Bioline) was used as the DNA ladder and 4 μl of the PCR product was loaded using 1μl of the 5x Loading buffer red. The bands were excised using a disposable scalpel under brief exposure to UV light; excised bands were placed in a sterile 1 ml centrifuge tube and weighed. See section 2.3.6 for sequencing preparation methodology.

2.3.6 Purification, sequencing and analysis of the ITS1–ITS4 region

The excised bands of the amplified products for the ITS1 to ITS2 regions were purified using the peqGold Gel Extraction Kit (Peqlab, U.K.) following the manufacturer's guidelines. The DNA content of the purified products was measured using the Nanodrop and a minimum of 1 ng/μl/100 bp was sent to Source Bioscience Nottingham, U.K. for Sanger sequencing using the ABI 3730 automated sequencer. Additionally 20 μl containing 3.2 pmol/1 μl of the ITS1 primer was sent for sequencing the yeast isolates. The sequences were analysed using the BioEdit program (v7.1.11) and converted to FASTA

format for sequence comparison against the NCBI database (www.ncbi.nlm.nih.gov/refseq/) and a fungal dedicated database called ISHAM ITS (http://its.mycologylab.org/).

2.4 Results

2.4.1 Culture profiling the microbiome of CF sputum samples for the isolation of the predominant species

Each patient's plates contained heavy bacterial growth on the neat to 10^{-2} plate but bacterial and fungal isolates where subcultured to ensure culture purity prior to testing. *P. aeruginosa* growth was merely noted for each of the patients, which varied in the number of cfu obtained per ml with a maximum of up to 10^6 observed, as the isolation of this microorganism from patients within this cohort was previously carried within our research team by Dr Rob Howlin. The colony morphology was noted for this species, with a mucoid strain observed in one of the patients sampled in this study, as shown in Table 2.3.

Identification of each species was first based on the colony morphology observed on the agar inoculated with liquefied sputum. Liquefied sputum diluted and inoculated onto chocolate agar and TSA agar continuously had confluent growth of a range of microorganisms similar to that shown previously in Figure 1.9. Presumptive isolates of interest were subcultured on selective and non-selective agar to aid in further characterizing the isolate and additionally Gram stained as shown in Figure 2.2. An outline of the microorganisms isolated and identified from 8 out of a total of 16 patient's samples in this study is shown in Table 2.3. The aforementioned table contains the microbiome for each patient, with microorganisms which were identified based on the results of colony morphology on non-selective and selective agar, Gram stain, biochemical and molecularly confirmed species meeting the requirements outlined in Table 2.4.

Table 2.3   Microorganisms isolated and identified from eight CF patients.

Patient	Microorganisms isolated
A08	*S. aureus*, *S. pneumoniae*, *P. aeruginosa*, Yeast
A12	*S. aureus*, *S. pneumoniae*, Yeast
A15	Yeast, *S. aureus*
A35	Mould (*Penicillium* spp.) ‡
A48	*S. aureus* LCV and SCV §
A57	*B. cepacia* complex, Yeast
A66	*S. aureus*, *S. pneumoniae*, *P. aeruginosa* mucoid strain, Mould (*Penicillium* spp.) ‡
A69	Mould (*Aspergillus* spp.) ‡
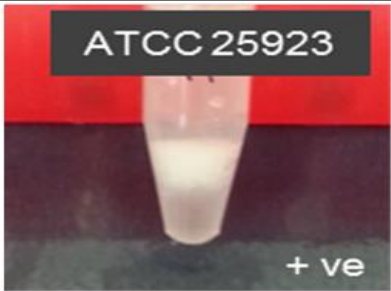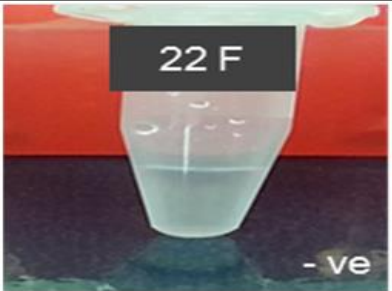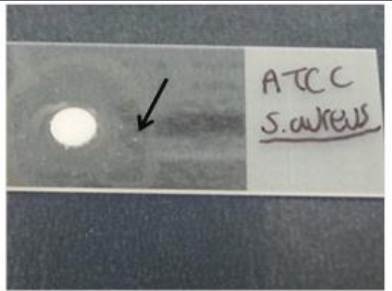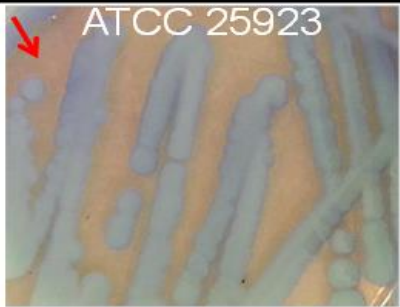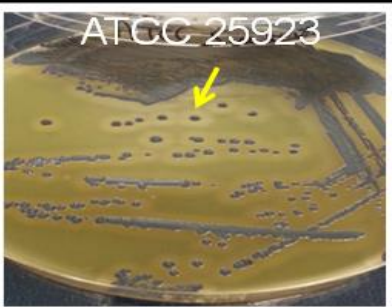
‡ Presumptive genus in brackets, based on colony morphology
§ Large colony variant (LCV), small colony variant (SCV)

The results for the biochemical tests with examples for the type and patient strain for each species is outlined in Figure 2.2. The DNase agar test to detect deoxyribonuclease activity showed positive results with pink zones observed around colonies against a blue background, Figure 2.3. Each organism was tested for the catalase enzyme using 3% hydrogen peroxide with a positive result noted on observing bubbles, all *Streptococci* isolates tested –ve for catalase, refer to Figure 2.3. *S. aureus* isolates were identified based on the colony appearance on Baird-Parker agar, with black-shiny colonies with halos around colonies indicating a positive reaction, refer to Figure 2.3. Additionally coagulase tests were carried out for each presumptive *S. aureus* isolate. The coagulase test used in this study detects bound coagulase; coagulase which is bound to the cell surface, Figure 2.3. All *S. aureus* isolates exhibited bound coagulase activity. The identification of a microorganism was confirmed on meeting the criteria outlined in Table 2.4.

Figure 2.2 Colony morphology and Gram staining techniques used in culture profiling of liquefied CF sputum. White arrows highlight alpha-haemolysis. Scale bar = 10 μm.

Catalase Test + ve reaction	Catalase Test - ve reaction	Coagulase Test + ve reaction
ATCC 25923 +ve	22 F -ve	ATCC S.aureus
DNase Agar Test using toluidine blue + ve reaction		Baird-Parker Agar secondary coagulase test + ve result
ATCC 25923		ATCC 25923

Figure 2.3 Biochemical tests, highlighting positive reactions for type strains. Arrows: black arrow shows clumping, red arrow highlights pink zones for + ve reaction and the yellow arrow points to the opaque halos for a coagulase + ve organism.

Table 2.4   Microorganism identification confirmed using the following requirements.

Bacterial species	Gram stain reaction	Colony morphology on		Catalase Test	DNase Activity	Coagulase Reaction	Molecular test
		Selective	Differential				PCR species specific target §
B. cepacia complex	Gram – ve Rod	• Grey to green colonies • Agar changes to a pink colour		+ ve	No	No	+ ve
S. aureus	Gram + ve Clusters of cocci	• Dark grey to black shiny colonies • Opaque halos around colonies		+ ve	Yes	Yes	+ ve
S. pneumoniae	Gram + ve Chain of cocci		Alpha-hemolysis	- ve	No	No	+ ve

§ Refer to Table 2.2 for species specific PCR assays

2.4.2 Molecular confirmation of microorganisms

Optimization for the *B. cepacia* complex PCR assay originally described by Mahenthiralingam *et al.* (2000) required a step-wise increase in the primer concentration and 1°C increments in annealing conditions. Final adjustments of 4°C in temperature from 56°C to 60°C and a reduction in the cycle time by 5 s from 45 s to 40 s provided a visible improvement in the amplicon obtained, as shown in Figure 2.3 gels 1 and 2). In Figure 2.4 (1) at the lower annealing temperature of 56°C non-specific bands occurred during amplification coinciding with the formation of primer-dimer complexes around the 50 bp region. DMSO was also added to the reaction mixture in order to prevent secondary structures from forming during amplification.
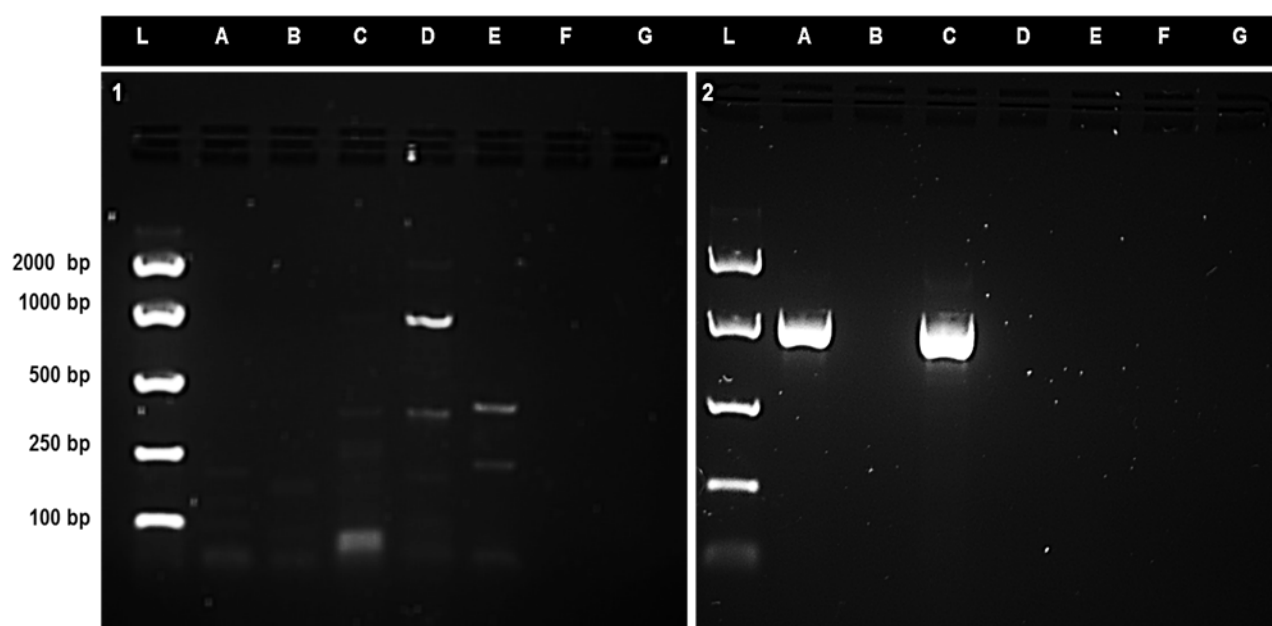
Figure 2.4   Optimization of *B. cepacia* complex specific *recA* PCR (Mahenthiralingam *et al.*, 2000). Gel 1 shows the results for the lower primer concentrations and annealing temperatures versus **Gel 2** with the higher levels for both parameters. For both 1.5% (w / v) agarose gels 1 & 2: lanes (L) for the Easyladder I, Lanes (A) for +ve control *B. cepacia* complex ATCC 25416. **Gel (1)** Lanes contained: (B) CF sputum isolate A57; (C) CF sputum A21; (D) *P. aeruginosa* PA01; (E) *S. aureus* ATCC 25923; (F) negative control Sigma water; lane G Empty. **Gel (2)** lanes contained: (B) empty; (C) CF sputum isolate A57; (D) empty; (E) *P. aeruginosa* PA01; (F) empty and (G) -ve control molecular grade water.

The PCR assay for *S. aureus* required an increase in the primer concentration, addition of DMSO, 2 cycle decreases along with an increase of 4°C in the annealing step from 55 to 59°C. After optimization of the PCR assay, a total of seven isolates obtained from CF sputum were confirmed as *S.* aureus isolates, with bands observed at ~ 270bp, refer to Figure 2.5. Each of these isolates were catalase positive and coagulase negative apart from two isolates of *S. aureus* from the one patient (AO8) which both tested positive for coagulase.

Figure 2.5 NUC primer set amplification run on 1.5% (w / v) agarose gel for presumptive *S. aureus* isolates from CF sputum. Lane (B) contains the DNA ladder Easyladder I (Bioline,U.K.); blank wells for lanes (A), (D), (F),(H),(J), (L), (N), (P), (R), (T) and (V). Contents of wells corresponding to the label above, as follows: (C) positive control *S. aureus* ATCC 25923, CF patient isolates: (E) A08.1, (G) A08.2, (I) A52, (K) CFSA1, (M) A08 (from sample obtained on 13 July 11), (O) A12, (Q) A66.2. Controls: (S) negative control *S. pneumoniae* serotype 14, (U) negative control mastermix without template DNA.
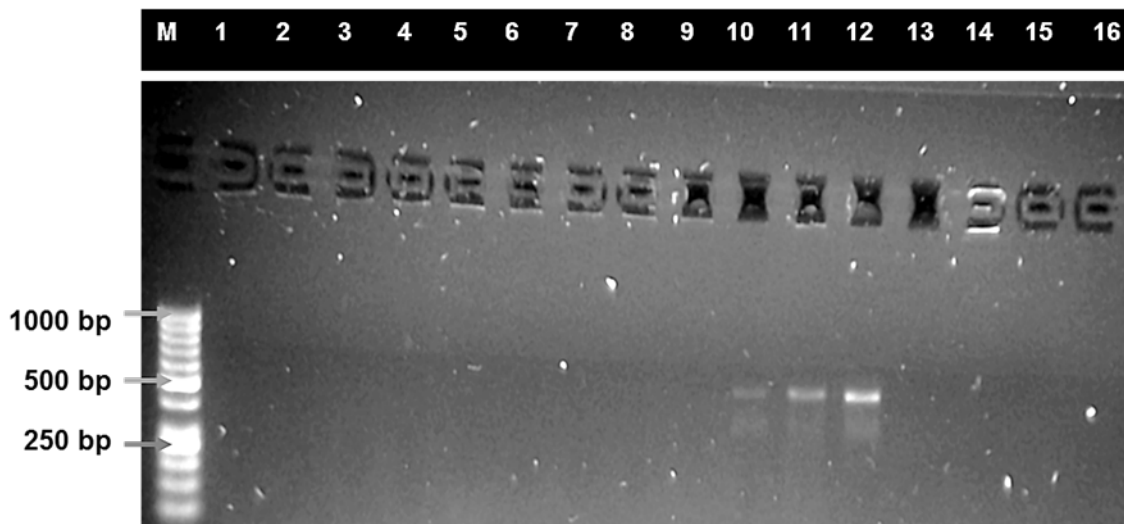
Figure 2.6 Amplification results for the MEC primer set run on a 1.5% (w / v) agarose gel. Molecularly confirmed *S. aureus* CF sputum isolates were tested to detect MRSA using the *mecA* primer set designed by Murakami *et al.* (1991). Well contents as follows: Lane (M) DNA ladder peqGold 50bp DNA (PEQLAB); lanes (1-4) *S. aureus* isolates (ENT mucosa source); lane (5-9) *S. aureus* isolates (ENT Polyp source); lane (10) positive control MRSA NCTC 13143; CF sputum isolates: (11) A08.1, (12) A08.2, (13) CFSA; (14) Negative control: MSSA ATCC 25923, (15) negative: control mastermix with no DNA, (16) negative control: molecular grade dH$_2$O.

The PCR reaction to detect MRSA isolates through targeting the *mecA* gene from CF sputum, mucosa and polyp (acquired from CF patients) samples was run with a lower primer concentration. *S. aureus* isolates from mucosa and polyp samples were used as additional test samples. Two isolates A08.1 and A08.2 obtained from the same patient were positively identified as MRSA isolates; with bands produced around 533bp region, refer to Figure 2.6 above. There was a low level of primer-dimer formation observed for this reaction and a fainter band for the amplicon for the positive control NCTC 13143 MRSA isolate in the well labelled 10 in Figure 2.6.
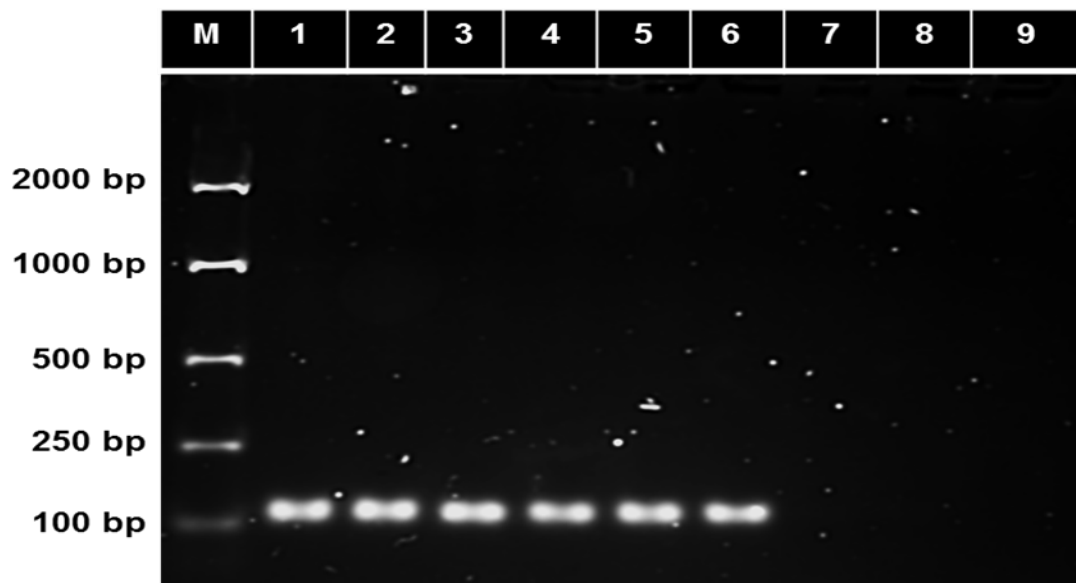
Figure 2.7 Amplicons from a PCR assay using the primer set STR1-DG74 (Matar *et al.*, 1998). Amplicons run on a 1.5% (w / v) agarose gel for presumptive isolates of *S. pneumoniae* obtained from CF sputum samples. The contents of the wells are as follows: Lane (M) DNA ladder Easyladder I; (1) positive controls at ~ 105bp *S. pneumoniae* serotype 14, (2) *S. pneumoniae* serotype 19, (3) *S. pneumoniae* serotype 22 F; CF *S. pneumoniae* patient isolates: (4) A48, (5) A12 and (6) A66. Negative controls: (7) *S. aureus* ATCC 25923; (8) negative control mastermix without template DNA; (9) blank well.

The optimization of the *S. pneumoniae* PCR assay involved the addition of 4 extra cycles with the annealing time reduced by 15 s from 60 s to 45 s. Three CF sputum isolates were confirmed as *S. pneumoniae* using three different serotypes of *S. pneumoniae* as positive controls; these serotypes were identified and molecularly confirmed by the PHE SUHT (Southampton University Hospital).

Sequencing results of yeast isolates

Two out of the three identified yeast isolates were identified as *C. albicans* by both the NCBI and ISHAM ITS databases; the isolates were assigned their corresponding patient designation number A08 and A15. Given only a small fraction of the patient cohort from the Southampton University Hospital's CF centre was sampled the prevalence of *C. albicans* was 12.5%. The yeast isolate obtained from patient A29 was identified as *C. dubliniensis* by both databases as above. This species is closely related to *C. albicans* and also exhibits similar phenotypic profiles, which can often lead to misidentification if molecular tests are not additionally carried out. In relation to the number of yeast isolates obtained from this small subset of the patient cohort sampled, the prevalence of *C. dubliniensis* was 6%. This figure is slightly higher but within the region of that reported by Gammelsrud *et al.* (2011) but considerably lower than that described by Wahab *et al.* (2014).

2.5 Discussion

In this study, a number of the predominant microorganisms were isolated through culture profiling with various agars. However, a greater appreciation of the vast number of microorganisms present within the CF microbiome is permitted through the use of molecular profiling (Cox *et al.*, 2010; Rogers *et al.*, 2004). Equally it has been recognized that the inadequacy in culture dependent methods may be due to the lack of a wide range of media, both selective and non-selective in combination with an inadequate length of incubation time during the culture profiling step. On the other hand the high throughput molecular techniques have been shown to have their shortcomings in the detection of the rare biosphere members as uncovered by Shade *et al.* (2012). Importantly, the isolation of as many microbial species as possible from the sputum samples from CF patients is required for studies into: (1) the biofilm forming ability of these isolates both as mono-species biofilms, (2) as multispecies biofilm in order to understand the dynamics of the microorganisms present pre and post exacerbation periods (Aaron *et al.*, 2002; Tunney *et al.*, 2011; Lopes *et al.*, 2014b) and (3) for antimicrobial susceptibility testing.

An example of the culture profiling for the species of interest data from 8 of the 16 patients sampled from the patient cohort is shown in Table 2.3. *S. aureus* predominated with a prevalence of 63% followed by *S. pneumoniae* at a prevalence rate of 38% within this subset of patients *;* which is similar to other studies (Guss *et al.*, 2011; Spicuzza *et al.*, 2009). Molecular confirmation of the microorganism isolated from CF sputum through the use of a species specific PCR assays are routinely carried out. Molecular assays to corroborate biochemical testing results are vital to ensure the correct identification of theses isolates is reported. Especially when certain microorganisms such as *B. cepacia* are associated with poor prognosis (Whitby *et al.*, 1998; Shelly *et al.*, 2000). The *recA* gene is involved in the repair of recombinant DNA in bacteria and was originally described as a target by Mahenthiralingam *et al.* (2000) for use in discriminating between *Burkholderia cepacia* complex members through the comparison of the restriction fragment length polymorphisms (RFLP) profiles. The primer set

targeting the *recA* gene used in this study was chosen based on the former study due to the specificity for the members of the *B. cepacia* complex over the primer set designed by the latter group, which aimed to identify members within the *Burkholderia* genus (Payne *et al.*, 2005). The primer set used herein has been used in other studies for the identification of *Burkholderia cepacia* complex members within CF sputum samples (McDowell *et al.*, 2001; Moore *et al.*, 2002). This primer set involved careful optimization as shown in Figure 2.4 due to non-specific binding to the DNA from *S. aureus* and *P. aeruginosa* which resulted in multiple amplicons. However post optimization the primer set proved highly specific for targeting *B. cepacia* complex members and resulted in the elimination of the amplicons initially observed using a lower annealing and primer concentration. The use of the *recA gene* region as a target to detect *B. cepacia* complex has offered more reliability in the discrimination of *B. cepacia* complex members than the use of 16S rDNA (Campbell *et al.*, 1995). Moore *et al.* (2002) described the poor specificity of the primers utilized in the latter study thereby making *recA* the more reliable target in the detection of *B. cepacia* complex members. *B. cepacia* complex members are considered as late stage colonizers in CF patient's lungs. This group are of extreme importance as they possess an intrinsic resistance to many antimicrobials (Papp-Wallace *et al.*, 2013; Tseng *et al.*, 2014) and are associated with deterioration in lung functioning and can result in the death of patients who succumb to cepacia syndrome.

S. aureus and *H. influenzae* are the predominately the first microorganisms isolated from the CF lung and many researchers view the initial colonization of the airways by these species as the first major trigger for the epithelial inflammatory response. Consequently, this results in damage to the lungs and thereby paves the way for later colonization by other microorganisms such as *P. aeruginosa* (Smith, 1997). The use of primers targeting the *nuc* gene (Brakstad *et al.*, 1992) for the confirmation of *S. aureus* (MSSA) are used in clinical laboratories (Koziol-Montewka *et al.*, 2006) in addition to phenotypic characterisation of isolates. It is well recognized that *S. aureus* MSSA is a colonizer of the CF lung (Kahl *et al.*, 1998). *S. aureus* was the most frequent microorganism isolated, with 63% of the patient cohort in this study culture positive for this species. Therefore work carried out by Fugère *et al.* (2014)

involving the use of the *nuc* gene for the confirmation of *S. aureus* MSSA isolates alongside the use of the *mecA* gene was a similar approach used in this study in order to additionally identify MRSA isolates obtained from CF sputum samples. Two MRSA isolates were identified in this study with two isolates obtained from the same patient. A review by Goss and Muhlebach, (2011) highlighted that within most European countries the level of MRSA has remained relatively constant between the years 2007 and 2008 whereas in the USA and Australia there has been a slight increase. Bacteria colonizing the CF lung form biofilm communities which permit persistence which in the case of infections with both MSSA and MRSA would allow the transfer of genetic information between the two but also between other species within the polymicrobial niche (Molina *et al.*, 2008). This supports the need for the identification of these species and the study of the biofilm forming ability of these and other microorganisms both as monospecies and mixed species biofilms to have a full appreciation of the survival dynamics of this highly diverse niche (Molina *et al.*, 2008).

The primer set designed by Matar *et al.* (1998) specific for *S. pneumoniae* targeting a region of the 16S rRNA gene was utilized to detect *S. pneumoniae* in otitis media effusion samples. *S. pneumoniae* is primarily a commensal associated with the nasopharynx (Faden, 2001) but this bacterium is routinely cultured and detected in CF sputum samples (Bauernfeind *et al.*, 1987; Goss and Muhlebach, 2011).The isolation of *S. pneumoniae* in CF sputum is not typically associated with exacerbations but instead is recognized as a colonizer within the early stage of life in CF patients (Høiby, 1982). Høiby, (1982) stated that the isolation of *S. pneumoniae* during an acute exacerbation episode was extremely low. The bacterium *S. pneumoniae* was isolated from patients across a range of ages in this study with a total of 38% of the patients being colonized with this bacterium; making it the second most commonly identified bacterium within this study cohort. Which is why *S. pneumoniae* is viewed as a transient colonizer of the CF lung (Renders *et al.*, 2001). But the work published by del Campo *et al.* (2005) highlighted the existence of a multi-resistant clone from the Serotype group 23 which was isolated from 30% of the patients within their study. Additionally, persistent colonization in the CF lung can be permitted through the formation of

biofilms as demonstrated by García-Castillo *et al.* 2007. This highlights the need for more work to be carried out to understand the relationship between the polymicrobial community existing as biofilms amongst a reservoir of multi-resistant isolates within the CF lung and how this influences the clinical status of patients as the existence of multi-resistant clones also poses a risk to other patients within the same treatment centre.

The number of yeast isolates identified in this study was in agreement to that observed among other groups (Peltroche-Llacsahuanga *et al.*, 2002; Gammelsrud *et al.*, 2011). The isolation of *C. albicans* accounted for a total of 68% of the yeast isolates obtained. This figure is corroborated by other studies analysing the prevalence of *C. albicans* and other *Candida* spp. within CF patients (Haase *et al.*, 1991; Peltroche-Llacsahuanga *et al.*, 2002; Muthig *et al.*, 2010). Only one of the yeast isolates was identified as *C. dubliniensis* based on the sequence obtained for the ITS1-IST2 region. *C. dubliniensis* was first reported as an atypical *C. albicans* infecting the oral cavity of HIV seropositive patients in Dublin, Ireland (Sullivan *et al.*, 1993) and was subsequently confirmed as a new species by Sullivan *et al.* (1995). Since the initial article identifying *C. dubliniensis* within CF sputum samples by Peltroche-Llacsahuanga *et al.,* 2002, there has been a steady increase in the number of reports of this organism inhabiting the CF lung (Wahab *et al.*, 2014).

The culture profiling of the sputum samples was primarily undertaken to isolate the widely accepted predominant microorganisms associated with CF patients, to investigate the response of *in vivo* biofilms formed by these microorganisms to nitric oxide, refer to Chapter 3. However, isolates for *A. xylosoxidans*, *S. maltophilia* and *H. influenzae* were not identified. The patient cohort sampled for this study did not include paediatric patients. This was a limiting factor of the sampled cohort in this study. Importantly, *H. influenzae* is recognized as an early colonizer of the CF lung (Smith, 1997). This factor limited the effectiveness of isolating *H. influenzae* through culturing the CF sputum of adults, due to the milieu of microorganisms colonizing the CF lung in older patients (Sibley *et al.*, 2011). Although *H. influenzae* has been

recognized as a transient colonizer of the CF lung (Román *et al*., 2004); due to the lower percentage of older patients testing positive for *H. influenzae* in the U.K. (Anonymous, 2013) and the difficulty in isolating this microorganism this bacterium was not included in the work carried out in Chapter 3. Isolates for *A. xylosoxidans* and *S. maltophilia* from CF patients in Norway were obtained for testing alongside the microorganisms acquired in this study for work in Chapter 3.

In summary, both fungal and bacterial species were isolated and characterised from CF sputum with a focus on the bacterial species for subsequent work involving biofilm growth.

Chapter 3

Investigation into the Potential Use of Nitric Oxide as a Dispersal Agent for Monospecies Biofilms Formed by Microorganisms Isolated From CF Sputum and Mixed Species *Ex vivo* CF Sputum Biofilm

3.1 Introduction

As discussed in Chapter 1, the discovery that low concentrations of exogenous NO where capable of inducing sessile bacterial cells within biofilms to undergo dispersal is initiated through the activation of c-di-GMP phosphodiesterase activity (Barraud *et al.*, 2009), this has been explored for a number of species (McDougald *et al.*, 2012). The use of nitric oxide as a potential anti-biofilm compound was first demonstrated to be effective in initiating dispersal of *P. aeruginosa* biofilms at picomolar to low nanomolar concentrations (Barraud *et al.*, 2006). Dispersal of monospecies biofilms formed by *Serratia marcescens*, *Vibrio cholerae*, *E. coli*, *Fusobacterium nucleatum*, *Bacillus licheniformis*, *S. epidermidis*, *Candida albicans* and multispecies biofilms from water systems, on exposure to low concentrations of NO has additionally been shown (Barraud *et al.*, 2009; McDougald *et al.*, 2012).

CF infection in the lungs is extremely difficult to eradicate despite continuous treatment with antimicrobials over the course of a patient's life, chronic infection persists and it has long been recognised that this can be attributed to the formation of biofilms by microorganisms within the lung (Yoon *et al.*, 2002; Høiby *et al.*, 2010a). Importantly, as biofilms are more tolerant to antimicrobials compared to their planktonic counterparts, due to a combination of factors as discussed in Chapter 1, methods of disrupting these multicellular communities are crucial in order to combat biofilm based infections.

A method of disrupting these multicellular communities would allow the antimicrobials to effectively attack the bacterial cells which are released from the biofilm on the dispersing. Due to this fact, nitric oxide was tested and shown to disperse *P. aeruginosa* biofilms formed by CF isolates obtained from our Southampton cohort by Dr Robert P. Howlin. This work demonstrated that ~450 - 500 nM of NO released from 500 µM SNP (based on direct NO measurements using a NO microsensor) was capable of inducing the dispersal of well-established biofilms formed by twelve different *P. aeruginosa* CF sputum isolates. Additionally, the author showed an increase in the biofilm biomass of *P. aeruginosa* CF isolates when dual antibiotic treatments of tobramycin and ceftazidime were administered at a minimum bactericidal concentration. Interestingly, the work showed a significant reduction in both

the biofilm biovolume and thickness for the biofilms formed by these *P. aeruginosa* CF isolates when a combined treatment of exogenous NO and antimicrobials was applied. A combination therapy consisting of NO + antimicrobials led to the dispersal of biofilms and killing of the released cells into the planktonic phase. Moreover, the combination therapy was more effective than antimicrobial treatments alone compared to the untreated. Due to the combined *in vitro* work, a randomized clinical trial was conducted to investigate if NO inhalation therapy could reduce the *P. aeruginosa* load in the sputum of CF patients. Through the use of FISH analysis, a reduction in *P. aeruginosa* biofilms within the sputum of 5 CF patients treated with inhaled NO (10 ppm) in conjunction with IV antibiotic therapy was demonstrated against the placebo group (Howlin, Cathie, Hall-Stoodley, Cornelius, Duignan *et al.*, 2017).

It is now widely accepted that CF lung infection is a polymicrobial infection (Rogers *et al.*, 2004; Sibley *et al.*, 2006; van der Gast *et al.*, 2011). With this in mind, it was decided to investigate whether NO can induce biofilm dispersal of other clinically relevant CF pathogens, similar to that observed for the biofilms formed with CF isolates of *P aeruginosa*. The effect of exogenous NO on the monospecies biofilms formed by the most commonly identified CF isolates, *B. cepacia* complex, *A. xylosoxidans, S. aureus, S. maltophilia* and *S. pneumoniae* will be addressed in this Chapter. These bacterial species were isolated from CF sputum collected from CF patients attending clinic at SUHT as outlined in Chapter 2. However, CF isolates for *A. xylosoxidans* and *S. maltophilia* were kindly donated by Prof Nørskov-Lauritsen. Additionally, work in this chapter will also investigate if exogenous NO can attenuate the biofilms formed by mixed species from enriched *ex vivo* CF sputum samples.

3.2 Materials and Methodology

3.2.1 *B. cepacia* complex monospecies biofilm assay

Preliminary assays were carried out to check the biofilm forming capabilities and the optimization of biofilm growth conditions. A modified Luria-Bertani broth (mod-LB) was prepared; which contained the same components as the LB broth with the exceptions of a lower sodium chloride concentration of 0.5 g / l instead of 5 g / l of NaCl as used in LB broth (Bertani, 1951) and the addition of 2 g / l of glucose (Sigma-Aldrich). A clinical isolate of *B. cepacia* complex was grown overnight in mod-LB at 37°C with 5% CO_2 - 95% air. For the biofilm inoculum, the overnight culture was pipetted into fresh mod-LB broth till an optical density (OD) of 0.2 measured at 600 nm was reached which equated to 1.5 x 10^6 CFU / ml using a Jenway 6300 spectrophotometer (used for all OD measurements). Biofilms for all species were grown on both 6-well plates and MatTek dishes unless otherwise stated, see Figure 3.1 for details of the plastic ware used. For biofilm growth on the 6-well plates and MatTek dishes, 2 ml of the biofilm inoculum was used to inoculate each well. The plates were incubated at 37°C with 5% CO_2 - 95% air with 75 rpm shaking for an attachment phase of 1.5 h. After the attachment phase the suspension was gently removed and either 4 ml or 3 ml of fresh mod-LB was gently pipetted into each well of the 6-well plates and MatTek dishes, respectively. To ensure an adherent biofilm biomass, biofilms were grown in both the 6-well plates and MatTek dishes at 37°C with 5% CO_2 – 95% air with 75 rpm (Stuart SI 500) shaking for a total of 84 h with fresh mod-LB applied every 24 h after carefully removing the planktonic suspension. After a total of 72 h of biofilm growth, the planktonic phase was gently removed from each well and mod-LB broth containing either sodium nitroprusside dihydrate (SNP) (Sigma-Aldrich, U.K.) or the chemical controls were applied to each biofilm at the concentrations outlined in section 3.2.7. Refer to sections 3.2.8 and 3.2.9 for an outline of the other methodologies applicable to the biofilms beyond this point.

MatTek dish   **6-well Nunc™ plate**
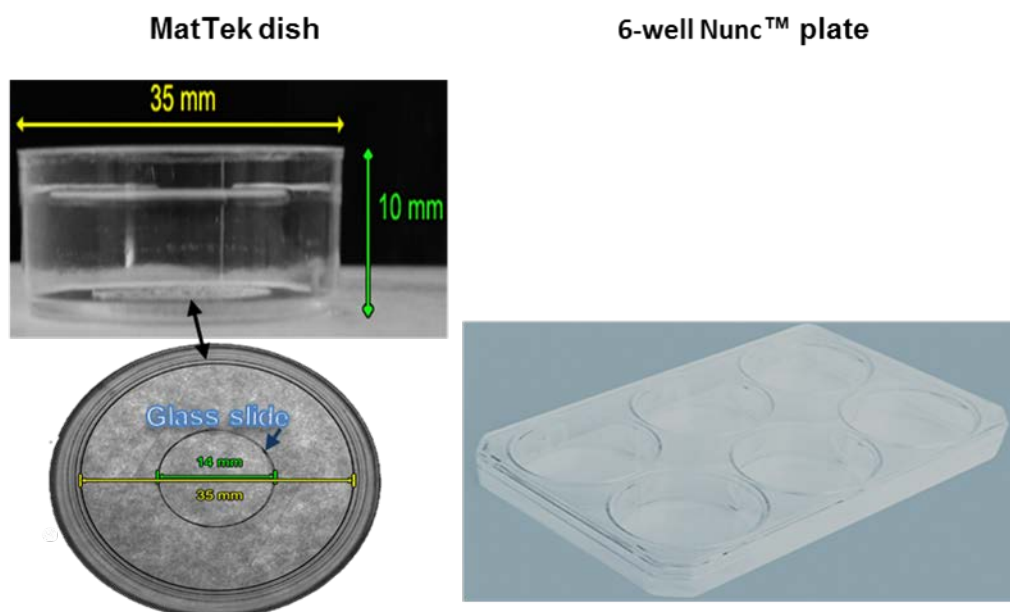
Figure 3.1 Plastic ware used for the growth of biofilm. The Nunc™ 6-well polystyrene flat bottom plates cell-culture treated (dry coating in the form of an energy treatment) (Thermo Scientific Nunc®, Nunclon™Δ) and the MatTek 35 mm dishes containing a microwell with a 14 mm diameter composed of glass with a thickness of No. 1.5 coated with poly-d-lysine (MatTek Corporation, USA) were used.

3.2.2 *Streptococcus pneumoniae* monospecies biofilm assay

Clinical isolates for this species obtained as outlined in Chapter 2 were used for this work. For the growth of this species media was prepared as follows: (1) 5% (v / v) sheep blood agar - was prepared using Blood agar base No.2 (Oxoid, U.K.) by following the manufacturer's instructions with sterilization at 121°C for 15 min; 5% (v / v) of sheep blood (Oxoid, U.K.) was added aseptically to the agar on cooling to ~ 50°C; (2) broth – full strength and 1/5 strength brain heart infusion broth (BHI) (Oxoid, U.K.) was prepared following the manufacturer's instructions with sterilized at 121 °C for 15 min. The clinical isolates were removed from the -80°C storage and streaked onto 5% sheep blood agar and incubated overnight at 37°C in 5% CO_2 - 95% air. Five colonies were selected using an inoculating loop to inoculate 15 ml of full strength BHI and then incubated for 12 - 15 h under static conditions at 37°C in 5% CO_2 -

95% air. For the biofilm inoculum, the overnight inoculum was used to inoculate fresh 1/5 BHI, with OD measurements taken at 600 nm for the suspension to adjust the OD to 1.5×10^7 CFU / ml. From this biofilm inoculum, 4 ml and 3 ml was used to seed biofilms on both 6-well plates and MatTek dishes, respectively. The plates and dishes were incubated at 37ºC in 5% CO_2 – 95% air for 6 days with the planktonic suspension gently removed on a daily basis from each biofilm to apply fresh 1/5 BHI. After a total of 6 days of biofilm growth the nitric oxide assay was commenced refer to sections 3.2.7, 3.2.8 and 3.2.9 for further methodologies.

3.2.3 *Achromobacter xylosoxidans* monospecies biofilm assay

Clinical isolates for this species obtained from CF patients treated at the Aarhus University Hospital Skejby were generously donated by Prof Nørskov-Lauritsen for this study. Media for growth was prepared as follows: (1) Agar - tryptone soy agar (TSA) (Oxoid, U.K.) was prepared following the manufacturer's instructions with sterilization at 121ºC for 15 min (2) Broth – tryptone soya broth (TSB) (Oxoid, U.K.) was prepared following the manufacturer's instructions with sterilization at 121ºC for 15 min. Clinical isolates for *A. xylosoxidans* were recovered from frozen stocks by being streaked onto TSA. The plates were incubated overnight at 37ºC in 5% CO_2 – 95% air. Five colonies were selected from the plate to inoculate a 50ml Falcon tube containing 15 ml of TSB and the tube was incubated overnight at 37ºC in CO_2 - 95% air with shaking at 250 rpm using a shaking platform (Stuart SSL1orbital shaker) . This overnight culture was used to inoculate fresh TSB until a cell density of 1.5×10^6 CFU / ml was reached by taking OD 620 nm measurements for the biofilm inoculum. Four ml and 3 ml of this biofilm inoculum was used to seed biofilms on both 6-well plates and MatTek dishes (as described above in section 3.2.2), respectively. The biofilms were grown at 37ºC in 5% CO_2 – 95% air under static conditions for 48 h with the planktonic suspension gently removed daily to apply fresh TSB. After 48 h of biofilm growth, the planktonic suspensions were carefully removed from each well and replaced with fresh TSB containing a range of concentrations of SNP with controls for testing the response of the biofilm to the presence of nitric oxide.

Refer to sections 3.2.7, 3.2.8 and 3.2.9 for biofilm methodologies beyond this point.

3.2.4 *Stenotrophomonas maltophilia* monospecies biofilm assay

Clinical isolates for *S. maltophilia* were donated by Prof Nørskov-Lauritsen. These clinical strains were obtained from patients treated at the Aarhus University Hospital Skejby, Denmark. For the growth of this species TSA and TSB were used and prepared as described in section 3.2.3 above. Clinical isolates from frozen stock were plated onto TSA agar and incubated at 37ºC in 5% CO_2 – 95% air. Five colonies were selected from the agar plate and used to inoculate 15 ml of TSB. This culture was incubated at 37ºC in 5% CO_2 – 95% air overnight. The OD of fresh TSB was adjusted through inoculation with the overnight culture, for a biofilm inoculum with a cell density of 1.5 x 10^6 CFU / ml; OD 560 nm measurements were taken. This biofilm inoculum was used to seed biofilms by pipetting 4 ml or 3 ml into 6-well plates and MatTek dishes, respectively. These plates and dishes were incubated at 37ºC in 5% CO_2 – 95% air for a total of 48 h. Every 24 h the planktonic suspension was gently removed and fresh TSB was applied. After 48 h the planktonic suspension was removed from all of the plates and replaced with fresh TSB containing varying concentrations of SNP ranging; refer to sections 3.2.7, 3.2.8 and 3.2.9 for biofilm methodologies beyond this point.

3.2.5 *Staphylococcus aureus* a cbcgdYW̯Wg˙biofilm assay

Clinical isolates of *S. aureus* were obtained as outlined in chapter 2. For the growth of this species TSB, mod-TSB and mod-TSA were used; the media was prepared as outlined in section 3.2.3 with the addition of 0.2% (w/v) glucose (Sigma-Aldrich) added to mod-TSA and mod-TSB. Patient isolate A52 was inoculated into a 50 ml Falcon tube containing 15 ml of TSB and was incubated overnight at 37ºC in 5% CO_2 – 95% air. The biofilm inoculum was prepared by using an overnight culture which had reached an OD 620 nm of 0.530 and was diluted in mod-TSB to a cell density of 1.5 x 10^6 CFU / ml. Either 4 ml or 3ml

per well of the biofilm inoculum was added to a 6-well plate and MatTek dish, respectively. All plates and dishes were incubated for 72 h at 37°C in 5% CO2 – 95% air. Every 24 h the planktonic suspension was gently removed and fresh mod-TSB was applied. After 72 h of biofilm formation the nitric oxide assay was conducted; refer to sections 3.2.7, 3.2.8 and 3.2.9 for biofilm methodologies beyond this point.

3.2.6 Enriched *ex vivo* mixed species biofilm

For the work carried out in this section, two expectorated sputum samples were collected from 1 patient, temporal sampling. A 1:1 volume of Mucolyse (Pro-lab Diagnostics, U.K.) was added to the samples to liquefy the sputum sample and incubated for 30 min at 37°C with 5% CO_2 – 95% air. The samples were homogenised by vortexing for 1 min. An equal volume of the liquefied sputum was used to inoculate MatTek dishes for each treatment. The MatTek dishes were incubated at 37°C with 5% CO_2 – 95% air for an attachment period of 1 h 30 min. After the attachment period the sputum suspension was slowly removed and the MatTek dish was rinsed with 4 ml of BHI broth. To each MatTek dish 3 ml of fresh BHI was applied and the dishes were incubated for 24 h at 37°C with 5% CO_2 – 95% air.

After 24 h of biofilm growth, the planktonic suspension was slowly removed and the dishes were rinsed twice using 3 ml of BHI broth; taking care not to disrupt the biofilm. Solutions were prepared for the nitric oxide assay; refer to section 3.2.7 for an outline of this procedure. In brief, 3 ml of fresh BHI was applied to MatTek dishes for control specimens and to MatTek dishes undergoing NO treatments, 3 ml of fresh BHI containing 500 µM of SNP was applied. The MatTek dishes were incubated for a further 15 h at 37°C with 5% CO_2 – 95% air. Refer to sections 3.2.9 and 3.2.11 for an outline of further relevant biofilm methodologies beyond this point. Aliquots containing the biofilm suspension for each were processed by a group at the SUHT for qPCR analysis, however the e*x vivo* biofilms imaged and analysed in this chapter were not analysed using qPCR analysis to identify *P. aeruginosa, S. aureus* MSSA and MRSA. Refer to section 3.3.7 for an overview of the qPCR analysis.

3.2.7 Nitric oxide assay– preparation of the NO donor sodium nitroprusside dihydrate (SNP), the NO scavenger PTIO and the SNP analogue potassium ferricyanide

A stock solution of sodium nitroprusside dihydrate (SNP) (Sigma-Aldrich) was freshly prepared in PBS, to a final concentration of 1 mM. All stock solutions in this section were sterilized by passage through a Millipore filter with a 0.22 µm pore size using a sterile syringe (VWR, U.K.). Various concentration of this SNP stock solution were added to fresh media for SNP concentrations ranging from 100 nM to 500 µM; refer to Table 3.1 for further information for each species. The concentration of SNP administrated equates to approximately 1000 fold lower concentration of NO released into the solution (Barraud *et al.*, 2009). A stock solution of potassium ferricyanide ($K_3Fe(CN)_6$; Sigma-Aldrich U.K.), an analogue for SNP lacking the NO moiety was also prepared in PBS and added to fresh media (Table 3.1) to a concentration of 1 µM as a chemical control for SNP. The potent NO scavenger 2-Phenyl-4,4,5,5- tetramethylimidazoline-1-oxyl 3-oxide (PTIO) (Goldstein *et al.*, 2003), was prepared in PBS and added at a final concentration of 1 µM to fresh media (Table 3.1); additionally SNP at a final concentration of 1 µM was added to this latter solution. For each nitric oxide assay, 1-well and 1-dish were used as controls; inoculated with only fresh media. After application of the treatments to each well, all 6-well plates and dishes were incubated for a further 12 h at 37°C in 5% CO_2 – 95% air. Refer to sections 3.2.8 and 3.2.9 for the remaining methodologies conducted.

Table 3.1 Nitric oxide assay conditions.

Species	Media		Nitric oxide assay treatments Concentration of SNP ‡, PF § and PTIO+SNP ¥ used	Duration of NO assay
	Broth	Agar		
A. xylosoxidans	TSB	TSA	100 nM, 250 nM, 500 nM, 1 µM, 15 µM, 50 µM, 100 µM, 250 µM, 500 µM ‡. 1 µM of PF §. 1 µM PTIO + 1 µM SNP ¥.	12 h
B. cepacia complex	Mod- LB	Mod- LB agar	100 nM, 250 nM, 500 nM, 1 µM, 15 µM, 50 µM, 100 µM, 250 µM, 500 µM ‡. 1 µM of PF §. 1 µM PTIO + 1 µM SNP ¥.	12 h
S. aureus	Mod- TSB	Mod- TSA	100 nM, 250 nM, 500 nM, 1 µM, 15 µM, 50 µM, 100 µM, 250 µM, 500 µM ‡. 1 µM of PF §. 1 µM PTIO + 1 µM SNP ¥.	12 h
S. maltophilia	TSB	TSA	100 nM, 250 nM, 500 nM, 1 µM, 15 µM, 50 µM, 100 µM, 250 µM, 500 µM ‡. 1 µM of PF §. 1 µM PTIO + 1 µM SNP ¥.	12 h
S. pneumoniae	1/5 BHI	5% Sheep Blood agar	100 nM, 250 nM, 500 nM, 1 µM, 15 µM, 50 µM, 100 µM, 250 µM, 500 µM ‡. 1 µM of PF §. 1 µM PTIO + 1 µM SNP ¥.	12 h
Ex-vivo sputum mixed species	BHI full strength	n/a	500 µM ‡	15 h

3.2.8 Culture analysis of planktonic and biofilm cells after treatment with SNP

After 12 h of nitric oxide treatment, the planktonic suspensions were removed from the 6-well plates for each species and serially diluted in PBS. The biofilms grown on the 6-well plates were rinsed slowly 3x using 3 ml of PBS. After the rinses, 1 ml of PBS was added to each well and each biofilm was removed from the surface using a cell scraper (Greiner Bio-One, U.K.). Care was taken to not remove any biofilm growth present on the edges of the well when using the cell scraper. The biofilm suspension was transferred to a 1.5 ml centrifuge tube. The biofilm suspensions were vortexed for 1 min and the centrifuge tube were placed in a sonication bath (operating frequency of 60 kHz at RT) containing 2% (v / v) Triton–X solution prepared in dH$_2$O. The biofilm suspensions were subjected to a total of three 5 min cycles in the sonication

bath at room temperature; with a total of 1 min of vortexing between each cycle. The biofilm suspension phase was then serially diluted in PBS. This methodology of sonication and vortexing cycles was tested using a Gram-positive and Gram-negative type strain to ensure damage to cells did not occur during this process thereby effecting cell viability, refer to Figure 3.3. All titers for the planktonic and biofilm suspensions were determined in quintuplicate and plated on the appropriate agar, refer to Table 3.1. All agar plates were incubated for 24 h at 37°C with 5% CO_2 – 95% air and CFUs were recorded for each treatment. Statistical analysis was carried out as outlined in section 3.2.11.

3.2.9 Microscopy and analysis of biofilms

For the MatTek dishes the planktonic phase was removed and the plate was rinsed 3x using PBS. A 1:1 mixture of the LIVE/DEAD BacLight kit (Invitrogen, U.K.) components SYTO9 and Propidium Iodide (PI) (2 μl / ml) were prepared in PBS. One ml of the prepared stain was applied to each dish. The dishes were incubated at room temperature for 20 min in the dark. The stain was removed taking care to not disrupt the biofilm and a 1 ml rinse of PBS was applied prior to imaging. For the biofilms in section 3.2.6, 500 μl of 90% (v / v) glycerol solution was applied gently to each dish prior to imaging. A Nikon Eclipse E800 Episcopic differential interference/epifluorescence (EDIC/EF) microscope (Best Scientific, U.K.) (Keevil, 2003) was used to take epifluorescent images at 10 different positions for all biofilms unless otherwise stated. Refer to Figure 3.2 for an image depicting the regions of biofilms where imaged on a MatTek dish. Images were taken for both the SYTO9 and PI channels using the FITC and TRITC filter cubes respectively with the 50x objective, long working distance lenses at each point. The excitation/emission for SYTO9 and PI dyes are 480/500nm and 490/635nm respectively. SYTO9 is a cell permeable which fluoresces green when bound to nucleic acid and was used to stain live biofilm cells. Propidium iodide is a cell impermeable dye which binds to both RNA and DNA and fluoresces in the red wavelength range; this dye was used to indicate dead or membrane comprised biofilm cells. Membrane comprised cells will fluoresce in the wavelength range from orange to red with dead cells emitting in the red wavelength. The images for both channels were combined to include

all adhered biofilm cells. Images were converted to 8 bit grayscale, manually thresholded and the percentage surface coverage was calculated using ImageJ (http://rsb.info.nih.gov/ij).
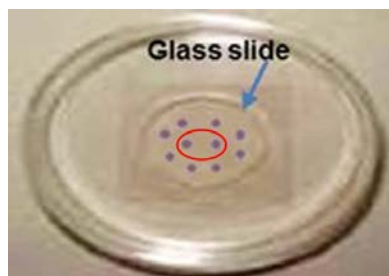
Figure 3.2   Microscopic analysis of biofilms formed on a MatTek dish. The purple circles mark the positions where 10 images of the biofilm biomass were taken for each species using the Nikon epifluorescence microscope. For CLSM, a total of 5 z-stacks were acquired. One representative z-stack for each region was acquired; the middle region is enclosed by a red circle.

The *ex vivo* sputum mixed species biofilm were analysed using a Leica SP5 CLSM (Leica Microsystems, Milton Keynes, U.K). Biofilm images were taken in five positions were acquired using the 63x/1.3 numerical aperture (NA) objective lens using glycerol immersion. The laser lines 488 nm and 561 nm were used to excite STYO9 and PI, respectively. Line average setting was set to 4, with a size of 1024x1024 pixels and the z-step size was set at 0.49 µm.

3.2.10 Statistical analysis

All CFU data collected for the biofilm, planktonic phases and for the sonication assay were transformed using log10 to normalize the data prior to statistical analysis. The surface percentage data analysed for the surface occupied by biofilm biomass as calculated using ImageJ was transformed using the Logit transformation (see formula below) in order to meet the requirement for

normal distribution; the residuals for the untransformed data were not normally distributed on observing the residual plots.

$$\text{Logit}(P) = \text{Log}_e \frac{P}{100 - P}$$

P = Percentage

The data was analysed using a general linear model (GLM) with orthogonal contrast for balanced analysis of variance using the Minitab software, version 16 (Minitab Inc., State College, Pennsylvania, USA). The program called Contrast.exe (Doncaster and Davey, 2007) was used to choose an appropriate set of balanced orthogonal contrasts to compare pooled groups of treatments which were of particular interest. As the analysis of variance tests assume equal variances across samples, the Levene's test was used to verify this assumption for the data sets tested. A GLM was used to uncover differences between treatments with Tukey's HSD post hoc tests for all pairwise comparisons. Box plots were used to demonstrate the results. The same methodology was used to analyse differences between the control and chemical controls 1 µM PF and 1 µM PTIO + 1 µM of SNP, these graphs can be found within Appendix 3. A two-tailed 2-sample t-test was used to compare if the sonication and vortexing treatment affected cell viability. All experimental repeats were conducted independently, $n = 3$ with the exception of the *ex vivo* sputum assay for which $n = 1$. Values for $P \leq 0.05$ were considered statistically different and highlighted by the one asterisk *, two asterisks ** for P values $\leq$ 0.01 and three asterisks *** for P values $\leq$ 0.001. Significant differences between the control and SNP treatments are highlighted within the graphs; all other significant differences between the various SNP treatment concentrations will be referred to in the text section of the results section 3.3.

3.2.11 Data analysis of the *ex vivo* sputum mixed species biofilms

The z-stack images were processed using Comstat2 (Heydorn *et al.*, 2000; Vorregaard, 2008). Otsu thresholding was carried out for each z-stack and the maximum thickness and total biomass (biofilm biovolume) were measured (Table 3.2; Figure 3.19). Images of the biofilms z-stacks were compiled using Leica LAS X Software and 2D aerial views were rendered using IMARIS v7.4.2 trial version (Bitplane).

3.3 Results

3.3.1 Does the use of a combination of sonication and vortexing cycles have an effect on the cell viability of Gram–positive and Gram–negative bacteria?

This experiment was carried out to ensure the methods used in handling the biofilm biomass recovered from the 6-well plates did not adversely affect cell viability. The use of sonication and vortexing cycles prior to serially diluting and plating did not adversely affect the cell viability of both the Gram-negative and Gram-positive type strains ($P < 0.01$; $P = 0.317$, two-tailed two sample t-test, respectively) similar to other studies using higher frequencies (Joyce *et al.*, 2003; Kobayashi *et al.*, 2009).
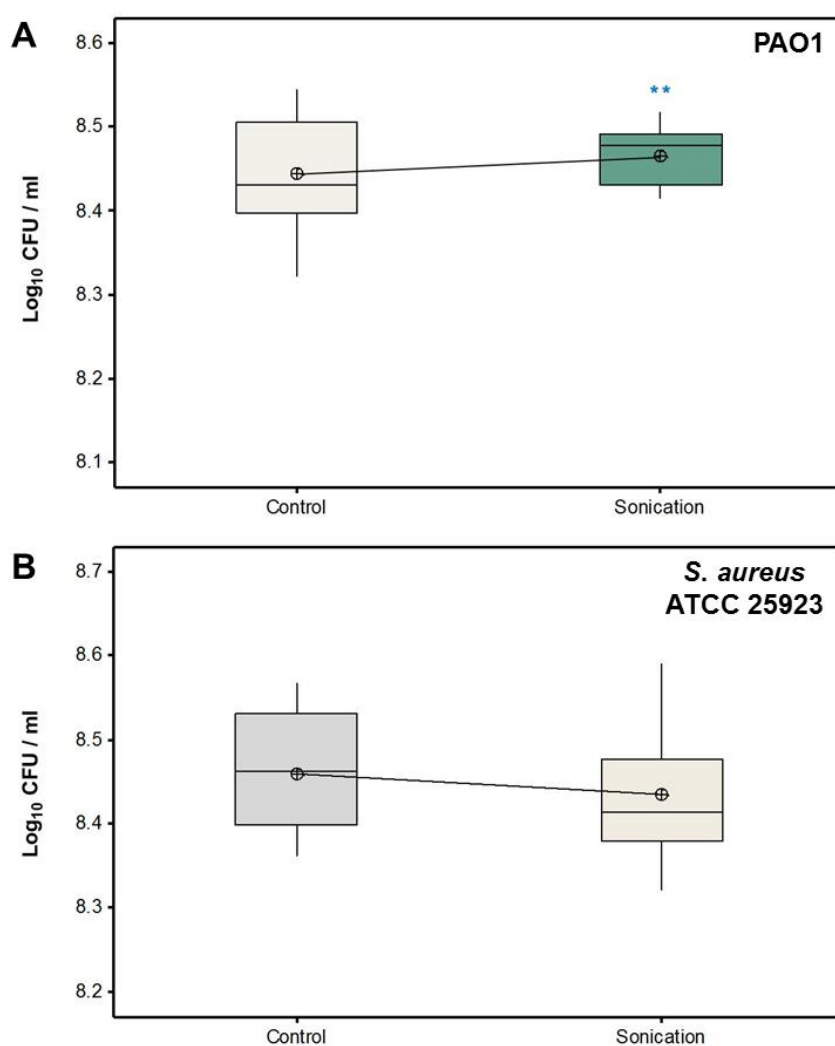
Figure 3.3   No negative effect on cell viability for both Gram-negative and Gram-

Figure 3.3 cont'd: positive type strains after sonication and vortexing. **A** shows an overall lower variability in CFU counts for the PA01 cultures with the sonication and vortexing methodology; with a modestly higher mean of 2.9 x 10^8 CFU /ml (8.47 ± 0.0079; $\log_{10}$ mean ± SEM) compared to the control with 2.8 x 10^8 CFU / ml (8.44 ± 0.018), $P \leq 0.01$. **B** shows no reduction in the viability for cultures of *S. aureus* ATCC 25923 treated with a combination of sonication and vortexing cycles. Box plots show median and inter-quartile ranges; means are shown as encircled cross, $n = 3$.

3.3.2 Positive control for NO mediated biofilm dispersal using *P. aeruginosa* biofilms

Refer to Appendix 4 which outlines the dispersal of monospecies biofilms formed by CF isolates of *P. aeruginosa*.

3.3.3 *In vitro* biofilms for a *B. cepacia* complex CF isolate did not undergo dispersal on exposure to SNP concentrations of 100 nanomolar to 500 micromolar of SNP

In vitro biofilms of a *B. cepacia* complex isolate were grown for 48 h to ensure a confluent biofilm biomass was established prior to exposure to NO. These biofilms were then treated with SNP concentrations of 100 nM – 500 μM for 12 h which corresponds to approximately NO concentrations of 100 pM – 500 nM into media as a result of the slow degradation of SNP (Barraud *et al.*, 2009; Bradley and Steinert, 2015). However, for this NO concentration range, biofilm dispersal was not observed in measurements for: a) the biofilm CFU / cm^2 – cell numbers did not decrease. Interestingly, there was a modest trend of increasing cell numbers; with the control $\log_{10}$ biofilm CFU / cm^2 at 6.30 ± 0.00, 6.47 ± 0.086 for 100 nM SNP, 6.46 ± 0.0791 for 1 μM SNP, 6.51 ± 0.0313 for 100 μM, and 6.46 ± 0.07 for 500 μM (mean ± SD); see Figure 3.4 (A). The planktonic phase CFU / ml – showed growth to be similar to that of the control until concentrations of SNP ≥ 50 μM are introduced. There is a statistically significant higher number of cells in the planktonic phase with 50 – 500 μM SNP ($F_{1, 140}$ = 37.01, $P < 0.001$). This has previously been used by

studies to demonstrate a dispersal event (Barraud *et al.*, 2009). However, this was not reflected in the biofilm CFU/ cm^2 or in the biofilm surface coverage data, see Figure 3.5 for the percentage of the surface covered by biofilm, there no significant difference observed for the control against the pooled SNP concentrations ($F_{1, 140}$ = 0.75, P = 0.388). There was a significantly lower level of surface coverage for the 250 nM SNP treatment compared to that for the 500 nM treatment ($P \leq 0.001$) and additionally when compared to the control (P = 0.024), refer to Figure 3.5. Importantly, this reduction in the surface coverage cannot be attributed to dispersal as this did not correlate with a reduction in the biofilm CFU / cm^2. Moreover, this reduction in the surface coverage from the controls 77% ± 2.58 to 68% ± 2.28 for the 250 nM SNP (untransformed % ± SEM) combined with the modest increase in biofilm CFU / cm^2 values at this concentration could be due to a more densely packed microcolonies as seen in image B within Figure 3.6. This could be further investigated using CLSM, to distinguish if an increase in the biofilm biovolume or biofilm thickness is observed at this SNP concentration.

The chemical controls for the SNP assay effectively demonstrated any noteworthy impact on the biofilm dynamics was due to the presence of NO. The analogue of SNP, PF demonstrated no negative effect on cell growth was observed due to cyanide release, refer to Appendix 3, Figure (i). Also the NO scavenger PTIO further demonstrated that any observable effect in the biofilms was mediated through the presence of exogenous NO release by SNP, refer to Appendix 3, Figure (i).
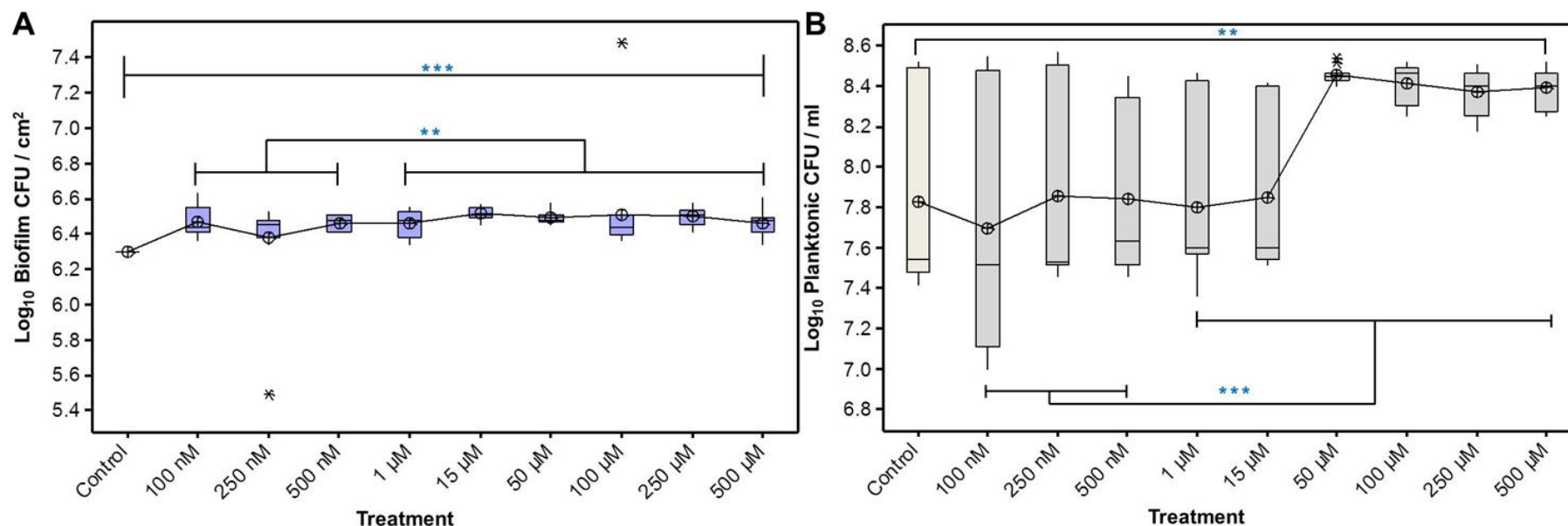
Figure 3.4 *In vitro B. cepacia* complex biofilm (CF isolate A57) treated with nanomolar to micromolar SNP concentrations. No reduction in the biofilm viable biomass noted, Figure A. In **A**, a greater significant difference in the control compared to the pooled SNP treatments as shown with a modest increase in CFU values of up to 0.2 (Log_{10} biofilm CFU / cm^2), $P \leq 0.001$. Nanomolar SNP concentrations differed significantly to the higher micromolar SNP concentrations (50 µM – 500 µM), $P = 0.021$; with a slightly higher biofilm CFU / cm^2 values evident for the micromolar SNP concentrations. In **B**, the planktonic phase showed a significant difference again between the control against the pooled SNP treatments, $P = 0.017$. The CFU / ml values were higher in the micromolar SNP range compared to that observed at nanomolar concentrations, $P \leq 0.001$. For significant differences, blue asterisk marks P values as follows: ** $P \leq 0.01$, *** $P \leq 0.001$. Box plots show median and inter-quartile ranges; means are shown as encircled cross, $n = 3$. Outliers are marked with a black asterisk.
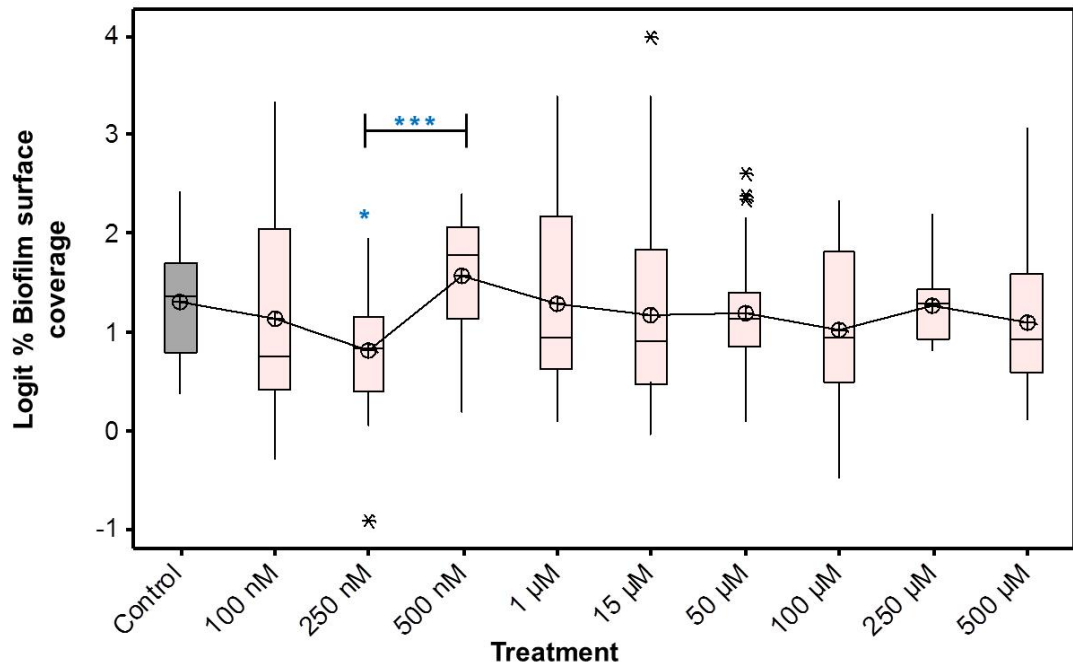
Figure 3.5   Minor reductions in the surface percentage biofilm coverage remaining in a 72 h *in vitro B. cepacia* complex biofilm post treatment with 250 nM SNP for 12 h. Overall no dispersal with SNP concentrations other than at 250 nM SNP; for which a significant difference compared to that of the control was noted, 0.815 ± 0.10 and 1.299 ± 0.10 (mean ± SEM), respectively, *P* = 0.02. A recovery of the biofilm biomass similar to that of the control is evident at 500 nM SNP; with a highly significant difference between the 250 nM and 500 nM SNP treatments, *P* < 0.001. Box plots show median and inter-quartile ranges; means are shown as encircled cross, *n* = 3. Outliers are marked as black asterisks. Blue asterisk highlight statistical significance for *P* values as follows, * *P* ≤ 0.05, *** *P* ≤ 0.001.
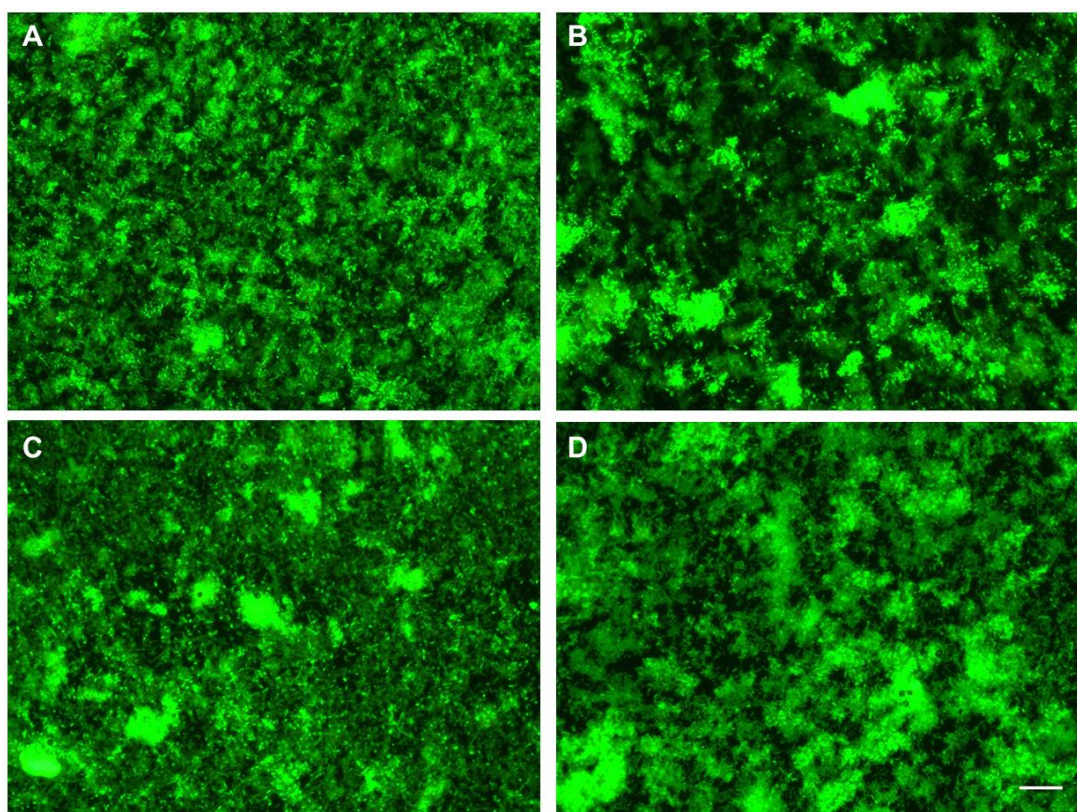
Figure 3.6 Minimal reduction in the surface coverage observed for 48 h *in vitro B. cepacia* complex biofilms treated with the NO donor SNP at 250 nM for 12h. No reduction of biofilm surface coverage noted for all other SNP concentrations. The biofilms were stained using Live/Dead *Bac*Light™ staining and examined using epifluorescent microscopy. (**A**) Control – mat-like coverage over the surface with medium sized microcolonies throughout the surface, (**B**) 250 nM SNP – a minor increase in voids of surface not occupied compared to that observed in the control but microcolonies appear more densely populated, (**C**) 500 nM SNP – biofilm surface coverage similar to that observed in the control and (**D**) 500 μM SNP – similar biofilm surface coverage to that of the control but with larger microcolonies. Images taken using 500x magnification. Scale bar = 20 μm.

3.3.3 A one log reduction in the biofilm biomass was observed for the *in vitro* biofilms of *A. xylosoxidans* treated with SNP concentrations of 100 nM and 50 – 500 µM cannot be attributed to biofilm dispersal

For concentrations of SNP at both 100 nM and ≥ 50 µM, a one log reduction in the biofilm CFU / cm^2 was observed; refer to Figure 3.7 (A). However, this reduction in the biofilm biomass was not as a result of biofilm dispersal triggered by the presence of exogenous NO as observed in other species (Barraud *et al.*, 2009). Firstly, an increase in the planktonic phase was not observed for this SNP concentration range compared to that of the control (*P* = 0.751; Figure 3.7 B). Secondly, there no was notable reduction observed in the biofilm surface coverage for the untreated compared against the pooled SNP treatments ($F_{1, 290}$ = 3.56, *P* = 0.06; Figure 3.8). Thirdly, the chemical controls for the SNP assays demonstrated that this effect cannot solely be attributed to the presence of exogenous NO into the surrounding media, as similarly in these treatments a log reduction in the CFU values was observed, refer to Appendix 3 Figure (ii). Collectively, these results demonstrated that under these experimental conditions, SNP concentrations of 100 nM and from 50 – 500 µM, elicit an effect on the viability of cells within the biofilm phase which cannot solely be attributed to the presence NO.
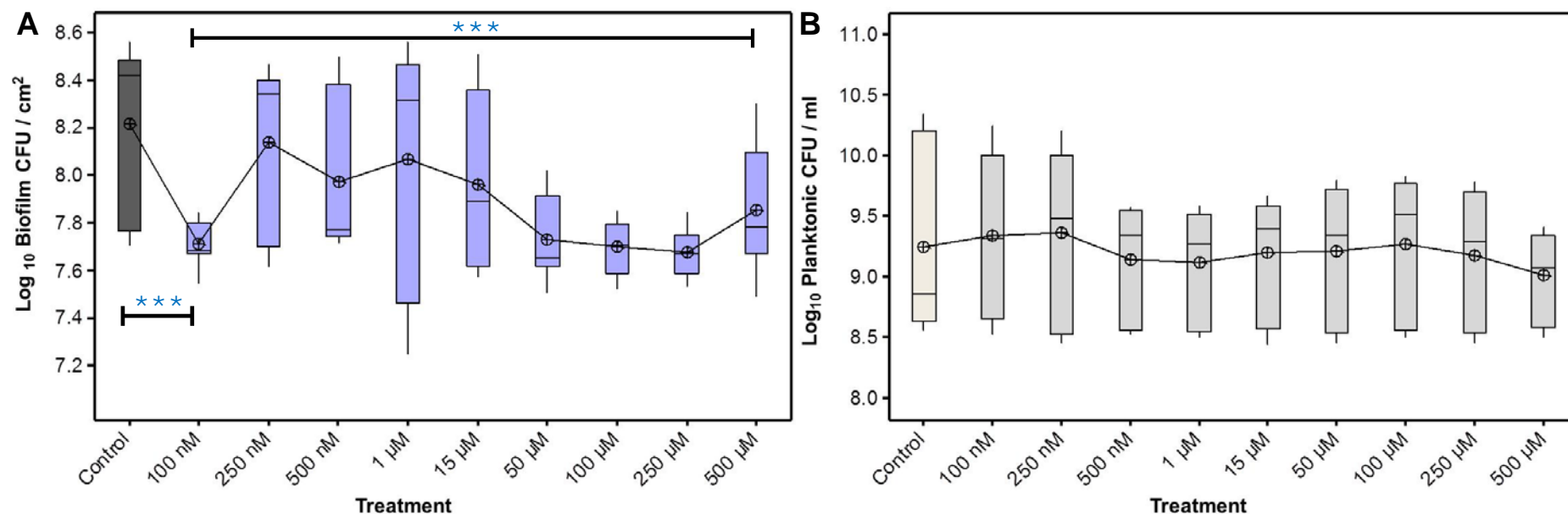
Figure 3.7 *In vitro* biofilms of *A. xylosoxidans* treated with SNP show a reduction in biofilm cells for SNP concentrations > 50 μM but lack an increase in the planktonic phase for CFU /ml at these concentrations. In **A**, the lowest concentration of SNP tested showed a marked decrease in the $\log_{10}$ biofilm CFU / cm^2, with 7.71 ± 0.0858 compared to the control with 8.21 ± 0.349 ($\log_{10}$ mean ± SD; $F_{1, 28}$ = 29.12, $P \leq$ 0.001; one-way Anova. Additionally, a significant reduction in the $\log_{10}$ CFU / cm^2 biofilm phase is noted for the control against the pooled SNP treatments ($F_{1, 140}$ = 18.91, $P < 0.001$). This reduction is evident in the SNP concentrations > 50 μM, with a significant reduction noted between 15 μM SNP compared against that for the 50 – 500 μM SNP treatments ($F_{1, 140}$ = 6.69, $P < 0.01$). However, in Figure **B** this reduction in the biofilm biomass does not result in an increase in the planktonic phase for the SNP treatments when compared to the control ($F_{1, 140}$ = 0.10, $P =$ 0.751), which would correlate with the reversion of the biofilm cells to a planktonic mode of growth. For significant differences, blue asterisk marks *P* values as follows: *** $P \leq 0.001$. Box plots show median and inter-quartile ranges; means are shown as encircled cross, *n* = 3.

116
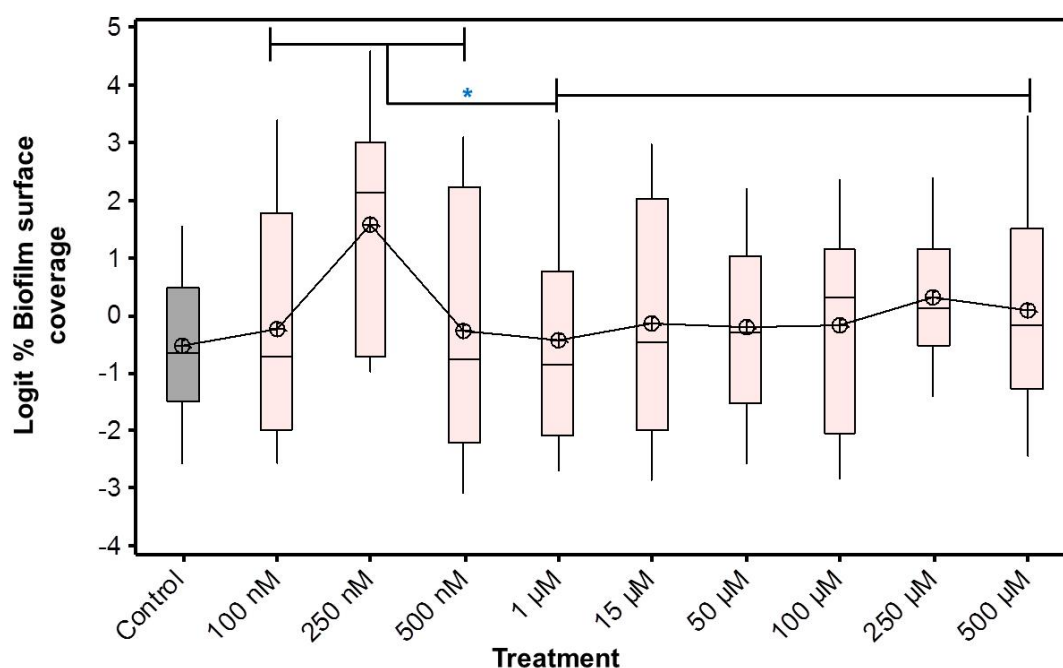
Figure 3.8 No reduction of biofilm surface coverage observed for the 48 h *in vitro A. xylosoxidans* biofilm on treatment with varying SNP concentrations for 12 h. The reduction of biofilm biomass observed in Figure 3.7 (A) for SNP concentrations > 50 µM was not the result of biofilm dispersal but possibly due to an effect exerted on the cell viability within the biofilm structure. There was no significant difference in the control against the pooled SNP treatments ($F_{1, 290}$ = 3.56, *P* = 0.06). The pooled nanomolar range of SNP concentrations showed a higher degree of surface coverage compared to the micromolar SNP concentration range ($F_{1, 290}$ = 4.51, *P* = 0.034). Box plots show median and inter-quartile ranges; means are shown as encircled cross, *n* = 3.
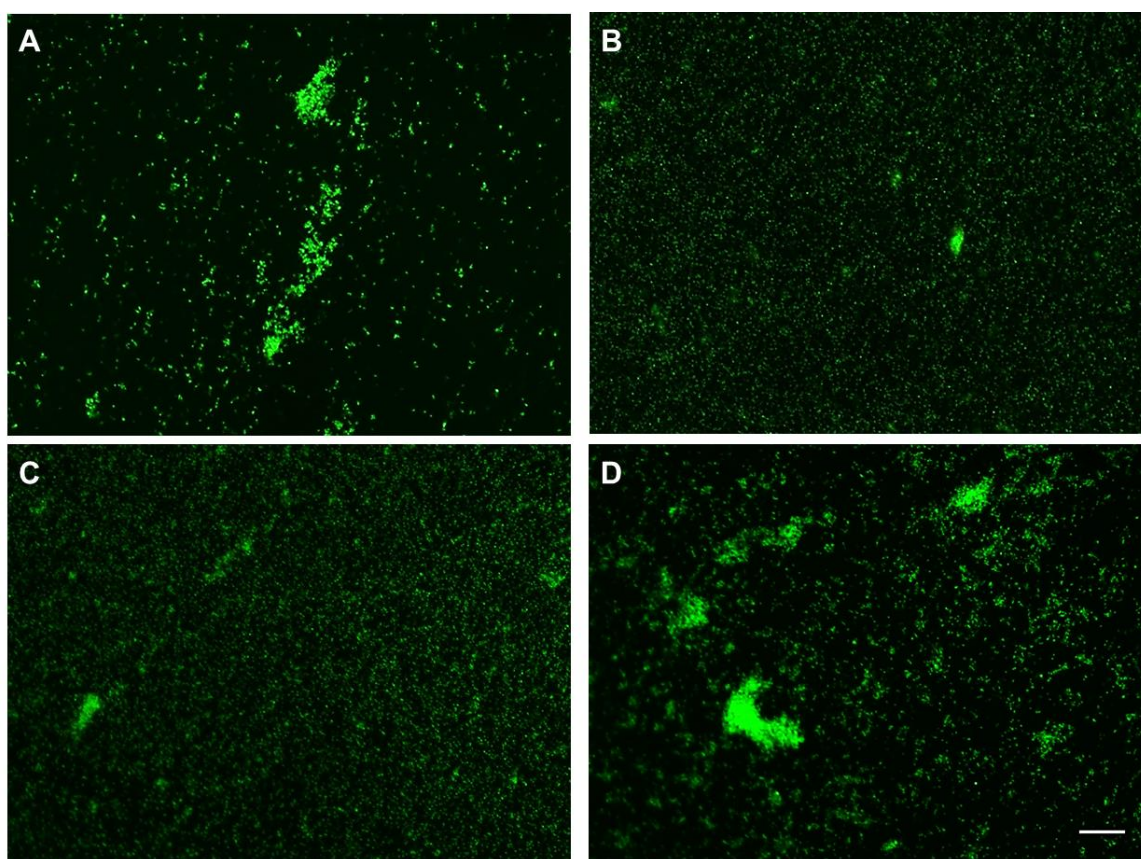
Figure 3.9 No reduction of the biofilm surface coverage observed for the 48 h *in vitro* biofilm of *A. xylosoxidans* after exposure to SNP for 12 h. The biofilms were stained using Live/Dead *Bac*Light™ staining and examined using epifluorescent microscopy. (**A**) Control – minimal surface coverage with medium sized microcolonies , (**B**) 100 nM SNP - showed less densely packed microcolonies a condense mat-like coverage, (**C**) 250 nM SNP – shows an increase in surface coverage and (**D**) 500 μM SNP – biofilm shows more microcolonies with more surface coverage visible, as highlighted in Figure 3.7. Images taken using 500x magnification. Scale bar = 20 μm.

3.3.4 *In vitro S. aureus* biofilms treated with micromolar concentrations of SNP showed a modest reduction in CFU for both the biofilm and planktonic phases

Under the experimental conditions used, no dispersal was observed for confluent 72 h *S. aureus* biofilms exposed to nanomolar and micromolar SNP concentrations. The largest reduction in biofilm surface coverage was 4%, which was observed at 250 µM SNP with a mean biofilm surface coverage of 83% ± 2.78 compared to 87% ± 2.90 for the control (untransformed % ± SEM) which was not significant ($F_{1, 58}$ = 2.78, P = 0.101), Figure 3.11. The only significant difference noted was that between the control compared against the pooled SNP treatments ($F_{1, 290}$ = 2.22, P = 0.021). The micromolar SNP concentrations showed an overall biofilm surface coverage similar to that of the control levels compared to the nanomolar SNP concentrations which showed a low level increase of biofilm surface coverage ($F_{1, 290}$ = 4.81, P < 0.05; Figure 3.11). Interestingly, although biofilm dispersal was not induced in the presence of exogenous picomolar to nanomolar NO by the SNP concentrations used in this study, an effect on the cell viability was observed for the nanomolar NO concentrations, see Figure 3.12. A reduction in cell viability was observed for both the planktonic and biofilm phases (Figure 3.10). A marked drop in the planktonic phase was noted starting from 50 µM SNP and was sustained up to 500 µM SNP which equates to approximately 50 nM – 500 nM of NO. For the biofilm cells, 8.35 ± 0.097 CFU $\log_{10}$ was noted for cells exposed to 100 nM NO and 8.41 ± 0.096 CFU $\log_{10}$ for 50 nM NO compared to the untreated with 8.44 ± 0.06 CFU $\log_{10}$. This observation is similar that noted in a study using NO releasing nanoparticles to reduce the cell burden of MRSA within subcutaneous abscesses in a mouse model, wherein they similarly showed that NO concentrations of 50 nanomolar in a steady-state release over 16 h was effective in reducing the MRSA cell viability (Han *et al.*, 2009a).
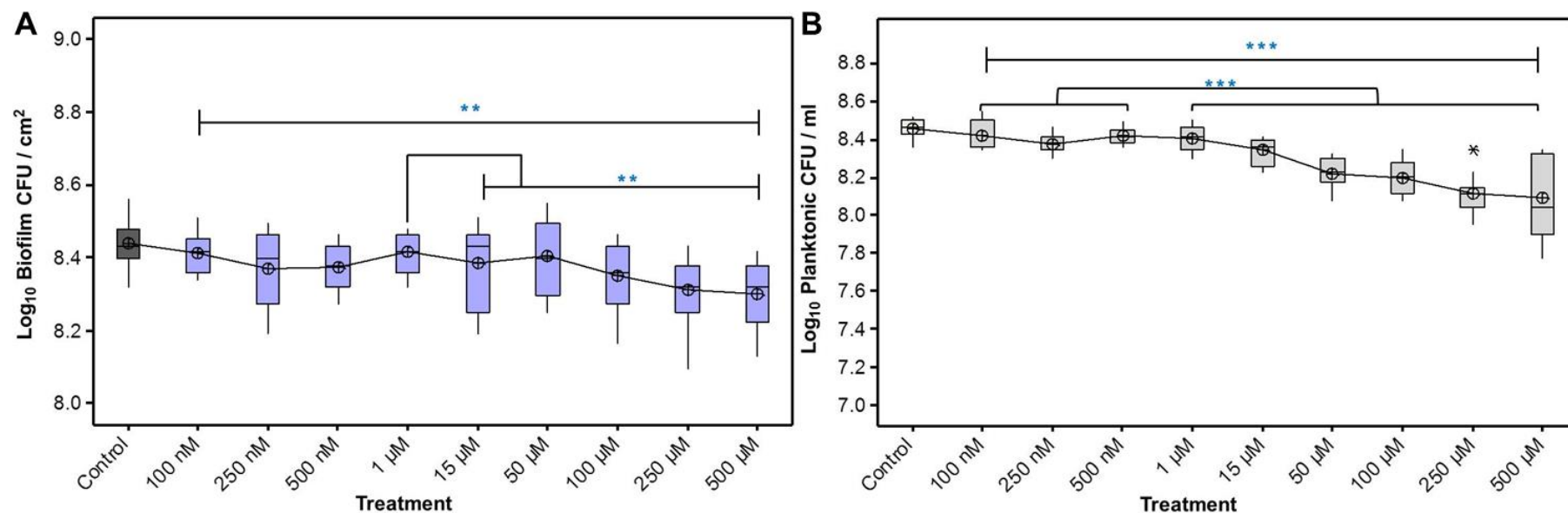
Figure 3.10   SNP concentrations ≥ 15 µM showed a minor decrease in the Log_{10} values for both the biofilm and planktonic phase for 72 h *in vitro S. aureus* biofilms. In Figure **A**, the pooled SNP treatments for the biofilm differed significantly to the control ($F_{, 139}$ = 8.92, P < 0.01). For the 1 µM SNP treatment on comparison against the higher micromolar concentrations of SNP used, there was a greater level of reduction for the higher micromolar treatments ($F_{1, 139}$ = 7.50, P < 0.01). In Figure **B**, a similarly modest reduction was observed for the aforementioned SNP concentrations compared to the control log_{10} CFU /ml values ($F_{1, 139}$ = 48.82, P < 0.001). Additionally, the micromolar concentrations of SNP demonstrated a higher level of cell reduction compared to that by the nanomolar SNP concentrations ($F_{1, 139}$ = 114.79, P < 0.001). For significant differences, blue asterisk mark P values as follows: ** P ≤ 0.01, *** P ≤ 0.001. Outliers are marked as black asterisks. Box plots show median and inter-quartile ranges; means are shown as encircled cross, n = 3.
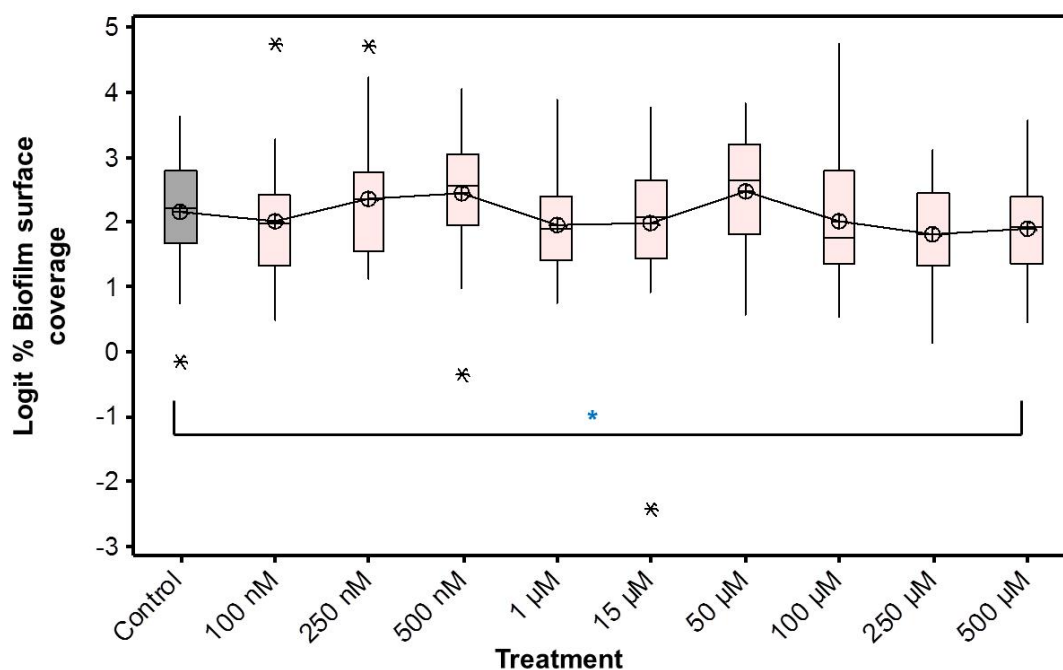
Figure 3.11 A fluctuation in the biofilm surface coverage response to the various SNP concentrations added to a 72 h *in vitro S. aureus* biofilm. For the control against the pooled SNP treatments there was a significant difference notes ($P = 0.021$) with some strong outliers for both the control, the nanomolar range and at 15 µM SNP concentrations was observed. The 100 nanomolar treatment had a significantly lower surface coverage value compared to the pooled higher nanomolar treatments ($F_{1, 290} = 4.81$, $P = < 0.05$). Blue asterisk marks $P < 0.05$. Outliers are marked as black asterisks. Box plot show median and inter-quartile ranges; means are shown as encircled cross, *n* = 3.

The chemical control results for this assay showed that the PTIO effectively scavenged NO with CFU and surface coverage levels similar to the untreated. However, for the PF treatment there was a reduction in both the biofilm and planktonic phase but importantly the reduction noted for both was not greater than observed for SNP concentrations ≥ 100 µM in the biofilm phase (Appendix 3, Figure (iii)). For the reduction observed below 100 µM SNP concentrations, the effect cannot solely but due to the presence of exogenous NO in the media but possibly due to a number of contributing factors such as a) low level of

cyanide release, b) accumulative effect of the continued formation of reactive nitrogen and oxygen species and c) an increase in the pH within the biofilm (Schlag *et al.*, 2007).
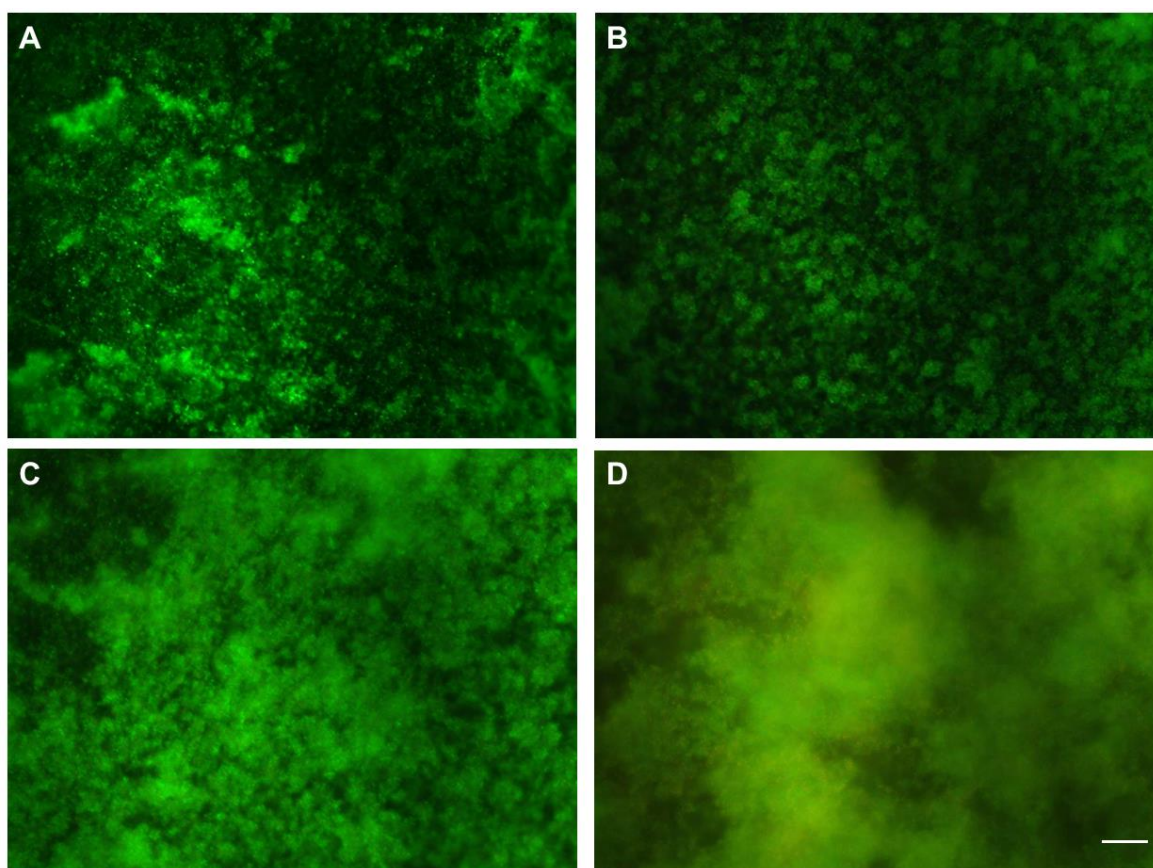
Figure 3.12 Biofilm dispersal not triggered for a 72 h *in vitro* biofilm of *S. aureus* with exposure to exogenous NO for 12 h. The biofilms were stained using Live/Dead *Bac*Light™ staining and examined using epifluorescent microscopy. (**A**) Control – confluent biofilm growth, (**B**) 500 nM SNP – similar level of surface coverage with microcolonies do not appear as dense as those in the control (**C**) 50 µM SNP – no visible reduction in biofilm surface coverage and (**D**) 500 µM SNP – confluent biofilm with more PI dye uptake; an indicator that biofilm cell viability is effected at this concentration. Images taken using 500x magnification. Scale bar = 20 µm.

3.3.5 Minor reduction in the biofilm surface coverage for a 48 h *in vitro* monospecies biofilms of *S. maltophilia* treated with 250 and 500 nM SNP for 12 h

To my knowledge, this is the first set of experiments characterizing the response of both the biofilm and planktonic phase for the *in vitro* biofilms of *S. maltophilia* after exposure to exogenous NO at concentrations ranging from ~ 100 pM – 500 nM. The response was measured using CFU counts (Figure 3.13) and the biofilm structure was imaged (Figure 3.15) to investigate if NO can similarly induce biofilm dispersal for this species as observed in other Gram-negative bacteria (Barraud *et al.*, 2009; McDougald *et al.*, 2012) , over a range of low dose SNP concentrations tested in this study. The largest reduction in biofilm surface coverage was observed for SNP concentrations of 250 and 500 nM, with the percentage surface coverage for these biofilms being 78% and 77%, respectively compared to 84% (untransformed %) for the untreated biofilm; however this difference was not significant ($F_{1, 58}$ = 1.57, P = 0.215) between the control with a logit value of 2.3 ± 1.48 compared to the 250 nM logit of 1.81 ± 1.58 due to the wide variation in the biofilm coverage (logit for the % ± SD; Figure 3.14). However, there was a significant difference between the 500 nM and the untreated ($F_{1, 58}$ = 4.81, P < 0.05). Importantly, this modest reduction in biofilm surface coverage was not reflected in the biofilm biomass CFU data with $\log_{10}$ CFU / cm^2 values of 7.71 ± 0.86 for the control, 7.89 ± 0.92 and 7.68 ± 0.78 observed for the 100 nM and 250 nM, respectively. Additionally, there was no reduction observed for the cells in the planktonic phase on exposure to low concentrations of NO.

Interestingly, there was a 0.39 $\log_{10}$ reduction in the cell viability for the 500 µM SNP concentration (Figure 3.13 (A)) and this effect on the cell viability for the cells within the biofilm structure is visible in the epifluorescent image in Figure 3.15 (D). Wherein, there are cells which have been visibly stained with PI, indicating the bacterial cell membrane has been comprised for these biofilm cells, thereby leading to a lower CFU count. It can be concluded that effects discussed in this section are NO mediated and not a result associated with the other properties of the chemicals based on the data for the chemical controls as shown in Appendix 3 Figure (iv).
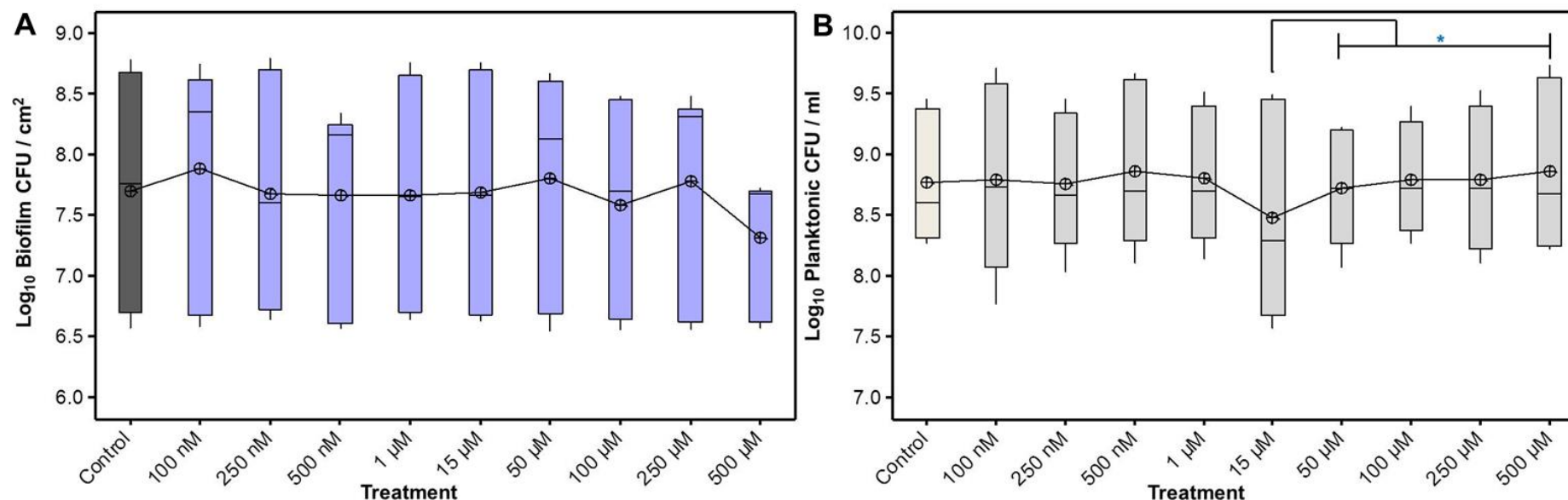
Figure 3.13 The addition of nanomolar to micromolar concentrations of SNP to a 48 h in vitro *S. maltophilia* biofilm did not induce dispersal or an effect on the cell viability for both modes of growth. For Figure **A**, there was no significant reduction in the biofilm CFU / cm^2 values for the control compared against the pooled SNP treatments ($F_{1, 140}$ = 0.02, *P* = 0.898) or for the control compared at the 500 µM SNP treatment ($F_{1, 28}$ = 2.18, *P* = 0.151). Figure **B**, there was a significant reduction in the log$_{10}$ CFU / ml for the cells in the planktonic phase treated with 15 µM SNP when compared to that for the 50 – 500 µM range ($F_{1, 140}$ = 3.81, *P* = 0.05) but not of significance when compared against the c comparedagainstthecontrol ($F_{1, 40}$ = 1.53, *P* = 0.227). Blue asterisk marks a *P* value ≤ 0.05. Box plots show median and inter-quartile ranges; means are shown as encircled cross, *n* = 3.
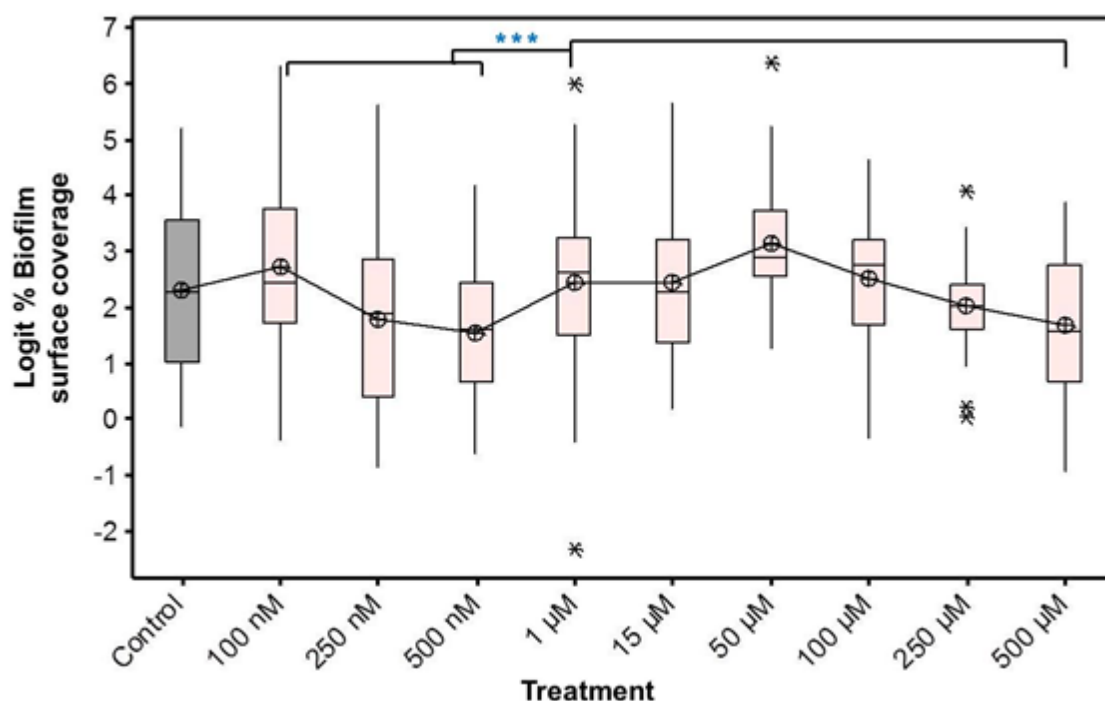
Figure 3.14 Low level of reduction in the biofilm surface coverage for 48 h *in vitro S. maltophilia* biofilms treated for 12 h with 250 – 500 nM SNP. This reduction was not significant when compared to the control ($F_{1,\,290}$ = 0.878, P = 0.878). But on comparing the 250 – 500 nM SNP treatments which showed a lower level of surface coverage compared to that in the 100 nM they differed significantly ($F_{1,\,290}$ = 11.15, $P \leq$ 0.001). This reduction in surface did not result in a log reduction in the CFUs for the biofilm. Blue asterisks for $P \leq$ 0.001. Outliers are marked as black asterisks. Box plot show median and inter-quartile ranges; means are shown as encircled cross, n = 3.
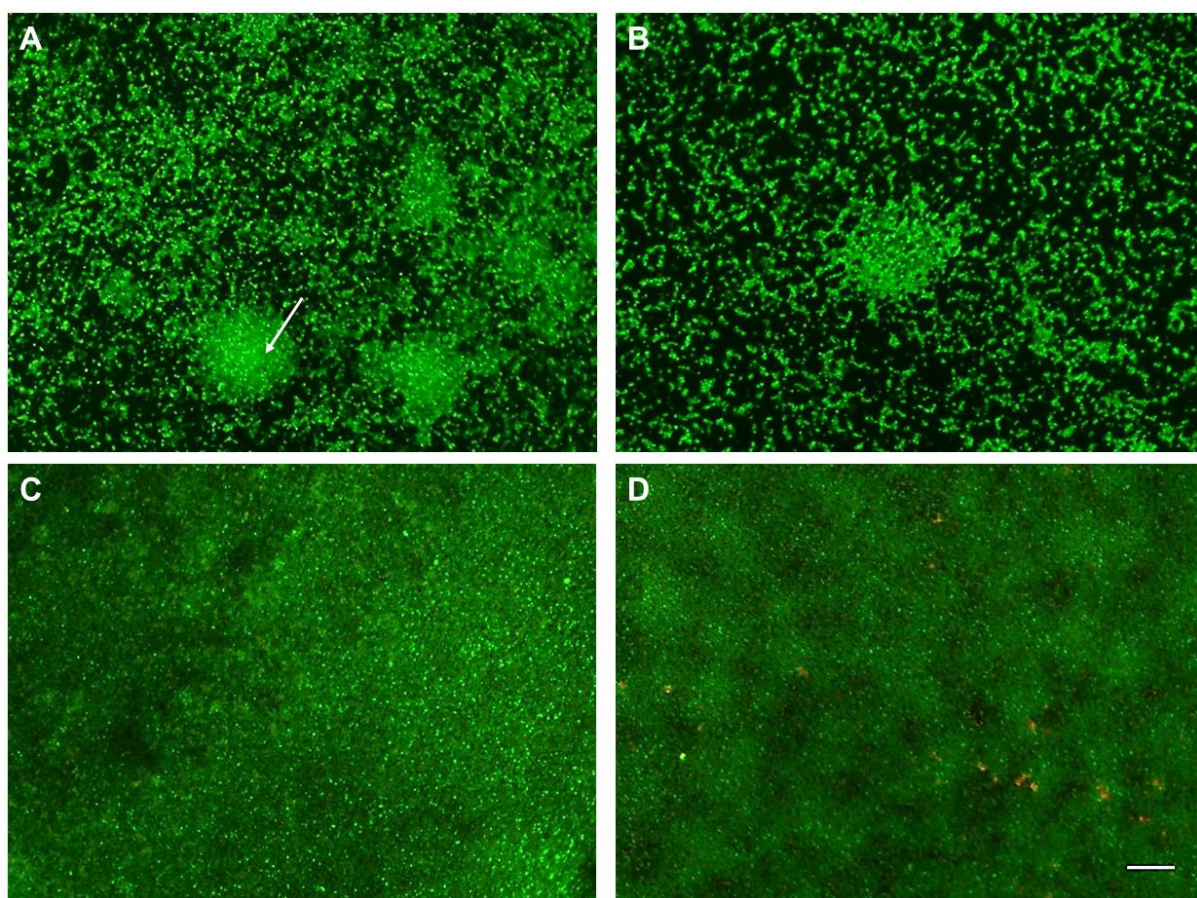
Figure 3.15 A low level of reduction in the biofilm surface coverage for 48 h *in vitro* biofilms of *S. maltophilia* when exposed to 250 – 500 nM SNP concentrations for 12 h. The biofilms were stained using Live/Dead *Bac*Light™ staining and examined using epifluorescent microscopy. (**A**) Control – different biofilm structure compared to the micromolar SNP concentrations but with visibly medium sized microcolonies with cells visibly supported within EPS clumps, denoted by the white arrow, (**B**) 250 nM SNP – a modest reduction in the surface coverage with similar biofilm structure as that observed for the control, (**C**) 50 µM SNP – biofilm surface coverage and topography is markedly different to that in the control compared to the SNP treatments as also seen in (**D**) 500 µM SNP – mat-like coverage of the biofilm with cells visible in the upper layer of biofilm which have PI dye uptake, indicating that biofilm cell viability has been effected. Images taken using 500x magnification. Scale bar = 20 µm.

3.3.6 Exogenous NO failed to induce biofilm dispersal in *S. pneumoniae* biofilms but instead reduced cell viability in sessile and planktonic cells

There was a 1.5 – 2 $\log_{10}$ reduction for the cells within the biofilm of a 6 day *in vitro* biofilm of *S. pneumoniae* treated with SNP concentrations ≥ 50 μM for 12 h, with the untreated $\log_{10}$ CFU / cm^2 data values of 5.97 ± 0.51 compared to that observed for the 500 μM treatment with 4.5 ± 1.27 (mean $\log_{10}$ ± SD; $F_{1,\ 28}$ = 17.73, $P \leq 0.001$; Figure 3.16 (A)). However, this reduction did not result with a decrease in biofilm surface coverage or notably affect the topography of the biofilm, Figure 3.18. Additionally, a 0.82 – 2.1 $\log_{10}$ reduction in the planktonic CFUs for the aforementioned SNP concentration range was noted (Figure 3.16 (B)). A recent study also demonstrated that low exogenous concentrations of NO released by SNP did not cause dispersal for this species (Allan *et al.*, 2016). Notably, the authors showed a marked reduction in viable cells for both the biofilm and planktonic phase exposed to 1 mM SNP (Allan *et al.*, 2016) which is double the highest concentration of SNP used in this study but corroborates that the biofilm reduction is not as a result of dispersal . Importantly, in this study the biofilms were exposed to exogenous NO treatment six times longer than that used by Allan *et al.*, 2016. This may explain the low level of cell reduction observed at the lower concentrations used in this study compared to the higher concentrations and shorter duration of the assay used in the other aforementioned study. Moreover, the longer duration of treatment would allow for the accumulative effect of toxic intermediates from cell death and increase the exposure to the reactive intermediates NO forms in the presence of oxygen and superoxide such as N_2O_4 and peroxynitrite, respectively.

The chemical controls used for the SNP assay showed the effects observed were due to the presence of NO, refer to Appendix 3 Figure (v).
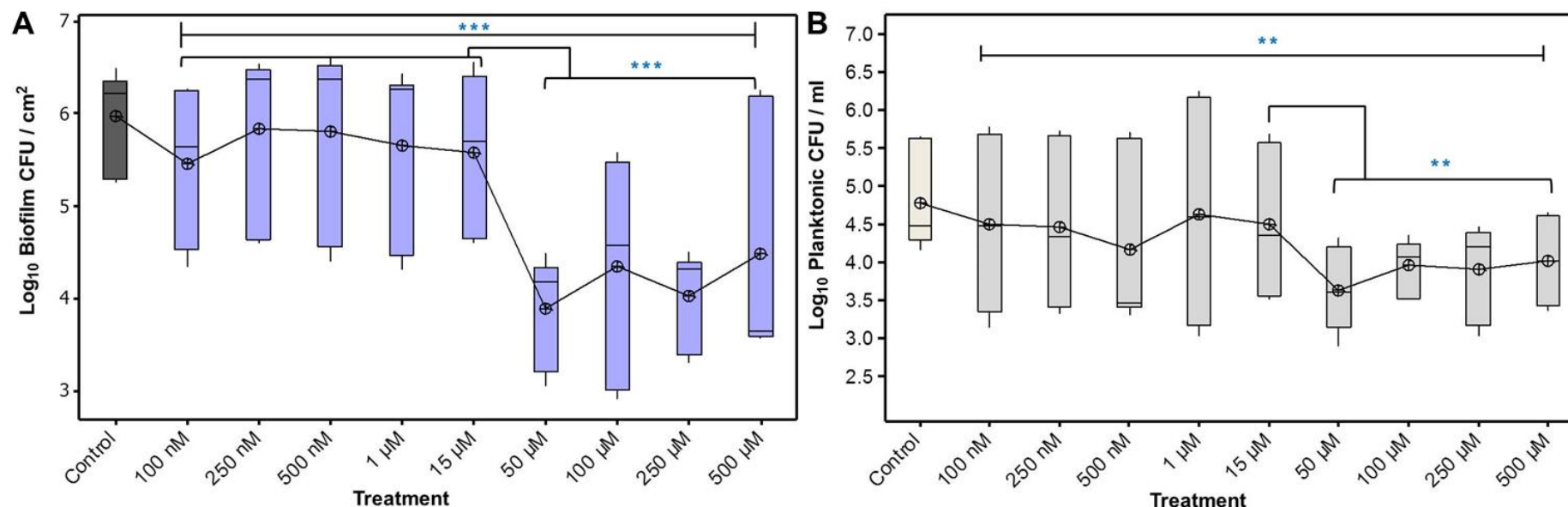
Figure 3.16 No dispersal but an effect on the cell viability of cells within the biofilm and planktonic phase was demonstrated for 6 day old *in vitro S. pneumoniae* biofilms treated with SNP for 12 h. Figure **A** for the $\log_{10}$ biofilm CFU /cm^2 showed a significant pooled effect compared to that of the control ($F_{1, 140}$ = 16.83, $P \le 0.001$). A greater reduction in the biofilm cells for SNP concentrations $\ge$ 50 µM was noted compared to that for the SNP concentrations $\le$ 1 µM ($F_{1, 140}$ = 31.73, $P \le 0.001$). Figure **B**, also demonstrates marked difference between the pooled SNP treatments against the control ($F_{1, 140}$ = 6.24, $P \le 0.01$). Similar to the biofilm phase, this effect was more pronounced in the 50 – 500 µM SNP range against that observed for the 15 µM SNP treatment ($F_{1, 140}$ = 6.74, $P \le 0.01$). Blue asterisk marks: ** indicates $P \le 0.01$ and *** indicates $P \le 0.001$. Box plots show median and inter-quartile ranges; means are shown as encircled cross, n = 3.
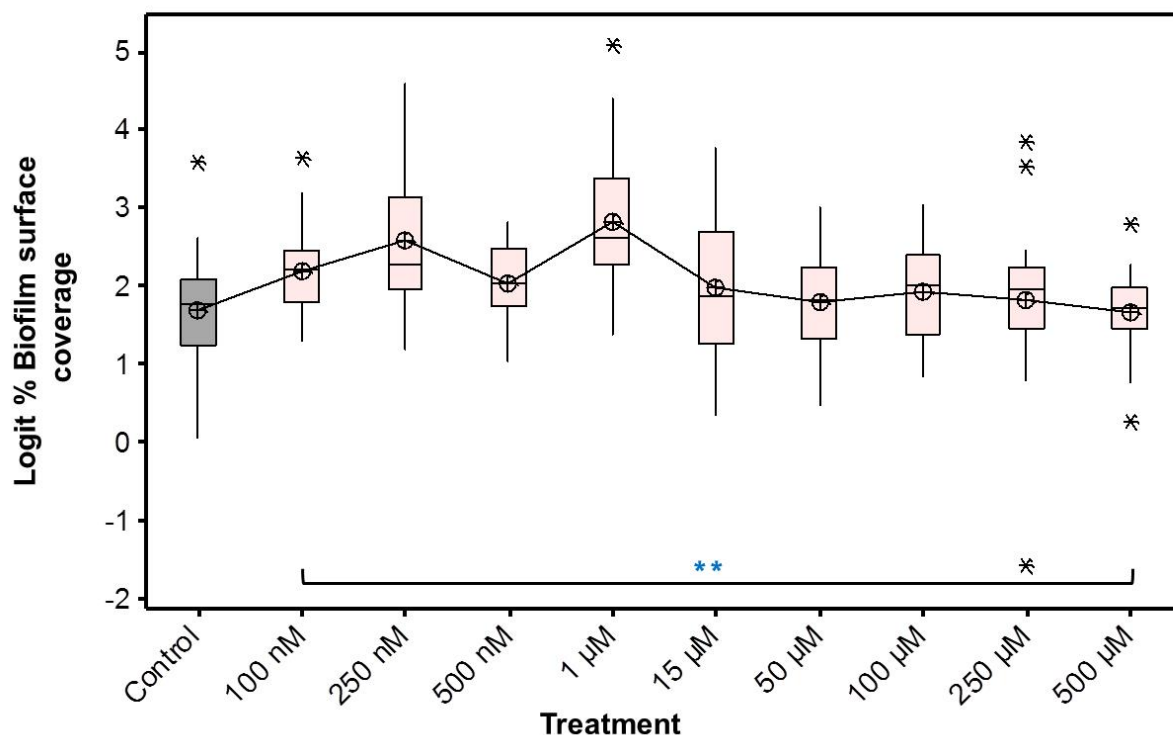
Figure 3.17 Exogenous NO did not induce biofilm dispersal for 6 day *in vitro S. pneumoniae* biofilms. On comparing the control against the pooled SNP treatments, there was a marked difference ($F_{1, 290}$ = 8.79, $P < 0.01$). This was due a modest increase in surface coverage observed for the SNP concentration of 1 μM compared to that observed in the higher micromolar concentrations, at this range a return to the control level is evident ($F_{1, 290}$ = 45.65, $P < 0.01$). Blue asterisk marks for $P < 0.01$. Black asterisk marks outlier values. Box plot show median and inter-quartile ranges; means are shown as encircled cross, n = 3.
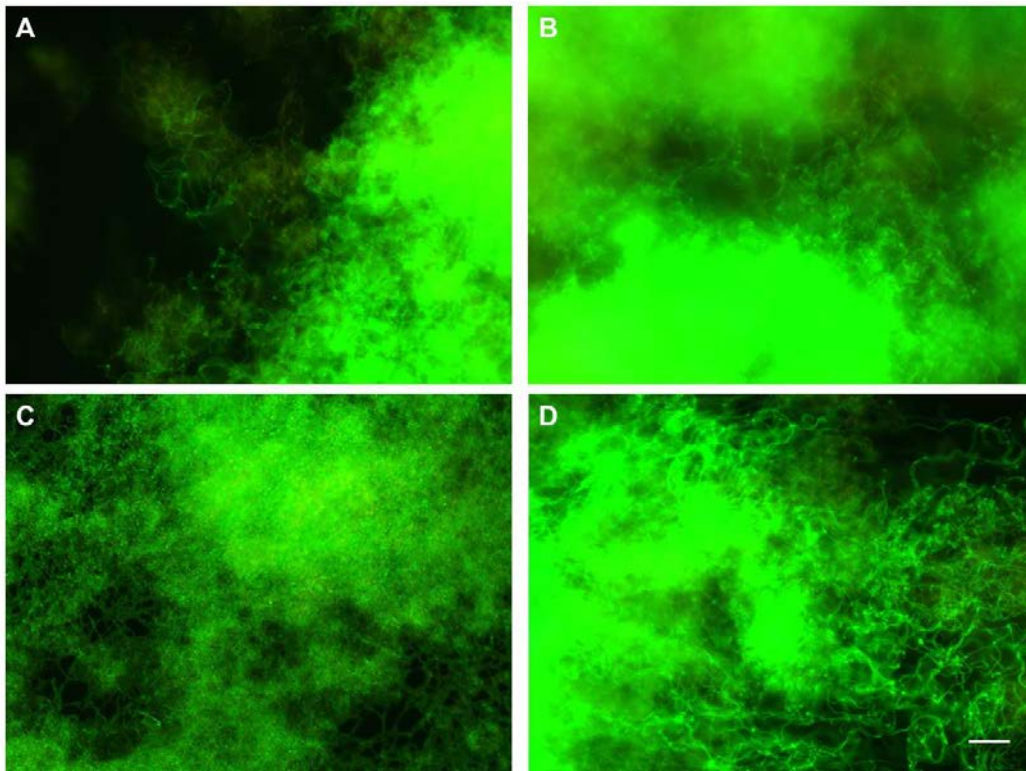
Figure 3.18 No dispersal observed for 6 day old *S. pneumoniae in vitro* biofilms treated with SNP for 12 h. The biofilms were stained using BacLight Live/Dead staining and examined using epifluorescent microscopy. (**A**) Control- confluent biofilms with pneumococcal chains visible with an abundance of EPS with a mean surface coverage of 82% ± 2.47, (**B**) 250 nM SNP – similar biofilm architecture but a higher mean surface coverage of 91% ± 3.04 , (**C**) 1 µM SNP – similar biofilm structure 93% ± 3.10 (**D**) 500 µM SNP – no change to the biofilm architecture but the biofilm surface coverage has returned to the untreated level, at 83% ± 2.77 (untransformed % biofilm surface coverage ± SEM). Images taken using 500x magnification. Scale bar = 20 µm.

3.3.7 *Ex vivo* CF sputum biofilms dispersed when treated with 500 μM SNP, biofilm dispersal induced for 3 *ex vivo* CF sputum biofilms

This study investigated if it is possible to disperse mixed species biofilms which form from enriched CF sputum samples. The biofilms where grown on MatTek dishes in the presence of a nutrient rich medium (BHI) and treated with 500 μM SNP for 15 h. The concentration and duration of the SNP treatment was used due to its effectiveness in dispersing well established biofilms formed by CF isolates of *P. aeruginosa*, based on work previously conducted Dr Robert P. Howlin (Howlin *et al.*, 2017).

The 24 h *ex vivo* biofilms dispersed when exposed to exogenous NO for 15 h. This reduction in the biofilm biovolume is clearly visible in Figure 3.19. The biofilm biovolume and average biofilm thickness parameters as measured in Comstat2 also showed a reduction (Figure 3.20; Table 3.2).

Table 3.2 Minor reduction in the *ex vivo* mixed-species' average biofilm thickness treated with 500 μM SNP.

Patient	Control Average Thickness (μm) SYTO9 Channel Mean (SD)	500 μM SNP Average Thickness (μm) SYTO9 Channel Mean (SD)
A03	4.89 (1.61)	4.25 (1.84)
A35 Sample (S1)	7.21 (2.89)	3.72 (0.23)
A35 Sample (S2)	5.78 (1.36)	4.52 (2.49)
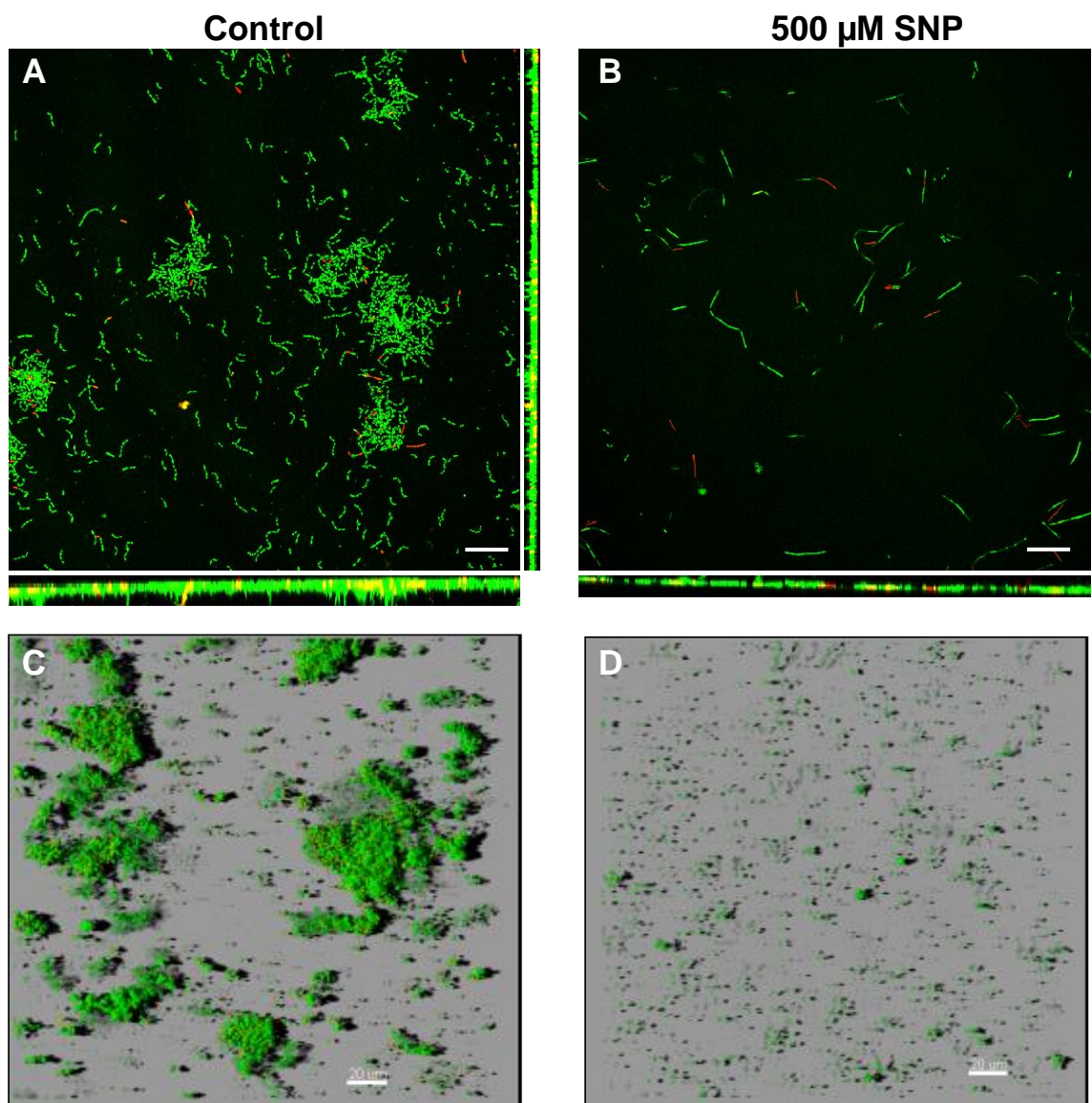
Figure 3.19 Micrographs representing z-stack images of *ex vivo* CF sputum mixed species biofilms, untreated and treated with 500 μM SNP. A visible reduction in the biofilm coverage was observed for the biofilms treated with ~ 500 pM exogenous NO. After Mucolyse treatment, the *ex vivo* CF sputum was added to a MatTek dish for a 1.5 h attachment period prior to removal. BHI broth was added to each MatTek and the biofilms formed after 24 h were treated with 500 μM SNP. The LAS X software from Leica was used to construct the micrographs for (**A**) and (**B**), which show a maximum projection of the biofilms with the panels below the image showing the xzy stack profile and the panel to the right shows the zyx profile of the biofilm. Micrographs for (**C**) and (**D**) represent aerial 3D images, obtained using IMARIS (v7.4.2 trial version). Micrographs : (**A**) untreated biofilm for Patient A03, (**B**) 500 μM SNP treated biofilm for Patient A03, (**C**) untreated biofilm for patient A35 (S1) and (**D**) 500 μM SNP treated biofilm for patient A35 (S1). Scale bars = 20 μm.
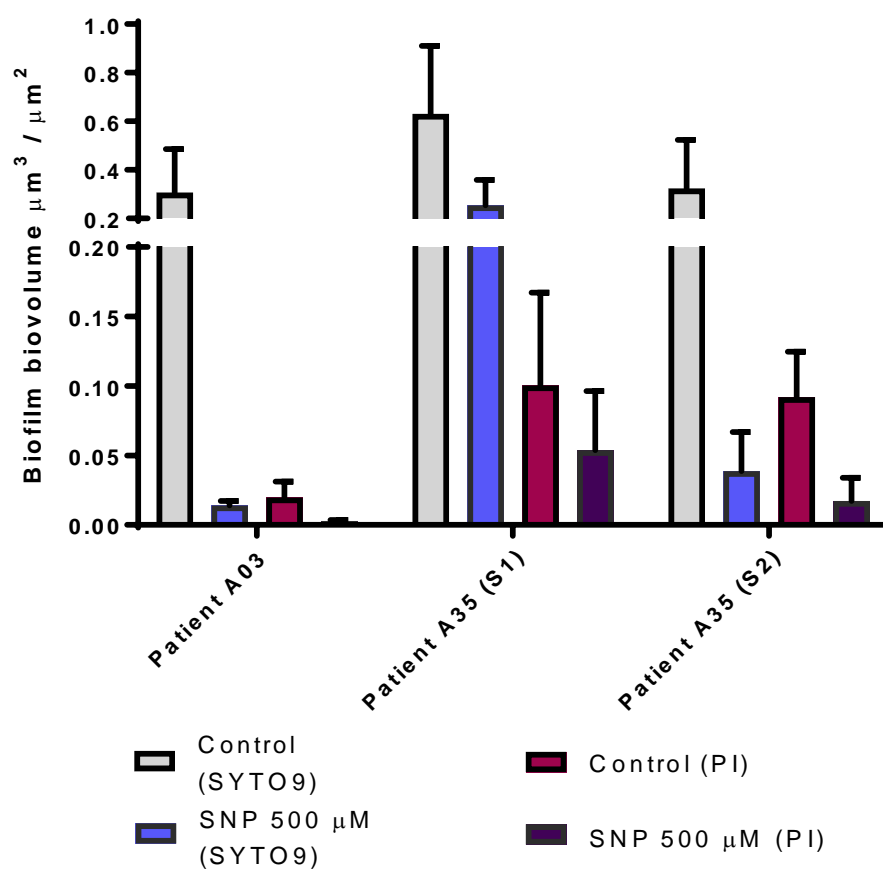
Figure 3.20 The mixed species biofilm biovolume formed from *ex vivo* CF sputum after 24 h of growth undergo dispersal on exposure to ~ 500 pM exogenous NO using the NO donor SNP. After treatment with 500 μM SNP for 15 h, a reduction in the biofilm biovolume was observed for all *ex vivo* biofilms in both the SYTO9 and PI channels imaged. Quantification of the biofilm biovolume was measured by Comstat2. Two sputum samples were collected from patient A35, sample 1 (S1) and sample 2 (S2) were sampled weeks apart. Error bars for ± SEM. Insufficient data for statistical purposes. Five representative z-stacks imaged per treatment per patient from one experiment (*n* = 1).

3.4 Discussion

In this Chapter, the application of low exogenous concentrations of NO to pre-established monospecies biofilms formed by CF isolates was investigated for the potential use as a biofilm dispersal agent to enhance the efficacy of antibiotic treatments. The work revealed 1) in contrast to the established dispersal response of *P. aeruginosa* to low exogenous concentrations of NO; this was not observed for the CF microorganisms tested, 2) the potential use of NO at higher concentrations as a bactericidal agent against monospecies biofilms formed by *A. xylosoxidans*, *S. aureus* and *S. pneumoniae*; which requires further investigation and 3) e*x vivo* mixed species biofilms formed from CF sputum could be successfully dispersed using 500 μM of the NO donor SNP, which merits further investigation.

Biofilm dispersal not induced for in vitro B. cepacia complex biofilms with low exogenous NO concentrations

It this chapter it has been demonstrated that the addition of picomolar to nanomolar exogenous NO concentrations to a mature *in vitro B. cepacia* complex biofilm was not shown to induce biofilm dispersal with the exception of one NO concentration in this species similar to that observed in other Gram-negative species (McDougald *et al*., 2012; Figure 3.4, 3.5 and 3.6). For 250 nM SNP a reduction of 9% in the biofilm surface coverage analysis was shown (Figure 3.5) and this was observable in the images of the biofilm structure as seen in Figure 3.6 B. Despite this reduction, no observable effect was measured in the biofilm CFU data and qualitatively based on the imaging, the biofilm architecture appeared more densely packed at 250 nM compared to the untreated biofilm. Instead, a modest increase of 0.2 $\log_{10}$ for the biofilm CFUs was observed for all SNP concentrations tested as shown in Figure 3.4 A, this increase was not mirrored in the biofilm surface coverage (Figure 3.5; Figure 3.6). In the planktonic phase for SNP concentrations $\geq$ 50 μM an increase in the CFUs was also observed (Figure 3.4 B). Importantly, a similar modest level of increase in both the planktonic and biofilm phases occurred in the SNP chemical controls, again without an impact on the biofilm surface coverage (Appendix 3 Figure (i)). Collectively, the results of this study demonstrate that

biofilm dispersal in the presence of low concentrations of exogenous NO was not achieved for the *in vitro* biofilms formed by this *B. cepacia* complex isolate.

Instead, the addition of SNP, PF and PTIO all resulted in a minor increase in the number of cultivable cells recovered from both the biofilm and planktonic phases, with the exception of the planktonic phase at concentrations of 100 nM to 15 μM SNP. This phenomenon may be due to a number of combinatorial factors relating to the interesting physiology of this species.

Firstly, both SNP and PF contain cyanide, which is slowly released during the breakdown of these compounds among other products such as NO_2^- and NO_3^- (Ikeda *et al.*, 1987). This is important as *B. cepacia* complex members have been shown to be cyanogenic during biofilm growth (Ben Ryall *et al.*, 2008) and therefore are capable of tolerating and utilizing low millimolar concentrations of cyanide (Adjei and Ohta, 1999). Intriguingly, in relation to CF lung infection the ability to produce, utilize and therefore tolerate cyanide is extremely beneficial against competing microorganisms with the exception of *P. aeruginosa*, which also been shown to produce cyanide (Ryall *et al.*, 2008a). Cyanide concentrations of up to 130 μM have been detected within CF sputum, a factor not independent of *P. aeruginosa* infection in the lungs (Ryall *et al.*, 2008b). This similar ability most likely explains why in the latter stages of CF lung infection both *P. aeruginosa* and *B. cepacia* complex can co-colonize the CF lung.

Secondly, the NO scavenger PTIO also showed a similar increase in CFUs which could possibly be explained by the low level of PTIO oxidizing NO forming PTI and $^\bullet NO_2$. This resulting breakdown product $^\bullet NO_2$ can react with NO to form N_2O_3; which is unstable in aqueous conditions and forms nitrite NO_2^- (Ignarro, 2000). Both factors mentioned additionally result in the accumulation of NO_2^- and NO_3^- during the degradation of these compounds and it has been demonstrated by Drevinek *et al.*, 2008 that the accumulation of these reactive nitrogen species resulted in *B. cenocepacia* up-regulating the expression of

NO$_2^-$ reductase. Moreover, *B. thailandensis* and *B. pseudomallei* have been shown to reduce nitrate under anaerobic conditions (Andreae, 2014). The above factors may account for the amelioration of the CFU counts observed in this study.

Finally, NO mediated dispersal of other bacterial species has been linked with the interference in the intracellular levels of c-di-GMP (Barraud *et al.*, 2009). The levels of c-di-GMP are controlled by GGDEF, EAL and HD-GYP domains (Ryan, 2013), it has been demonstrated the *B. pseudomallei* KHW has an EAL domain which produces an active phosphodiesterase called *cdpA* which was shown to have a direct effect on biofilm formation (Lee *et al.*, 2010). Although, these domains have been shown to be present within *Burkholderia* spp., dispersal of this species through the addition of exogenous NO was not demonstrated under the conditions used in this study.

Varied response to treatment with SNP for the in vitro A. xylosoxidans biofilms

A log reduction in the biofilm CFU counts was observed at SNP concentrations of 100 nM and ≥ 50 µM (Figure 3.7 (A)) and this was also observed in both the SNP chemical controls used as seen in Appendix 3, Figure (ii). The planktonic phase however was not affected. This reduction was not reflected in the biofilm surface coverage data for all SNP treatments, each of which showed an increase of ~ 10% in the mean percentage surface coverage analysed compared to the untreated (Figure 3.8). *A. xylosoxidans* is a denitrifying bacterium and therefore has systems which are capable of reducing nitrite, nitrate and importantly NO in low oxygen conditions (Farver *et al.*, 1998). There are two key factors which are of direct importance in this study: 1) the *in vitro* biofilms were not grown under low oxygen or anaerobic conditions and 2) the biofilms where exposed to SNP for a period of 12 h and therefore steady levels of exogenous NO would be maintained under these conditions. Importantly, previous studies have shown that denitrifiers can maintain NO concentration levels varying between 1 – 65 nanomolar (Goretski *et al.*, 1990; Cutruzzolà, 1999) and therefore at this range denitrifying bacteria are capable of preventing the cytotoxic nature of NO within this nanomolar range. Therefore,

the reduction observed in this study could possibly be due to a metabolic arrest for the SNP treatments ≥ 50 μM which would correspond with the release of ~ 50 nM – 500 nM NO for this SNP range used and explain the combined effect for the reduction in the biofilm CFUs but modest increase in the biofilm surface coverage.

In a study using *Nitrosomonas europaea,* a bacterium capable of denitrification, increasing NO exposure was shown to influence the metabolic activity and result in greater biofilm formation compared to that observed on the removal of NO or lowered concentrations of NO (Schmidt *et al.*, 2004). Moreover, the biofilm architecture as seen in Figure 3.9 is notably different to that of the untreated; as the SNP concentration increases the biofilm shows more of a mat coverage with visibly larger microcolonies evident at the 500 μM SNP treatment which could be a response to nitrosative stress. Also, if conditions were so unfavourable then a greater log reduction in CFUs would be expected after the 12 h of treatment. The change in biofilm architecture would also result in a higher gradient of oxygen concentrations thereby creating low oxygen niches, an environment more suited to the denitrification process. The 100 nM SNP treatment showed a similar level of biofilm surface coverage to that of the untreated. Additionally, the biofilm displayed a less dense mat coverage with undefined microcolonies in contrast to that observed on increasing the SNP concentrations (Figure 3.9). So the reduction in the biofilm CFU counts observed at this SNP concentration would need to be investigated both under aerobic and anaerobic conditions to distinguish if the environmental conditions alone can ameliorate this effect when the biofilm structure is less densely packed. Collectively, this study shows that the low exogenous concentrations of NO used do not mediate biofilm dispersal for *A. xylosoxidans* biofilms.

Low concentrations of exogenous NO did not result in biofilm dispersal for in vitro S. aureus biofilms but affect cell viability

Biofilm dispersal of pre-established *in vitro S. aureus* biofilms was not observed for the SNP range of concentrations used in this study (Figure 3.11

and Figure 3.12). However, from treatments of SNP at concentrations above 250 nM a reduction trend in the CFU data for both the biofilm and planktonic phase was observed, albeit a modest reduction, refer to Figure 3.10. Additionally, the effect in cell viability is particularly notable for the *in vitro* biofilm treated with 500 µM SNP, in which there appears to be more of an uptake of PI, with yellow fluorescence visible, indicating the cell membrane integrity has been comprised for some biofilm cells at this concentration (Gião *et al.*, 2009) (Figure 3.12). There are currently a number of studies which have demonstrated a reduction in *S. aureus* biofilm cell viability through the use of nitric oxide releasing nanoparticles (Hetrick *et al.*, 2009), gaseous nitric oxide (Ghaffari *et al.*, 2007), NO probiotic patches (Jones *et al.*, 2010) and NO loaded zeolites (Fox *et al.*, 2010). In a study by Han *et al.*, 2009b, they used a mouse model to show a subcutaneous abscesses infected with MRSA was reduced when treated with NO nanoparticles and additionally, work by Martinez *et al.*, 2009 showed the NO releasing nanoparticles were bactericidal for *S. aureus* at NO concentrations of 12.5 nM for MSSA and 25 nM for MRSA. These NO concentrations correspond to that used in this study, in which only a minor reduction was noted.

An important difference, between the work in this chapter and the aforementioned studies, pre-established confluent biofilms were not tested. However, other studies using NO releasing nanoparticles have shown that NO concentrations of 1.25 – 5 µM are required before a bactericidal effect can be observed against *S. aureus* biofilms and against the biofilms of other Gram-positive and Gram-negative bacteria (Hetrick *et al.*, 2009). Collectively, this implies that NO is more effective as a bactericidal agent against *S. aureus* biofilms, this could be explored as a potential treatment in CF lung infection.

Low picomolar to nanomolar concentrations of nitric oxide did not induce biofilm dispersal for in vitro S. maltophilia biofilms

This is the first study to my knowledge which has evaluated the effect low concentrations of exogenous NO have on pre-established *in vitro* biofilms of *S. maltophilia.* The quantification of the biofilm and planktonic phase overall

showed no significant reduction in the CFU counts. The only notable observations were: 1) the surface topography of the biofilms became more of a mat/uniform coverage with micromolar concentrations of SNP compared to medium sized microcolonies in the untreated and in the nanomolar SNP treatments, as seen in Figure 3.15; 2) A small fraction of cells within the biofilms treated with 500 µM SNP are visibly red indicating that the PI stain has out competed SYTO9 stain and therefore there is considerable damage to the cell membranes of the cells in the upper section of the biofilm as seen in Figure 3.15 D. Therefore, further work with higher concentrations of SNP would be required to establish the concentration at which exogenous NO becomes a bactericidal agent against pre-established *S. maltophilia* biofilms.

Dispersal not triggered but an adverse effect on cell viability for pre-established S. pneumoniae biofilms was observed

Low exogenous concentrations of NO did not trigger biofilm dispersal in *S. pneumoniae* biofilms grown for 6 days prior to a 12 h treatment with varying concentrations of SNP (Figure 3.16, Figure 3.17 and Figure 3.18). This observation was noted in another recent study by Allan *et al*., 2016, in which they too demonstrate that low concentrations of exogenous NO did not trigger biofilm dispersal. Importantly, these authors showed that at SNP concentrations of 1 mM a highly significant 3 log reduction in biofilm CFUs was achieved which was not attributed to biofilm dispersal, as no visible change in the biofilm architecture was noted. In this study, a smaller reduction in CFUs was noted for the biofilm and planktonic phases for SNP concentrations of 50 µM and higher. This can be explained due to the differing length of exposure between this study and that used by Allan *et al*., 2016. In the aforementioned study a 3 log reduction for a SNP treatment of 1 mM was achieved in 2 h compared to a 1.5 – 2 log reduction for SNP concentrations higher than 50 µM after 12 h of exposure. They also demonstrated that NO could ameliorate the effectiveness of amoxicillin-clavulanic acid killing. Collectively, this evidence points to the potential use of NO as an additional bactericidal agent towards biofilms which can be used alongside other antimicrobials improving their action and therefore would need to be explored for treating CF infections.

Ex vivo CF sputum mixed species biofilms dispersed with 500 µM SNP

The mixed species biofilms formed from the sputum samples collected from 3 CF patients after 24 h of growth were successfully dispersed after treatment with 500 µM SNP for a period of 15 h, which is evident in the micrographs in Figure 3.19. A reduction was observed in the biofilm biovolume for all 3 CF patients, refer to Figure 3.20. Although the biofilms in this set of work were not assessed using qPCR analysis, e*x vivo* sputum biofilms grown using the same methodology for other patients showed both *P. aeruginosa* and *S. aureus* where identified as the microorganisms contributing to the mixed species biofilms formed in these assays. The main limitations in this set of work were: 1) using the sputum sample collected to form one replicate; 2) limit to the number of microorganisms which could be successfully grown. This was due to the use of BHI medium, which would not be sufficient to allow for the growth of other microorganism such as *Haemophilus influenzae* which would require nicotinamide adenine dinucleotide and hemin as supplements. 3) The biofilms were grown under aerobic conditions which therefore eliminated anaerobes. However, this is the first set of work showing the successful dispersal of these *ex vivo* mixed species biofilms from CF sputum. The only other study observing the dispersal of a mixed species consortium is that observed from the mixed species biofilms formed in a water system by Barraud *et al.*, 2009.

In conclusion, the work here demonstrates that while dispersal of *P. aeruginosa* monospecies biofilms can be induced using low concentrations of exogenous NO, the dispersal of monospecies biofilms formed by *A. xylosoxidans*, *B. cepacia* complex, *S. aureus*, *S. maltophilia* and *S. pneumoniae* was not achieved with the low exogenous concentrations of NO used in this study. However, higher concentrations of NO could potentially be used in combination with other antimicrobials to kill the bacteria within biofilms; this observation merits future investigation. The observed dispersal of the *ex vivo* CF sputum mixed-species biofilms will be investigated in the next Chapter using *in vitro* dual-species biofilms formed by two of the most prevalent CF microorganisms *P. aeruginosa* and *S. aureus*.

Chapter 4

Determination of cell viability and species abundance following nitric oxide treatment in dual-species biofilms formed by CF clinical isolates of *Pseudomonas aeruginosa* and *Staphylococcus aureus*

4.1 Introduction

Biofilms are a ubiquitous form of life and is the preferred mode of lifestyle for bacteria, both in the environment and within a host. A biofilm's composition can be solitary or diverse in it's collection of sessile cells. Biofilms are composed of self-produced scaffolding, referred to as the matrix. The matrix consists of eDNA, lipids, exopolysaccharides, proteins and lipoteichoic acids (Flemming and Wingender, 2010). The composition of the matrix and the protection it offers to the biofilm inhabitants is an extremely important part of biofilm research (Flemming *et al.*, 2007; Xiao *et al.*, 2012; Doroshenko *et al.*, 2014). However, there is a gap in knowledge for multispecies biofilm interactions and how these interactions have an impact on both the colonisation of human hosts and on the treatments administrated. This poses issues in the effort to effectively eradicate these biofilm infections as shown in a study by Dalton *et al.*, (2011) using *in vivo* wound models with multispecies biofilms.

The advent of molecular biology has led to an increasing appreciation of the species richness encountered within human infections, as discussed in Chapter 1 section 1.2.2. A number of important pitfalls have been highlighted (Zhao *et al.*, 2012a), in relation to the molecular techniques used to identify and quantify the microorganisms present in a sample. The principal two concerns are: 1) the possibility for biased extraction of genomic DNA (gDNA) and 2) the inclusion of DNA from dead cells. This Chapter addresses these concerns using a model dual-species *P. aeruginosa* and *S. aureus* biofilm. Firstly, the DNA extraction from prokaryotic cells can be divided into approximately four stages (a) lysis of a cell, (b) separation of the DNA from its associated nucleoproteins (the macromolecular proteins bound to DNA, (c) removal of cellular proteins, carbohydrates, lipids and RNA and (d) inactivation of DNA nucleases. Gram-negative and Gram-positive bacteria often require different approaches for the effective extraction of gDNA. This is due to the differences in their cell wall structure. Gram-positive bacteria have simple cell wall with sheets of peptidoglycan containing teichoic acids. In contrast, Gram-negative bacteria have a complex cell wall with a single layer of peptidoglycan and an outer membrane composed of lipopolysaccharides. The first stage in the DNA

extraction process for prokaryotic cells provides the biggest challenge due to the robust properties of the cell wall. A combination of mechanical, chemical and enzymatic treatments can be employed to lyse the Gram-negative and Gram-positive bacteria (Bhaduri and Demchick, 1983; Chapaval *et al.*, 2008; Zhao *et al.*, 2012b). Collectively, if these treatments prove to be too harsh for certain microorganisms within the population being examined, then these treatments can cause damage to the DNA extract and therefore interfere with further downstream analysis (Leff *et al.*, 1995). Equally important, if the cell lysis process is not adequate to crack open all of the Gram-positive species or the more resistant Gram-negative species within a sample then the analysis immediately becomes biased. This has a knock on effect, in the accurate determination of microbial species present and their relative abundance (Krsek and Wellington, 1999; Carrigg *et al.*, 2007; Salonen *et al.*, 2010).

Secondly, the issue of including dead cells in the estimation of the species abundance within a dual-species biofilm was addressed by using propidium monoazide (PMA). Propidium monoazide is not membrane permeable and therefore can only enter cells with damaged membranes. It binds to dsDNA and upon light exposure; at the sites of PMA binding the azide group converts to a nitrene radical which in turns reacts with organic moieties forming a strong covalent bond with the DNA. This action makes the DNA from dead cells and the eDNA within in the matrix unavailable for PCR amplification (Nocker *et al.*, 2007; Rogers *et al.*, 2008; Alvarez *et al.*, 2013; Tavernier and Coenye, 2015).

In this Chapter, a dual-species biofilm model was designed to investigate *in vitro* the effect NO exerts on a dual-species biofilm composed of two of the most predominate bacterial species identified within the CF lung. This was primarily undertaken due to the reduction noted in the *ex vivo* CF sputum mixed species biofilms on exposure to exogenous NO, as observed in Chapter 3. Additionally, various DNA isolation methodologies were explored. To ensure only viable cells there enumerated from both *P. aeruginosa* and *S. aureus* within the dual-species biofilm, PMA was applied to the biofilms prior to DNA extraction. Therefore, PMA-qPCR enabled the enumeration of the viable cell

fractions and concomitantly estimates the relative species abundance of dual-species biofilm both untreated and SNP treated.

4.2 Materials and Methodology

4.2.1 Monospecies biofilm assays for CF isolates of *S. aureus* and *P. aeruginosa* for use in the evaluation of DNA extraction methods

A CF clinical isolate of *P. aeruginosa* assigned the patient designation number of PA68 which was previously isolated by Dr Robert P. Howlin was inoculated into 15 ml of LB-broth Miller (Formedium, U.K.) and incubated at 37°C with 5% CO_2 – 95% air overnight. The overnight culture was used to inoculate fresh LB until an OD 620 nm of 0.06 was reached, corresponding to 10^6 cells per ml. A total of 4 ml was used to inoculate one 6-well polystyrene flat bottom plate (Thermo Scientific Nunc®, Nunclon™Δ). The 6-well plate was incubated at 37°C with 5% CO_2 – 95% air for a total of 48 h. After 24 h of biofilm growth, fresh LB was applied to three of the wells and for the remaining three wells the supernatant was removed. The biofilm was washed gently 3x using 3 ml of PBS. After rinsing, 1 ml of PBS was applied to each of the wells and the biofilm was removed from the well surface using a cell scraper (Greiner Bio-One). The remaining 3 wells were incubated 37°C with 5% CO_2 – 95% air for a further 24 h after which the biofilm was removed from the well's surface as outlined previously.

A CF clinical isolate of *S. aureus* assigned the patient designation number of A52 (isolated previously, refer to Chapter 2) was inoculated into 15 ml TSB and incubated at 37°C with 5% CO_2 – 95% air overnight. The overnight culture with an OD 620 nm of 0.530 was used to inoculate fresh TSB to a cell density of 10^6 cells per ml. Biofilms were grown as outlined for *P. aeruginosa* above with the exception of 4 ml of fresh TSB being applied at the 24 h time point.

The 24 h and 48 h biofilm suspensions for *P. aeruginosa* and *S. aureus* were used to evaluate the DNA extraction methods in section 4.2.2.

4.2.2 Evaluation of DNA extraction methods from biofilm

Biofilm suspensions for a Gram-positive CF isolate *S. aureus* and a Gram-negative CF isolate *P. aeruginosa* grown as outlined in section 4.2.1 were used for testing in studies 1 to 5 below; sections 4.2.2.1 – 4.2.2.5.

4.2.2.1 Study 1 – Bead beating versus sonication from *P. aeruginosa* biofilms

For this study, 24 h and 48 h *P. aeruginosa* biofilm suspensions were used to test the procedures below. Final concentrations used for the enzymes lysozyme and lysostaphin are within brackets, unless otherwise stated.

(i) Bead beating the biofilm suspension prior to DNA extraction

Two 2 mm glass beads (Sigma-Aldrich, U.K.) were placed into the 1 ml biofilm suspensions recovered for both the 24 h and 48 h monospecies *P. aeruginosa* biofilms sampled. The suspensions were vortexed for 30 sec at ~ 5,000 rpm prior to following the CTAB method based on a protocol by Wilson, 2001, with modifications as outlined in section 4.2.2.1 (iii).

(ii) Sonicating the biofilm suspension prior to DNA extraction

A sonication bath (operating frequency of 60 kHz at RT) was filled with a 2% (v/v) Triton–X (Sigma-Aldrich) solution prepared using dH_2O. The biofilm suspensions within 1.5 ml centrifuge tube were placed within the sonication bath tray and subjected 3x to 6 min sonication cycles, with a 30 sec vortex cycle at ~ 5,000 rpm carried out between sonication cycles. The CTAB method was carried out using a protocol by Wilson, 2001, with modifications as outlined in section 4.2.2.1 (iii).

(iii) CTAB DNA extraction method

All biofilm suspensions were centrifuged at 12,000 g for 5 min in a Thermo Scientific Heraeus Fresco 21 centrifuge (centrifuge used unless otherwise stated).The PBS supernatant was removed and a 740 µl volume of TE (10 mM Tris pH 8.0 and 1 mM EDTA) (Sigma-Aldrich) was added to resuspend the biofilm pellet. The suspension was vortexed at ~ 5,000 rpm (used throughout, unless otherwise stated) for 30 sec and 8 µl of lysozyme (100 mg / ml) (Sigm-Aldrich) was added to the centrifuge tube. The centrifuge tube was vortexed for 30 sec and the centrifuge tube was left at room temperature for 5 min. The centrifuge tube was vortexed after the addition of 40 µl of 10% SDS. Proteins were degraded with the addition of 8 µl of Proteinase K (10 mg / ml) and the tube was vortexed for 30 sec. The centrifuge tube was placed in a 37 ℃ incubator for 1 hr. A 10 µl drop of the suspension was placed on a microscope

slide and viewed under bright field using an Olympus BX61 microscope with a 100x objective. A 100 µl volume of 5 M NaCl was pipetted into the solution and vortexed for 30 sec. Hexadecyltrimethyl ammonium bromide (CTAB) / NaCl (Sigma-Aldrich) was heated at 65°C prior to use. A volume of 100 µl of CTAB/NaCl was added to the centrifuge tube and the suspension was vortexed for 1 min. After homogenisation, 500 µl of chloroform:isoamyl alcohol (24:1) (Sigma-Aldrich) was pipetted into the centrifuge tube and vortexed for 30 sec. The centrifuge tube was centrifuged at 12,000 g for 10 min. The aqueous phase was transferred to a fresh centrifuge tube and 500 µl of phenol:chloroform:isoamyl alcohol (25:24:1) (Sigma-Aldrich) was added to the suspension and vortexed for 30 sec. The centrifuge tube was centrifuged at 12,000 g for 10 min. The aqueous phase was transferred to a clean centrifuge tube and 600 µl of isopropanol (Sigma-Aldrich) was added to this phase. The centrifuge tube was incubated at room temperature for 35 min and was centrifuged at 12,000 g for 15 min. The aqueous layer was removed and the pellet was washed using 200 µl cooled 70% ethanol (stored at - 20°C) and centrifuged at 12,000 g for 5 min. The supernatant was removed and the pellet was left to air dry in a microbiological safety cabinet (MSC). The dried pellet was resuspended in 20 µl of TE + RNAse (99 µl TE + 1 µl RNAse 10 mg / ml) (Sigma-Aldrich). The DNA extract was transferred to a sterile centrifuge tube and incubated at 37°C for 20 mins prior to storing at -20°C.

(iv) Bead beating post addition of lysozyme

The CTAB protocol outlined above was followed up to the addition of Proteinase K. Two 2 mm glass beads were placed in the centrifuge tube and the centrifuge tube was immediately vortexed for 3 min. A 10 µl aliquot was placed on a microscope slide for visualization under bright field using an Olympus BX61 microscope with the 100x objective, to view the level of lysis. The glass beads were removed from the suspension and the chemical DNA extraction protocol was reconvened starting with the 1 h incubation step at 37°C as outlined in section 4.2.2.1 (iii).

4.2.2.2 Study 2 – Combined mechanical and enzymatic cell wall disruption versus enzymatic cell wall disruption for S. aureus biofilms

For this study, 24 h and 48 h *S. aureus* biofilm suspensions were used to test the procedures below.

(i) Mechanical - Bead beating 2x cycles

The scraped biofilm suspension for *S. aureus* was centrifuged and the supernatant was removed. The pellet was resuspended using 560 µl of TE. Two 2 mm glass beads were placed in the centrifuge tube and the centrifuge tube was vortexed for 20 sec x2 cycles. The suspension was transferred into a fresh centrifuge tube and 20 µl of lysozyme (100 mg /ml) was pipetted into the suspension. The suspension was incubated for 5 min at room temperature. A volume of 30 µl of 10% SDS was added to the centrifuge tube and the centrifuge tube was vortexed. A volume of 6 µl of Proteinase K (20 mg/ml) was pipetted into the solution and two glass beads (2 mm) were placed into the centrifuge tube. The centrifuge tube was vortexed for 30 sec. The suspension was placed in a fresh centrifuge tube and incubated for 1 h at 37°C. A 10 µl aliquot was placed on a microscope slide and visualized under bright field using an Olympus BX61 microscope with a 100x objective, to assess cell lysis. A volume of 100 µl of 5 M NaCl was pipetted into the centrifuge tube and vortexed for 30 sec. To this suspension, 80 µl of preheated (at 65°C) CTAB/NaCl was added to the centrifuge tube and incubated at 65°C for 10 min. An equal volume of chloroform:isoamyl alcohol (24:1) was added and the suspension was vortexed for 30 sec. The centrifuge tube was centrifuged at 12,000 g for 4 min. The aqueous phase was transferred to a new centrifuge tube and an equal volume of phenol:chloroform:isoamyl alcohol (25:24:1) was added and the suspension was mixed thoroughly by vortexing for 30 sec. The centrifuge tube was centrifuged at 12,000 g for 4 min and the supernatant was transferred to a new centrifuge tube. The remaining steps of the CTAB protocol as above in section 4.2.2.1 were followed.

(ii) Mechanical - Bead beating 1x cycle

A 500 µl aliquot of a *S. aureus* biofilm pellet was resuspended in 560 µl of TE as above in section (i). Two 2 mm glass beads were placed in the centrifuge tube and the centrifuge tube was vortexed for 30 sec.

The suspension was pipetted into a fresh centrifuge tube. The CTAB DNA extraction protocol was followed as outlined above in section 4.2.2.2 (i) commencing with the addition of lysozyme step.

(iii)   CTAB DNA extraction with 1 h lysozyme treatment

A 500 µl aliquot of a *S. aureus* biofilm pellet was resuspended in 560 µl of TE as above in section 4.2.2.2 (i). The centrifuge tube was vortexed for 50 sec. The CTAB method was followed as outlined in section 4.2.2.2 (i) with a 1 h incubation period at 37°C with lysozyme.

(iv)   CTAB DNA extraction with 2 h lysozyme treatment

A 500 µl aliquot of a *S. aureus* biofilm pellet was resuspended in 560 µl of TE. The centrifuge tube was vortexed for 1 min. The CTAB method was followed as outlined above in section 4.2.2.2 (i) with the following exception, after the addition of Proteinase K the incubation period was extended to 2 h at 37°C.

4.2.2.3   Study 3 – Enzyme concentration modifications for cell wall disruption of cells from a S. aureus V]cZ]`a ·

For this study, 24 h and 48 h *S. aureus* biofilm suspensions were used to test the procedures below.

(i) Lysostaphin 10 mg / ml

The chemical CTAB DNA extraction protocol used in Study 2 section 4.2.2.2 (i) was followed with the following modifications. A 5 µl volume of RNase A (10 mg / ml) and 5 µl of Lysostaphin (10 mg / ml) (Sigma-Aldrich) were added to the resuspended biofilm pellet and vortexed for 1 min. The centrifuge tube was incubated at 37°C for 1 h. A volume of 30 µl of 10% SDS was pipetted into the centrifuge tube and vortexed for 30 sec. To this suspension, 10 µl Proteinase K (10 mg / ml) was added and the CTAB method used in Study 2 section 4.2.2.2 (i) was followed from the incubation step.

(ii) Lysostaphin 50 mg / ml

The CTAB method used in Study 2 section 4.2.2.2 (i) was followed with the following modifications. To the suspension, a 5 µl volume of RNase A (10 mg / ml) and 37.5 µl of Lysostaphin (50 mg / ml) were added to the resuspended

pellet and for 30 sec. The centrifuge tube was incubated at 37°C for 40 min. A volume of 30 μl of 10% SDS was pipetted into the centrifuge tube and vortexed for 30 sec. A 10 μl volume of Proteinase K 10 mg / ml was added and the centrifuge tube was vortexed for 30 sec. The centrifuge tube was incubated for 20 min at 37°C and the CTAB method was followed as outlined in Study 2 section 4.2.2.2 (i), commencing with the 5 M NaCl step.

(iii) No enzyme

The CTAB method used in Study 2 section 4.2.2.2 (i) was followed with the following modifications. A volume of 5 μl of RNase A (10 mg / ml) was added to the resuspended pellet and vortexed for 30 sec. The centrifuge tube was incubated at 37°C for 1 h. A volume of 30 μl of 10% SDS was pipetted into the centrifuge tube and vortexed for 30 sec. To this suspension, 10 μl Proteinase K (10 mg / ml) was added, the centrifuge tube was vortexed for 30 sec. The CTAB method used in Study 2 section 4.2.2.2 (i) was then followed commencing with the incubation step.

(iv) Lysostaphin 2.5 mg / ml

The CTAB method used in Study 2 section 4.2.2.2 (i) was followed with the following modifications. A volume of 5 μl of RNase A (10 mg / ml) and 2.5 μl of Lysostaphin (2.5 mg / ml) were added to the resuspended pellet and vortexed for 30 sec. The centrifuge tube was incubated at 37°C for 40 min. A volume of 30 μl of 10% SDS was pipetted into the centrifuge tube and vortexed for 30 sec. A volume of 10 μl of Proteinase K (10 mg / ml) was added and the centrifuge tube was vortexed for 30 sec. The centrifuge tube was incubated for 20 min at 37°C and the CTAB method used in Study 2 section 4.2.2.2 (i) was then followed commencing with the 5 M NaCl step.

4.2.2.4 Study 4 – Chemical and enzymatic DNA extraction protocols for S. aureus biofilms

For this study, 24 h and 48 h *S. aureus* biofilm suspensions were used to test the procedures below.

(i) Lysostaphin (0.088 mg / ml) with the CTAB DNA extraction method

One ml of a 48 h *S. aureus* biofilm suspension was centrifuged at 12,000 g for 10 min. The pellet was resuspended in 560 µl TE. A total of 5 µl of RNase (10 mg / ml) and 5 µl of lysostaphin (final concentration of 0.088 mg / ml) were added to the suspension and vortexed for 30 sec. The suspension was incubated at 37°C for 1 h. After incubation, 30 µl of 10% of SDS, 5 µl of RNase (10 mg / ml) and 10 µl Proteinase K (10 mg / ml) were added and the suspension was vortexed. The tube was incubated for 1 h at 37°C. A 100 µl volume of 5 M NaCl was added followed by the addition of CTAB - NaCl (10% CTAB, 0.7 M NaCl) which was preheated at 65°C. The suspension was incubated at 65°C for 10 min. An equal volume of chloroform (Sigma-Aldrich) was added to the suspension and vortexed for 30 sec. The suspension was centrifuged for 5 min at 12,000 g to produce layers; the top viscous layer was removed and placed in a fresh centrifuge tube. An equal volume of phenol-chloroform-isoamyl alcohol (25:24:1) and the centrifuge tube was inverted well prior to being centrifuged at 12,000 g for 10 min. The aqueous phase was transferred to a fresh tube. The chloroform step and the phenol:chloroform:isoamyl alcohol steps was carried out two times. To the final aqueous phase an equal volume of chloroform-isoamyl alcohol was added to the contents. The centrifuge tube was mixed by gentle inversion and the centrifuge tube was centrifuged at 10,000 g for 10 min. The upper aqueous phase was pipetted into a fresh centrifuge tube and 500 µl of isopropanol was added to precipitate the DNA. The centrifuge tube was centrifuged at 12,000 g for 10 min and the supernatant was removed. A 200 µl volume of 70% ethanol was added to wash the pellet and the tube was vortexed for 30 sec. The tube was centrifuged at 10,000 g for 5 min. The pellet was left to air dry in a MSC. The DNA pellet was resuspended in 30 µl of DNase, RNase free molecular grade water (Sigma-Aldrich) and stored at -20°C.

(ii) Guanidinium thiocyanate

This method was based on a protocol developed by Pitcher *et al.*, 1989. In brief, 500 µl of the biofilm suspension was centrifuged at 12,000 g for 10 min, the

supernatant was removed. The pellet was resuspended in 100 µl of lysostaphin (0.088 mg / ml) dissolved in 0.1 M sodium phosphate pH 7 and the suspension was incubated at 37°C for 30 min. Guanidinium thiocyanate solution (GES) was prepared as follows: 60 g of guanidinium thiocyanate (Sigma-Aldrich) was added to 20 ml of 0.5 M EDTA at pH 8 and 20 ml of dH_2O while heating at 65°C and stirred until it was completely dissolved. To this GES solution, 5 ml of 10% (v / v) sarkosyl (Sigma-Aldrich) was added after cooling. The GES solution was made up to 100 ml with dH_2O and filtered through a Nalgene filter 0.45 µm unit. A volume of 500 µl of the GES solution was added to the biofilm suspension and after 10 min, a 20 µl aliquot was viewed under bright field using an Olympus BX61 microscope using the 100x objective; to observe cell lysis. The tube was left on ice and 250 µl of 7.5 M ammonium acetate was pipetted into the cooled suspension and the tube was left on ice for 10 min. A volume of 500 µl of chloroform:isoamyl alcohol (24:1) was added in and the tube was vortexed for 1 min. The tube was centrifuged at 2,500 g for 10 min. The upper aqueous phase was transferred to a fresh centrifuge tube and 540 µl of isopropanol stored at − 20°C was added. The tube was inverted to mix the contents. The tube was centrifuged at 6,500 g for 20 sec. The supernatant was removed and the DNA pellet was washed with 200 µl of 70% ethanol. The tube was vortexed for 30 sec and centrifuged at 10,000 g for 5 min. This ethanol wash step was carried out two times. The DNA pellet was resuspended in 30 µl of TE and stored at -20°C.

(iii) Acetone and Ethanol with the CTAB DNA extraction method

The DNA extraction procedure was based on a protocol by Birnbiom, 1983. A 1 ml biofilm suspension was centrifuged at 12,000 g for 10 min. The supernatant was removed and 700 µl of TE was added to resuspend the pellet. A 500 µl volume of cold acetone: ethanol suspension was added (50% acetone, 50% ethanol; stored at -20°C) and the tube was incubated on ice for 5 min. The tube was centrifuged at 12,000 g for 2 min. The supernatant was removed and the pellet was washed with 1 ml of TE. The suspension was centrifuged at 12,000 g for 2 min and the supernatant was removed. A 3 µl volume of lysostaphin (0.044 mg / ml) was added to the pellet and the tube was vortexed for 30 sec. The CTAB DNA extraction protocol in section 4.2.2.1 (iii) was followed, commencing at the incubation step for the enzyme cell wall lysis treatment with

the exception of a shorter incubation period of 10 min.

(iv) Dual-enzymatic method at lower concentrations:
Lysostaphin (0.044 mg / ml) and Lysozyme (0.176 mg / ml) with CTAB.
A 500 µl biofilm suspension was centrifuged at 12,000 g for 10 min. The supernatant was removed and the pellet was resuspended in 541 µl of TE buffer. A total of 10 µl of lysostaphin (0.044 mg / ml) and 10 µl of lysozyme (0.176 mg / ml) were added to the suspension and the tube was incubated at 37°C for 1 h. A 20 µl aliquot was placed on a microscope slide. Cell lysis was viewed under bright field using an Olympus BX61 microscope with the 100x objective. The CTAB DNA extraction protocol was followed as outlined in section 4.2.2.4 (i), commencing with the addition of SDS step.

(v) Polyvinylpyrrolidone (1%) combined with the CTAB DNA extraction protocol
A method described by Chapaval *et al.*, 2008 was followed. In brief, a 100 µl biofilm suspension was centrifuged at 12,000 g for 10 min. The polyvinylpyrrolidone (PVP) extraction buffer contained 1.4 M NaCl, 100 mM Tris-HCL pH 8, 200 mM EDTA pH 8, 1% (w / v) PVP- 40 (Sigma-Aldrich), 2% (w / v) CTAB, 20 mg / ml Proteinase K, lysozyme (0.044 mg / ml) and 0.2% (v / v) ß-mercaptoethanol (Sigma-Aldrich) were prepared in dH$_2$O. PVP – extraction buffer **B** contained 1.4 M NaCl, 100 mM Tris-HCL pH 8, 200 mM EDTA pH 8, 1% (w / v) PVP- 40 (Sigma-Aldrich), 2% (w/v) CTAB, 20 mg / ml and 0.2% (v / v) ß-mercaptoethanol were prepared in dH$_2$O.

The biofilm pellet was resuspended in 700 µl of the PVP- extraction buffer **A** and the suspension was heated at 65°C for 30 min using a hotplate; the tube was vortexed for 30 sec at 10 min intervals, to insure homogenisation of the buffer for cell lysis. The suspension was allowed to cool briefly before 650 µl of chloroform-isoamyl alcohol (24:1) was added to the suspension and the tube was gently inverted. The tube was centrifuged at 20,000 g for 7 min and the aqueous phase was transferred to a fresh tube. A volume of 200 µl of PVP – extraction buffer **B** was added to aqueous phase and the tube was inverted three times. A 650 µl volume of chloroform:isoamyl (24:1) was added to the tube and inverted three times. The tube was centrifuged at 20, 000 g for 7 min. The aqueous phase was transferred to a fresh tube and 650 µl of chloroform: isoamyl alcohol (24:1) step was repeated. The centrifuge tube was centrifuged at 12,000 g for 10 min at the aqueous phase was transferred to a fresh

centrifuge tube. An equal volume of isopropanol was added and the tube was inverted three times. The tube was centrifuged at 12,000 g for 10 min. The supernatant was removed and the DNA pellet was washed with 70 µl of cold 70% ethanol twice with a step centrifugation at 10,000 g for 5 min in between washes. The pellet was left to air dry in a MSC and resuspended in 40 µl TE buffer (10 mM Tris-HCL pH8, 1 mM EDTA pH 8, 10 µg / ml RNAse) and incubated at 37°C for 30 min. The DNA was stored at -20°C.

(vi) Polyvinylpyrrolidone (2%) combined with the CTAB DNA extraction protocol

The above PVP protocol in section 4.2.2.4 (v) was followed with the exception of 2% PVP-40 was used in the preparation of both PVP - extraction buffers A and B (Chapaval *et al.*, 2008).

4.2.2.5 Study 5 – Commercial kit versus Bead beating with the CTAB DNA Extraction methodology

The same biofilm suspension for both monospecies biofilms of *S. aureus* and *P. aeruginosa* which were sampled after 48 h of biofilm growth were split between the two test methodologies for this study.

(i) M 1 - Commercial kit PowerBiofilm® DNA Isolation Kit

The protocol for the PowerBiofilm® DNA Isolation Kit was followed (MoBio Laboratories, Inc., U.S.) with the exception of 100 µl of the biofilm suspension being added to the bead beating tube; separate tests for *S. aureus* and *P. aeruginosa* monospecies biofilms were conducted.

(ii) M 2 – PowerBiofilm® Bead Beating Tubes with the CTAB DNA Extraction Method

Another 100 µl aliquot from the same biofilm suspensions used in section 4.2.2.5 (i) was added to a PowerBiofilm® bead beating tube composed of a mixture of 0.1 mm glass beads, 0.5 mm glass beads and 2.4 mm ceramic mix (MoBio Laboratories, Inc., U.S.). The bead beating tubes were placed in the MoBio vortex adapter and vortexed at 5,000 rpm for 30 sec using the Vortex-Genie® (MoBio Laboratories, Inc., U.S.). The CTAB DNA extraction method outlined under section 4.2.2.1 (iii) was followed with the following modifications based on the observations made from studies 4.2.2.1 – 4.2.2.4; a) a lysozyme concentration of 80 mg / ml was used, b) the CTAB solution was

preheated to 65°C, c) centrifugation steps during chloroform:isoamyl alcohol and phenol:chloroform:isoamyl alcohol steps were reduced to 4 min, d) immediately after the addition of isopropanol the tubes were cooled at –20°C for 30 min, e) 70% ethanol was cooled at -20°C prior to washing the DNA pellet and f) an incubation period of 30 min at 60°C was carried out after the addition of 20 µl of TE buffer containing RNAse (10 mg / ml).

4.2.3 Evaluation of DNA quantity and quality

All DNA samples were stored at –20°C. The DNA concentration for each assay was measured using the Nanodrop® instrument ND-1000 (Thermo Fisher Scientific, Wilmington, DE, USA). The Nanodrop® was blanked using the same TE buffer used to resuspend the DNA extract. The DNA quality was evaluated by running it through a 0.8% (w / v) agarose gel, with 10 µl of 10,000x SYBR Green I stain (Invitrogen). The agarose (Bioline, U.K.) was dissolved in 1x TBE (Sigma-Aldrich) prior to heating, the gel was allowed to cool with 1 mm comb x24 wells insert placed in the gel. The DNA was pipetted into the gel after mixing with 5x DNA loading buffer red (Bioline, U.K.). The 5 µl volume of the DNA standard molecular weight ladder Hyperladder I was loaded into the agarose gel, refer to Appendix 2 for band sizing. The gel was set to run at 80 V 80 mA 7W using the Consort EV243 power pack for 1 h. The agarose gel was visualized using the UV transilluminator in the G:box (Syngene, UK).

4.2.4 Formation of dual-species biofilm and treatment with the NO donor SNP

(i) S. aureus and P. aeruginosa dual-species biofilm assay

A CF isolate for *S. aureus* with the patient designation number A52 (isolated previously, refer to Chapter 2) and a CF isolate for *P. aeruginosa* with the patient designation number PA21 (isolated by Dr Robert P. Howlin) were used to form a dual-species biofilm. The biofilm inoculum cell numbers, different media compositions and biofilm growth conditions were chosen based on preliminary optimization experiments (data not shown). Overnight cultures were prepared from the frozen stock cultures by inoculating into 15 ml LB and 15 ml TSB, for *P. aeruginosa* PA21 and *S. aureus* A52 respectively. The cultures

were incubated at 37ºC with 5% CO_2 – 95% air to an OD 620 nm of ~ 0.530. The dual-species biofilm inoculum was prepared by adding 10^5 cells / ml of *P. aeruginosa* PA21 and 10^5 cells / ml of *S. aureus* A52 to ½ strength BHI broth (Oxoid, U.K.). A total of 1 ml of this biofilm inoculum was added to each well of a 6-well Thermo Scientific Nunc®, Nunclon™Δ plate and MatTek dish. The 6-well plates and MatTek dishes were incubated for an attachment phase of 6 h under agitation at 50 rpm at 37°C with 5% CO_2 – 95% air. A 1/5 strength BHI broth with hemin was prepared as follows: 96 ml of dH_2O was autoclaved with a magnetic stirrer. After the dH_2O had cooled to RT, 4 ml off triethanolamine was added aseptically. A total of 100 mg of hemin (Sigma-Aldrich) was weighed and added aseptically and the solution was placed on a magnetic stirrer for 5 min. The hemin solution was heated for 30 min at 65°C. The solution was stored at 4°C. Hemin was aseptically added (after 5 mins on a magnetic stirrer) to 1/5 strength BHI broth to a final concentration of 1.25 µg / ml. After the attachment phase, the suspension was removed and either 4 ml or 3 ml of 1/5 strength BHI broth + hemin was added to the 6-well plates and MatTek dishes respectively. The plates and dishes were incubated for a total of 48 h under agitation at 50 rpm at 37°C with 5% CO_2 – 95% air with fresh medium applied after 24 h of incubation. Three biological replicates were carried out for this assay, performed independently.

(ii) SNP treatment of a S. aureus and P. aeruginosa dual-species biofilm

After 48 h of incubation each well and dish were treated with either 1/5 strength BHI broth + hemin for the controls or a treatment as follows: 1/5 strength BHI broth + hemin with 500 µM SNP, 1/5 strength BHI broth + hemin with 100 µM PTIO + 500 µM SNP or 1/5 strength BHI broth + hemin with 0.4 µM PF. Refer to section 3.27 for an outline of the preparation of these chemicals. All biofilms were incubated for a maximum of 24 h under agitation at 50 rpm at 37°C with 5% CO_2 – 95% air and exposed to a full spectrum lamp for the duration of SNP treatment. The dual-species biofilms in the 6-well plates were sampled at the following time points post SNP addition: 1 h, 2 h, 5 h, 12 h, 15 h, 24 h, with PF and PTIO + SNP sampled at the 24 h time point. Biofilm removal from the surface was carried out as outlined in section 3.2.8, with the following exception – no sonication of the biofilm suspension was

followed. The biofilm suspensions were split into 500 μl aliquots into 1.5 ml centrifuge tube. One of these aliquots per treatment was used for the extraction of genomic DNA form the dual-species biofilm, see section 4.2.6 and 4.2.7. The dual-species biofilms on the MatTek dishes were sampled at the following time points post SNP addition: 1 h, 12 h, 15 h, 24 h, with PF and PTIO + SNP sampled at the 24 h time point. The dishes were stained and imaged using CLSM as outlined under section 3.2.9.

4.2.5 Testing the antibacterial activity of the CF isolated strains for *S. aureus* and *P. aeruginosa* used in the dual-species biofilm assay

The antibacterial activities of both CF strains were evaluated by observing the zone of inhibition on a lawn of bacteria. The antibacterial activity of the cells and the cell supernatant was tested for both species. Overnight cultures of *S. aureus* A52 and *P. aeruginosa* PA21 were prepared by inoculating the frozen glycerol stock cultures into 15 ml TSB and 15 ml LB, respectively. The cultures were incubated at 37ºC with 5% CO_2 – 95% air. The overnight cultures were diluted to a cell density of 10^6 in fresh TSB and LB for *S. aureus* A52 and *P. aeruginosa* PA21, respectively. Briefly, 100 μl of this suspension was spread onto a BHI agar plate containing 1.25 μg / ml of hemin, 4x agar plates for both strains were streaked. The plates were allowed to dry in a MSC for ~ 25 min. Supernatant suspension prepared as follows: 1 ml of the overnight culture was centrifuged at 12,000 g for 10 min at 4ºC and sterile filtered using a Millipore 0.22 μm filter unit. Four 10 μl drops of the test supernatant suspension were applied to the streaked plates and allowed to dry for ~ 25 min in a MSC. Cell suspension: Four 10 μl drops of the test overnight adjusted culture were applied to the streaked plates and allowed to dry for ~ 25 min in a MSC. Control plates for each species were streaked onto the BHI agar supplemented with hemin, 1.25 μg / ml of molten agar. The plates were incubated at 37ºC with 5% CO_2 – 95% air for 20 h. The plates were examined for zones of inhibition. This assay was conducted on three different occasions with two technical replicates.

4.2.6 Propidium monoazide cross-linking

The following procedure is based on work carried out by Nocker *et al.*, 2007. Propidium monoazide (PMA) (Biotium, Inc., Hayward, CA, USA) was centrifuged using the pulse function, prior to the addition of 20% dimethylsulphoxide (DMSO) (Sigma-Aldrich, Co., St. Louis, MO) to prepare a 20 mM stock solution. PMA was added to the 500 µl biofilm suspensions to a final concentration of 50 µM. The suspensions were incubated in the dark for 30 min (Rogers *et al.*, 2008), with occasional mixing. The biofilm suspensions in the 1.5 ml centrifuge tube were placed horizontally on the ice and exposed to light from a 650-W halogen light source (Kaiser Videolight 6; Kaiser Fototechnik, Bunchen, Germany) at a distance of 20 cm for a total of 3 min, and vortexed briefly to ensure homogenisation after 1.5 min of light exposure. The biofilm suspension was centrifuged at 5,000 g for 5 min. The supernatant was removed and 500 µl of TE was used to resuspend the pellet prior to gDNA isolation.

4.2.7 Isolation of genomic DNA (gDNA) from a dual-species biofilm composed of CF strains of *S. aureus* and *P. aeruginosa*

After PMA-cross linking, the isolation of gDNA from the resuspended biofilm pellet was carried out as outlined in section 4.2.2.5 (ii), with the following exception: 25 µl of TE was used to resuspend the gDNA pellet. The DNA quality was assessed by running 5 µl on a 0.8% agarose gel and the DNA concentration was assessed using a Nanodrop® blanked using TE buffer, as described in section 4.2.3.

4.2.8 Quantitative analysis of the two bacterial species in a dual-species biofilm using quantitative polymerase chain reaction (Q-PCR)

Primers and probes for the qPCR assay were designed by PrimerDesign™ Ltd. (Southampton, U.K.). The primers and probe targeted the *femB* gene for the quantification of *S. aureus*; accession number GQ284649 for the EMBL-Bank Sequence Database (http://www.ebi.ac.uk/). The *P. aeruginosa* primers and probe targeted the *regA* gene; EMBL-Bank accession number X12366. Both

species target genes are designed to cover a range of sequences while remaining species specific. The quantification of the composition of both species was carried out in separate qPCR reactions from the same DNA extract. The Genesig® standard kit components were used to prepare the qPCR reaction mixtures for both species and for the template used in the creation of a standard curve to a final volume of 15 µl as follows: 10 µl of the 2x PrecisionPLUS™ qPCR mastermix, 1 µl of the species specific primer/probe mix, 4 µl RNAse/DNAse free water. The qPCR mastermix was pipetted into a 96-well low profile Thermo Scientific PCR plate and 5 µl of the biofilm gDNA extra was pipetted each well. The 96-well plate was sealed using an adhesive PCR plate seal (Thermo Scientific). The 96-well plate was centrifuged at 280 g for 1 min prior to the reaction run. Test qPCR reactions were carried prior to the quantification assays, to identity the appropriate amount of biofilm gDNA extract to be added for both species. An undiluted gDNA extract, 1:1 gDNA extract diluted in RNAse/DNAse free water and 1:10 gDNA extract diluted in RNAse/DNAse free water were tested. Due to these observations: an undiluted biofilm gDNA extract for the quantification of *S. aureus* was used and a 1:1 dilution of the biofilm gDNA extract for the quantification of *P. aeruginosa* were utilized. The final qPCR endpoint values collected for *P. aeruginosa* were doubled to adjust for dilution of the original biofilm extract. The positive template was used to create a standard curve range from 2×10^0 to 2×10^5 copies / µl through a serial ten-fold dilution series prepared using RNAse/DNAse free water. For each biofilm experimental repeat, two technical repeats were conducted for all qPCR reactions for both species. Negative and positive controls were employed as follows: a) –ve non template control (NTC) – 15 µl qPCR mastermix with 5 µl RNAse/DNAse free water, b) –ve NTC - 20 µl RNAse/DNAse free water and c) +ve control – for each fold dilution: 5 µl of the diluted positive control template with 15 µl qPCR mastermix. The positive template was added to the 96-well plate post addition of test samples and these wells were also sealed to prevent cross contamination with the positive template. The qPCR reactions were carried out using the Bio-Rad iQ™5 real time PCR detection system, amplification was monitored in the FAM channel. The qPCR reaction was conducted using an initial cycle of 95°C for 2 min, followed by 50 cycles of denaturation at 95°C for 10 s, annealing at 60°C for 60 s. For a dissociation curve, temperature increments of 0.5°C starting at 55°C and

ending at 95°C was conducted over the course of 81 cycles. Analysis of qPCR data was carried out using the Bio-Rad iQ™5 cycler software. For both species the standard curve created by the positive template with a known gene copy number was used to calculate the PCR amplification efficiency (*E*) and absolute quantification of the unknown samples. The unknown sample gene copy number was calculated by interpolation from the standard curve using their respective threshold cycle (Ct) values.

4.2.9 Quantitative image analysis of the *S. aureus* and *P. aeruginosa* dual-species biofilm

The biofilm z-stacks were analysed as outlined in section 3.2.11 using Comstat2 (Heydorn *et al.*, 2000; Vorregaard, 2008). Otsu thresholding was carried out for each z-stack and the average biofilm thickness, biofilm roughness (formula below) – a measure of the biofilm heterogeneity and the biofilm biovolume were measured. A 3D rendering of the biofilm z-stacks was carried out using the Imaris x64 v8.2.1 trial package (Bitplane, AG, Zurich, Switzerland).

$$R_a^* = \frac{1}{N \cdot t_{avg}} \sum_{i=1}^{slices} spots[i] \cdot (thickness\ [i] - t_{avg})$$

N = total number of spots, spots*[i]* contains the spots of slice *i* and thickness *[i]* is for the slice *i*. t_{avg} for average thickness

4.2.10 Statistical analysis

All statistical analysis was performed using the Minitab software, version 16 (Minitab Inc., State College, Pennsylvania, USA). The qPCR data were transformed using the log10 to normalize the data prior to statistical analysis. The qPCR transformed data were compared using one-way analysis of variance (ANOVA), followed by Tukey's comparison test. Results were considered significant when *P* – values ≤ 0.05. The biofilm image analysis data was checked for normal distribution and differences between the untreated and SNP treatments for each time point were investigated by a one-way ANOVA, followed by Tukey's comparison test. Significant *P* – values are highlighted

using an asterisk as follows: * for a *P* -value ≤ 0.05, ** for a *P* – value ≤ 0.01 and *** for a *P* – value ≤ 0.001.

4.3   Results

4.3.1 Genomic DNA extraction from monospecies biofilms using physical, enzymatic and chemical disruption yielded insufficient and/ poor quality DNA

Bead beating, sonication and enzymatic treatment of P. aeruginosa biofilms

Mechanical disruption of the monospecies biofilms formed by this bacterium was investigated by using either a) bead beating with 2 mm glass beads or b) sonication at 60 kHz at RT. Both of these approaches additionally used lysozyme for the enzymatic degradation of the cell wall in conjunction with the CTAB DNA extraction protocol (Doyle and Doyle, 1987). Twice as much intact gDNA was obtained using the bead beating methodology when compared to that obtained using sonication. Bead beating was more effective when used directly after biofilm removal as opposed to after enzyme treatment. However, DNA damage on using the bead beating method was evident with DNA smears observed using agarose gel electrophoresis.

Bead beating, sonication and enzymatic treatment of S. aureus biofilms

The same mechanical disruption methodologies listed above for a) and b) were performed on the monospecies biofilms formed by this bacterium. A higher gDNA yield of 1347 ng / µl was obtained for bead beating compared to 468 ng / µl acquired using the sonication methodology. The use of 2 mm glass beads resulted in poor quality gDNA, with visible shearing of the gDNA on evaluation of agarose gel electrophoresis results. Next, the enzymatic treatment was explored as 100 mg / ml of lysozyme proved ineffective on increasing the incubation period of the enzyme to 2 h at 37°C; with insufficient lysis of cells observed under brightfield. Due to the efficiencies observed in the lysis of *S. aureus* cells within the biofilm with lysozyme, a range of lysostaphin concentrations were tested in combination with the CTAB methodology. The

lowest concentration of lysostaphin 2.5 mg / ml yielded a high concentration of intact gDNA.

4.3.2 Chemical and dual-enzymatic gDNA extraction methodologies for *S. aureus* monospecies biofilms produced undetectable DNA levels and degraded DNA

The following chemical DNA extraction protocols were chosen by searching through literature to investigate if alternative methods could yield higher concentrations of intact gDNA from *S. aureus*: 1) polyvinylpyrrolidone (PVP) DNA extraction by Chapaval *et al.*, 2008, 2) guanidinium thiocyanate DNA extraction by Pitcher *et al.*, 1989 and 3) 1:1 acetone, ethanol DNA extraction by Birnboim, 1983. A dual-enzymatic treatment with lysozyme (0.176 mg / ml) and lysostaphin (0.044 mg / ml) employed to lyse the cells followed by the CTAB DNA extraction method. Additionally, a higher concentration of lysostaphin (0.088 mg / ml) in conjunction with the CTAB DNA extraction method was tested. The PVP method yielded extremely low gDNA concentrations although Chapaval *et al.*, 2008 reported yields of 45 to 714 ng /ml. In this study, the yields were considerably lower for a 24 h and 48 h monospecies biofilm, 1.19 ng / µl and 1.96 ng / µl, respectively using 1% PVP-40. No significant increase in the gDNA concentration was observed when 2% PVP-40 was used; 1.83 ng / µl and 1.65 ng / µl was obtained for 24 h and 48 h biofilms respectively. No detectable gDNA was obtained using the 1:1 acetone: ethanol (Birnboim, 1983) in conjunction with the CTAB DNA extraction, as shown in Lane C Figure 4.1. The protocol using guanidinium thiocyanate resulted in a high yield of gDNA, with a gDNA extract of 2024 ng / µl isolated for a 24 h biofilm and 2413 ng / µl extracted for a 48 h biofilm. However, on assessing the gDNA quality via agarose gel electrophoresis, shearing of gDNA during the DNA isolation procedure occurred with a visible DNA smear noted via agarose gel electrophoresis, refer to Lane B in Figure 4.1. Moreover, an additional band which migrated ahead of the gDNA is visible in Lane B Figure 4.1; which could be a sheared fragment of gDNA and additionally equally be due to the presence of some RNA contamination. On observing the A_{260} / A_{280} (nm) ratio readings, 2.01 and 2.03 were obtained for the 24 h and 48 h biofilm gDNA extracts. These values are not greatly elevated from a value near 1.8,

which indicates DNA purity compared to RNA readings which are close to 4.0 due to the presence of uracil.
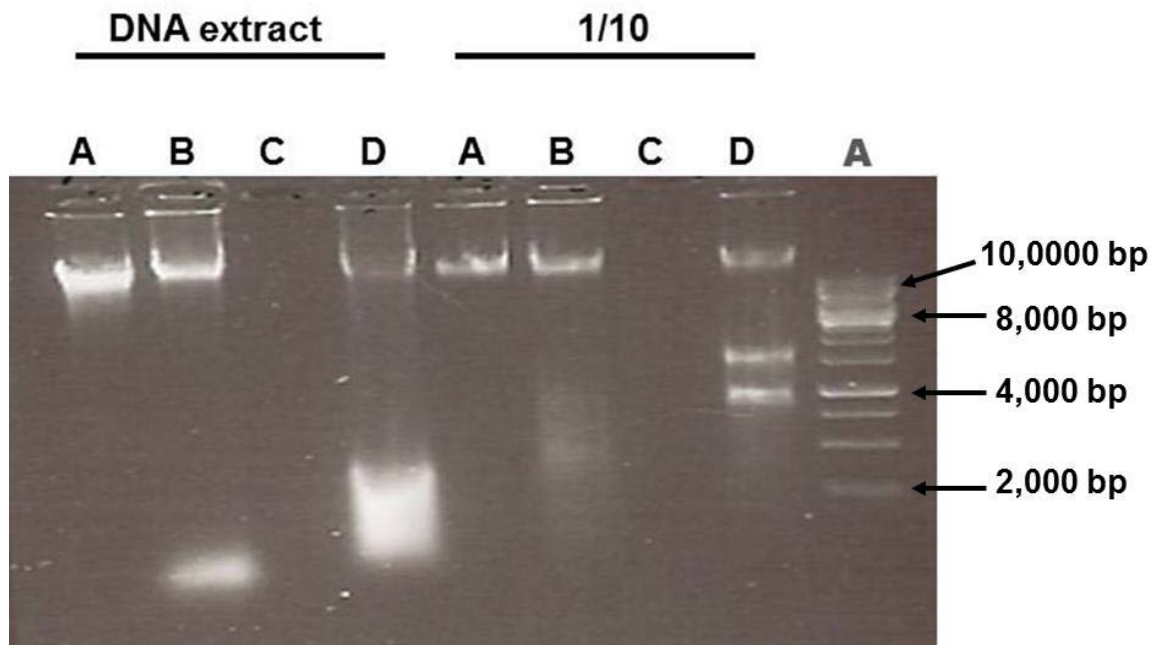
Figure 4.1 Assessment of chemical and enzymatic DNA extraction protocols for *S. aureus* monospecies biofilms formed by the CF patient isolate. Genomic DNA (gDNA) extracted from a biofilms run through a 0.8% agarose gel. Lanes under the label DNA extract – contain the undiluted gDNA biofilm extract and the lanes under the label 1/10 - contain a 1 in 10 dilution of the gDNA biofilm extract. Genomic DNA extracts for the various DNA extraction methods in the lanes are outlined by the black letters represent: **A**) Lysostaphin (0.088 mg / ml) with the CTAB DNA extraction method: good quality gDNA extract obtained from the biofilm, **B**) Guanidinium thiocyanate: poor quality of gDNA extract with two bands present; as a result of RNA contamination combined with DNA degradation resulting is a second band. Degradation of DNA is clearly visible in lane B containing the 1 in 10 dilution fraction with smearing of the biofilm gDNA extract, **C**) 1:1 Acetone and Ethanol with the CTAB DNA extraction method: no detectable DNA extract and **D**) Lysostaphin (0.044 mg / ml) and Lysozyme (0.176 mg / ml): visible DNA smear in the undiluted fraction. Further supported by the clear fragmentation of gDNA in the 1/10 dilution of the biofilm gDNA extract, indicating damage to gDNA during this methodology. The grey letter **A** marks the lane with the molecular weight ladder, Hyperladder I (Bioline, U.K.); black arrows indicate the base pair size for the corresponding DNA fragment.

Finally, the dual-enzymatic treatment combined with the CTAB DNA extraction method resulted in gDNA yields of 960 ng / μl and 2794 ng / μl for the 24 h and 48 h biofilm, respectively. However, the gDNA quality was extremely poor; with a high level of shearing of the gDNA visible coupled with a considerable reduction in the higher molecular weight gDNA band fraction on agarose gel electrophoresis evaluation; refer to Lane D Figure 4.1. The DNA extraction protocol using lysostaphin at a concentration of 0.088 mg / ml combined with the CTAB DNA extraction method resulted in higher gDNA extract yields of 531 ng / μl and 372 ng / μl for 24 h and 48 h biofilms, respectively. The A_{260} / A_{280} (nm) ratio readings were 1.84 and 1.85 for the 24 h and 48 h biofilms respectively, indicating high purity for the biofilm gDNA extract. Additionally, agarose gel electrophoresis evaluation showed the gDNA extract was intact; refer to Lane A Figure 4.1. The fraction of gDNA extracted from the 48 h *S. aureus* biofilm was lower than that for the 24 h. Due to this observation; the use of a commercial kit was explored for the gDNA extraction from both *S. aureus* and *P. aeruginosa* monospecies biofilms in order to ensure the equal extraction of intact gDNA.

4.3.3 The commercial PowerBiofilm® DNA isolation kit yields lower gDNA levels from monospecies biofilms compared to a method combining the PowerBiofilm® bead beating tubes with the CTAB DNA isolation protocol

This study involved an evaluation of gDNA recovery from both a Gram-negative and Gram-positive monospecies biofilm using two approaches: 1) the commercial kit PowerBiofilm® DNA isolation kit (M1) and 2) the PowerBiofilm® bead beating tubes combined with the CTAB DNA extraction method (M2). Moreover, due to the shearing of the gDNA on using 0.2 mm glass beads, the use of a combination of smaller beads for the lysis of both Gram-negative and Gram-positive cells within biofilms required investigation. A comparison of both methodologies clearly demonstrated that M2 out performed M1. The gDNA recovery was the highest for both the Gram-negative and Gram-positive biofilms using M2, refer to Table 4.1. Additionally, based on the ratio readings A_{260} / A_{280} and A_{260} / A_{230} nm, the gDNA purity was high with values close to 1.8 and the gDNA was recovered with minimal contaminants from the DNA isolation method with values between 2.27 – 2.43, respectively, refer to Table

4.1. Intact gDNA was recovered using both methodologies as evidenced from agarose gel electrophoresis, refer to Figure 4.2.

Table 4.1 Comparing the mean yields of DNA extracted from a Gram-negative and Gram-positive monospecies biofilm using the PowerBiofilm® DNA Isolation kit (MoBio) versus PowerBiofilm® bead beating tubes (MoBio) together with the CTAB methodology; refer to section 4.2.2.5. The DNA concentration was measured using the Nanodrop®.

Monospecies Biofilm		DNA Extraction Method	Concentration of DNA extract ng / µl ¥	Absorbance 260 / 280 nm ∂	Absorbance 260 / 230 nm §
Sample time (h) Bacteria	Patient Designation				
48 h P. aeruginosa	A68	M1	1684	2.02	2.27
48 h P. aeruginosa	A68	M2	2259	2.07	2.34
48 h S. aureus	A52	M1	584	2.02	2.33
48 h S. aureus	A52	M2	1717	2.01	2.43

M1 PowerBiofilm® DNA Isolation Kit (MoBio).
M2 PowerBiofilm® Bead-Beating tube (composed of a 0.1 mm glass, 0.5 mm glass and 2.4 mm ceramic mix) (MoBio) + CTAB DNA Extraction Method.
∂   Indicates protein contamination of DNA samples, values ≥ 1.8 indicate a pure DNA sample.
§   Indicates contamination of the DNA extract with reagents used during the extraction process. Values close to 1.8 indicate a pure DNA sample.
¥   Means from duplicate reads.
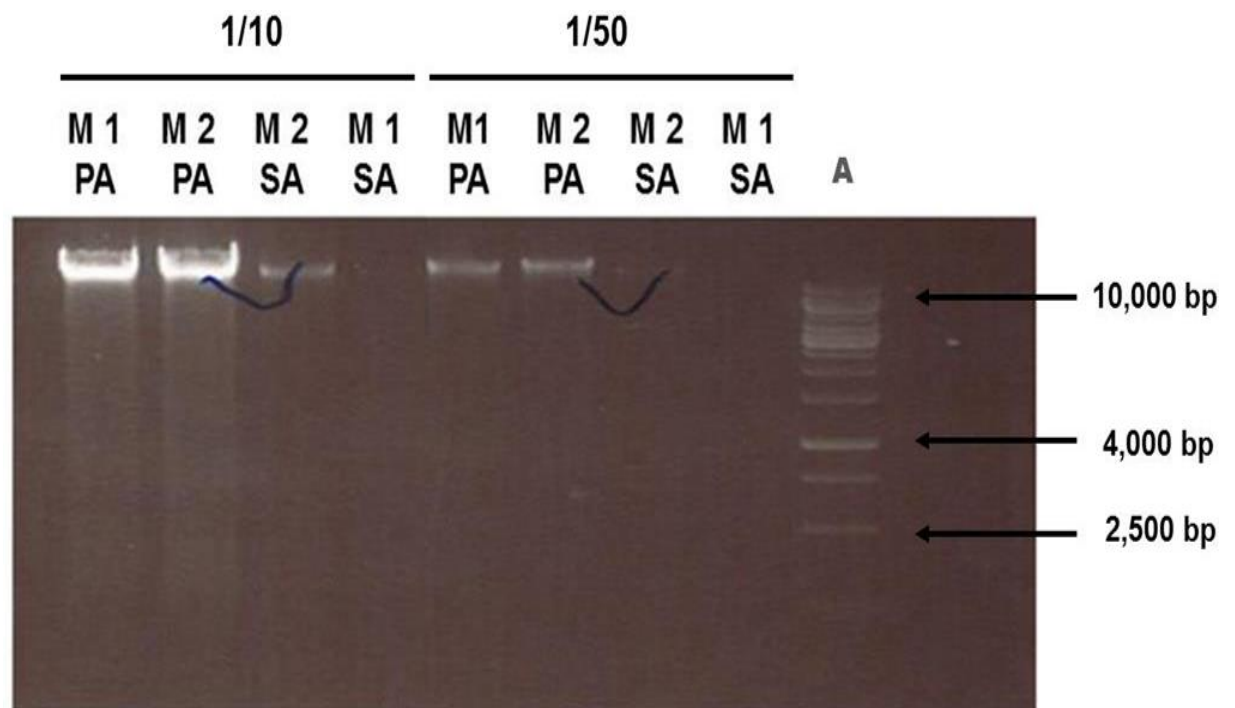
Figure 4.2 PowerBiofilm® bead beating tubes (MoBio Laboratories, Inc., U.S.) in conjunction with the CTAB DNA extraction method yields higher quantities of intact DNA. Image of a 0.8% agarose gel showing, a higher recovery of intact gDNA extract from 48 h monospecies biofilms formed by the CF isolates of *P. aeruginosa* PA68 (PA) and *S. aureus* A52 (SA) using the PowerBiofilm® bead beating tubes with the CTAB methodology in lanes labelled M1 compared to that obtained using the PowerBiofilm® kit (MoBio, Laboratories, Inc., U.S.) in lanes labelled M2. Lanes labelled 1/10 represent lanes for which the gDNA extract was diluted 1 in 10 in TE buffer; lanes labelled 1/50 highlight a 1 in 50 dilution of the gDNA extract in TE buffer. The V-shape marks the lanes which contain a higher amount of gDNA recovered based on the Nanodrop® readings, refer to Table 4.1. The grey letter **A** marks the lane which contains the molecular weight ladder, Hyperladder I (Bioline, U.K.); black arrows indicate the base pair size for the corresponding DNA fragment.

4.3.4 The cell suspension of a *P. aeruginosa* CF isolate exhibits limited antimicrobial activity against the growth of a *S. aureus* CF isolate

This antimicrobial activity test was carried to investigate if the cell suspensions or cell-free supernatant suspensions of this *P. aeruginosa* CF clinical isolate exhibited antimicrobial activity against the *S. aureus* CF clinical isolate as other studies have previously shown (Machan *et al.*, 1991; Filkins *et al.*, 2015).
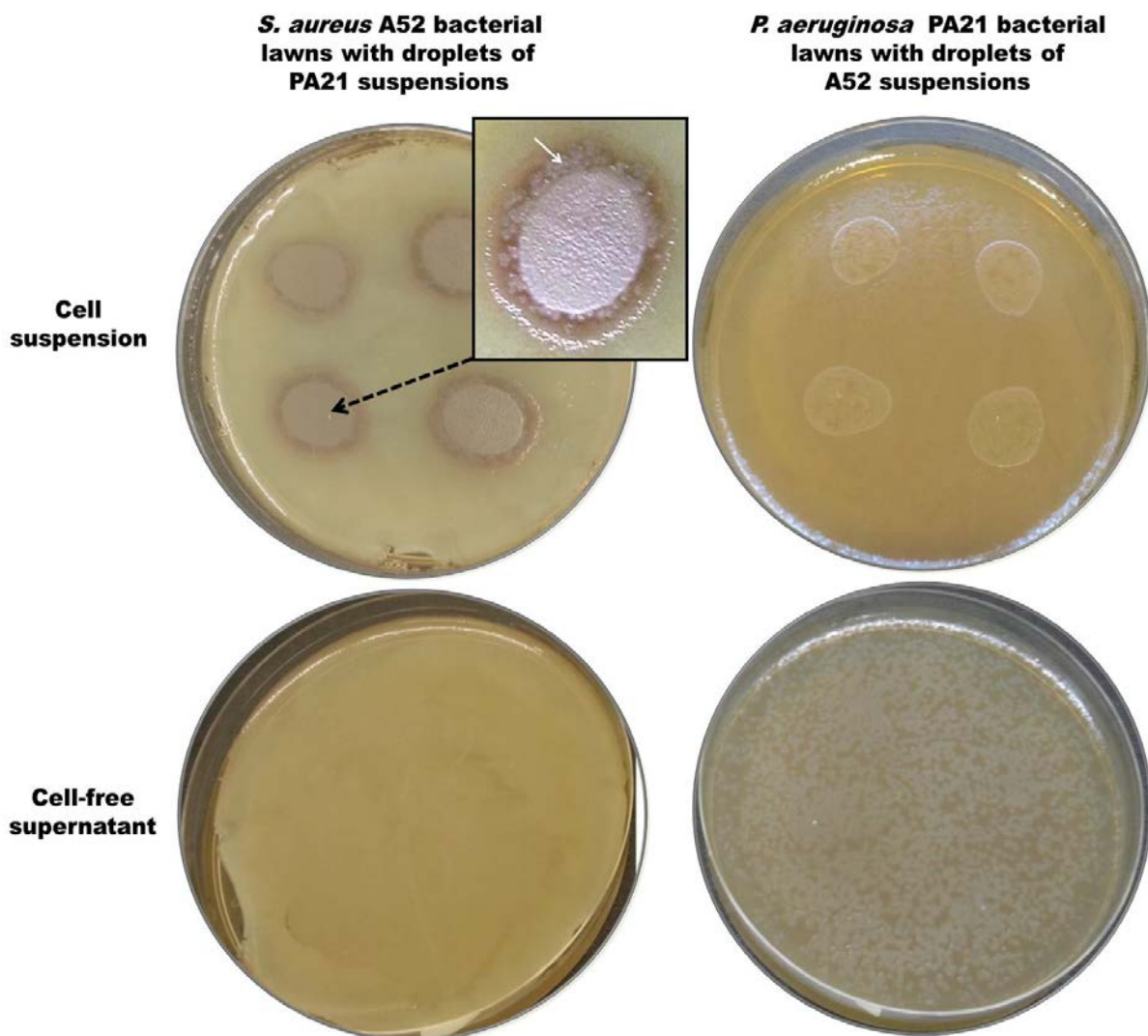
Figure 4.3   Investigating the antibacterial activity of the CF isolates used for the dual-species biofilm assay using the agar spot assay. Partial antibacterial activity exerted by the cell suspension of the *P. aeruginosa* CF isolate PA21 against the *S. aureus* CF isolate A52 bacterial lawn. Regrowth of *S. aureus* occurs within the inhibition zone (top left). This is highlighted by a white arrow in a closer image of the

Figure 4.3 cont'd: colony which points to the colonies of *S. aureus* regrowth within the small halo of clearance around the PA21 *P. aeruginosa* bacterial cell suspension colony. No inhibition zone observed for the *S. aureus* A52 cell suspension against the *P. aeruginosa* PA21 bacterial lawn (top right). The cell free supernatants did not inhibit bacterial growth of the opposing species. The bacterial suspensions were spread onto BHI agar supplemented with hemin, 1.25 μg / ml of molten BHI agar; representative images shown for the agar plates. The bacterial lawns for *P. aeruginosa* display plaque-like clearings, which are clearly visible with the dense growth and is indicative of autolysis for this particular *P. aeruginosa* CF strain.

The cell suspension of *P. aeruginosa* exerted only a partial inhibition of *S. aureus* growth, Figure 4.3. There is visible *S. aureus* regrowth evident within the halo around the *P. aeruginosa* cell suspension, refer to Figure 4.3. The *S. aureus* cell suspension exerted no inhibitory effect on the growth of the *P. aeruginosa* bacterial lawn, refer to Figure 4.3. Interestingly, the cell free supernatants from both bacterial species exerted no inhibitory effect on the growth of the opponent species, refer to Figure 4.3. Moreover, the interaction between these two bacterial species isolated from CF sputum is not an antagonistic relationship but is a commensal relationship. Other authors have reported similar synergistic observations such as Hoffman *et al.*, 2006 and Michelsen *et al.*, 2014. Equally, antagonistic interactions for co-cultures of these two species have also been previously described by Mashburn *et al.*, 2005 and Beaume *et al.*, 2015. Interestingly, this CF isolate of *P. aeruginosa* displayed plaque like clearing which is a result of autolysis which could possibly be due to cell signalling molecules such as PQS (McKnight *et al.*, 2000) or as a result of the triggering of induction of a prophage (Winstanley *et al.*, 2009).

4.3.5 Quantitative analysis of a 48 h dual–species biofilm's morphology on temporal exposure to ~ 500 pM exogenous NO

Quantitative analysis was performed on the images obtained from confocal laser microscopy (CLSM) using the software Comstat2, to compare the differences in the biofilm morphology between the control and NO treated dual-species biofilms using three parameters: Biofilm biovolume (μm^3 / μm^2) (Figure 4.5), average biofilm thickness (μm) (Figure 4.5) and the biofilm roughness coefficient (dimensionless) (Table 4.2) (Heydorn *et al.*, 2000).

After 1 h of exposure to ~ 500 pM NO, the dual-species biofilm biovolume showed no significant reduction compared to the control, for both the SYTO9 (P = 0.095) and propidium iodide (PI) channels (P = 0.69), refer to Figure 4.5. This modest dual-species biofilm biovolume reduction after 1 h of NO exposure can be visualized in the 3D image in Figure 4.4; wherein there is more unoccupied black voids in the NO treated dual-species biofilm coverage. The dual-species biofilm average thickness values for the 1 h NO biofilms did not decrease for the SYTO9 (7.94 μm ± 1.30; P = 0.06) or the PI (7.86 μm ± 1.29; P = 0.07) channels compared to the control (4.96 μm ± 0.83 for SYTO9; 4.97 μm ± 0.78 for PI; (mean μm ± SEM). The biofilm roughness coefficient, a measure of the level of biofilm heterogeneity was not significantly altered to that of the control (P = 0.313 for SYTO9; P = 0.50 for PI), refer to Table 4.2. Interestingly, after 12 h and 15 h of exposure to NO the dual-species biofilm biovolume increases temporally compared to the control. This is evidenced in the CLSM images in Figure 4.4. The dual-species biofilm architecture is notably changed after 12 h of NO exposure, with less black voids visible compared to the control, refer to Figure 4.5. Additionally, the 12 h NO treated dual–species biofilm is composed of a dense layer of tightly packed cells compared to the control at 12 h which shows a greater number of black voids combined with mature microcolony structuring. This is further reflected by a significantly lower biofilm roughness coefficient value of 0.45 ± 0.46, P ≤ 0.001 compared to the control's value of 1.1 ± 0.29, P ≤ 0.001 for the SYTO9 channel (similar significant values for the PI channel), refer to Table 4.2. The temporal increase in the biofilm biovolume for the dual-species biofilms treated with ~ 500 pM NO continues after 24 h of treatment.

However, this difference is not statistically significant ($F_{1, 29}$ = 1.86, P = 0.183) with values of 0.69 ± 0.89 μm^3 / μm^2 and 1.13 ± 0.84 μm^3 / μm^2 in the SYTO9 channel for the control and SNP biofilm respectively (mean biofilm biovolume ± SEM). The dual-species' biofilm morphology after 24 h of NO treatment displays larger microcolonies compared to the untreated with a modest increase in unoccupied voids similar again to the untreated (Figure 4.4). After 24 h of NO exposure the dual-species biofilm heterogeneity returns to the control levels as evident in the biofilm roughness values, refer to Table 4.2. Interestingly, for the PI channel after 24 h of exposure to ~ 500 pM exogenous NO the biofilm biovolume increases significantly compared to the control ($F_{1, 29}$ = 4.96, P = 0.034), refer to Figure 4.5. Although there is a higher level of biofilm biovolume in the PI channel compared to the control this is not as a result of the presence of dead cells exhibiting red fluorescence but could be due to PI binding to more extracellular DNA in the dual-species biofilm matrix and/ a number of bacterial cells may have incurred damage to the cell membrane, refer to Figure 4.4. The PTIO + SNP treatment (sampled at 24 h) serves as a control to show that differences in the NO treatments are as a result of the presence of NO. The aforementioned treatment, displayed a significant increase in only the biofilm average thickness parameter compared to the control at 24 h ($F_{1, 28}$ = 13.49, P = 0.001 for the SYTO9 channel; similar values obtained for the PI channel), refer to Figure 4.5. This difference is statistically significant for the PTIO + SNP treatment with average thickness value of 21.78 μm ± 2.26 compared to the control's value of 12.53 μm ± 1.10 (means ± SEM) it does not correlate with an increase in the biofilm biovolume values. Importantly, the biofilm biovolume for the dual-species biofilm has demonstrated a temporal dependent increase from 12 h onwards on exposure to exogenous NO which based on this study, has been the principal biofilm parameter affected by NO, refer to Figure 4.5. Collectively, this difference in the PTIO + SNP treatment does not impact on the observations made in this section. Finally, the biofilm average thickness showed a significant increase (P = 0.004 for SYTO9: P = 0002 for PI) in the SNP treatment compared to the control at the 12 h time point. This is in conjunction with the increase observed in the biofilm biovolume for this time point, Figure 4.5.
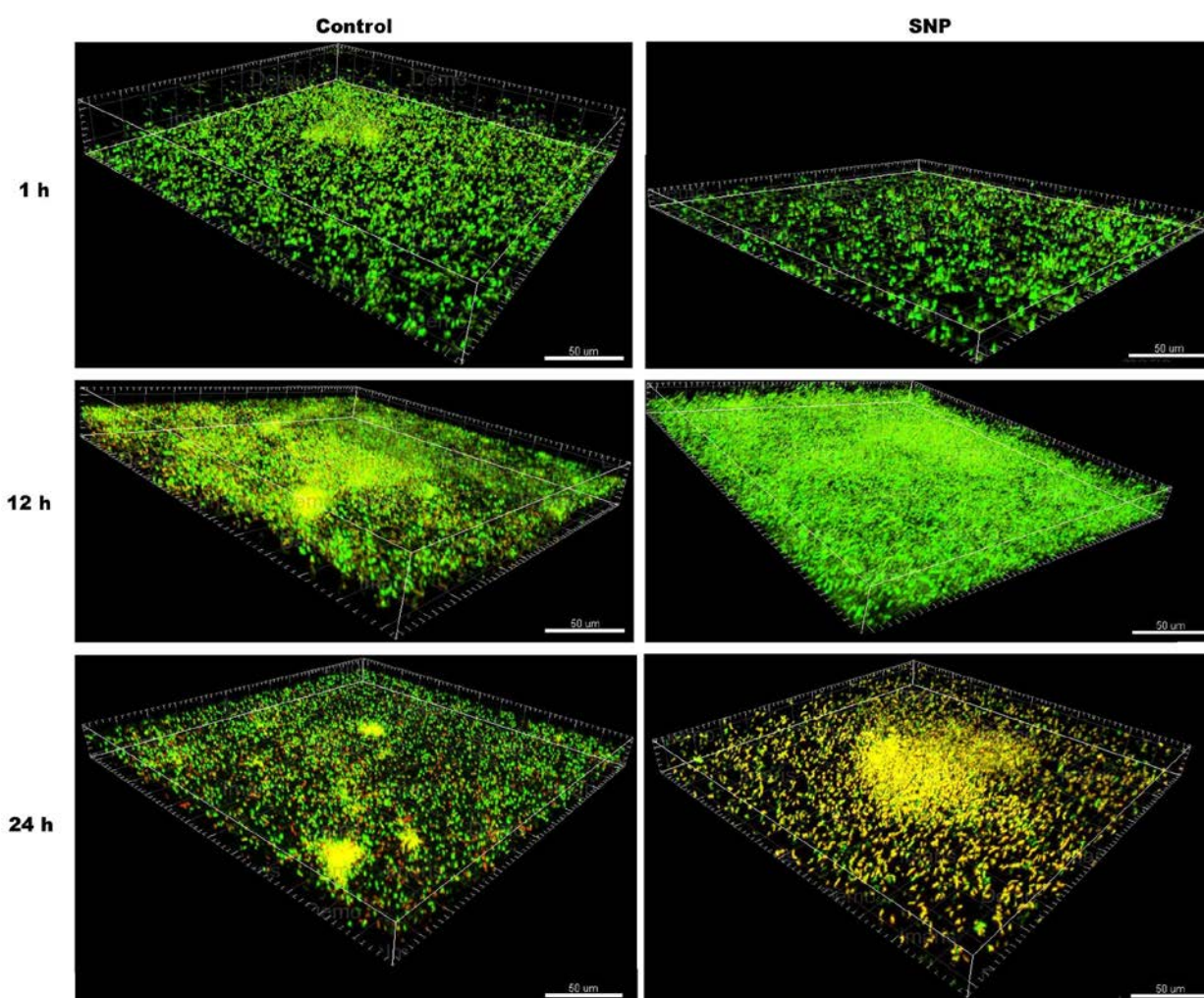
Figure 4.4 CLSM images of the dual-species biofilms formed by the CF isolates of *S. aureus* A52 and *P. aeruginosa* PA21 to track the temporal effect of NO on the dual-species biofilm architecture. The dual-species biofilm were grown for 48 h prior to treatment with ~ 500 pM NO via the addition of 500 μM of the NO donor sodium nitroprusside (SNP). The dual-species biofilms were stained using Live/Dead® *Bac*Light™, representative z-stacks shown for the merge of the SYTO9 and PI channels were 3D rendered using Imaris x64 (v8.2.1 trial package). A modest non-significant reduction in the dual-species biofilm biovolume compared to the untreated dual-species biofilm after 1 h of exposure to the NO donor SNP is visible (top right z-stack). A temporal increase in the dual-species biofilm is clearly visible commencing after 12 h of exposure to ~ 500 pM NO. Moreover, the biofilm architecture of the dual-species biofilms treated with NO display a more homogenous biofilm structure after exposure to NO from 12 h up to 24 h compared to the heterogeneous biofilm structure observed for the controls. Scale bar = 50 μm.
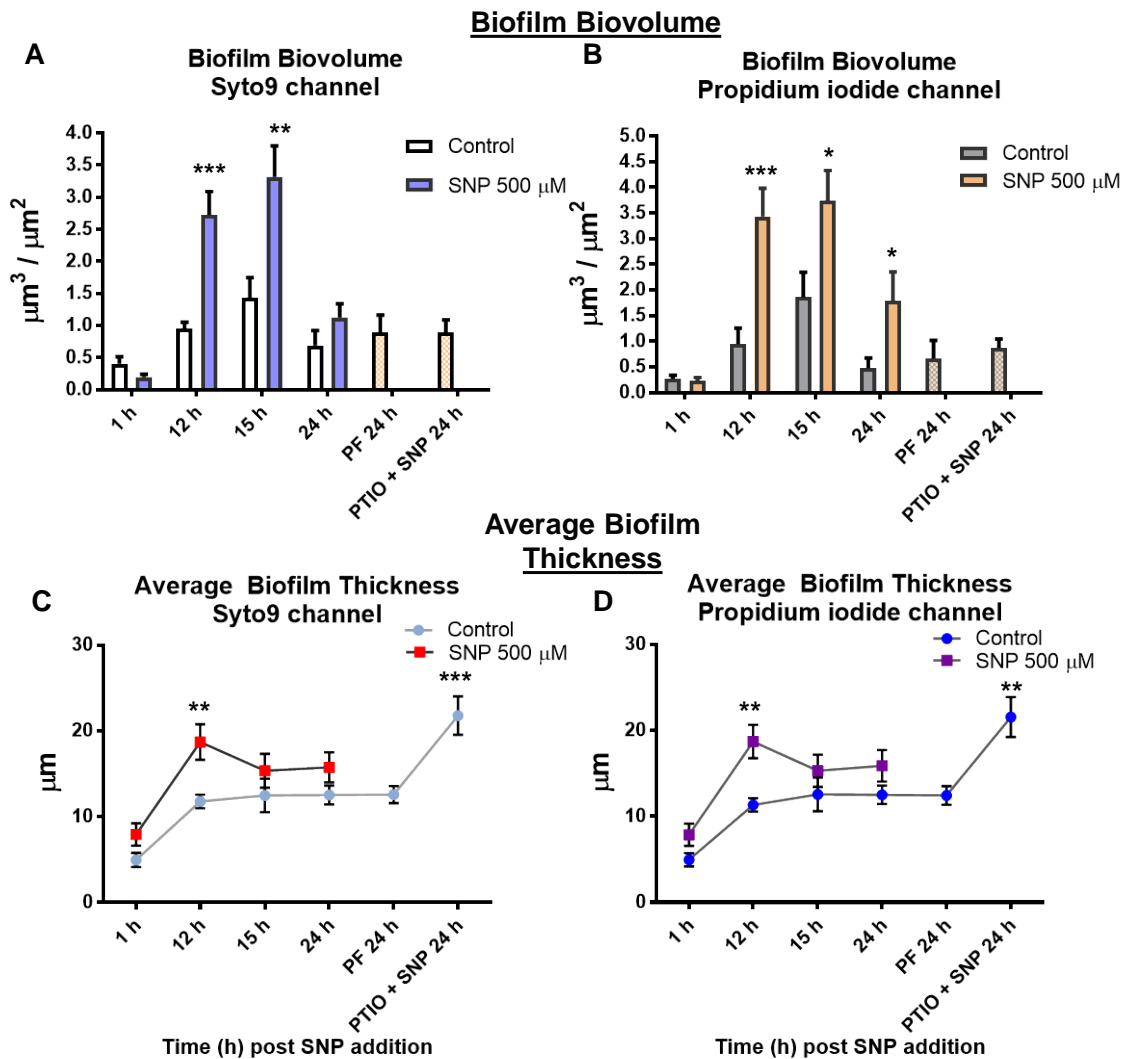
Figure 4.5 The effect of NO on the biofilm parameters of a dual-species biofilm formed by the CF isolates *S. aureus* A52 and *P. aeruginosa* PA21. Quantitative analysis of the biofilm biovolume (**A** and **B**) and the average biofilm thickness (**C** and **D**) were calculated using Comstat2. The biofilm biovolume (μm^3 / μm^2) of the dual-species biofilm for both the SYTO9 and PI channels increases after 12 h ($P = 0.000$ for SYTO9; $P = 0.000$ for PI) and 15 h ($P = 0.003$ for SYTO9; $P = 0.02$ for PI) of exposure to NO for both SYTO9 and PI; Figures **A** and **B** respectively. After 24 h of exposure to NO the dual-species biovolume in the PI increases significantly ($P = 0.038$ for PI). The average biofilm thickness (μm) parameter shows a significant increase for both the SYTO9 and PI channels commencing after 12 h of exposure to NO; Figures **C** and **D** respectively. With the PTIO + SNP treatment showing a significant increase in average biofilm thickness ($P = 0.001$ for SYTO9; $P = 0.002$ for PI). Values are means with error bars for SEM, five representative z-stacks per treatment for three biological replicates, $n = 15$. Statistical comparisons were made using one-way ANOVA. Asterisk marks significant differences from the control as follows: * $P \leq 0.05$, ** $P \leq 0.01$, *** $P \leq 0.001$.

173

Table 4.2 A temporal effect of nitric oxide on reducing the biofilm roughness co-efficient (dimensionless) for established dual-species biofilms formed by the CF isolates *S. aureus* A52 and *P. aeruginosa* PA21, as calculated by Comstat2.

	Roughness Coefficient				
	Mean ± Standard Deviation				
Channel	**Control 1 h**	**Control 12 h**	**Control 15 h**	**Control 24 h**	**PF 24 h**
Syto 9	1.5 ± 0.59	1.1 ± 0.29	0.9 ± 0.67	1.4 ± 0.59	1.3 ± 0.60
Propidium Iodide	1.6 ± 0.51	1.3 ± 0.33	0.9 ± 0.69	1.7 ± 0.32	1.5 ± 0.48
Channel	**500 µM SNP 1 h**	**500 µM SNP 12 h**	**500 µM SNP 15 h**	**500 µM SNP 24 h**	**100 µM PTIO + 500 µM SNP 24 h**
Syto 9	1.7 ± 0.3	0.4 ± 0.46 ***	0.5 ± 0.43	1.1 ± 0.50	1.2 ± 0.50
Propidium Iodide	1.7 ± 0.32	0.5 ± 0.46 ***	0.6 ± 0.42	1.1 ± 0.54 **	1.3 ± 0.45 **

Statistically different from untreated controls: ** $P \leq 0.01$; *** $P \leq 0.001$

4.3.6 Enumeration of the temporal effect on the species composition of a 48 h dual–species biofilm exposed to exogenous NO using PMA–qPCR

The PMA-qPCR approach (Nocker *et al.*, 2007; Rogers *et al.*, 2008) was used to quantify the viable cell population remaining within 48 h dual-species biofilms post exposure to ~ 500 pM exogenous NO over the course of 24 h. Additionally, the effect exogenous NO treatment exerted on the population composition of the dual-species biofilms formed by CF isolates of *P. aeruginosa* and *S. aureus* was also measured. This work was carried out to determine if biofilm dispersal was triggered within this dual-species biofilm on exposure to exogenous NO, similar to that reported for a biofouling mixed species biofilms (Barnes *et al.*, 2013).

Overall, a high linearity of the Ct values plotted in the standard curves was demonstrated by r^2 values from 0.95–0.99 and amplification efficiencies ranging from 74% - 99% (Appendix 5).
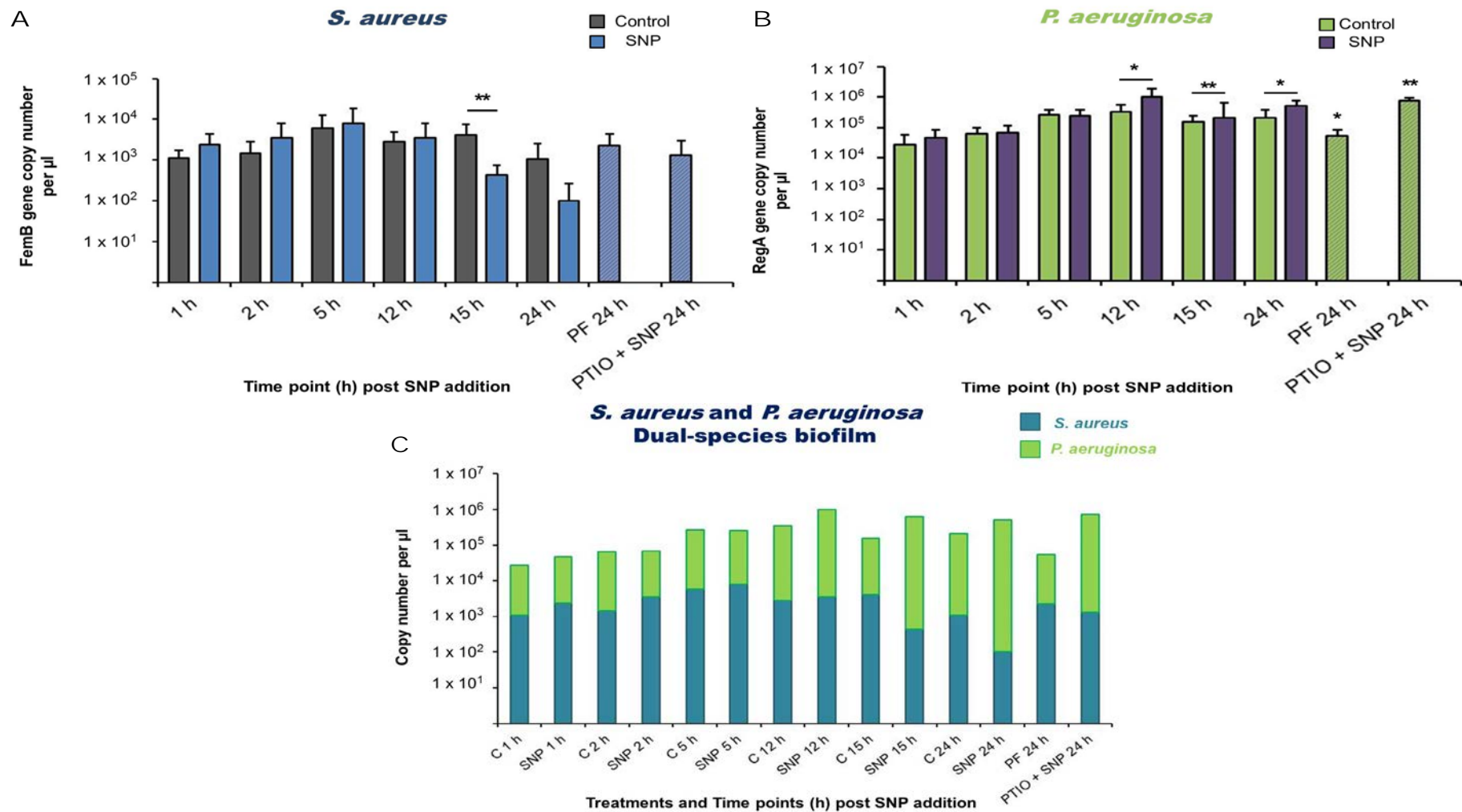
Figure 4.6 Enumeration of the viable population dynamics of an established dual-species biofilm, formed by CF isolates *S. aureus* A52 and *P. aeruginosa* PA21 post exposure to NO over a 24 h period using PMA-qPCR. Figures **A** shows a significant reduction of *S. aureus* within

Figure 4.6 cont'd: the dual-species biofilm after 15 h of exposure to ~500 pM NO (*P* = 0.002). However, after 24 h of exposure to NO the reduction is not significant compared to the control (*P* = 0.06). Figure **B** shows a minor but significant increase in the proportion of *P. aeruginosa* cells in the dual-species biofilm after 12 h (*P* = 0.02), 15 h (*P* = 0.01) and 24 h (*P* = 0.02) of exposure to ~ 500 pM NO compared to their corresponding control values. Figure **C** shows the collated PMA-qPCR data for the viable proportion of *S. aureus* and *P. aeruginosa* cells remaining in a dual-species biofilm grown for 48 h prior to exposure to ~ 500 pM NO over the course of 24 h. Statistical differences from the control highlighted using asterisks as follows: * *P* ≤ 0.05 and ** *P* ≤ 0.01. Means with error bars for standard deviation; all reactions were performed in duplicate with three independent biological experiments (*n* = 6).

The NO donor SNP was added to established dual-species biofilm composed of the CF isolates *P. aeruginosa* and *S. aureus;* both untreated controls and SNP treated biofilms were sampled after 1 h, 2 h, 5 h, 12 h, 15 h and 24 h of exposure by removal from the surface. All biofilm suspensions were treated with PMA to ensure the extracellular DNA (eDNA) and DNA from dead cells would be excluded from quantification through qPCR. The gDNA was isolated from the dual-species biofilms using an optimized method (section 4.2.2.5 (ii)). An aliquot of this gDNA extract was used in separate qPCR assays, to detect the copy number per microliter for the *femB* and *regA* gene to quantify remaining viable *S. aureus* and *P. aeruginosa* cells within the untreated and SNP treated dual-species biofilms, respectively.

The results from the qPCR analysis revealed, that overall the addition of ~ 500 pM of exogenous NO did not cause an increase or decrease of the viable *S. aureus* bacterial load within the dual-species biofilms compared to the untreated biofilms sampled after 1 h (*P* = 0.28), 2 h (*P* = 0.41), 5 h (*P* = 0.88), 12 h (*P* = 0.49) and 24 h (*P* = 0.06) of NO exposure (Figure 4.6 A). However, after 15 h of treatment with NO, a statistically significant reduction (*P* = 0.002) in the viable proportion of *S. aureus* remaining within the dual-species biofilm was noted. No observable effect for the SNP chemical controls was observed on the *S. aureus* bacterial load within this dual-species biofilm.

In contrast to these effects of NO on *S. aureus* in the dual-species biofilm, a statistically significant increase is observed for the viable *P. aeruginosa* bacterial load remaining in the dual-species biofilm post treatment with exogenous NO, Figure 4.6 B. The addition of NO to the established dual-species biofilm after 1 h, 2 h and 5 h of exposure did not result in significant differences in the viable proportion of *P. aeruginosa* load within the biofilm compared to that of the untreated biofilms; (1h $P = 0.24$, 2 h $P = 0.68$, 5 h $P = 0.91$; Figure 4.6 A). After 12 h onwards of exogenous NO exposure, the *P. aeruginosa* bacterial load within the dual-species biofilms showed a consistent statistically significant increase compared to the untreated biofilms (12 h $P = 0.018$, 15 h $P = 0.014$ and at 24 h $P = 0.024$; Figure 4.6 A). This temporal increase in the bacterial load for *P. aeruginosa* within the dual-species biofilm formed with *S. aureus* post exposure to NO, is further supported by the increase observed for the biofilm biovolume as calculated by Comstat2 at these time points, Figure 4.5 A and B. Moreover, qualitatively this biofilm biovolume increase can be observed in the CLSM images for the NO treated dual-species biofilms with representative images shown for the 12 h and 24 h time points post NO addition, refer to Figure 4.4.

The SNP controls PF and PTIO, showed a statistically significant difference from the 24 h control, with a lower and higher bacterial load of *P. aeruginosa* within the dual-species biofilm quantified, with 4.4 ± 0.28, $P = 0.02$ for PF and 5.5 ± 0.16, $P = 0.004$ for 100 µM PTIO + 500 µM SNP compared to the control levels of 4.9 ± 0.36 (mean $\log_{10}$ value $\pm$ standard deviation $\log_{10}$ value). The increase in the *P. aeruginosa* bacterial load within the dual-species biofilms treated with 100 µM PTIO and 500 µM SNP, can possibly be explained by the non-selective reactions of PTIO binding to superoxide radicals (O_2^-); thereby sequestering otherwise damaging radical accumulation from the dual-species biofilm (Haseloff *et al.*, 1997). This reactivity has been further discussed by other authors (Goldstein *et al.*, 2003). The lower levels of *P. aeruginosa* detected within the dual-species biofilms treated with PF ($P = 0.02$) suggests there may be a possible shift in the species dynamic for the dual-species biofilms treated with PF, as a similar reduction in the viable load of *S. aureus* if not observed, Figure 4.6.

In Figure 4.6 C, the qPCR data from both the *S. aureus* and *P. aeruginosa* detection assays is collated data to allow for the appreciation of the viable proportions of both species within the dual-species biofilm. *P. aeruginosa* is the predominate member within this dual-species biofilm community, both temporally in the untreated and NO treated biofilms, Figure 4.6 C. The *S. aureus* population fluctuates between 10^3 – 10^4 copies / µl, remaining ~1 log below the bacterial load detected for *P. aeruginosa*, whose population fluctuates between 10^4 - 10^5 copies / µl.

4.4 Discussion

It has long been recognised that in nature biofilms consist of a highly complex consortia, which can be composed of both bacteria, fungi, protozoa and algae (Costerton *et al.*, 1978; Ellwood *et al.*, 1982; Ramanan *et al.*, 2016). Whereas, until the last decade, biofilms involved in human infections were largely considered to lack species richness, as evident by biofilm research largely confined to studying monospecies biofilms formed by microorganisms commonly associated with human infection (Lam *et al.*, 1980; Lee *et al.*, 2005; Davis *et al.*, 2008). The long term colonisation of the CF lung by *P. aeruginosa* within biofilms is a classic example of why perhaps monospecies biofilm research was largely pursued in relation to human infection. Importantly, a shift towards polymicrobial biofilm research is being increasingly pursued (Wolcott *et al.*, 2009; Tavernier and Coenye, 2015), especially within the CF biofilm research field, due to the observations made for example by Rogers *et al.*, (2009); Sibley *et al.*, (2008) and van der Gast *et al.*, (2011).

The work in this Chapter was undertaken to investigate the findings in Chapter 3 (section 3.37). Wherein, an overall decrease in the biofilm biovolume for *ex vivo* sputum mixed species biofilms treated with ~ 500 pM NO was observed, as quantified using Comstat2 analysis of the CLSM images. A number of these enriched *ex vivo* sputum biofilms were shown to be composed of *P. aeruginosa* and *S. aureus*. Biofilm dispersal of *S. aureus* monospecies biofilms was not achieved over a range of NO concentrations, as described in Chapter 3. However, based on previous work within our group and from other studies (Barraud *et al.*, 2006), exogenous NO concentrations of ~ 500 pM have been shown to trigger biofilm dispersal of *P. aeruginosa* biofilms. Therefore, the work in this chapter was undertaken to investigate if NO was capable of inducing biofilm dispersal of a dual-species biofilm formed by CF clinical isolates of *P. aeruginosa* and *S. aureus*.

In this Chapter, (i) various gDNA extraction methodologies were explored to ensure unbiased estimations of bacterial community dynamics within a dual-species biofilm could be accurately quantified by downstream methodologies, namely qPCR for this study, (ii) PMA-qPCR: addition of PMA prior to gDNA isolation and qPCR analysis of dual-species biofilms was used as an approach characterise the viable bacterial community with the dual-species biofilm post

addition of exogenous NO, (iii) an *in vitro* dual-species biofilm model composed of CF isolates of *P. aeruginosa* and *S. aureus*, to investigate if exogenous NO can trigger biofilm dispersal is described. Comstat2 analyse of the dual-species biofilm enabled quantitative results of biofilm parameters to characterise the effect NO had on the established dual-species biofilms.

A large number of protocols exist for the extraction of gDNA from microorganisms. The primary issues relating to the extraction of DNA is firstly, the material in which the microorganisms are found (i.e. soil and sputum) and the effective disruption of the cell wall. Additionally, efficient extraction of DNA from cells within biofilms needs to be fully tested and/ optimized for every system to cater for latter downstream use. The main concern in the extraction of DNA from Gram-positive bacteria is the effective lysis of cells. The choice of enzyme for the cell wall disruption of Gram-positive isolates is important. Lysozyme is one of the most widely used cell lysis enzymes and may not effectively disrupt all Gram-positive isolates (Chapaval *et al.*, 2008). Therefore, the use of both lysozyme and lysostaphin combined and singly at different concentrations was also investigated, as initially insufficient cell lysis for this *S. aureus* CF isolate was observed despite increasing the incubation period. Lysostaphin was used as an alternative enzyme replacement because it can cleave the polyglycine bridges which cross-link glycopeptide chains in the peptidoglycan cell wall of Gram-positive and is routinely used to replace lysozyme. The results obtained show that a low concentration of lysostaphin (0.088 mg / ml) lysed cells and the use of a dual-enzymatic treatment resulted in a high yield of DNA but crucially DNA damage was clearly visible, refer to Figure 4.1.

Work pertaining to the use of dual lytic enzyme combinations of lysostaphin–lysozyme compared to the use of a commercial lysis buffer from Roche Applied Science in the extraction of DNA from CF sputum prior to pyrosequencing was tested by Zhao, Carmody, *et al.*, (2012b) with the specific focus on the detection of *S. aureus*. Interestingly, their sequencing results found that lysis involving the dual enzyme combination resulted in a lower level of species richness for the overall community but a greater detection level of

Staphylococcus versus that obtained from using the manufactured lysis buffer, which showed the opposite scenario. The combined use of lysostaphin and bead-beating was not an approach used for the extraction of DNA from biofilms which contain Gram-negative bacteria, as this treatment proved damaging to the gDNA extract for the Gram-positive isoalte. Instead, a lower concentration of lysozyme (80 mg /ml) combined with bead-beating methodology was used to extract gDNA from biofilms composed of Gram-positive and Gram-negative bacteria. A number of DNA extraction methods for *S. aureus* were explored. However, the polyvinylpyrrolidone (PVP) DNA extraction as described by Chapaval *et al.*, (2008), guanidinium thiocyanate DNA extraction described by Pitcher *et al.*, (1989) and 1:1 acetone, ethanol DNA extraction described by Birnboim, 1983 produced either non detectable levels of DNA or DNA which was visibly sheared as observed on agarose gel electrophoresis evaluation, Figure 4.1.

The extraction of intact and pure DNA from biofilms which are composed of both Gram-negative and Gram-positive bacterial species need to be tested in order to verify whether a protocol is biased in the level and purity of DNA which is extracted for all species (Vishnivetskaya *et al.*, 2013). Additionally, in the case of extraction of pure DNA from biofilms the removal of the extracellular matrix as a contaminant involves tailoring the extraction process to mechanical disrupt this structure and chemically elute compounds such as polysaccharides, proteins and lipids. One of the most widely used chemical DNA extraction methods is the CTAB method, which is traditionally used for DNA extraction of plants and fungi (Doyle and Doyle, 1987). This method has proven useful in the extraction of DNA from *B. cepacia* complex members within the CF sputum samples (Ergunay *et al.*, 2008). CTAB is a cationic detergent which binds to the polysaccharides and glycoproteins which are abundant in bacterial biofilms. This quality coupled its low cost when combined with phenol chloroform isoamyl alcohol steps; make it a low cost methodology for implementing in laboratories constantly carrying out a large number of DNA extractions.

The poor performance of sonication at 60 kHz at RT for the cell lysis of Gram-positive and Gram-negative bacteria within biofilms compared to that obtained using bead-beating, led to the bead-beating approach being further investigated. Importantly, the sole use of 2 mm glass beads led to sheared DNA from the *S. aureus* biofilms with the effects most noticeable when 2 cycles were utilized. Due to this issue, the use of a combination of bead types with smaller diameters was investigated as designed by MoBio and used within their PowerBiofilm® DNA Extraction Kits. The bead beating tube used in this set of work are composed of a mixture of 0.1 mm glass beads, 0.5 mm glass beads and a 2.4 mm ceramic mix. This bead beating tube was coupled with the CTAB DNA extraction methodology (including modifications made within this study) and tested for performance against the PowerBiofilm® DNA Extraction Kit. The PowerBiofilm® commercial kit gave high yields of undamaged and pure gDNA; with 1,684 ng / μl and 584 ng / μl of gDNA extracted from *P. aeruginosa* and *S. aureus* respectively (Figure 4.2 and Table 4.1). Intriguingly, this kit was out performed when compared to the level of gDNA recovered using the PowerBiofilm® bead-beating tube coupled with the CTAB methodology utilized in this study (section 4.2.2.5 (ii)). Genomic DNA levels of 2,259 ng / μl and 1,717 ng / μl were recovered from monospecies biofilms formed by *P. aeruginosa* and *S. aureus*, respectively using the aforementioned methodology (Figure 4.2 and Table 4.1).

Crucially, other authors investigating the composition and abundance of members within the CF microbiome through whole genome sequencing approached and qPCR analysis, acknowledge that the detection level of microorganisms varied largely between groups based on the DNA extraction methodologies employed (Momozawa *et al.*, 2011; Goddard *et al.*, 2012; Hauser *et al.*, 2014). Moreover, as shown in this study, a difference in the gDNA levels was observed between the chemical components used in a commercial kit from PowerBiofilm® compared to the widely used CTAB DNA extraction method, as the same bead-beating tube was used in both methodologies. Based on these results, the PowerBiofilm® bead-beating tube combined with the CTAB DNA extraction methodology refined in this Chapter

was utilised for extracting gDNA from the dual-species biofilms for downstream qPCR analysis.

To my knowledge, this is the first study experimentally testing an *in vitro* dual-species biofilm formed by *P. aeruginosa* and *S. aureus* isolates obtained from CF sputum and quantitatively determining if biofilm dispersal can be achieved on the addition of exogenous NO. The NO donor SNP was added at a concentration of 500 μM which equates to approximately 450 -500 pM of NO release due to the work carried out within our group (Howlin, Cathie, Hall-Stoodley, Cornelius, Duignan *et al.*, 2017).

There are currently a number of papers which have investigated co-culturing and biofilm dynamics for these two species (Mashburn *et al.*, 2005; Hoffman *et al.*, 2006; Baldan *et al.*, 2014; Michelsen *et al.*, 2014; Filkins *et al.*, 2015). Interestingly, Mashburn *et al.*, 2005 put forward evidence that *S. aureus* served as an iron source for *P. aeruginosa* as a possible reason for *P. aeruginosa* out competing *S. aureus* during colonisation of the CF lung. Which can undoubtedly be a factor in the co-colonisation of these microorganisms (Hutchins *et al.*, 1999) or in fact, any other microorganisms both in nature and in human infection (Skaar, 2010). However, in relation to the colonisation of the CF lung, there is ample bioavailability of iron within the CF lung as demonstrated by Hunter *et al.*, (2013), with total iron concentrations ranging from 18 - 62 μM for mild to severe CF lung infections, respectively. Based on this observation, I used hemin to supplement the 1/5 BHI medium used to grow the dual-species biofilms for 48 h in an effort to mimic similar conditions in the CF lung; with the recognition that this medium does not resemble the composition or viscosity of CF sputum. Importantly, hemin is composed of an iron-containing porphyrin and as iron containing proteins (e.g. haemoglobin, cytochrome c) have a high affinity for binding to NO (Drapier *et al.*, 1993; Cooper, 1999), the concentration of hemin used for this study is several fold lower than that found in CF lung infections as stated above and shown by Hunter *et al.*, (2013). Furthermore, the bioavailability of iron would be lowered within this model due to it being sequestered by (1) *P. aeruginosa*'s siderophores; pyoverdine and pycochelin (Banin *et al.*, 2005; Cornelis and

Dingemans, 2013) and (2) by *S. aureus* through the surface bound IsdA domain part of the Isd (iron regulated surface determinant) system (Skaar and Schneewind, 2004; Grigg *et al.*, 2010). Therefore, the use of NO as a potential therapy *in vivo* would similarly encounter the above and a number of other interactions which would have an effect on its optimal dose. Preliminary optimization experiments on cell number, medium for biofilm growth and duration of biofilm growth, informed the conditions required for the formation of an established dual-species biofilm by the CF isolates *P. aeruginosa* PA21 and *S. aureus* A52 to test the effect NO had on the dual-species biofilm (data not shown).

Additionally, the antimicrobial activity of both the cell suspensions and cell free supernatants for both species was investigated (Figure 4.3). Overall, the *P. aeruginosa* PA21 cell suspension was the only suspension which exhibited antimicrobial activity. Importantly, only partial inhibition of *S. aureus* A52 growth was observed, with a number of *S. aureus* colonies growing within the *P. aeruginosa* PA21 cell suspension halo. Similar reports of partial inhibition of growth for CF isolates of *P. aeruginosa* tested against *S. aureus*, the Newman strain (a human clinical isolate) have been described Baldan *et al.*, (2014).

A comparative analysis of the temporal effect exogenous NO had on the biofilm architecture of an established dual-species biofilm versus an untreated dual-species biofilms was revealed by both CLSM imaging and quantitative analysis of the CLSM data using Comstat2. The dual-species biofilm architecture 1 h post the addition of NO displayed early microcolony formation with a visibly unoccupied areas of the substratum compared to the untreated at 1 h, which contained showed the opposite (Figure 4.4). Similar roughness coefficient values for both the untreated and NO treated dual-species were obtained. The roughness coefficient is a parameter which describes the degree of heterogeneity of the biofilm examined; heterogeneous biofilms display pockets of microcolony structures with visible voids/water channels throughout the biofilm structure; in contrast the opposite occurs for homogenous biofilms which display lower roughness coefficient values due to a lack of voids, with a characteristic undifferentiated biofilm architecture.

Intriguingly, after 12 h of exposure to NO the dual-species biofilm biovolume increases by 1.77 μm^3 / μm^2 compared to the control in the SYTO9 channel; a similar statistical difference for the PI channel also; Figure 4.5 A and B). This biofilm biovolume increase is clearly visible in the architectural difference in the NO treated dual-species biofilms compared to the control, Figure 4.4. A condensed mat with a clear uniform/undifferentiated biofilm structure is observed. A NO dependent homogenous biofilm structure with a low roughness value was noted, in striking contrast to the higher roughness value for the untreated dual-species biofilm, which displays heterogeneous biofilm architecture. The control is composed of mid-late stage microcolony development with voids throughout the biofilm structure, Figure 4.4. A similar statistically significant increasing trend in the biofilm biovolume is observed for the NO treated dual-species biofilms after 15 h of exposure to NO.

After 24 h of NO treatment, there was an increase observed in both channels for the biofilm biovolume; more evident in the PI channel however. The dual-species biofilm displays a greater uptake of the PI dye, as evident by yellow-orange fluorescence emitted by the biofilm which appears more in the upper layer of the biofilm. This can be indicative of bacteria cell walls which have incurred damage but are not dead VBNC (Gião *et al.*, 2009) or could possibly be due to an increase in eDNA, as PI outcompetes SYTO9 due to its stronger affinity for nucleic acids (Wang *et al.*, 2015). In summary, both qualitative and quantitative analysis do not show a dispersal effect for the dual-species biofilms exposed to NO.

Furthermore, supporting evidence provided by PMA-qPCR analysis of the untreated and NO treated dual-species biofilms sampled over a 24 h period, further demonstrated an increase in the dual-species biofilm biovolume for the biofilms treated with NO, see Figure 4.6. The combined used of PMA treatment prior to gDNA isolation to remove dead cells and the extracellular DNA in the milieu allowed for the accurate estimation of the viable population proportions for both bacterial species within these dual-species biofilms. Thereby preventing the overestimation of bacterial species fraction with a biofilm (Nocker *et al.*, 2007; Rogers *et al.*, 2008; Tavernier and Coenye, 2015). The

qPCR results showed the bacterial community dynamics temporally post NO treatment over a 24 h period, see Figure 4.6 C. It revealed that *P. aeruginosa* was the dominant species within this dual-species biofilm, with at least a one log difference throughout the 24 h period.

The population proportions for *S. aureus* remained relatively stable during treatment with exogenous NO with only a statistically significant lowering of the viable population fraction observed after 15 h of NO treatment (see Figure 4.6 A). This difference was not statistically significant after 24 h of treatment with NO (see Figure 4.6 A). Intriguingly, the opposite case for the *P. aeruginosa* viable cell fraction within the dual-species biofilm was observed, see Figure 4.6 B. The data shows a significant increase in the viable *P. aeruginosa* cell population on treatment with NO, from 12 h to 24 h, see Figure 4.6 B. Interestingly, this result was not expected as *P. aeruginosa* has been shown to undergo biofilm dispersal (Barraud *et al.*, 2006; Li *et al.*, 2013). Crucially, however the work in this study involves a dual-species biofilm model containing *P. aeruginosa* and *S. aureus*, not a *P. aeruginosa* monospecies biofilm which has been shown to undergo biofilm dispersal. Further work is required to understand the components of this co-localisation interaction which have played a factor in the increase of the *P. aeruginosa* population and why biofilm dispersal was not triggered with exogenous NO.

The work in this Chapter has outlined an approach for the unbiased recovery of gDNA from biofilms and further demonstrated the use of PMA-qPCR for the estimation of the viable community dynamics of dual-species post NO treatment. Moreover, the work in this Chapter highlights the need for a continued focus on understanding the interspecies dynamics of mixed and multispecies biofilms, as these interactions most likely alter the effect observed for treatments tested solely on monospecies biofilms. Additionally, I recognise that not only is it important to shift biofilm research attentions towards the interspecies interactions but concomitantly when *in vivo* work cannot be carried out, these multispecies biofilm models should be carried out under conditions which more closely resemble the human infection.

Chapter 5

Adapting the Fluorescence *in situ* Hybridisation (FISH) Methodology – Combinatorial Labelling and Spectral Imaging FISH (CLASI-FISH) for the Identification and Spatial Analysis of the CF Microbiome

5.1 Introduction

Fluorescence *in situ* hybridisation (FISH) is a technique in which the user can design a complementary oligonucleotide bound to a fluorescent probe for a specific nucleic acid sequence of interest, so that on binding the probe can be detected via fluorescence microscopy or flow cytometry. The first publications outlining *in situ* hybridisation were concomitantly produced by two groups, Gall and Pardue, 1969 and John, Birnstiel and Jones, 1969. Wherein, they demonstrated a methodology to directly visualize *in situ* within a frog egg, the position of the complementary DNA sequence within a chromosome as result of the binding of a radioactive copy of ribosomal DNA. Hybridisation can be carried out using DNA or RNA sequence bound to a label which is referred to as a probe. Labels commonly used *in situ* hybridisations can range from (1) radioactive elements such as ^{3}H, ^{32}P, ^{35}S and ^{125}I, (2) non-isotopic such as biotin and digoxigenin and (3) fluorescent dyes (Lakatošová and Holečková, 2007). The very first application of *in situ* hybridisation technique within the field of microbiology was described by Giovannoni *et al.*, 1988 wherein rRNA oligonucleotides with the radioactive label ^{35}S were used to distinguish between the primary kingdoms archaebacteria, eubacteria and eukaryotes. Although the wide ranging applications *in situ* hybridisation was providing this promising technique was being hampered by the lack of resolution offered by some radioactive labels such as ^{35}S for use in microbiology (Giovannoni *et al.*, 1988). This issue was resolved with the use of fluorescent dyes. DeLong *et al.*, 1989 provided the first methodology detailing the use of fluorescence *in situ* hybridisation (FISH) in the detection of single cells of *Escherichia coli* and also its use to estimate rRNA molecules within the cell due to the 1:1 ratio of probe and target binding.

The first use of FISH in the identification of microorganisms in CF sputum was conducted by Hogardt *et al.*, 2000, wherein, FISH was used to detect *P. aeruginosa, B. cepacia* complex, *S. maltophilia*, *S. aureus* and *H. influenzae* within the sputum and throat swab samples obtained from CF patients. This study demonstrated the ability of the FISH probes to detect up to two bacterial species within the same field view in a shorter period of time. This methodology yields results relatively quickly within the laboratory and as they

191

explained, would benefit a more rapid decision in informing the course of antimicrobial therapy to patients undergoing a pulmonary exacerbation. Later studies, further detailed the use of FISH in detecting microorganisms and the ability to determine the growth rate of a microorganism within sputum (Yang and Zeyer, 2003; Wellinghausen *et al.*, 2005). Although FISH is a highly specific technique with a wide number of applications it is limited by the number of fluorophores which can be utilized and reliably separated within one experimental system using traditional confocal microscopy. Up to four fluorophores can be imaged simultaneously using a two-photon laser scanning microscope (Lansford *et al.*, 2001). Therefore in experiments deciphering the microbial spatial arrangement within a biofilm where cells from a number of different species can reside in close proximity, the use of a large number of different fluorophores would result in a greater number of overlapping spectra. Luckily an intriguing solution has been described, spectral imaging/hyperspectral imaging is a technique which incorporates spectroscopy and high resolution CCD imaging which provides more spectral information for each pixel within a sample (Zimmermann *et al.*, 2003). On acquisition of an image across the spectral plane the image can be separated using a linear unmixing method, to permit the use of seven fluorophores to analyse the one thymic tissue sample from a mouse (Tsurui *et al.*, 2000). All these advancements combined within the field of microbial ecology can permit the analysis of cells in close proximity from a number of different species within both human and environmental samples to understand the community structuring of biofilms within these niches. One of the key influential advancements and examples of the potential spectral imaging holds, was recently demonstrated by Valm *et al.*, 2011, 2012. Wherein, they describe the technique they coined combinatorial labelling and spectral imaging-fluorescence *in situ* hybridisation (CLASI-FISH). They used a binary combination of fluorophores each attached to its own oligonucleotide targeting its 16S rRNA counterpart for FISH. This group acquired the spectral images or lambda stack (λ stack); then these λ stacks were processed using the linear unmixing principle and intensity measurements to gauge the contribution of a fluorophore in order to decipher the spatial positioning of the 15 different taxon members within a dental plaque sample.

Considering these recent advancements, the use of CLASI-FISH as a diagnostic technique to identify the microorganisms within a biological specimen obtained from a patient would be beneficial. Apart from the identification of the microorganisms present within the CF sputum, the identification of the species which are found within biofilm aggregates could be achieved by employing CLASI-FISH as a diagnostic technique. The use of FISH as a diagnostic technique to determine whether an infection is caused by a biofilm infection was recommended by a number of biofilm experts working in the field of biofilm infections (Høiby *et al.,* 2015). Despite the benefit of advanced molecular techniques, these techniques cannot determine what microorganisms are present within biofilms hence the benefit of using FISH.

The work in this Chapter, focuses on firstly optimizing the CLASI-FISH methodology for targeting a number of the predominate microorganisms routinely isolated from the lungs of CF patients. Additionally, I commenced the development of CLASI-FISH as a diagnostic technique to be used on CF sputum samples.

5.2 Materials and Methodology

5.2.1 Microbial species

E. coli NCTC 9001, *P. aeruginosa* PAO1 and *B. cepacia* complex were separately grown in 15 ml of LB broth overnight at 37°C under static conditions. *S. aureus* ATCC 25923, *S. maltophilia* ATCC 13637 and *A. xylosoxidans* ATCC 9220 were separately grown in 15 ml TSB overnight at 37°C under static conditions. *H. influenzae* ATTC 49766 and *S. pneumoniae* Serotype 22F were separately grown overnight in BHI broth (supplemented with hemin 10 μg / ml and 2 μg / ml of nicotinamide adenine dinucleotide) and BHI broth respectively at 37°C with 5% CO_2 – 95% air under static conditions. Overnight cultures were diluted using fresh media at O.D. readings as follows: OD_{600} of 0.5 for *E. coli* NCTC 9001, OD_{620} of 0.3 and 0.4 for *P. aeruginosa* PAO1 and *S. aureus* ATCC 25923 respectively, OD_{601} of 0.2, 0.3, 0.2 and 0.2 *B. cepacia* complex, *A. xylosoxidans* ATCC 9220, *H. influenzae* ATTC 49766 and *S. pneumoniae* Serotype 22F and finally and OD_{560} of 0.4 for *S. maltophilia* ATCC 13637. Five millilitres of the diluted overnight suspensions were centrifuged at 4,000 rcf for 10 min. The supernatant was removed and 5 ml of Hank's Balanced Salt Solution (HBSS; Sigma-Aldrich). A 4% solution of paraformaldehyde (Alfa Aesar, U.K.) was prepared using 30 ml of 3x PBS (10x PBS stock diluted using Ultrapure water) added to 10 ml of 16x paraformaldehyde. A 1:1 volume of 4% paraformaldehyde was added to each bacterial culture. The suspensions were left on ice for 1.5 h. After fixing with paraformaldehyde the suspensions were centrifuged at 4,000 rcf for 10 min. The supernatant was discarded and 5 ml of 1x PBS was added to resuspend the cell pellet. The suspensions were vortexed for 1 min at ~ 5000 rpm and 1 ml aliquots were pipetted into 2 ml centrifuge tube. The centrifuge tube were centrifuged at 10,000 g for 5 min, the supernatant was removed and 1 ml of 1x PBS was applied; a total of 3 1X PBS washes were carried out. Finally, the cells were resuspended using 800 μl of a PBS:EtOH solution prepared using a 1:1 (v /v) of 100% ethyl alcohol added to 1x PBS. The cells were stored at -20°C, fresh cell suspensions prepared after a 6 mth period.

5.2.2 Oligonucleotide probes

The oligonucleotide probes used in this study to target the bacterial species of interest are outlined in Table 5.1. Candidate probes were selected from the database probeBase (http://www.probebase.net/). For the experiments involving *E. coli* eight Eub338 oligonucleotides were synthesised by IDT, each labelled with a different fluorophore conjugated to the 5´ end. The fluorophores conjugates used in this study for testing purposes: Alexa Fluor (AF) 350, AF 405, AF 488, AF 555, AF 594, AF 647, Cy3 and Rhodamine Red X. For the type strain collection of bacteria representing the most predominant members of the CF microbiome, six different fluorophores were used AF 488, AF 555, AF 594, AF 647, Cy3 and Rhodamine Red X; with two oligonucleotide probes synthesised for each species. Refer to Table 5.1 for the fluorophore combination used to label each species.

5.2.3 FISH methodology

All FISH assays were performed as described by Nistico *et al.*, 2009; Valm *et al.*, 2011 with some modifications as outlined below, informed from preliminary experiments conducted for the work in this chapter.

The fixed cell suspension was vortexed upon removal from -20°C and a 20 µl aliquot was pipetted into a fresh 2 ml centrifuge tube tube. The tube was centrifuged at 12,000 g for 6 min. The supernatant was removed and 100 µl of 2 mg / ml lysozyme (based on preliminary testing) dissolved in a buffer containing 100 mM Tris-HCL, 50 mM EDTA, pH 8.0 was added to the cell pellet. The pellet was gently resuspended by vortexing and incubated for 10 min at 37°C. The suspension was centrifuged at 8,000 g for 6 min and the supernatant was removed. A rinse of 100 µl of ultrapure water was added to resuspend the pellet briefly by vortexing before a centrifugation step of 8,000 g for 6 min was followed. The pellet was subjected to a series of increasing ethanol concentrations: 50%, 80% and 100%. One hundred microliters of the ethanol suspension was added to the pellet and incubated at room temperature for 2 min followed by centrifugation at 8,000 g for 3 mins between the ethanol series. Finally, the cell pellet was resuspended using the hybridization buffer. The cells were resuspended using 100 µl of the

hybridization buffer containing 0.9 M NaCl, 0.02 M Tris (pH 7.5), 0.01% SDS and either 10% - 50% Hi-Di formamide (ThermoFisher). Each probe was added to the hybridization buffer at a final concentration of 2 μM, protected from light. The tubes were vortexed briefly and incubated in a hybridization oven at 46°C for 3 h or 18 h, for cell suspensions being labelled singly and cells being labelled with two different fluorophores (binary labelling), respectively. After hybridization the tubes were centrifuged at 10,000 g for 6 min before 100 μl of Wash buffer 1 containing 0.9 M NaCl, 0.02 M Tris (pH 8.0), 0.01% SDS and the corresponding formamide concentration was added. The tubes were vortexed briefly and incubated in a water bath at 48°C; protected from light for 15 min. Wash buffer 1 was removed by centrifugation at 10,000 g for 6 min. The cell pellet was resuspended using 200 μl of Wash buffer 2 containing 0.9 M NaCl, 0.02 M Tris (pH 8.0) and 0.01% SDS and vortexing briefly. The tubes were incubated in a water bath at 48°C for 15 min; protected from light. Wash buffer 2 was removed by centrifugation at 10,000 g for 6 min and the cell pellet was resuspended using 20 μl / 40 μl of a resuspension buffer containing 0.025 M NaCl and 0.02 M Tris (pH 8.0). Microscope slides were cleaned using ethanol and ultrapure water washes prior to coating with poly-L-lysine for 20 min (Sigma-Aldrich). A hydrophobic ring was drawn on the cleaned microscope slides using an ImmEdge™ Pen (Vector Laboratories). The resuspended cell pellet was pipetted onto the microscope slide surface within the ring outline. The microscope slides were allowed to dry at 37°C in a humid chamber protected from light. A drop of Vectashield was applied prior to the adding a coverslip. The microscope slides were stored in a microscope slide box protected from light.

Table 5.1 Oligonucleotide sequences and fluorophores used in this study.

Probe probeBase no. / Reference	Target species	Sequence (5' - 3')	Target	Fluorophore
Sau pB-349	*S. aureus*	GAA GCA AGC TTC TCG TCC G	16S	Cy3, AF 647
Haeinf pB-348	*H. influenzae*	CCG CAC TTT CAT CTT CCG	16S	AF 488, AF647
Ach-221 pB-1233	*A. xylosoxidans*	CGC TCY AAT GCA AGG TC	16S	AF488, Rhodamine Red X
Spn pB-350	*S. pneumoniae*	GTG ATG CAA GTG CAC CTT	16S	AF 594, AF 647
PseaerA pB-383	*P. aeruginosa*	GGT AAC CGT CCC CCT TGC	16S	Cy3, Rhodamine Red X
Stemal pB-345	*S. maltophilia*	GTC GTC CAG TAT CCA CTG	16S	Cy3, AF 594 / AF 555
Bcc spp Bauernfeind et al., 1999	*Burkholderia* spp.	CCG RCT GTA TTA GAG CCA	16S	AF 488, AF 594
EUB338 pB-159	Eubacteria (~ 90%)	GCT GCC TCC CGT AGG AGT	16S	AF 488, AF 555, AF 594, AF647, Cy3, Rhodamine Red X, AF 405

197

5.2.4 Testing formamide concentrations and specificity of FISH probes

Optimization of formamide concentration

For each of the type strains, FISH assays were carried out using the methodology outlined in section 5.2.3, across a range of formamide concentrations. Formamide concentration of 10%, 20%, 30%, 40% and 50% were tested for all type strains, with 50% tested solely for *B. cepacia* complex type strain. A list of the probes used for each bacterial species for testing the formamide concentration follows: AF 555 for *E. coli* NCTC 9001, Cy3 for *P. aeruginosa* PAO1, AF 647 for *S. aureus* ATCC 25923, AF 488 for *B. cepacia* complex, Rhodamine Red X for *A. xylosoxidans* ATCC 9220, AF 488 for *H. influenzae* ATTC 49766 and AF 555 for *S. pneumoniae* Serotype 22F. A total of 3 images were acquired for each specificity test (other locations were visually observed to ensure non-specific binding did not occurred) using CLSM, refer to section 5.2.5.

Specificity Testing

The specificity for each probe was tested against all type strains using the probe's optimal formamide conditions. Ten images for each formamide concentration were acquired using a Leica SP5 CLSM as outlined in section 5.25 and 5.2.6; images were randomly selected.

5.2.5 CLASI–FISH methodology applied to CF sputum samples

The collection of CF sputum samples for this study was approved by NHS Research Ethics Committee 08/H0502/126 in Southampton, U.K. CF patients were recruited in the Adult Cystic Fibrosis Clinic at Southampton General Hospital, United Kingdom. Expectorated sputum samples were processed in the lab within a maximum of 2 h after collection from the CF patient. Sputum samples were liquefied using 1:1 volume of mucolyse (Pro-Lab Diagnostics), vortexed to homogenise and placed in an incubator at 37ºC for 15 - 30 min with shaking at 200 rpm (Stuart SI500). After the sputum was liquefied, the sputum was vortexed for 1 min and 100 µl was pipetted into a sterile 2 ml centrifuge tube. CF isolates for all 6 species either isolated in Chapter 2 or

gifted were used as follows with one type strain used for the 7th species: *B. cepacia* complex A57, *S. aureus* A52, *H. influenzae* ATTC 4976 (non-CF isolate), *P. aeruginosa* (gifted by Dr R.P. Howlin), *S. pneumoniae* A66, *S. maltophilia* and *A. xylosoxidans* (gifted by Prof Nørskov-Lauritsen) were grown as outlined in section 5.2.1. Equal cell volumes of ~ 1 x 10^6 CFU / ml were added to a 2 ml centrifuge tube and centrifuged at 10,000 g for 5 min. The supernatant was removed and 10 µl of the hybridization buffer was added to the tube to resuspend the cells. This cell suspension was then used to spike the liquefied CF sputum. The FISH methodology outlined under section 5.2.3 was followed from the lysozyme step using 30% Formamide. Additionally, the binary labelling approach was used for an initial test of the CLASI-FISH methodology on CF sputum. The oligonucleotides probes tagged with fluorophore AF594 were used instead of the AF555 tagged probes, refer to Table 5.1 for the oligonucleotide probes and fluorophores used for each bacterial species.

5.2.6 Image acquisition

Formamide and Specificity Testing

All images were acquired using a Leica SP5 CLSM (Leica Microsystems, Milton Keynes, U.K). The 63x/1.3 numerical aperture (NA) objective lens under glycerol immersion was utilized for imaging. Laser lines (nm) used to excite fluorophores: 488 nm for AF 488, 561 nm for AF 555, 561 nm for Cy3, 496 nm for Rhodamine Red X and 633 nm for AF 647.

Spectral Imaging

Images were acquired using a Zeiss LSM780 (Carl Zeiss) inverted confocal laser scanning microscope; with 7 laser lines and a 32 channel GaAsP array. Images were acquired using a 63x/1.4 N/A or 40x/1.3 objective oil immersion objective with 9 nm band between each channel; 414 to 691 nm. Fluorophores were excited starting with laser line 633 nm descending to 405 nm. A line average of 4 was used for the acquisition of each field.

5.2.7 Linear unmixing

The procedure outlined by Valm *et al.*, 2011, 2012 was followed. Linear unmixing was carried out using the Zeiss Zen software. Reference spectra for each fluorophore were obtained using *E. coli* NCTC 9001 tagged cells, to create a data bank of the spectral properties of each fluorophore using the same microscope settings. Additionally, untagged cells were imaged under the same settings as that used for the reference spectra to create an auto-fluorescence reference image, to enable removal of noise on acquiring a λ stack.

5.2.8 Image Analysis

Formamide concentration image analysis

The images assessing the formamide concentration series were processed using DAIME software version 2.1 (Digital image analysis in microbial ecology) (Daims *et al.*, 2006). The images were thresholded prior to analysis using 2D segmented coupled with RATS-L, images were inspected to ensure larger clumps of cells were not included in the analysis. Post thresholding, the mean intensity was calculated within DAIME v2.1 using the evaluate formamide function. The mean intensities with standard errors are reported for each type strain in Figure 5.1.

Binary labelling assignment

The resulting image stacks generated after linear unmixing where exported as TIFF files. The unmixed image stacks where segmented in ImageJ by first applying the global thresholding to the image at a level which picked up all cells within the image. To separate cells within the image a watershed algorithm was applied to the image. ImageJ was then used to find the local maxima within the unmixed image which was then used to further segment the image by superimposing the resulting image onto the thresholded image. After image segmentation, the resulting pixel-based fluorophore data acquired from the linear unmixing was then used to assign each cell it's binary labelling components. Image stacks were imported into Mathematica version 10 in order to assign each cell it's combinatorial label type.

Custom built functions were designed within Mathematica v10 for carrying out the following operations. The mean fluorophore intensity values were computed for each segmented cell across all 5 fluorophores used in the experiment. The two fluorophores with the highest intensities values were assigned as the segmented cell's binary label make up/combinatorial label. For segmented cells wherein the fluorophore intensity values for each channel were equal the segmented cell was labelled as an unknown cell, identified by the pseudocolour grey. For the work in this Chapter, as I used five fluorophores (n) in groups of two (k objects) the formula below was used to determine the number of combinations. Therefore, a total of 10 possible combinatorial label outcomes are possible with the fluorophore set used for this work.

$$_nC_k = \frac{n!}{k!\,(n-k)!}$$

Refer to Table 5.2 for an outline of the pseudocolours applied based on the results for each segment. The pseudocolours were mapped back onto the image for the assignment of the combinatorial labelling for each of the cells.

Table 5.2 Fluorophores and pseudocolour assignment. Fluorophores codes (A) and corresponding pseudocolour applied for CLASI-FISH assays (B).

A

Letter Code	Fluorophore
A	AF 488
B	Cy3
C	Rhodamine Red-X
D	AF594
E	AF647

B

Combinatorial Labelling with two fluorophores	Pseudocolour assignment
AB	Green
AC	Yellow
AD	Orange
AE	Light Blue
BC	Cyan
BD	Magenta
BE	Blue
CD	Purple
CE	Pink
DE	Red
Unknown	Grey

5.3 Results

5.3.1 Optimization of the formamide concentration and testing probe specificity

The mean intensities for the formamide concentrations calculated by DAIME v2.1 showed varying degrees of response to the formamide concentration. The optimal formamide concentration for single FISH assays for each species under the conditions outlined in this study were: 20% for *P. aeruginosa* PAO1, 10 - 30% for *S. aureus* ATCC 25923, 50% for *B. cepacia* complex, 30% for *A. xylosoxidans* ATCC 9220, 10% / 40% for *H. influenzae* ATTC 49766 and 10% for *S. pneumoniae* Serotype 22F; Figure 5.1. The formamide testing results for the EUB338 probe to label *E. coli* NCTC 9001 showed a more consistent pattern of decreasing fluorescence intensity on increasing the formamide concentration, with mean fluorescence intensity values and SEM values reported as follows for each formamide concentration: 68 ± 0.9 for 10%, 62 ± 62 for 20%, 44 ± 0.8 for 30% and 22 ± 0.2 for 40%.

Each probe was tested against all other type strains for specificity at the probe's most optimal conditions. No non-specific binding was noted, refer to Figure 5.2.
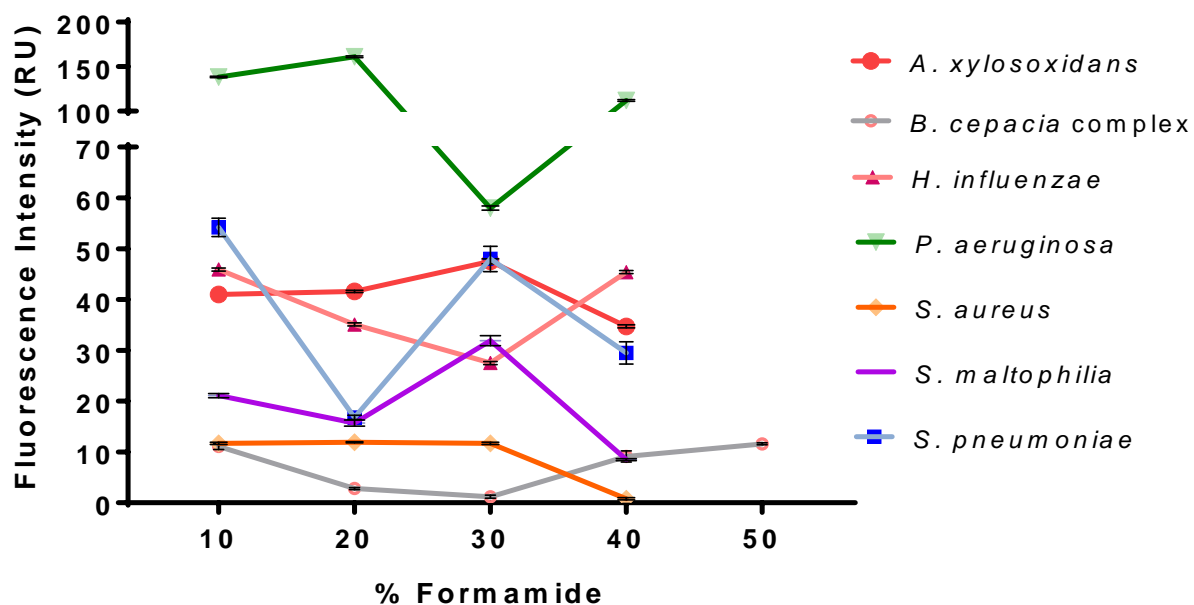
Figure 5.1 Mean fluorescence intensity relative units (RU) as calculated by DAIME across each formamide concentration. Each ATCC bacterial isolate and serotype 22F of *S. pneumoniae* tested. Data for mean values with error bars representing SEM.
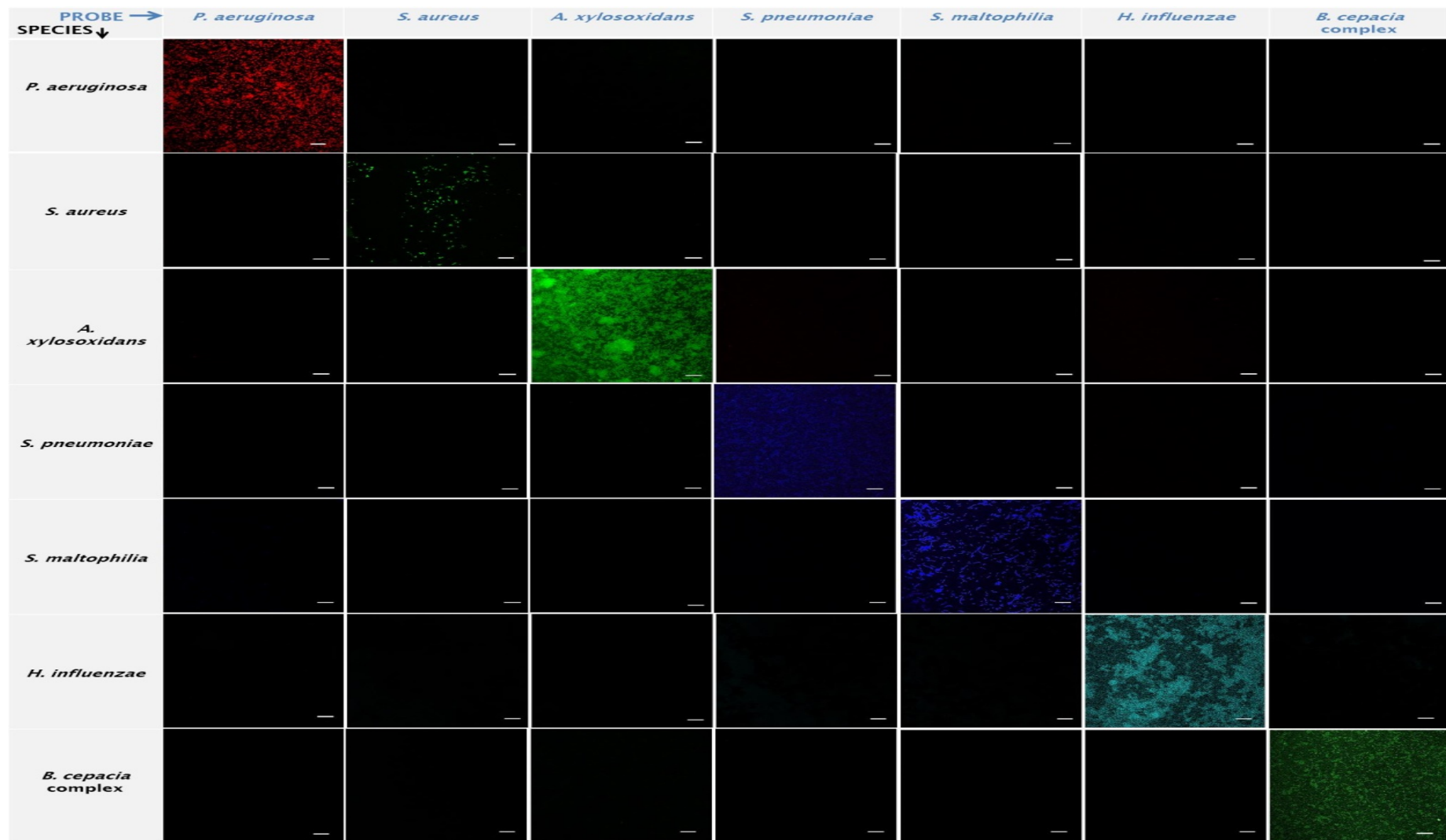
Figure 5.2 Probe specificity testing for all oligonucleotide probes used in this study. Scale bar = 20 μm.

5.3.2 Testing single and binary combinations of probes with type strains

First a database containing the spectral characteristics for each fluorophore (see Table 5.1) used in this study was conducted. Second, a test was first conducted for the spectral acquisition of 6 fluorophores in the one field of view for testing the equipment set up. Six separate FISH assays were conducted concomitantly for *E. coli* NCTC 9001. The Eub338 probe was used with each tube of *E. coli* NCTC 9001 tagged with a different fluorophore. All six fluorophores were successfully imaged and identified using the reference spectra database, refer to Figure 5.3. Binary combinations of the fluorophores were tested using *E. coli* NCTC 9001, an example is shown in Figure 5.4.

AF 405   AF 594   Cy3   Rhodamine Red X
AF 488   AF 647
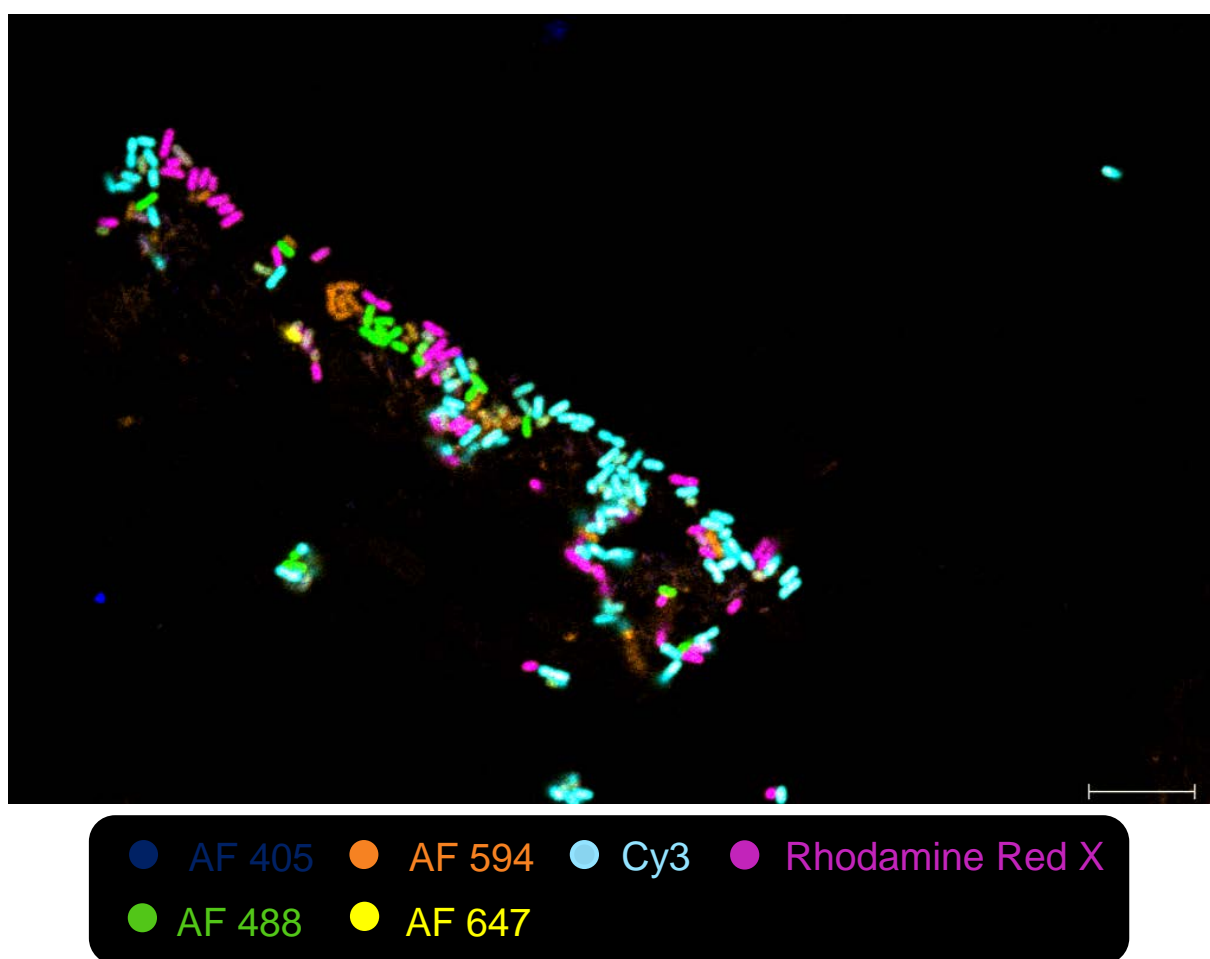
Figure 5.3   Micrograph of a raw spectral image for a mixture of six singly labelled *E. coli* NCTC 9001. Each EUB 338 probe tagged with a different fluorophore. Legend outlines fluorophore and pseudocolour designation. Scale bar = 10 μm.
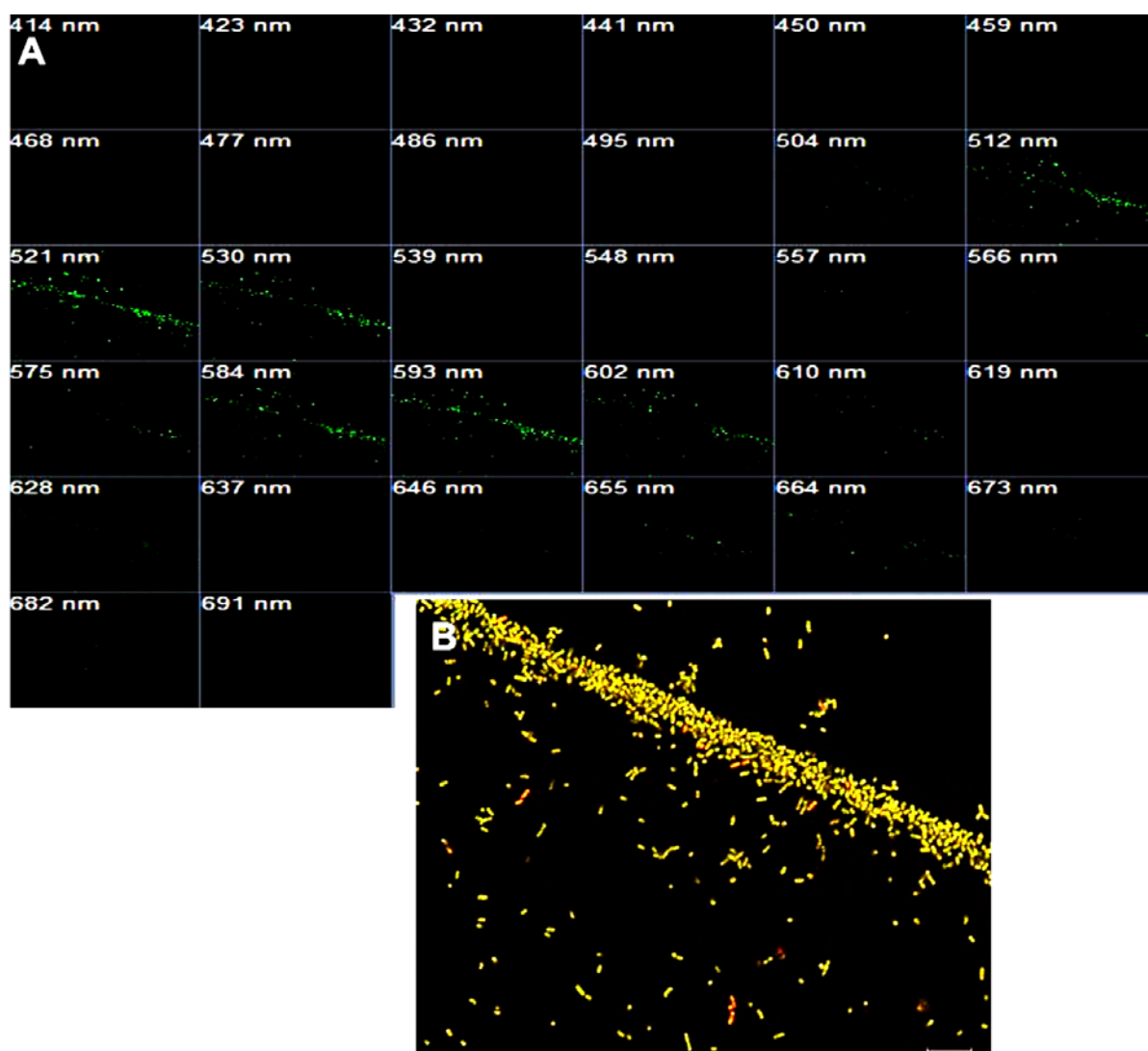
Figure 5.4 Spectral imaging acquisition and linear unmixing for binary labelled *E. coli* NCTC 9001cells. A) Spectral images across each of the 32- channels acquired for *E. coli* NCTC 9001cells labelled with AF 488 and Rhodamine Red X. B) Linear unmixed image for CLASI-FISH assay. Pseudocolours were applied for fluorophores: *E. coli* NCTC 9001cells coloured green for AF 488, *E. coli* NCTC 9001cells coloured red for Rhodamine Red X and for *E. coli* NCTC 9001cells labelled in binary combination, cells appear as a faint yellow colour. Scale bar = 10 µm.

Binary combinations of *E. coli* NCTC 9001 were successfully linearly unmixed using the reference spectra database created, refer to Figure 5.4. Additionally, all 10 populations of *E. coli* NCTC 9001which were labelled in binary combination then mixed in equal quantities were successfully labelled and assigned their combinatorial label using the CLASI-FISH methodology as shown in Figure 5.5. In Figure 5.6, all 7 of the type strains were labelled, each with

their own species specific probe in the one FISH assay and identified within a mixture containing an equal quantity of each of the type strains.

AB: AF488 + CY3   AC: AF488 + Rhodamine Red X   AD: AF488 + AF594   AE: AF488 + AF647
BC: CY3 + Rhodamine Red X   BD: CY3 + AF594   BE: CY3 + AF647   CD: Rhodamine Red X + AF594
CE: Rhodamine Red X + AF647   DE: AF594 + AF647   Unknown
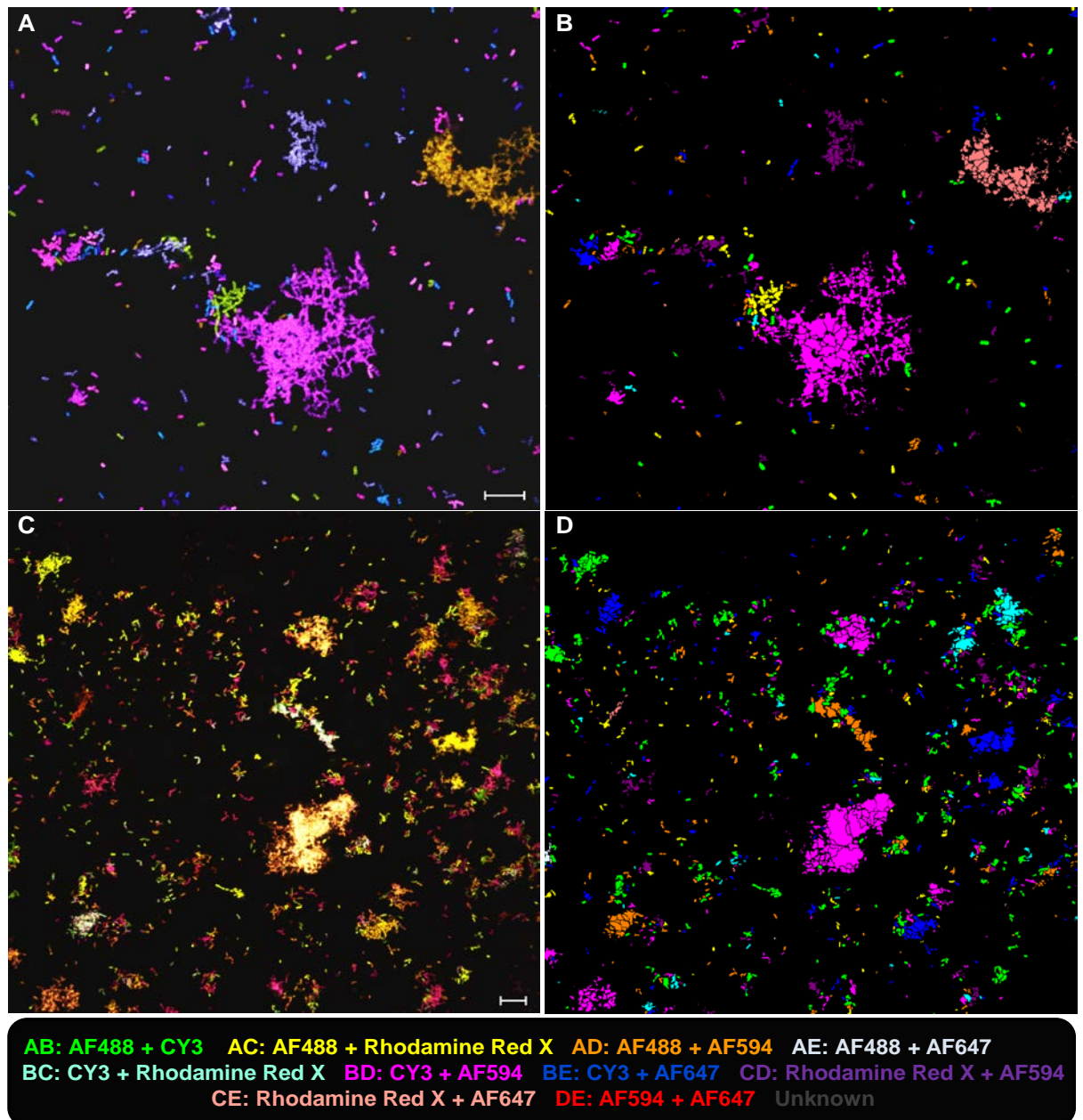
Figure 5.5   CLASI-FISH images for 10 different populations of *E. coli* NCTC 9001 labelled in binary combination. Images (A) and (C) are linear unmixed images of different fields of view for image of the same CLASI-FISH assay; images acquired using the 63x objective and the 40x objective respectively. Images (B) and (D) show the resulting combinatorial label assignment for the segmented images. All 10 possible label types were identified, unknown segments are coloured grey. Scale bar = 10 μm.
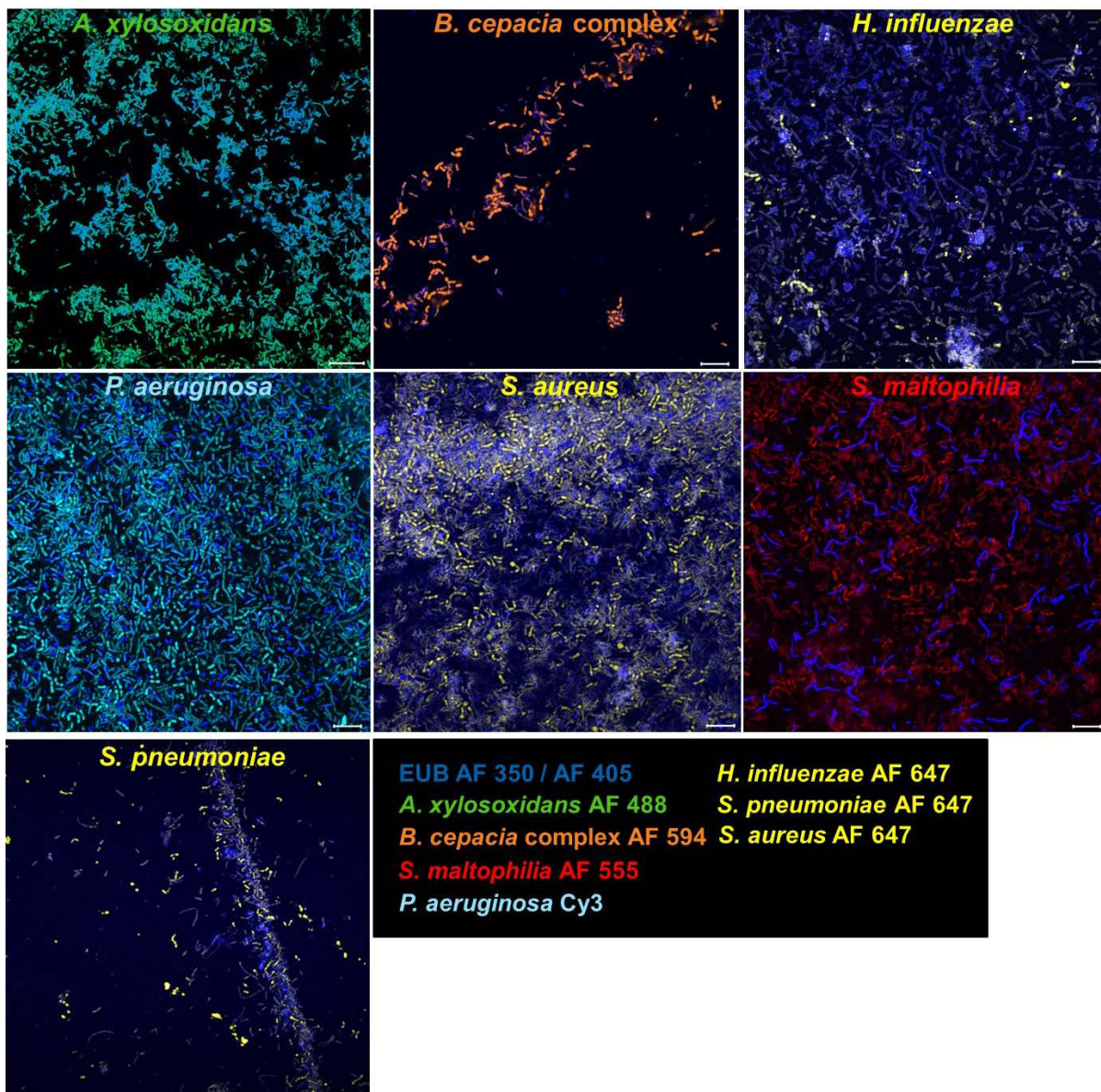
Figure 5.6 Spectral image acquisition and linear unmixing for a mixture of the type strains labelled with one species specific probe. An equal mixture of the type strains were combined for seven separate FISH assays using a 20% formamide concentration with one species specific probes added per assay and a EUB 338 probe. Image post linear unmixing with pseudocolours applied for each fluorophore. The figure legend matches the microbial species with its corresponding pseudocolour. Fluorophores were coloured within the Zeiss Zen software as follows: Dark blue for AF 405, green for AF 488, orange for AF 594, cyan for Cy3 and yellow for AF647. Scale bar = 20 μm.

The laser intensity had to be increased in order to capture sufficient signal from the *B. cepacia* complex strain labelled with AF594. This practice had the knock on effect of over exposure for the species labelled with the same fluorophore, for which the signal intensity is otherwise adequate. Next, a test for labelling the type strains (CF related strains) was conducted using a formamide concentration of 20% for cells labelled in binary combination; using a species specific probe and a EUB338 probe conjugated to either AF 350 or AF 405. This assay was conducted to test how labelling these microbes in binary combination under the same conditions as that used in Figure 5.6 would affect the labelling efficiencies of each probe, refer to Figure 5.7. The EUB338 probe conjugated to AF 350 was used in the FISH assays for *H. influenzae, P. aeruginosa, S. aureus, S. pneumoniae* 22F and *S. maltophilia*. The EUB338 probe conjugated to AF 405 was used in the FISH assays for *A. xylosoxidans* and *B. cepacia* complex, refer to Figure 5.7. An equal volume of the individual 7 assays were mixed and spotted for imagining. The EUB signal was not used to identify each species in the resulting linear unmixed image which was processed within Mathematica. This assay was conducted to qualitatively determine how well each of the individual species specific probes perform when added to a cell mixture containing approximately equal cell quantities of each the 7 bacterial species (Figure 5.7). As outlined in Figure 5.7, *B. cepacia* complex, *S. maltophilia, A. xylosoxidans and P. aeruginosa* were successfully assigned their species specific probe as these species had their own unique fluorophore. However, as *H. influenzae, S. aureus* and *S. pneumoniae* were all labelled with the fluorophore AF647 these species could not be individual identified as therefore were all assigned the same label/pseudocolour.

Based on the above results from Figure 5.1 and 5.6, the *B. cepacia* complex probe with both fluorophores shows the lowest level of signal out of all probes. Which therefore would impact on the imaging for all other probes when used in a binary combination (CLASI-FISH assay) as both probes signals are spread across the spectrum of signal acquired during spectral imagining.
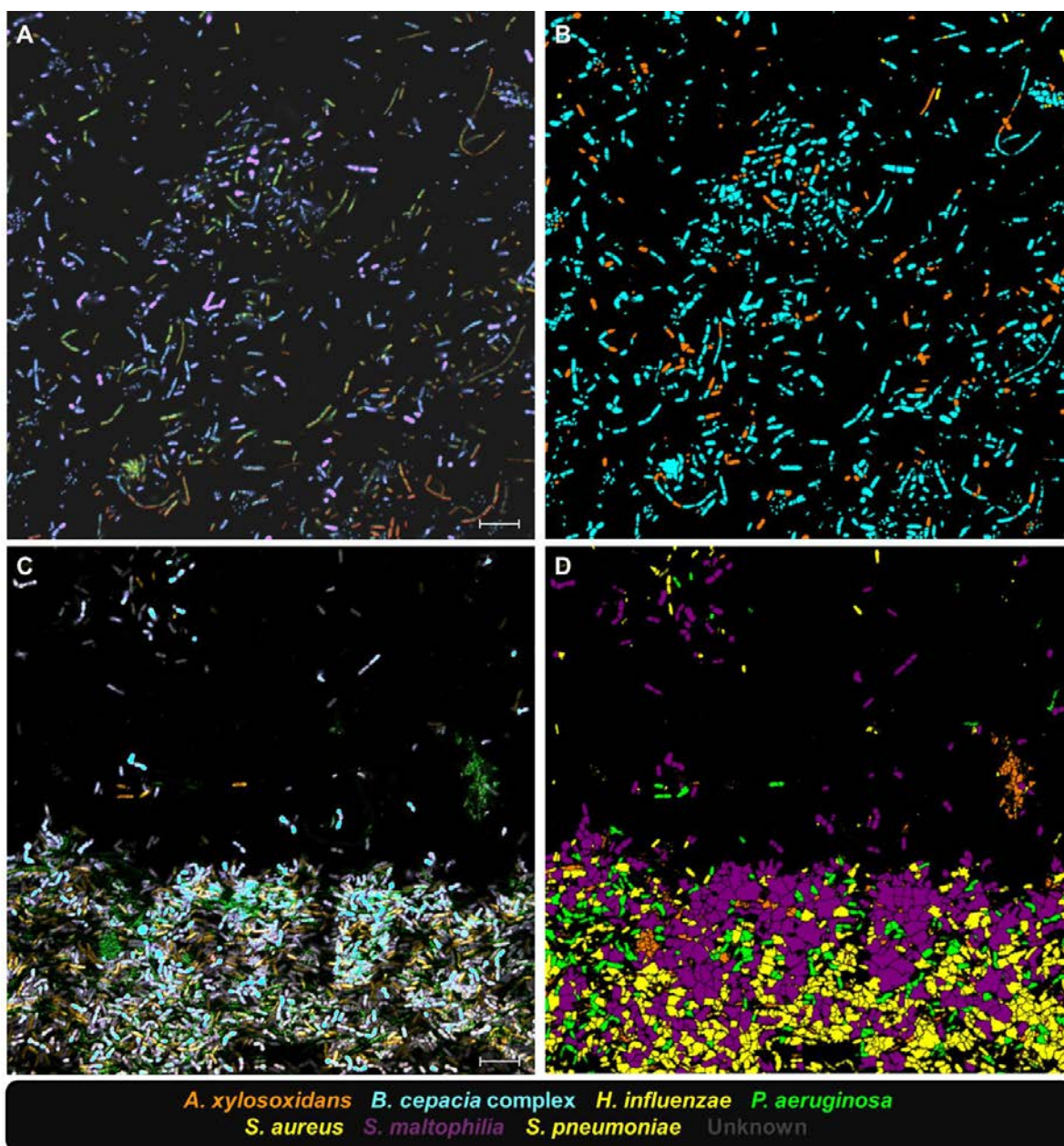
Figure 5.7 Pseudocoloured images for linear unmixed combinations of probes used against a suspension containing all the microbial type strains. One species specific probe was used in combination with a EUB338 probe for 7 individual CLASI-FISH assays against the same microbial type mixture. Only the signal from the species specific probes was used to identify the fluorophore with the highest signal in each segmented cell to assign a species label to the cell. Images (A) and (C) represent the linear unmixed images acquired using the 63x objective of different fields of view. Images (B) and (D) represent the corresponding label assigned to identify 4 out of the 7 species specifically. *H. influenzae*, *S. aureus* and *S. pneumoniae* are labelled with the same fluorophore and therefore not individually distinguishable. The figure legend details the colour of the species specific probe for images B and D. Scale bar = 10 µm.

A primarily test to determine the spectral output when using CLASI-FISH in the identification of 7 CF microbial species used to spike a CF sputum sample was conducted (Figure 5.8).
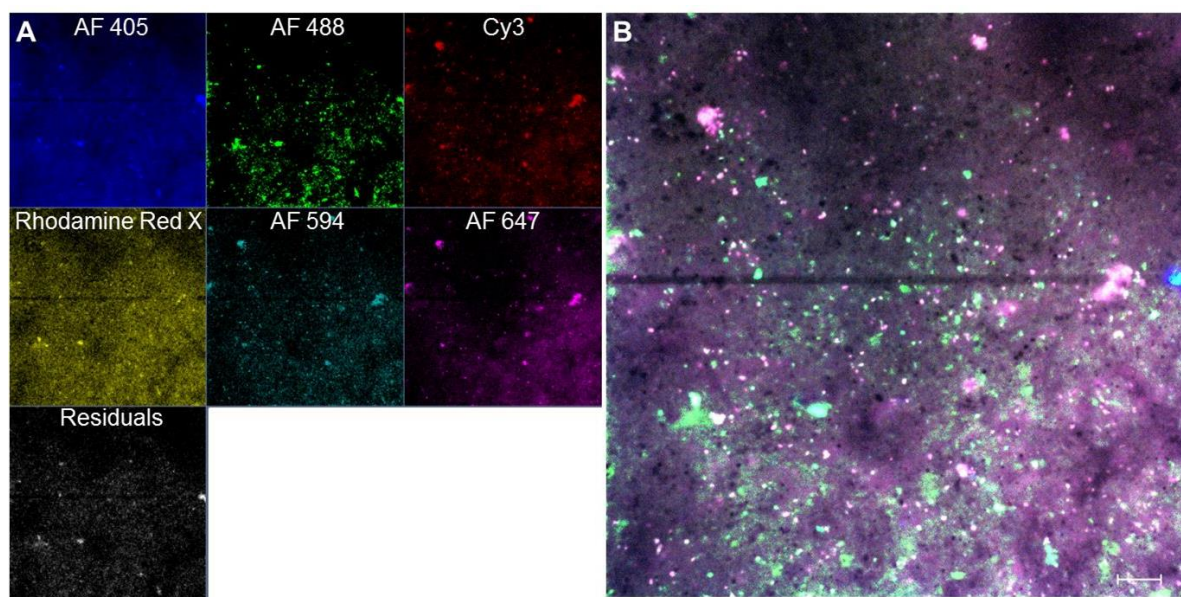
Figure 5.8 An example of a CLASI-FISH image of CF sputum spiked with 7 CF isolates. Six microbial species isolated from CF sputum and one type strain for *H. influenzae* were used to spike a CF sputum sample and all binary combinations of species specific probes for a CLASI-FISH assay were added. A) Image shows the resulting signal for each of the fluorophores used in the experiment post linear unmixing operation. The residual channel shows a high level of signal not attributed to the fluorophores used in the CLASI-FISH assay. B) Image of the merged fluorophore channels of the CF sputum imaged after the linear unmixed operation was applied. Scale bar = 10 μm.

As shown above in Figure 5.8 the level of signal output contained a high amount of signal noise evident in the residual channel post linear unmixing. Additionally, the linear unmixed image of the CF sputum in Figure 5.8 (B) showed high level of signal lacking which does not allow for the ability to determine morphological features of the bacteria within the CF sputum sample.

This is due in part to the compensation made during spectral imaging of the probes which show weaker signals when used in a CLASI-FISH assay, as noted above for the *B. cepacia* complex probes. Furthermore, the level of autofluorescence of the CF sputum was removed during the linear unmixing operation which therefore cannot account solely for the high level of noise encountered during spectral imaging, refer to Appendix 6, Figure (vi).

5.4 Discussion

Previous studies (Hogardt *et al.*, 2000; Wellinghausen *et al.*, 2005) have outlined the importance of FISH for the identification of bacterial species within CF sputum samples for up to 2 microbial species within the one assay. The work presented in this Chapter outlines the identification of seven of the most predominant microbial species routinely isolated from the lungs of CF patients and a primarily in applying CLASI-FISH for imagining CF sputum samples. As discussed earlier, a recent method described by Valm *et al.*, 2011, 2012 outlines a FISH technique called CLASI-FISH, wherein they showed they could identify 15 taxa within a plaque sample.

The formamide conditions for each type strain varied widely excluding the data for the EUB338 probe (Figure 5.1 and section 5.3.1) which is not an issue for FISH assays focused on the identification of one microbial species. This variation in the formamide concentration levels across each species becomes an issue when a multiplex FISH assay is being designed. Firstly, the probe specificity was tested and no non-specific hybridization was observed for each of the probes. There was a small amount of background noise for the *H. influenzae* species on testing against the *S. pneumoniae* probe when using 561 nm laser line but this was not observed at lower wavelengths of excitation; indicating a level of autofluorescence, importantly no labelling of *H. influenzae* cells was observed, refer to Figure 5.2.

After developing the reference spectra database for each of the fluorophores used (Table 5.1) a mixture containing an equal proportion of the singly labelled *E. coli* cells was combined to test if the reference spectra database could enable discrimination of six fluorophores in the one field of view. This test was successful and moreover, the addition of a reference spectrum for the untagged *E. coli* cells enabled the removal of autofluorescence during image processing, to produce clearer images (Figure 5.3). After the reference spectra was set up, binary combinations of the Eub338 probe were tested against *E. coli* cells to investigate if the reference spectra could be successfully employed in the linear unmixing of the spectral images acquired for binary labelled *E. coli* cells similar to (Valm *et al.*, 2011; Figure 5.4). The CLASI-FISH methodology and the custom built functions designed within the Mathematica v10 platform

were further tested using 10 populations of *E. coli* NCTC 9001. Each population was labelled with a binary combination of fluorophores which were then equally mixed and imaged using the spectral imaging parameters used for acquiring CLASI-FISH images (Figure 5.5). As shown in Figure 5.5 all 10 populations of *E. coli* were identified and mapped back onto the linear unmixed images.

Prior to conducting specificity testing and formamide testing, the EUB338 probe was used to investigate the effect of varying lysozyme concentrations for the efficient permeabilization of the cells for each bacterial species. Lysozyme concentrations of 1 mg and 2 mg / ml (Nistico *et al.*, 2009) were tested with incubation periods of 10 min and 30 min at 37°C, for each microbe. The most efficient conditions for cell permeabilization of the cell walls for FISH analysis, was obtained using 2 mg / ml of lysozyme for 10 min, followed by an ethanol series, with 50%, 80% and 100% applied in succession at room temperature. Ethanol series are usually used for the purpose of dehydrating cell samples prior to FISH analysis or to reduce chlorophyll autofluorescence in seawater samples (Cruz-López and Maske, 2015). For this study, subjecting the cells to an increasing ethanol series improved the cell permeabilization procedure.

Based on the proof of concept tests above, separate FISH assays were first conducted for the single labelling of each of the CF related type strains using each probe's optimal formamide concentration. This was carried out to test if the reference spectra could be used to linear unmix a community of seven different species within the one field of view, refer to Figure 5.6. Each of the microorganisms were identified, with some species such as *P. aeruginosa* tagged with Cy3 being slightly over-exposed (Figure 5.6); as this probe displays a high intensity signal (Figure 5.1). This has previously been reported for cells stained with Cy3, a characteristically higher fluorescence intensity is acquired for oligonucleotides tagged with this fluorophore (Stoecker *et al.*, 2010). Finally, labelling the type strains cells in binary combination was explored. For this CLASI-FISH assay, in order to avoid competition between two differently tagged oligonucleotides for each CF related type strain, an equal mixture of the type strains was prepared. For this CLASI-FISH assay one species

specific probe and one EUB338 probe labelled either AF 530 or AF 405 added to the type strain mixture, with the CLASI-FISH assay carried out using 20% formamide (Figure 5.7). Each of the species were identified within the type strain mixture with *B. cepacia* complex, *S. maltophilia, A. xylosoxidans and P. aeruginosa* individual identified and assigned a pseudocolour to identify the species in the segmented image (Figure 5.7, images B and D). This was due to the labelling of these species with different fluorophores refer to Figure 5.7. For the segmented cells containing *H. influenzae*, *S. aureus* and *S. pneumoniae* they were all labelled with the same pseudocolour due as their species specific probes were tagged with AF647. Importantly, the success of the binary labelling for each of the species varied under 20% formamide, with *A. xylosoxidans*, *P. aeruginosa* and *H. influenzae* successfully labelled to varying degrees with their species specific probe and the EUB338 probe. However, binary labelling of *S. aureus, B. cepacia* complex, *S. pneumoniae* and *S. maltophilia* was not as successful for these species with the species specific probe labelling the corresponding bacterium in the type strain mixture. This test was conducted to ensure no competition between the two same oligonucleotide sequences labelled with a different fluorophore was the cause of an unsuccessful binary FISH assay. The EUB338 probe targets a different 16S region and therefore was not in direct competition with another oligonucleotide sequence.

Further testing is underway to design a CLASI-FISH assay which successfully labels each of the CF related type strains within the same assay. This includes conducting multiple CLASI-FISH assays, whereby the test sample is subjected to increasing formamide concentrations with species specific probes added at their optimal formamide concentrations, as the formamide concentration affects the efficient binary labelling of a mixture of different microbial species (Santos *et al.*, 2014).

Moreover, the first application of CLASI-FISH for the identification of microorganisms within CF sputum was additionally explored. To the best of my knowledge, this is the first such application of CLASI-FISH. This primarily test was conducted in order to identify the signal levels of the fluorophores and

determine the level of autofluorescence of the CF sputum. Although, the autofluorescence was removed from the spectrally acquired image of the CF sputum there still remained a high level of signal in each of the fluorophore channels. This is due to unbound probe which is not successfully removed during the wash steps due primarily to the higher viscosity of CF sputum.

These issues will be explored, as the CLASI-FISH methodology is essential for an understanding of the spatial arrangement of the CF microbiome within the CF lung. Furthermore, the important use of FISH assays as a rapid diagnostic technique which can be used to identify what species are forming biofilms within a CF patient's lung has been advised by biofilm experts in the paper by Høiby *et al.,* 2015.

Chapter 6

General Conclusions

and

Future Work

The CF microbiome has been shown to have a vast array of microorganisms (Rogers *et al.*, 2004; van der Gast *et al.*, 2011). Moreover, it has long since been recognized that chronic persistent CF lung infections are as a result of bacteria establishing biofilms within the CF lung (Ciofu *et al.*, 2005; Hall-Stoodley and Stoodley, 2009; Høiby *et al.*, 2010b; Mulcahy *et al.*, 2010). Over the course of a number of years, a greater number of biofilm based studies focused solely on *P. aeruginosa* biofilms formed by CF sputum isolates (Jesaitis *et al.*, 2003; Hill *et al.*, 2005; Anderson *et al.*, 2008; Mulcahy *et al.*, 2010). In recent years, there is a growing number of biofilm based research shifting towards the analysis of multispecies biofilms (Filkins *et al.*, 2015; Tavernier and Coenye, 2015).

Firstly, CF sputum isolates for *S. aureus*, *A. xylosoxidans*, *S. maltophilia*, *B. cepacia* complex and *S. pneumoniae* had to be isolated from CF sputum samples collected within our CF patient cohort, who attend the CF clinic at SUHT (Chapter 2). This then allowed for the work presented in the remaining chapters in this thesis to be undertaken. This was conducted in order to study the biofilms formed by the most predominant microorganisms isolated across CF patients other than *P. aeruginosa.* Secondly, the monospecies biofilms formed by these CF isolates were tested to analyse the monospecies' biofilm response to nitric oxide (Chapter 3). This was undertaken due to the observations that biofilm dispersal effects are triggered by low concentrations of nitric oxide for *P. aeruginosa* monospecies formed by both type strains and CF isolates of this bacterium (Barraud *et al.*, 2006). Preliminary observations of *ex vivo* mixed species sputum biofilms (Chapter 2) displaying a reduction in biofilm biovolume led to the design of an *in vitro* mixed species biofilm model to test this observation. As a result, a gDNA isolation methodology for mixed species biofilms was developed for the enumeration of the viable population fractions remaining in the biofilm post nitric oxide treatment using PMA-qPCR (Chapter 4). The work in Chapter 5 was undertaken in an effort to apply the new FISH methodology coined CLASI-FISH to identify seven of the most predominant members of the CF microbiome, namely *P. aeruginosa*, *S. aureus*, *H. influenzae*, *A. xylosoxidans*, *S. maltophilia*, *B. cepacia* complex and *S. pneumoniae* (Sibley *et al.*, 2006; Bittar *et al.*, 2008; Sibley *et al.*, 2009) with the

ultimate aim of designing a diagnostic tool which can additionally be built upon for the identification more CF microorganisms within the one sample.

Culture dependent techniques were applied to CF sputum samples collected from the SUHT CF clinic (Kilbourn *et al.*, 1968). The primary focus of the work in Chapter 2 was the isolation of the following microorganisms; *S. aureus*, *A. xylosoxidans*, *S. maltophilia*, *B. cepacia* complex and *S. pneumoniae.* Additionally, presumptive isolates for the aforementioned microorganisms and fungal microorganisms were first isolated on agar and tested for purity before being added to a library of microorganisms isolated from CF sputum (microorganism numbered according to patient designation). The microorganisms were molecularly confirmed either by PCR or by sequencing. The culture profiling for a small fraction of the Southampton cohort revealed that *S. aureus*, *P. aeruginosa*, *C. albicans*, *B. cepacia* complex and *S. pneumoniae* were easily and routinely cultured from the CF sputum samples. The frequency of these microorganisms within our CF patient cohort was aligned with that observed by other groups (Peltroche-Llacsahuanga *et al.*, 2002; Molina *et al.*, 2008; Guss *et al.*, 2011; Wahab *et al.*, 2004). I recognise that the focus of this work was aimed at the isolation of aerobic bacterial species. I understand that anaerobic microorganisms colonise the CF lung and suggest that future work isolating these microorganisms from the CF sputum should be encouraged. Biofilm model studies representing a collection of microorganisms mirroring conditions that are observed in the CF lung will enable a better understanding of the effect these communities have on a patient's health. Furthermore, the interspecies interactions can have an impact on therapies aimed at combating biofilm infections (Smith *et al.*, 2006; Michelsen *et al.*, 2014; Tavernier and Coenye, 2015).

A number of groups have reported that *P. aeruginosa* biofilms can be triggered to undergo biofilm dispersal in the presence of low concentrations of exogenous NO (Barraud *et al.*, 2006, 2012). Furthermore, work carried out within our group has demonstrated that NO can mediate the biofilm dispersal of *P. aeruginosa* biofilms formed by isolates collected from CF patients. Additionally, a clinical trial was conducted and a reduction in the microcolony size of *P. aeruginosa* within the CF sputum was observed using FISH (Howlin *et*

al., 2017). Collectively, due to these observations, the potential use of NO as an adjunctive therapy in CF was investigated for other CF microbiome members. The biofilm dynamics for the monospecies biofilms formed by the microorganisms isolated within Chapter 2 *S. aureus*, *A. xylosoxidans*, *S. maltophilia*, *B. cepacia* complex and *S. pneumoniae* was first established, to ensure a mature biofilm was established prior to testing the effect NO had on the monospecies biofilm. Collectively, for each of monospecies biofilms the addition of low exogenous concentrations of NO did not result in biofilm dispersal. However, for *ex vivo* sputum mixed species biofilms a reduction in the biofilm biovolume was observed. Although, I recognise that this observation was limited as only one sample was imaged for 3 patients. This combined with the fact that the enriched *ex vivo* community structure and/abundance for both the untreated and SNP treated could be markedly different: therefore any reduction in the biofilm biovolume cannot solely be attributed to the addition of NO. For monospecies biofilms formed by the *B. cepacia* complex CF isolate, a minor increase in the biofilm biovolume as measured by CFU counts was observed. For the remaining monospecies biofilms either a change in the biofilm architecture on exposure to NO was observed or a minor reduction in CFU counts was attributed to a reduction in cell viability as a result of the presence of NO. A reduction in cell viability was attributed to this observed effect based on the observation that biofilm dispersal was not concomitantly observed, similar observations has been outlined by other authors (Allan *et al.*, 2016). To my knowledge, no other studies have investigated the effect NO has on the biofilms formed by these isolates, with the exception of *S. aureus* (Hetrick *et al.*, 2009; Friedman *et al.*, 2011) and *S. pneumoniae* (Allan *et al.*, 2016). Future work examining the potential use of higher concentrations of NO in an effort to affect the viability of cells within a monospecies and mixed species biofilm needs to be explored. Treatment with NO may enhance the effect of existing antimicrobial treatments and therefore is worth exploring.

The work described in Chapter 4 further contributed to the research being carried out recently on the biofilms dynamics of mixed species biofilms composed of *P. aeruginosa* and *S. aureus* (Baldan *et al.*, 2014; Michelsen *et al.*, 2014; Filkins *et al.*, 2015). This study has outlined a mixed species biofilm

model which can be utilised for biofilm studies investigating interspecies interactions for any *P. aeruginosa* and *S. aureus* CF isolate. Additionally, it has been highlighted by a number of groups that a range of different gDNA extraction methodologies and commercial kits can have a profound effect on the species diversity and accurate enumeration of the microbial content of a sample (Leff *et al.*, 1995; Krsek and Wellington, 1999; Carrigg *et al.*, 2007; Salonen *et al.*, 2010; Zhao, Schloss, *et al.*, 2012). Therefore, I tested a number of gDNA extraction methodologies and discovered that combining the PowerBiofilm™ with a modified CTAB methodology improved the quantity of DNA recovered from both Gram-positive and Gram-negative monospecies biofilms. The mixed species biofilm model was used to investigate whether NO could trigger the dispersal of biofilms formed by a defined set of species, PA21 a *P. aeruginosa* CF isolate and A52 a *S. aureus* CF isolate. However, biofilm dispersal was not observed as measured by Comstat2 analysis of CLSM data and by PMA-qPCR (Nocker *et al.*, 2007; Rogers *et al.*, 2008) which was employed to measure the viable population of cells for both species. Although, biofilm dispersal was not successfully induced in the presence of ~ 500 pM exogenous NO, a minor increase in the viable proportion of *P. aeruginosa* cells within the mixed species biofilm was observed. Further work is required to examine if this effect is observed over a longer duration of NO treatment. In addition, an examination focused on the interspecies interaction between these two species is required to tease apart whether the following effects: QS signals, reduction in nutrient content, oxygen and pH levels and antimicrobials have on the biofilms dynamics observed in this assay. Additionally, an examination of biofilm dynamics across a longer duration of time may reveal a recovery of *S. aureus* occurs in the mixed species biofilm. Collectively, this work outlines the importance of using mixed species biofilm models in the future to test the effectiveness of an antimicrobial therapies being tested (Bragonzi *et al.*, 2012a; Ren *et al.*, 2015; Tavernier and Coenye, 2015).

The final chapter outlines the testing of a new FISH based method called CLASI-FISH. To date FISH in the field of microbiology has proven to be a powerful technique for the rapid detection and visualisation of microorganisms within the clinical setting (Michael Hogardt *et al.*, 2000; Forrest *et al.*, 2006; Brown and Govan, 2007). In relation to CF, FISH has previously been used in the direct

identification of *P. aeruginosa*, *S. aureus*, *H. influenzae*, *S. maltophilia* and *B. cepacia* complex within CF sputum samples (Michael Hogardt *et al.*, 2000), wherein the authors outlined the detection of two species simultaneously within CF sputum. The obvious limitation to this methodology is the limited number of probes which can be applied to a sample before the overlapping spectra of a number of fluorophores becomes the limiting factor in the ability to distinguish fluorescence signals, using the traditional confocal microscopy practices (Zimmermann *et al.*, 2003). Given the diversity of the CF microbiome (Cox *et al.*, 2010; van der Gast *et al.*, 2011) and the fact that the microorganisms colonize the lung forming biofilms, the use of 5 fluorophores would provide minimum information about the structuring of this species rich community.

The use of this recent new FISH method, CLASI-FISH has been shown to dramatically increase the number of microorganisms which can been identified simultaneously (Valm *et al.*, 2011, 2012). The aim of this chapter was to adapt this technique for the identification of seven of the most predominant microorganisms in the CF lung. The work in Chapter 5 set out to use five fluorophores, which when used in binary combination would permit the identification of up to 10 taxa within the one field of view. FISH assays using both singly and binary labelled *E. coli* NCTC 9001cells were successfully separated through linear unmixing operations using the database of reference spectra acquired for each fluorophore. Moreover, 10 populations of *E. coli* were successfully labelled and assigned their combinatorial label using custom built functions designed within the Wolfram Mathematica platform. These tests ensured that methodology could then be applied to identify the seven CF microbial strains of interest.

An equal mixture of the type strains for *P. aeruginosa*, *S. aureus*, *H. influenzae*, *A. xylosoxidans*, *S. maltophilia*, *B. cepacia* complex and *S. pneumoniae* were singly labelled with their species specific probe. However, for some of the species, a dim fluorescence signal was observed. Finally, testing of a CLASI-FISH assay using a binary combination of probes, one species specific probe and one EUB338 allowed for the identification of regions of the assay which

could be further improved. Furthermore, a primarily test for the first step in understanding the parameters required to be optimized in using CLASI-FISH to identify the seven CF microbial species used to spike a CF sputum sample was explored. This initial test provided evidence that autofluorescence alone did not contribute to the high level of noise; as this artefact could be removed during linear unmixing operation. This importantly pointed to issues with sufficiently removing the unbound probes from the sputum post CLASI-FISH.

These issues observed for the type strains and application of CLASI-FISH to CF sputum are currently being investigated to ameliorate the negative effects observed for multiplexing all specifies specific probes under the same formamide concentration within CF sputum. The ultimate goal of this technique is to provide a rapid diagnostic tool for laboratories which would enable clinicians to know which microorganisms are forming biofilms within the CF patient's lung. And additionally, to describe a FISH assay which enables a researcher to study directly the species interactions observed within CF sputum and therefore enable a better understanding of the dynamics of biofilm infection over the course of a CF patient's life.

Appendices

Appendix 1

Sequencing Results for the Three Yeast Isolates Obtained from Three CF Patients (Chapter 2)

C. albicans isolate from patient A08 sequencing result for the ITS1‑ ITS4 region

>410936501_08_ITS1

NNNNNNNNNNNNNNNNNNNNNNNNNGCCCNNTGTGTTTTTCTTTGANCANACTTGC
TTTGGCGGTGGGCCCAGCCTGCCNCCAGAGGTCTAAACTTACAACCAATTTTTTAT
CAACTTGTCACACCAGATTATTACTAATAGTCAAAACTTTCAACAACGGATCTCTTG
GTTCTCGCATCGATGAAGAACGCAGCGAAATGCGATACGTAATATGAATTGCAGAT
ATTCCTGAATCATCCAATCTTTGAACGCACATTGCGCCCTCTGGTATTCCGGAGGG
CATGCCTGGTTGAGCGTCGTTTCTCCCTCAAACCGCTGGGTTTGGTGTTGAACAAT
ACCACTTGGGTTTGCTTGAAAGACGGTAGTGGTAAGGCGGGATCCCTTTGACAATG
GCTTAAGTCTAACCAAAAACATTGCTTGCGGCGGGAACGTCCACCACCTATATCTT
CAAACTTTGACCTCCAATCAAGTAGGACTACCCCCTGAAATTCAGCATATCAATAA
GCGGAAGAANAANNGAAGAAACN

NCBI and ISHAM ITS database results

C. albicans isolate from patient A08

NCBI Database top three matches for Isolate A08

Description of matches	Max Score	Total score	Query cover	E value	Ident	Accession ID
C. albicans strain M357	798	798	91%	0.0	96%	KP675591.1
C. albicans strain M193A	798	798	91%	0.0	96%	KP675369.1
C. albicans strain M188B	798	798	91%	0.0	96%	KP675365.1

ISHAMITS Database result for the matches for A08 sequence. Sequence alignment for the top hit (Ref) to that of isolate A08 (Qry)

#	Reference description	Score	Probability	Similarity	Fragments	Overlap%	Direction	Rating
1	MITS468, Candida albicans, WM 01.160, N437: ITS sequence Alignment	661.736	0	95.614	1	86.364	+/+	****

Reference sequence:
MITS468, Candida albicans, WM 01.160, N437: ITS sequence

Sequence length: 494

Similarity: 436/456 [95.614 %], Gaps: 0 [0.000 %], Coverage: 456/456 [100.000 %]

Score: 661.736, Probability: 0, Direction: +/+

```
Qry 36    TTTTTCTTTGANCANACTTGCTTTGGCGGTGGGCCCAGCCTGCCNCCAGAGGTCTAAACT  95
          ||||  ||  | ||  |||||||||||||||||||||||||||  |||||||||||||||
Ref 37    TTTTCTTTGAAACAAACTTGCTTTGGCGGTGGGCCCAGCCTGCCGCCAGAGGTCTAAACT  96

Qry 96    TACAACCAATTTTTTATCAACTTGTCACACCAGATTATTACTAATAGTCAAAACTTTCAA  155
          |||||||||||||||||||||||||||||||||||||||||||||||||||||||||||
Ref 97    TACAACCAATTTTTTATCAACTTGTCACACCAGATTATTACTAATAGTCAAAACTTTCAA  156

Qry 156   CAACGGATCTCTTGGTTCTCGCATCGATGAAGAACGCAGCGAAATGCGATACGTAATATG  215
          ||||||||||||||||||||||||||||||||||||||||||||||||||||||||||||
Ref 157   CAACGGATCTCTTGGTTCTCGCATCGATGAAGAACGCAGCGAAATGCGATACGTAATATG  216

Qry 216   AATTGCAGATATTCCTGAATCATCCAATCTTTGAACGCACATTGCGCCCTCTGGTATTCC  275
          ||||||||||||| |||||||||| ||||||||||||||||||||||||||||||||||||
Ref 217   AATTGCAGATATTCGTGAATCATCGAATCTTTGAACGCACATTGCGCCCTCTGGTATTCC  276

Qry 276   GGAGGGCATGCCTGGTTGAGCGTCGTTTCTCCCTCAAACCGCTGGGTTTGGTGTTGAACA  335
          |||||||||||||||||||||||||||||||||||||||||||||||||||||||||| ||
Ref 277   GGAGGGCATGCCTGTTTGAGCGTCGTTTCTCCCTCAAACCGCTGGGTTTGGTGTTGAGCA  336

Qry 336   ATACCACTTGGGTTTGCTTGAAAGACGGTAGTGGTAAGGCGGGATCCCTTTGACAATGGC  395
          ||||| ||||||||||||||||||||||||||||||||||||||||| |||||||||||||
Ref 337   ATACGACTTGGGTTTGCTTGAAAGACGGTAGTGGTAAGGCGGGATCGCTTTGACAATGGC  396

Qry 396   TTAAGTCTAACCAAAAACATTGCTTGCGGCGGGAACGTCCACCACCTATATCTTCAAACT  455
          |||| |||||||||||||||||||||||||||| |||||||||||||||| |||||||||||
Ref 397   TTAGGTCTAACCAAAAACATTGCTTGCGGCGGTAACGTCCACCACGTATATCTTCAAACT  456

Qry 456   TTGACCTCCAATCAAGTAGGACTACCCCCTGAAATT  491
          ||||||||| ||||| ||||||||||||||| |||| ||
Ref 457   TTGACCTCAAATCAGGTAGGACTACCCGCTGAACTT  492
```

229

C. albicans isolate from patient A15 sequencing result for the ITS1-ITS4 region

>410936501_15_ITS1

NNNNNNNNNNNNNTNNANNNTGCNCCNCATGTGTTTTTCTTTGAACAAACTTGCT
TTGGCGGTGGGCCCAGCCTGCCGCCAGAGGTCTAAACTTACAACCAATTTTTTATC
AACTTGTCACACCAGATTATTACTAATAGTCAAAACTTTCAACAACGGATCTCTTGG
TTCTCGCATCGATGAAAAACGCAGCGAAATGCGATACGTAATATGAATTGCAAATA
TTCGTGAATCATCCAATCTTTGAACGCACATTGCGCCCTCTGGTATTCCGGAAGGC
ATGCCTGTTTGAGCGTCGTTTCTCCCTCAAACCGCTGGGTTTGGTGTTGAACAATA
CCACTTGGGTTTGCTTGAAAGACGGTAGTGGTAAGGCGGGATCCCTTTGACAATGG
CTTAAGTCTAACCAAAAACATTGCTTGCGGCGGTAACGTCCACCACGTATATCTTC
AAACTTTGACCTCAAATCAGGTAGGACTACCCGCTGAACTTAAGCATATCACTAAC
CGGAGGAAACANNNNCATACCGANTTNNTTAATTGNNANATGTGTTNTTCNTTGA

NCBI and ISHAM ITS database results

C. albicans isolate from patient A15

NCBI Database top three matches for isolate A15

Description of matches	Max Score	Total score	Query cover	E value	Ident	Accession
C. albicans strain H108A	857	857	88%	0.0	98%	KP674802.1
C. albicans strain m79b	852	852	88%	0.0	98%	KP675281.1
C. albicans strain m79a	852	852	88%	0.0	98%	KP675280.1

ISHAMITS Database result for matches to the A15 sequence.
Sequence alignment for the top hit (Ref) to that of isolate A15 (Qry)

```
Alignment
Reference sequence:
MITS441, Candida albicans, IHEM 9582, N437: ITS sequence

Sequence length: 499

Similarity: 467/478 [97.699 %], Gaps: 1 [0.209 %], Coverage: 477/478 [99.791 %]
Score: 703.723, Probability: 0, Direction: +/+

Qry 21    TGCNCCNCATGTGTTTTTCTTTG-AACAAACTTGCTTTGGCGGTGGGCCCAGCCTGCCGC   79
          ||| ||  ||||||||||||||| |||||||||||||||||||||||||||||||||||||
Ref 22    TGCACCACATGTGTTTTTCTTTGAAACAAACTTGCTTTGGCGGTGGGCCCAGCCTGCCGC   81

Qry 80    CAGAGGTCTAAACTTACAACCAATTTTTTATCAACTTGTCACACCAGATTATTACTAATA   139
          ||||||||||||||||||||||||||||||||||||||||||||||||||||||||||||
Ref 82    CAGAGGTCTAAACTTACAACCAATTTTTTATCAACTTGTCACACCAGATTATTACTAATA   141

Qry 140   GTCAAAACTTTCAACAACGGATCTCTTGGTTCTCGCATCGATGAAAAACGCAGCGAAATG   199
          |||||||||||||||||||||||||||||||||||||||||||||||  |||||||||||
Ref 142   GTCAAAACTTTCAACAACGGATCTCTTGGTTCTCGCATCGATGAAGAACGCAGCGAAATG   201

Qry 200   CGATACGTAATATGAATTGCAAATATTCGTGAATCATCCAATCTTTGAACGCACATTGCG   259
          ||||||||||||||||||||||| |||||||||||||||| |||||||||||||||||||
Ref 202   CGATACGTAATATGAATTGCAGATATTCGTGAATCATCGAATCTTTGAACGCACATTGCG   261

Qry 260   CCCTCTGGTATTCCGGAAGGCATGCCTGTTTGAGCGTCGTTTCTCCCTCAAACCGCTGGG   319
          |||||||||||||||||| |||||||||||||||||||||||||||||||||||||||||
Ref 262   CCCTCTGGTATTCCGGAGGGCATGCCTGTTTGAGCGTCGTTTCTCCCTCAAACCGCTGGG   321

Qry 320   TTTGGTGTTGAACAATACCACTTGGGTTTGCTTGAAAGACGGTAGTGGTAAGGCGGGATC   379
          |||||||||||| ||||||| |||||||||||||||||||||||||||||||||||||||
Ref 322   TTTGGTGTTGAGCAATACGACTTGGGTTTGCTTGAAAGACGGTAGTGGTAAGGCGGGATC   381

Qry 380   CCTTTGACAATGGCTTAAGTCTAACCAAAAACATTGCTTGCGGCGGTAACGTCCACCACG   439
          ||||||||||||||||| |||||||||||||||||||||||||||||||||||||||||||
Ref 382   GCTTTGACAATGGCTTAGGTCTAACCAAAAACATTGCTTGCGGCGGTAACGTCCACCACG   441

Qry 440   TATATCTTCAAACTTTGACCTCAAATCAGGTAGGACTACCCGCTGAACTTAAGCATAT   497
          ||||||||||||||||||||||||||||||||||||||||||||||||||||||||||
Ref 442   TATATCTTCAAACTTTGACCTCAAATCAGGTAGGACTACCCGCTGAACTTAAGCATAT   499
```

C. dubliniensis isolate from patient A29 sequencing result for the ITS1-ITS4 region

>410936501_29_ITS1

NNNNNNNNNNNNNNNNNNNNNNNNNNCNNNTGTGTTTTGNTCTGGACAAACTTG
CTTTGGCGGTGGGCCCCTGCCTGCCNCCNGAGGACATAAACTTACAACCAAATTTT
TTATAAACTTGTCACGAGATTATTTTTAATAGTCAAAACTTTCAACAACGGATCTCT
TGGTTCTCGCATCGATGAAGAACGCAGCGAAATGCGATACGTAATATGAATTGCAG
ATATTCGTGAATCATCGAATCTTTGAACGCACATTGCGCCCTCTGGTATTCCGGAG
GGCATGCCTGTTTGAGCGTCGTTTCTCCCTCAAACCCCTAGGGTTTGGTGTTGAGC
AATACAACTTGGGTTTGCTTGAAAGATGATCGTGGTATAAGGCGGACATGCTTGAC
AATGGATAACGTGTAACCAAAANTNTCGCTAAAGCGGTCTCNGGTTGCNCCCCCTN
NATTCTGGAAATTTAGCCGTCNGGGCANAGNNAAGTGTTCTCCNTCNNGNGCTAT
CCTCANGGTNCGGACCCATCAAGCNAACTNTCATAANGATCGAGGCTGGNAGCTT
TTCACNGNNGNAANTTGCGTCCTGGCTAANTCCTACNTCNNNTGNNCTTNNTTCCT
TGCTCTGGTTTCTCTTATGCTCNNAAGAANGGCATTNTCAANGATANGAANC

NCBI and ISHAM ITS Database results

C. dubliniensis isolate from patient A29

NCBI Database top three matches for isolate A29

Description of matches	Max score	Total score	Query cover	E value	Ident	Acession ID
C. dubliniensis strain PMM08-3042L	675	675	60%	0.0	97%	KP131697.1
C. dubliniensis strain PMM08-2297L	675	675	60%	0.0	97%	KP131696.1
C. dubliniensis strain WM 03.460	675	675	60%	0.0	97%	KP068727.1

ISHAMITS Database result for matches to the A29 sequence. Sequence alignment for the top hit (Ref) to that of isolate A29 (Qry)

```
Alignment
Reference sequence:
MITS581, Candida dubliniensis, Lcd5, N437: ITS sequence

Sequence length: 453

Similarity: 403/428 [94.159 %], Gaps: 0 [0.000 %], Coverage: 428/428
[100.000 %]
Score: 600.701, Probability: 1.71805E-172, Direction: +/+

Qry 31     TGTGTTTTGNTCTGGACAAACTTGCTTTGGCGGTGGGCCCCTGCCTGCCNCCNGAGGACA
  90
           |||||||| |||||||||||||||||||||||||||||||||||||||| || |||||||
Ref 25     TGTGTTTTGTTCTGGACAAACTTGCTTTGGCGGTGGGCCCCTGCCTGCCGCCAGAGGACA
  84

Qry 91     TAAACTTACAACCAAATTTTTTATAAACTTGTCACGAGATTATTTTTAATAGTCAAACT
 150
           |||||||||||||||||||||||||||||||||||||||||||||||||||||||||||
Ref 85     TAAACTTACAACCAAATTTTTTATAAACTTGTCACGAGATTATTTTTAATAGTCAAACT
 144

Qry 151    TTCAACAACGGATCTCTTGGTTCTCGCATCGATGAAGAACGCAGCGAAATGCGATACGTA
 210
           ||||||||||||||||||||||||||||||||||||||||||||||||||||||||||||
Ref 145    TTCAACAACGGATCTCTTGGTTCTCGCATCGATGAAGAACGCAGCGAAATGCGATACGTA
 204

Qry 211    ATATGAATTGCAGATATTCGTGAATCATCGAATCTTTGAACGCACATTGCGCCCTCTGGT
 270
           ||||||||||||||||||||||||||||||||||||||||||||||||||||||||||||
Ref 205    ATATGAATTGCAGATATTCGTGAATCATCGAATCTTTGAACGCACATTGCGCCCTCTGGT
 264

Qry 271    ATTCCGGAGGGCATGCCTGTTTGAGCGTCGTTTCTCCCTCAAACCCCTAGGGTTTGGTGT
 330
           ||||||||||||||||||||||||||||||||||||||||||||||||||||||||||||
Ref 265    ATTCCGGAGGGCATGCCTGTTTGAGCGTCGTTTCTCCCTCAAACCCCTAGGGTTTGGTGT
 324

Qry 331    TGAGCAATACAACTTGGGTTTGCTTGAAAGATGATCGTGGTATAAGGCGGACATGCTTGA
 390
           ||||||||||| ||||||||||||||||||||||||| |||||||||||||| ||||||||
Ref 325    TGAGCAATACGACTTGGGTTTGCTTGAAAGATGATAGTGGTATAAGGCGGAGATGCTTGA
 384

Qry 391    CAATGGATAACGTGTAACCAAAANTNTCGCTAAAGCGGTCTCNGGTTGCNCCCCCTNNAT
 450
           ||||||| | | ||||||||||||   |  | ||||| ||||||||| ||   | |||  | ||
Ref 385    CAATGGCTTAGGTGTAACCAAAAACATTGCTAAGGCGGTCTCTGGCGTCGCCCATTTTAT
 444

Qry 451    TCTGGAAA   458
           ||| |||
Ref 445    TCTTCAAA   452
```

Appendix 2

DNA molecular weight markers used for agarose gel electrophoresis work in this thesis

peqGold 50 bp DNA ladder
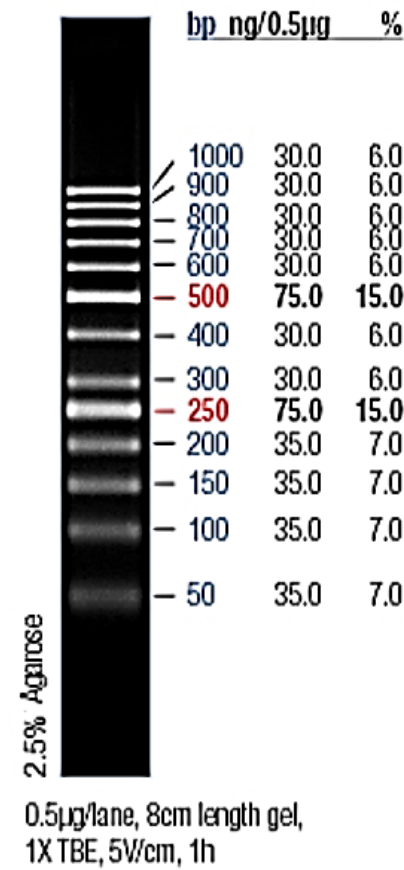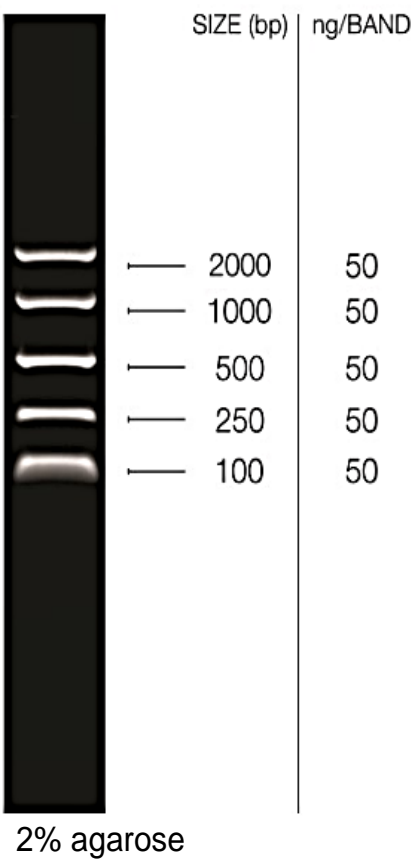
bp	ng/0.5µg	%
1000	30.0	6.0
900	30.0	6.0
800	30.0	6.0
700	30.0	6.0
600	30.0	6.0
500	75.0	15.0
400	30.0	6.0
300	30.0	6.0
250	75.0	15.0
200	35.0	7.0
150	35.0	7.0
100	35.0	7.0
50	35.0	7.0

2.5% Agarose

0.5µg/lane, 8cm length gel, 1X TBE, 5V/cm, 1h

Easyladder™ I

SIZE (bp)	ng/BAND
2000	50
1000	50
500	50
250	50
100	50

2% agarose

235

Appendix 2

DNA molecular weight markers used for agarose gel electrophoresis work in this thesis

Hyperladder I

SIZE (bp)	ng/BAND
10037	100
8000	80
6000	60
5000	50
4000	40
3000	30
2500	25
2000	20
1500/1517	15/15
1000	100
800	80
600	60
400	40
200	20

1% agarose gel
5µl per lane
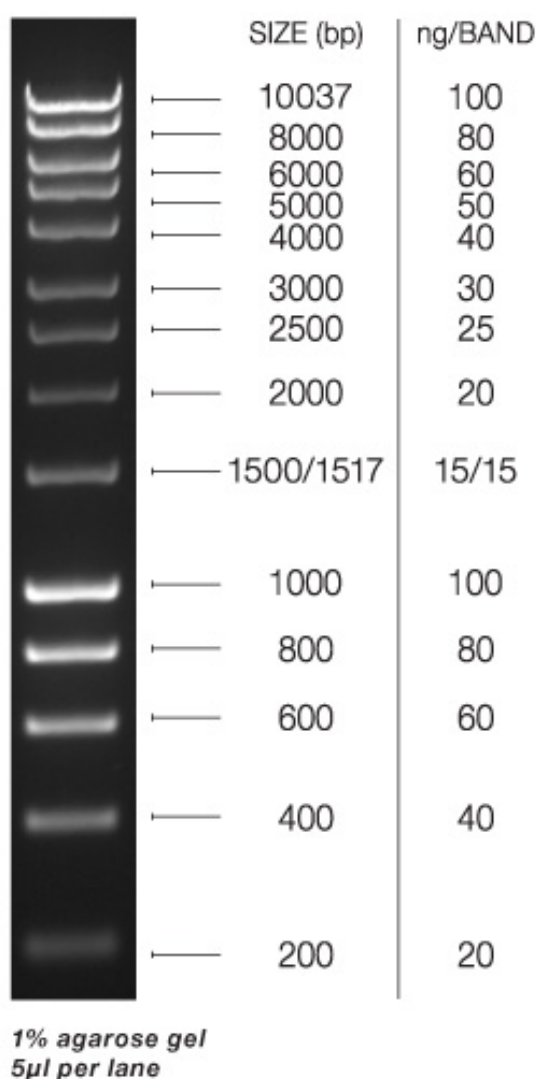
Appendix 3

Chemical controls used for the SNP assays

The results in this section are related to the data obtained in Chapter 3. The boxplots outline the effect the chemical controls for SNP had on the biofilm biomass (CFU / cm^2), planktonic phase (CFU / ml) and the percentage surface coverage compared to the control for the five monospecies biofilms tested. The SNP chemical controls are: 1) PF, which is a chemical analogue of SNP lacking NO but contains a ferricyanide moiety similar to SNP, serves as a control for the potential effects of cyanide and breakdown products of SNP released into the medium may present (Wang *et al.*, 2002). PTIO acts as a scavenger of NO thereby ensuring any reduction in CFU values or biofilm surface coverage is NO mediated (Goldstein *et al.*, 2003). All *in vitro* monospecies biofilms were treated with one micromolar PF for 12 h. The concentration of PTIO added to each *in vitro* monospecies biofilm was one micromolar, for sequestering the NO released from one micromolar SNP added to the same medium. The concentration of PTIO for this assay is 3 fold higher than that of the concentration of NO released from one micromolar SNP (Venkataraman *et al.*, 2002), which would approximately equate to 0.7 – 1 nanomolar NO (Bradley and Steinert, 2015). Therefore, this PTIO concentration is sufficient to remove the NO released in this assay and confirm any effect observed in the SNP treatments is due to presence of NO.

In vitro *B. cepacia* complex biofilm response to PF and PTIO treatments
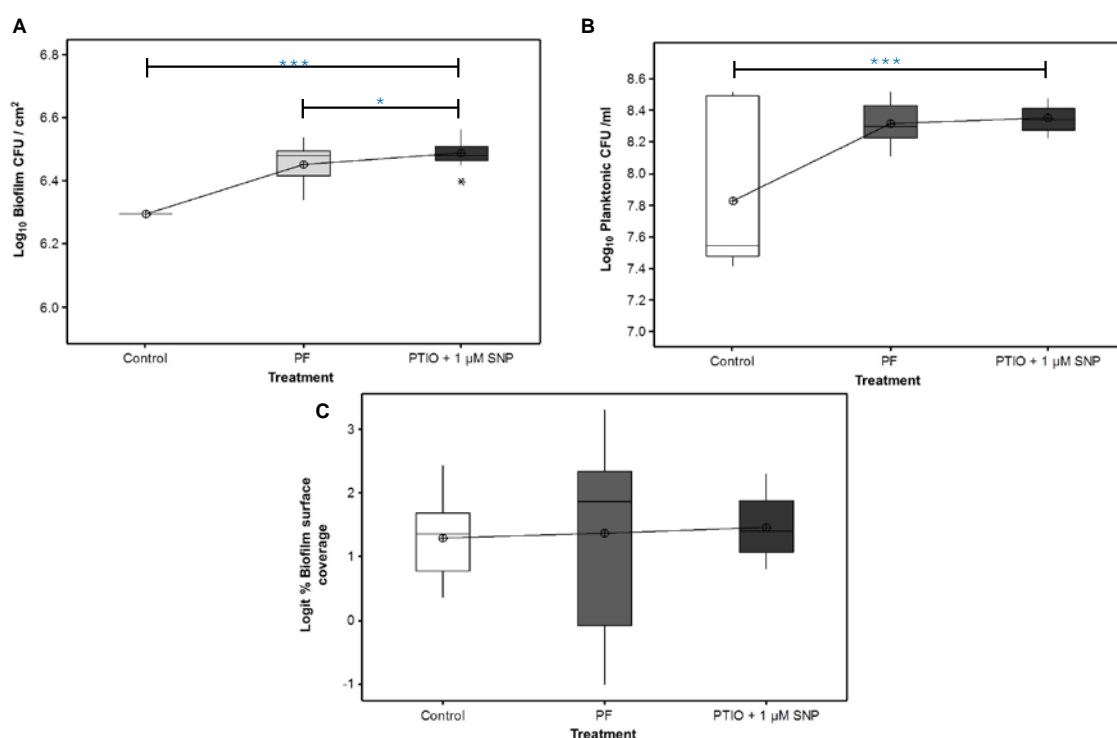
Figure (i) No negative effect observed for the *B. cepacia* complex biofilm treated with the SNP chemical controls. Figure A shows the Log_{10} biofilm CFU /cm^2 data; with a highly significant difference between the control and the chemical controls and between the chemical controls, due to the modest increase of CFU values not of biological significance ($F_{1, 42}$ = 25.48, P < 0.001; $F_{1, 42}$ = 5.46, P = 0.021, respectively). Figure B shows the response of the planktonic phase (Log_{10} CFU / ml) to the chemical controls. A highly significant difference is noted for the control against the pooled treatments ($F_{1, 42}$ = 29.86, P < 0.001); again no reduction in CFU values in the treatment, a wider variation in the CFU values across the control group accounts for this difference. Figure C shows the Logit values for the percentage of biofilm present after treatment, no significant or negative effect observed. Box plots show the median and inter-quartile ranges; means are shown as encircled crosses, n = 3. Black asterisk marks an outlier.

Influence of PF and PTIO on the *in vitro A. xylosoxidans* biofilm phase
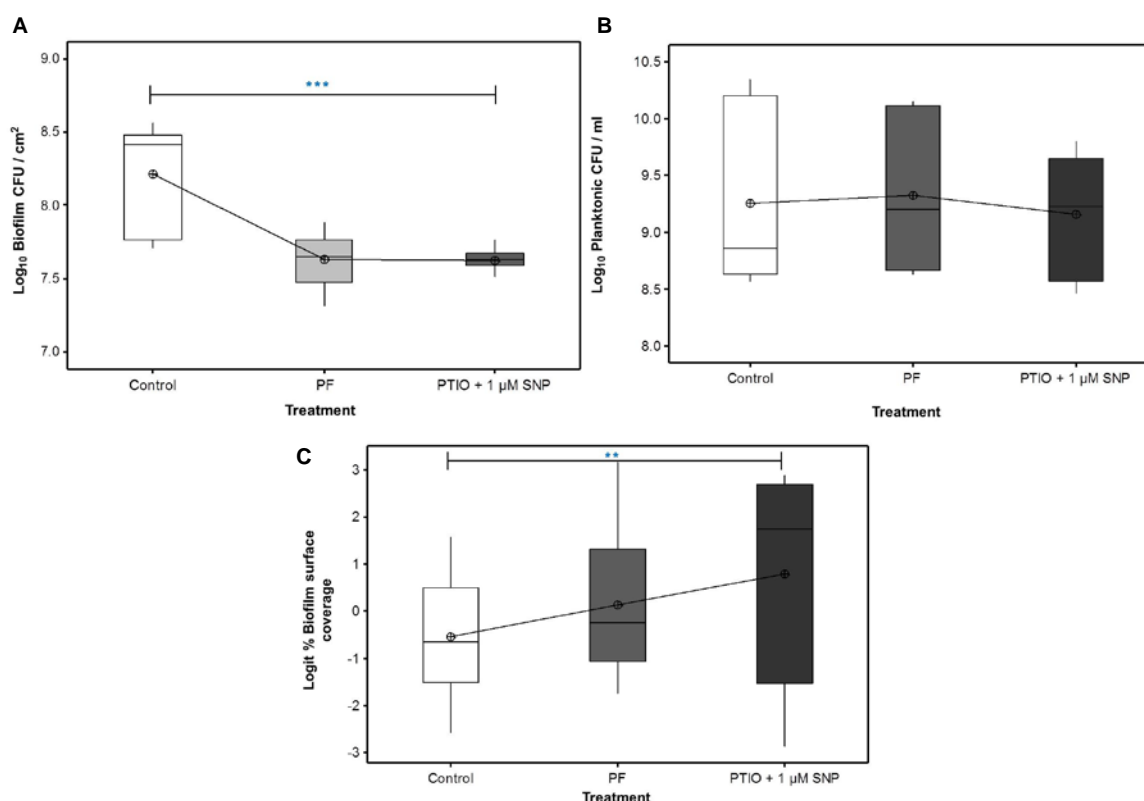
Figure (ii) A significant negative effect observed for the *in vitro A. xylosoxidans* biofilms treated with PF and PTIO. Figure A shows a significant reduction ($F_{1, 42}$ = 67.89, *P* < 0.001) of 0.59 to 0.60 in the $\log_{10}$ CFU / cm² for the biofilm biomass in the PTIO and PF treatments, respectively. **Figure B**, no negative effect observed for the PF and PTIO treatments for the planktonic phase. **Figure C** for the logit % surface coverage shows a significant trend towards a modest increase in surface coverage of the biofilm biomass ($F_{1, 42}$ = 7.87, *P* < 0.01). The biofilm surface coverage did not correlate with the reduction $\log_{10}$ reduction in biofilm CFU / cm² observed for the PTIO and PF treatments thereby showing these chemical controls did not trigger biofilm dispersal but had an effect on biofilm cell viability. Box plots show the median and inter-quartile ranges; means are shown as encircled crosses, *n* = 3.

In vitro S. aureus biofilm response to PF and PTIO treatments
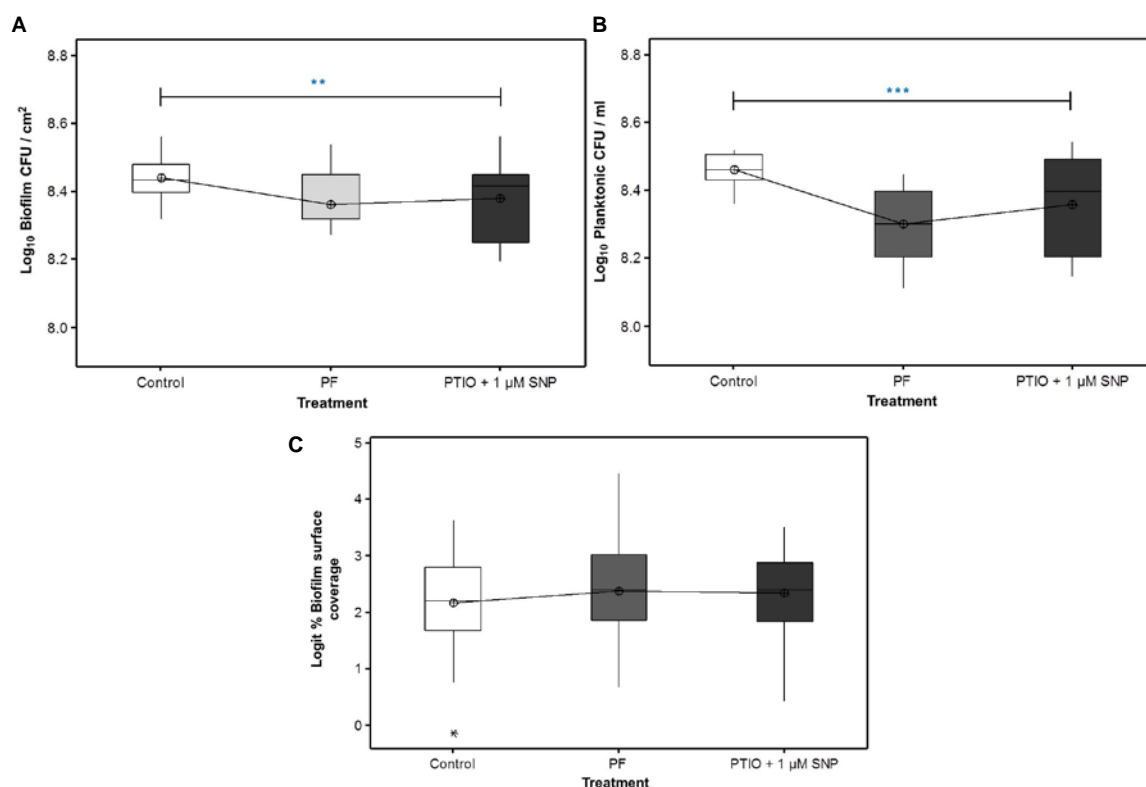
Figure (iii)   *S. aureus in vitro* biofilms exposed to PF and PTIO are not adversely affected and do not induce a biofilm dispersal effect. **Figure A** for the $\log_{10}$ biofilm CFU / cm² showed a reduction from 8.44 ± 0.06 for the control compared to the pooled PF and PTIO treatments with 8.36 ± 0.08 and 8.38 ± 0.11 (mean ± SD), respectively ($F_{1,\,42}$ = 6.60, P < 0.01). **Figure B** shows a similarly low level of reduction in for the planktonic phase when the control is compared against the pooled treatments for PF and PTIO. Albeit, this reduction is statistically significant for the $\log_{10}$ values of 8.46 ± 0.05, 8.35 ± 0.14, 8.30 ± 0.11 observed for the control, PTIO and PF treatments, respectively, it is not of biological importance (mean ± SD; $F_{1,\,42}$ = 15.54, P < 0.001). **Figure C** for the logit % biofilm surface coverage showed no reduction in surface coverage ($F_{1,\,87}$ = 1.08, P = 0.302). Box plots show the median and inter-quartile ranges; means are shown as encircled crosses and any outlier is marked as a black asterisk, n = 3.

Response for the _in vitro_ biofilm of _S. maltophilia_ treated with the SNP chemical controls, PF and PTIO
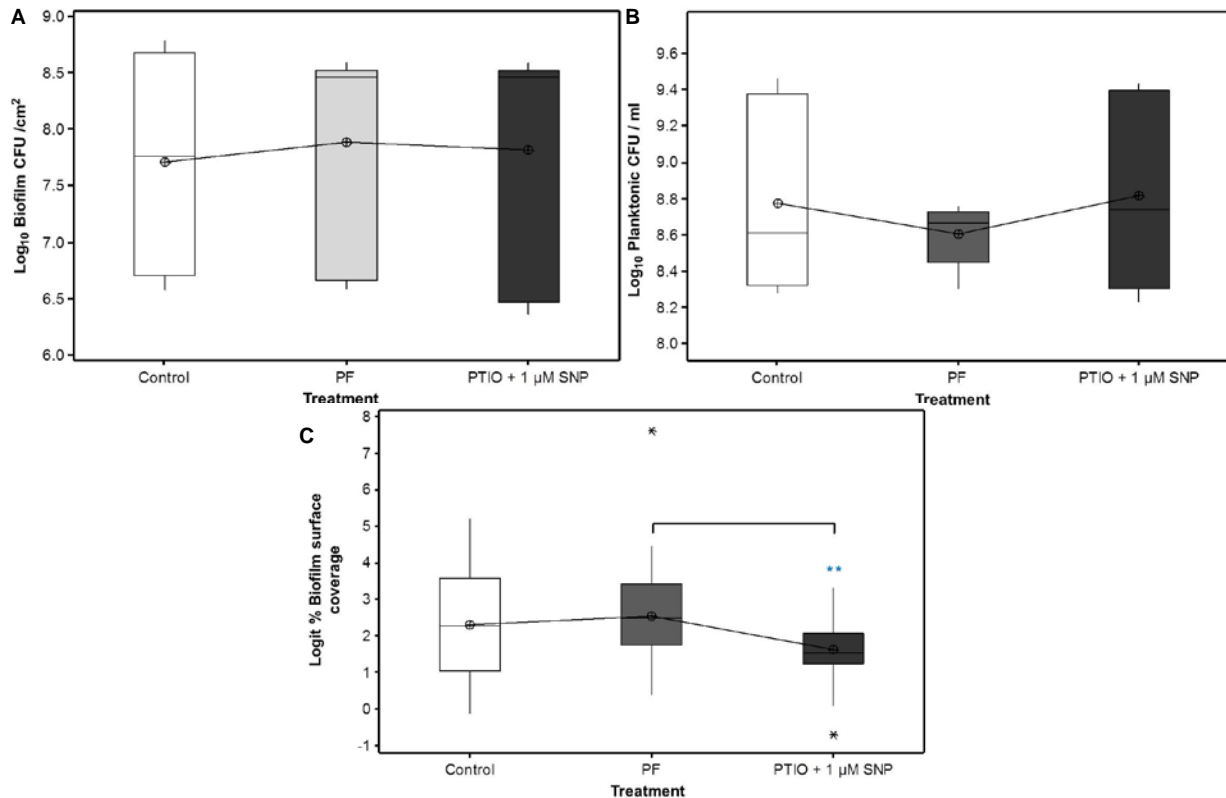
Figure (iv)   **The chemical controls for SNP have no adverse effect on the _in vitro S. maltophilia_ biofilm. Figure A** and **Figure B** do not show any negative impact of these chemicals on comparing the control against the pooled treatments groups for both the biofilm biomass $\log_{10}$ CFU / cm^2 and the planktonic CFU /ml values, respectively. There is considerable variation within each treatment group ($F_{1,\ 42}$ = 0.23, P = 0.633; $F_{1,\ 42}$ = 0.04, P = 0.842, respectively). **Figure C** for the logit transformed percentage surface coverage shows the only significant difference noted is between the PF and PTIO treatments ($F_{1,\ 87}$ = 7.66, $P < 0.01$). For the untransformed data, the control, PF and PTIO had percentage surface coverage values of 84% ± 2.81, 88% ± 2.94 and 81% ± 2.69, respectively (mean ± SEM). Box plots show the median and inter-quartile ranges; means are shown as encircled crosses and outliers are marked with a black asterisk, n = 3.

The chemical controls PF and PTIO have no negative effect on the *in vitro* biofilm for *S. pneumoniae*
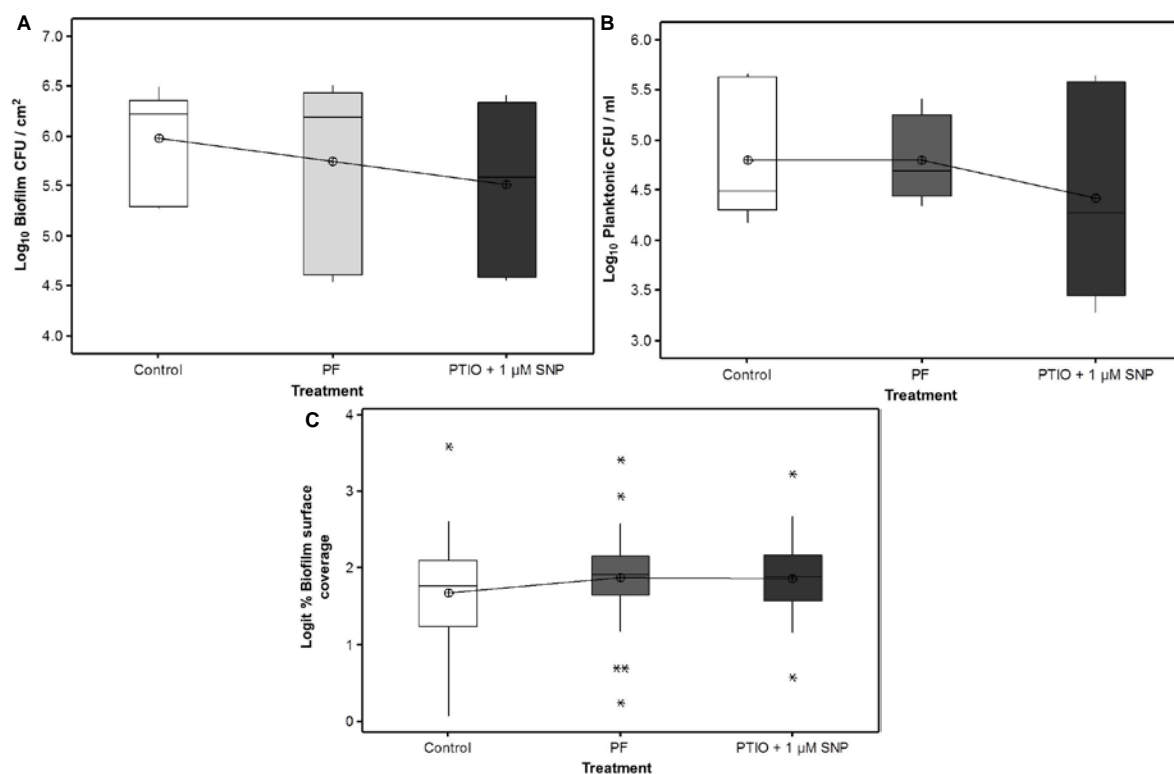
Figure (v) The SNP chemical controls used do not affect the cell viability and show the NO is effectively scavenged by PTIO. Therefore, any effects observed are mediated due to the presence of NO for the SNP concentrations tested. **Figure A** shows no significant reduction in the biofilm biomass via the $\log_{10}$ CFU / cm^2 for which the control, PF and PTO values are 5.97 ± 0.51, 5.74 ± 0.85 and 5.51 ± 0.76 (mean ± SD; $F_{1, 42}$ = 2.25, P = 0.141). **Figure B** shows similar results for the planktonic phase $\log_{10}$ CFU /ml ($F_{1, 42}$ = 0.76; P = 0.389). **Figure C** for the transformed (logit) percentage surface data similarly show no adverse effect between the control against the pooled treatments was noted ($F_{1, 87}$ = 1.89, P = 0.173). Box plots show the median and inter-quartile ranges; means are shown as encircled crosses and outliers are marked by a black asterisk, n = 3.

No reduction in biofilm biomass, planktonic phase growth and biofilm surface coverage for four out of the five *in vitro* monospecies biofilms treated with the SNP chemical controls

The only *in vitro* monospecies biofilm exhibiting a significant biofilm reduction was that observed via the one log reduction in the biofilm CFU data for the *A. xylosoxidans* biofilm. The biofilm phase showed a one log reduction in the biofilm CFU / cm^2 for both the PF and PTIO treatments, 7.63 ± 0.161 and 7.62 ± 0.064, respectively when compared to 8.21 ± 0.349 for the control (mean $\pm$ SD). This reduction in biofilm biomass was not observed for the cells in planktonic phase and did not result in a reduction in the biofilm surface coverage. Refer to section 3.4, wherein this observation is further discussed.

Appendix 4

Positive control for NO mediation dispersal using a _P. aeruginosa_ biofilm

The following work outlines a positive control for NO mediated biofilm dispersal using a _P. aeruginosa_ biofilm. _In vitro_ biofilms formed by _P. aeruginosa_ isolates from the CF lung were dispersed using the NO donor SNP. In Figure (vi) (A) an increase in the planktonic phase via optical density measurements of established _in vitro_ biofilms post treatment with SNP is shown to commence from the 5 h time point across NO concentrations from 450 pM – 450 nM. Furthermore, in Figure (vi) (B) this increase is demonstrated to be a response to the presence of exogenous NO introduced to the established in vitro _P. aeruginosa_ biofilms through the NO donor SNP. The NO scavenger PTIO prevents this effect and the chemical analogue for SNP potassium ferricyanide (PF) shows that the breakdown products are not responsible for the increase observed. Figure (vi) (C) and (D) show representative fluorometric measurements and CLSM images respectively for the reduction in biofilm biomass of established biofilms treated with ~ 450 nM NO (500 μM SNP) compared to an untreated control. This work was conducted across 12 different _P. aeruginosa_ CF clinical biofilm-forming isolates. It was found that an NO concentration of 450 nM effectively induced biofilm dispersal in all _in vitro_ biofilms formed by the 12 CF clinical isolates. Additionally, this work lead to a proof of concept double blind clinical trial to show that NO could be used as an adjunctive therapy to disperse _P. aeruginosa_ biofilms within a CF patient's lung and thereby enable antibiotics to carry out their function (Howlin, Cathie, Hall-Stoodley, Cornelius, Duignan _et al._, 2017).
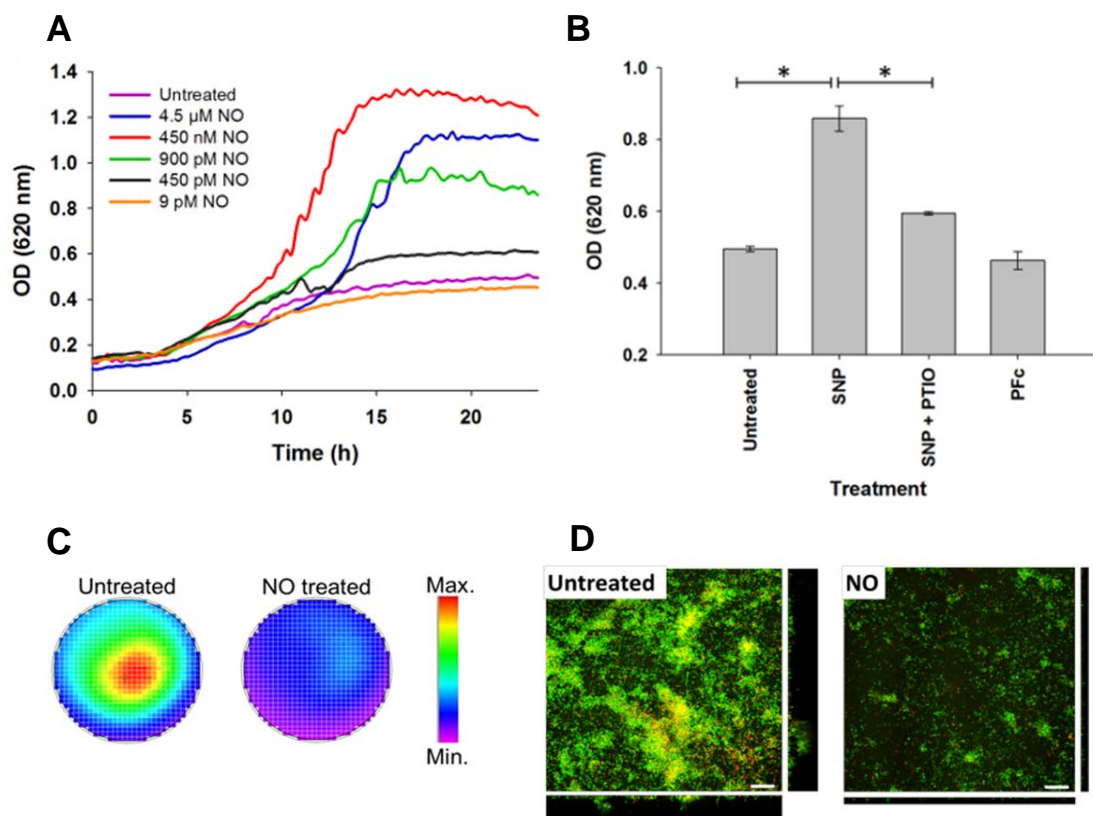
Figure (vi)   Nitric oxide (NO) induces dispersal of *in vitro* biofilms formed by *P. aeruginosa* CF isolates. **A**) An increase in the mean optical density in the planktonic phase following treatment with the NO donor SNP over a low NO concentration range (9 pM – 4.5 µM). **B**) NO dependent increase in the planktonic phase post treatment of *in vitro* biofilms with SNP (500 µM) for 15 h. The NO scavenger PTIO reduces this effect and the SNP chemical analogue potassium ferricyanide is redundant. **C**) Fluorometric measurements showing a reduction of the biofilm biomass attached to the surface of 6-well plates for biofilms treated with NO (450 nM) compared to the untreated. Wells stained with the nucleic acid stain SYTO9. The scale bar indicates maximum (red) to minimum (blue-purple) fluorescence intensity for bound SYTO 9 to the biofilm biomass. **D)** Representative images are X-Y orthogonal z-stack views for biofilm dispersal in the biofilms treated with NO (450 nM) compared to the untreated control. Asterisk indicates statistical difference for $P < 0.05$. Adapted from Howlin, Cathie, Hall-Stoodley, Cornelius, Duignan *et al*., 2017).

Appendix 5

Evaluation of qPCR performance

Table A   Linearity and efficiency for the qPCR reactions

Plate Species	R^2	E
Plate 1 P. aeruginosa	0.994	90.2%
Plate 2 P. aeruginosa	0.949	90.9%
Plate 1 S. aureus	0.970	74.2%
Plate 2 S. aureus	0.975	99.5%

R^2 indicates the regression coefficient.
PCR efficiency (E) expressed as a percentage:
% Efficiency = (E − 1) x 100% as calculated from the
standard curve from E = $10^{-1/slope}$

The qPCR assays were conducted using duplicate technical repeats and plated as follows: Plate 1 had three biological replicates for the untreated and NO treated biofilms sampled at time points 1 h to 5 h analysed within the same plate and equally for Plate 2, biofilms sampled at time points 12 h to 24 h, all biological replicates were analysed within the same plate.

The melt curve analysis did not show detectable peaks for non-specific amplification or primer-dimer associations.

Appendix 6

Level of Autofluorescence of CF sputum

414 nm 423 nm 432 nm 441 nm 450 nm 459 nm 468 nm 477 nm

A

486 nm 495 nm 504 nm 512 nm 521 nm 530 nm 539 nm 548 nm

557 nm 566 nm 575 nm 584 nm 593 nm 602 nm 610 nm 619 nm

628 nm 637 nm 646 nm 655 nm 664 nm 673 nm 682 nm 691 nm

B
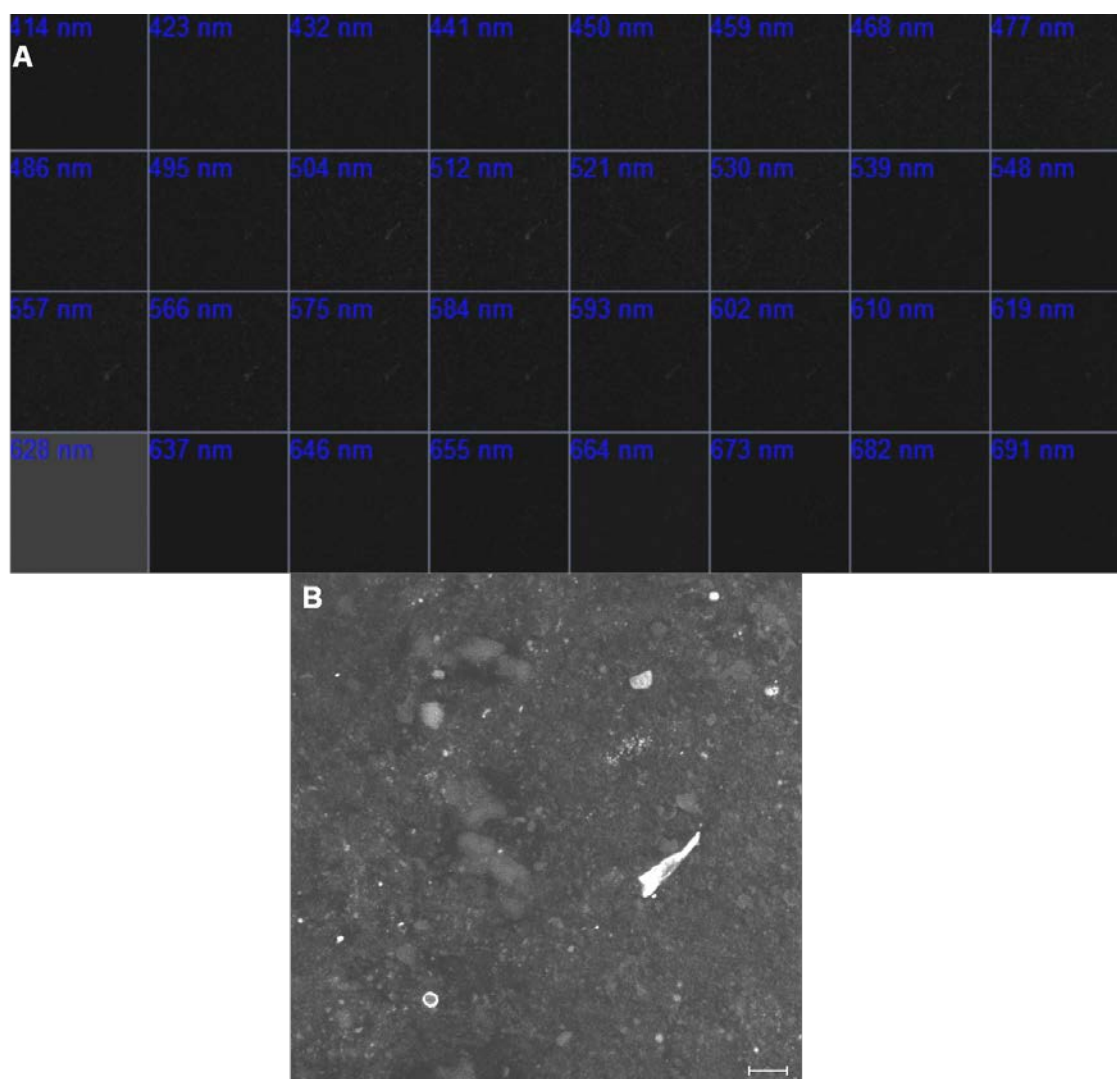
Figure (vii)   Spectral Imaging of a CF sputum sample to determine the level of autofluorescence. A) Image showing the 32-channel spectral images of a CF sputum sample prior to treatment with DTT and PFA.

B) Merged image for all channels. Scale bar = 10 µm

The level of autofluorescence signal is highest between 504 – 610 nm. This output was added to the spectral database for the linear unmixing operation used for the CLASI-FISH image of the CF sputum as shown in Chapter 5 Figure 5.8 (B). The resulting image still contained a high amount of signal not attributed to the autofluorescence levels of the CF sputum imaged.

List of References

Aaron SD, Ferris W, Ramotar K, Vandemheen K, Chan F, Saginur R. (2002). Single and combination antibiotic susceptibilities of planktonic, adherent, and biofilm-grown *Pseudomonas aeruginosa* isolates cultured from sputa of adults with Cystic Fibrosis. *J Clin Microbiol* **40**:4172–4179.

Abdul Wahab A, Janahi IA, El-Shafie SS. (2004). *Achromobacter xylosoxidans* isolated from the sputum of a patient with cystic fibrosis mutation I1234V with *Pseudomonas aeruginosa*. *Saudi Med J* **25**:810–811.

Adak S, Aulak KS, Stuehr DJ. (2002). Direct evidence for nitric oxide production by a nitric-oxide synthase-like protein from *Bacillus subtilis*. *J Biol Chem* **277**:16167–16171.

Adamou JE, Wizemann TM, Barren P, Langermann S. (1998). Adherence of *Streptococcus pneumoniae* to human bronchial epithelial cells (BEAS-2B). *Infect Immun* **66**:820–822.

Adjei MD, Ohta Y. (1999). Isolation and characterization of a cyanide-utilizing *Burkholderia cepacia* strain. *World J Microbiol Biotechnol* **15**:699–704.

Alderton WK, Cooper CE, Knowles RG. (2001). Nitric oxide synthases: structure, function and inhibition. *Biochem J* **357**:593–615.

Alhede M, Bjarnsholt T, Jensen PØ, Phipps RK, Moser C, Christophersen L, *et al.* (2009). *Pseudomonas aeruginosa* recognizes and responds aggressively to the presence of polymorphonuclear leukocytes. *Microbiology* **155**:3500–3508.

Allan RN, Morgan S, Brito-Mutunayagam S, Skipp P, Feelisch M, Hayes SM, *et al.* (2016). Low concentrations of nitric oxide modulate *Streptococcus pneumoniae* biofilm metabolism and antibiotic tolerance. *Antimicrob Agents Chemother* AAC.02432-15-.

Allison DG, Ruiz B, SanJose C, Jaspe A, Gilbert P. (1998). Extracellular products as mediators of the formation and detachment of *Pseudomonas fluorescens* biofilms. *FEMS Microbiol Lett* **167**:179–184.

Alvarez G, González M, Isabal S, Blanc V, León R. (2013). Method to quantify live and dead cells in multi-species oral biofilm by real-time PCR with propidium monoazide. *AMB Express* **3**:1.

Amann RI, Ludwig W, Schleifer K-H. (1995). Phylogenetic identification and in situ detection of individual microbial cells without cultivation. *Microbiol Rev* **59**:143–169.

Amoureux L, Bador J, Fardeheb S, Mabille C, Couchot C, Massip C, *et al.* (2013). Detection of *Achromobacter xylosoxidans* in hospital, domestic, and outdoor environmental samples and comparison with human clinical isolates. *Appl Environ Microbiol* **79**:7142–7149.

Andersen DH. (1938). Cystic fibrosis of the pancreas and its relation to celiac disease: a clinical and pathologic study. *Am J Dis Child* **56**:344–399.

Andersen DH, Hodges RG. (1946). Celiac syndrome: V. Genetics of cystic fibrosis of the pancreas with a consideration of etiology. *Am J Dis Child* **72**:62–80.

Anderson GG, Moreau-Marquis S, Stanton BA, O'Toole GA. (2008). In vitro analysis of tobramycin-treated *Pseudomonas aeruginosa* biofilms on cystic fibrosis-derived airway epithelial cells. *Infect Immun* **76**:1423–1433.

Andreae CA. (2014). Understanding the role of anaerobic respiration in *Burkholderia thailandensis* and *B. pseudomallei* survival and virulence. https://ore.exeter.ac.uk/repository/handle/10871/15284 (Accessed April 30, 2016).

Anonymous. (2012). Cystic Fibrosis Foundation Registry Report 2011. Bethesda, MD.

Anonymous. (2013). UK CF Registry Annual Data Report 2011.

Armougom F, Bittar F, Stremler N, Rolain J-M, Robert C, Dubus J-C, *et al.* (2009). Microbial diversity in the sputum of a cystic fibrosis patient studied with 16S rDNA pyrosequencing. *Eur J Clin Microbiol Infect Dis* **28**:1151–1154.

Armstrong DS, Grimwood K, Carlin JB, Carzino R, Gutierrez JP, Hull J, *et al.* (1997). Lower airway inflammation in infants and young children with cystic fibrosis. *Am J Respir Crit Care Med* **156**:1197–1204.

Azeredo J, Oliveira R. (2000). The role of exopolymers produced by *Sphingomonas paucimobilis* in biofilm formation and composition. *Biofouling* **16**:17–27.

Bagge N, Hentzer M, Andersen JB, Ciofu O, Givskov M, Høiby N. (2004). Dynamics and spatial distribution of β-lactamase expression in *Pseudomonas aeruginosa* biofilms. *Antimicrob Agents Chemother* **48**:1168–1174.

Bakker-Woudenberg IAJM, Marian T, Guo L, Working P, Mouton JW. (2002). Ciprofloxacin in polyethylene glycol-coated liposomes: efficacy in rat models of acute or chronic *Pseudomonas aeruginosa* infection. *Antimicrob Agents Chemother* **46**:2575–2581.

Baldan R, Cigana C, Testa F, Bianconi I, De Simone M, Pellin D, *et al.* (2014). Adaptation of *Pseudomonas aeruginosa* in cystic fibrosis airways influences virulence of *Staphylococcus aureus in vitro* and murine models of co-infection Palaniyar, N (ed). *PLoS One* **9**:e89614.

Baltimore RS, Christie CDC, Smith GJW. (1989). Immunohistopathologic localization of *Pseudomonas aeruginosa* in lungs from patients with cystic fibrosis. *Am Rev Respir Dis* **140**:1650–1661.

Banin E, Vasil ML, Greenberg EP. (2005). Iron and *Pseudomonas aeruginosa* biofilm formation. *Proc Natl Acad Sci U S A* **102**:11076–11081.

Barbaree JM, Payne WJ. (1967). Products of denitrification by a marine bacterium as revealed by gas chromatography. *Mar Biol* **1**:136–139.

Barber CE, Tang JL, Feng JX, Pan MQ, Wilson TJG, Slater H, *et al.* (1997). A novel regulatory system required for pathogenicity of *Xanthomonas campestris* is mediated by a small diffusible signal molecule. *Mol Microbiol* **24**:555–566.

Barlow M. (2009). What antimicrobial resistance has taught us about horizontal gene transfer. *Methods Mol Biol* **532**:397–411.

Barnes RJ, Bandi RR, Wong WS, Barraud N, McDougald D, Fane A, *et al.* (2013). Optimal dosing regimen of nitric oxide donor compounds for the reduction of *Pseudomonas aeruginosa* biofilm and isolates from wastewater membranes. *http://dx.doi.org/101080/0892701420 12760069*.

Barraud N, Hassett DJ, Hwang S-H, Rice SA, Kjelleberg S, Webb JS. (2006). Involvement of nitric oxide in biofilm dispersal of *Pseudomonas aeruginosa*. *J Bacteriol* **188**:7344–7353.

Barraud N, Kardak BG, Yepuri NR, Howlin RP, Webb JS, Faust SN, *et al.* (2012). Cephalosporin-3'-diazeniumdiolates: targeted NO-donor prodrugs for dispersing bacterial biofilms. *Angew Chem Int Ed Engl* **51**:9057–60.

Barraud N, Schleheck D, Klebensberger J, Webb JS, Hassett DJ, Rice SA, *et al.* (2009). Nitric oxide signaling in *Pseudomonas aeruginosa* biofilms mediates phosphodiesterase activity, decreased cyclic di-gmp levels, and enhanced dispersal . *J Bacteriol* **191**:7333–7342.

Barraud N, Storey M V, Moore ZP, Webb JS, Rice SA, Kjelleberg S. (2009). Nitric oxide-mediated dispersal in single-and multi-species biofilms of clinically and industrially relevant microorganisms. *Microb Biotechnol* **2**:370–378.

Bauernfeind A, Hörl G, Jungwirth R, Petermüller C, Przyklenk B, Weisslein-Pfister C, *et al.* (1987). Qualitative and quantitative microbiological analysis of sputa of 102 patients with cystic fibrosis. *Infection* **15**:270–277.

Bayer AS, Speert DP, Park S, Tu J, Witt M, Nast CC, *et al.* (1991). Functional role of mucoid exopolysaccharide (alginate) in antibiotic-induced and polymorphonuclear leukocyte-mediated killing of *Pseudomonas aeruginosa*. *Infect Immun* **59**:302–308.

Beaume M, Köhler T, Fontana T, Tognon M, Renzoni A, van Delden C. (2015). Metabolic pathways of *Pseudomonas aeruginosa* involved in competition with respiratory bacterial pathogens. *Front Microbiol* **6**:321.

Beckman JS, Koppenol WH. (1996). Nitric oxide, superoxide, and peroxynitrite: the good, the bad, and ugly. *Am J Physiol* **271**:C1424–C1437.

Bendinger, B., Rijnaarts, H.H.M., Altendorf, K. and Zehnder AJB. (1993). Physicochemical cell surface and adhesive properties of coryneform bacteria related to the presence and chain length of mycolic acids. *Appl Environ Microbiol* **59**:3973–3977.

Bergström S, Theorell H, Davide H. (1946). On a metabolic product of *P. pyocyanea*. pyolipic acid, active against *M. tuberculosis*. *Ark Kemi Mineral och Geol* **23A**:1–12.

Bertani G. (1951). Studies on lysogenesis I.: The mode of phage liberation by lysogenic *Escherichia coli. J Bacteriol* **62**:293.

Besier S, Smaczny C, von Mallinckrodt C, Krahl A, Ackermann H, Brade V, *et al.* (2007). Prevalence and clinical significance of *Staphylococcus* aureus small-colony variants in cystic fibrosis lung disease. *J Clin Microbiol* **45**:168–172.

Bhaduri S, Demchick PH. (1983). Simple and rapid method for disruption of bacteria for protein studies. *Appl Environ Microbiol* **46**:941–943.

Bigger J. (1944). Treatment Of *Staphylococcal* Infections with penicillin by intermittent sterilisation. *Lancet* **244**:497–500.

Bilton D, Pye A, Johnson MM, Mitchell JL, Dodd M, Webb AK, *et al.* (1995). The isolation and characterization of non-typeable *Haemophilus influenzae* from the sputum of adult cystic fibrosis patients. *Eur Respir J* **8**:948–953.

Birnboim HC. (1983). A rapid alkaline extraction method for the isolation of plasmid DNA. *Methods Enzymol* **100**:243–255.

Bittar F, Richet H, Dubus J-C, Reynaud-Gaubert M, Stremler N, Sarles J, *et al.* (2008). Molecular detection of multiple emerging pathogens in sputa from Cystic Fibrosis patients. *PLoS One* **3**:e2908.

Bittar F, Rolain J. (2010). Detection and accurate identification of new or emerging bacteria in cystic fibrosis patients. *Clin Microbiol Infect* **16**:809–820.

Bjarnsholt T, Jensen PØ, Fiandaca MJ, Pedersen J, Hansen CR, Andersen CB, *et al.* (2009). *Pseudomonas aeruginosa* biofilms in the respiratory tract of cystic fibrosis patients. *Pediatr Pulmonol* **44**:547–558.

Bjarnsholt T, Kirketerp-Møller K, Jensen PØ, Madsen KG, Phipps R, Krogfelt K, *et al.* (2008). Why chronic wounds will not heal: a novel hypothesis. *Wound Repair Regen* **16**:2–10.

Blessing J, Walker J, Maybury B, Yeager AS, Lewiston N. (1979). *Pseudomonas cepacia* and *maltophilia* In The Cystic-Fibrosis Patient. In:*American Review of Respiratory Disease*, Vol. 119, Amer Lung Assoc 1740 Broadway, New York, NY 10019, p. 262.

Bloch KD, Ichinose F, Roberts JD, Zapol WM. (2007). Inhaled NO as a therapeutic agent. *Cardiovasc Res* **75**:339–348.

Bobadilla JL, Macek M, Fine JP, Farrell PM. (2002). Cystic fibrosis: a worldwide analysis of CFTR mutations—correlation with incidence data and application to screening. *Hum Mutat* **19**:575–606.

Böckelmann U, Janke A, Kuhn R, Neu TR, Wecke J, Lawrence JR, *et al.* (2006). Bacterial extracellular DNA forming a defined network-like structure. *FEMS Microbiol Lett* **262**:31–38.

Bogosian G, Bourneuf E V. (2001). A matter of bacterial life and death. *EMBO Rep* **2**:770–774.

Boles BR, Thoendel M, Singh PK. (2004). Self-generated diversity produces 'insurance effects' in biofilm communities. *Proc Natl Acad Sci U S A* **101**:16630–16635.

Bradley SA, Steinert JR. (2015). Characterisation and comparison of temporal release profiles of nitric oxide generating donors. *J Neurosci Methods* **245**:116–24.

Bragonzi A, Farulla I, Paroni M, Twomey KB, Pirone L, Lorè NI, *et al.* (2012a). Modelling co-infection of the cystic fibrosis lung by *Pseudomonas aeruginosa* and *Burkholderia cenocepacia* reveals influences on biofilm formation and host response. *PLoS One* **7**:e52330.

Bragonzi A, Farulla I, Paroni M, Twomey KB, Pirone L, Lorè NI, *et al.* (2012b). Modelling co-infection of the cystic fibrosis lung by *Pseudomonas aeruginosa* and *Burkholderia cenocepacia* reveals influences on biofilm formation and host response. *PLoS One* **7**:e52330.

Brakstad OG, Aasbakk K, Maeland JA. (1992). Detection of *Staphylococcus aureus* by polymerase chain reaction amplification of the nuc gene. *J Clin Microbiol* **30**:1654–1660.

Brown AR, Govan JRW. (2007). Assessment of fluorescent in situ hybridization and PCR-based methods for rapid identification of *Burkholderia cepacia* complex organisms directly from sputum samples. *J Clin Microbiol* **45**:1920–6.

Bucki R, Sostarecz AG, Byfield FJ, Savage PB, Janmey PA. (2007). Resistance of the antibacterial agent ceragenin CSA-13 to inactivation by DNA or F-actin and its activity in cystic fibrosis sputum. *J Antimicrob Chemother* **60**:535–45.

Burmølle M, Thomsen TR, Fazli M, Dige I, Christensen L, Homøe P, *et al.* (2010). Biofilms in chronic infections–a matter of opportunity–monospecies biofilms in multispecies infections. *FEMS Immunol Med Microbiol* **59**:324–336.

Burns JL, Emerson J, Stapp JR, Yim DL, Krzewinski J, Louden L, *et al.* (1998). Microbiology of sputum from patients at cystic fibrosis centers in the United States. *Clin Infect Dis* **27**:158–163.

Burns JL, Rolain J-M. (2014). Culture-based diagnostic microbiology in cystic fibrosis: Can we simplify the complexity? *J Cyst Fibros* **13**:1–9.

Campbell PW, Phillips JA, Heidecker GJ, Krishnamani MRS, Zahorchak R, Stull TL. (1995). Detection of *Pseudomonas* (*Burkholderia*) *cepacia* using PCR. *Pediatr Pulmonol* **20**:44–49.

del Campo R, Morosini M-I, de la Pedrosa EG-G, Fenoll A, Muñoz-Almagro C, Máiz L, *et al.* (2005). Population structure, antimicrobial resistance, and mutation frequencies of *Streptococcus pneumoniae* isolates from cystic fibrosis patients. *J Clin Microbiol* **43**:2207–2214.

Carlsson K, Danielsson P-E, Liljeborg A, Majlöf L, Lenz R, Åslund N. (1985). Three-dimensional microscopy using a confocal laser scanning microscope. *Opt Lett* **10**:53–55.

Carrigg C, Rice O, Kavanagh S, Collins G, O'Flaherty V. (2007). DNA extraction method affects microbial community profiles from soils and sediment. *Appl Microbiol Biotechnol* **77**:955–964.

CFTRScience. (2015). Most common CFTR mutations around the world. http://www.cftrscience.com/?q=epidemiology.

Chapaval L, Moon DH, Gomes JE, Duarte FR, Tsai SM. (2008). An alternative method for *Staphylococcus aureus* DNA isolation. *Arq Bras Med Veterinária e Zootec* **60**:299–306.

Chotirmall SH, Greene CM, McElvaney NG. (2010). *Candida* species in cystic fibrosis: a road less travelled. *Med Mycol* **48**:S114–S124.

Ciofu O, Mandsberg LF, Wang H, Høiby N. (2012). Phenotypes selected during chronic lung infection in cystic fibrosis patients: implications for the treatment of *Pseudomonas aeruginosa* biofilm infections. *FEMS Immunol Med Microbiol* **65**:215–225.

Ciofu O, Riis B, Pressler T, Poulsen HE, Høiby N. (2005). Occurrence of hypermutable *Pseudomonas aeruginosa* in cystic fibrosis patients is associated with the oxidative stress caused by chronic lung inflammation. *Antimicrob Agents Chemother* **49**:2276–2282.

Cole JR, Chai B, Farris RJ, Wang Q, Kulam SA, McGarrell DM, *et al.* (2005). The Ribosomal Database Project (RDP-II): sequences and tools for high-throughput rRNA analysis. *Nucleic Acids Res* **33**:D294–D296.

Cooper CE. (1999). Nitric oxide and iron proteins. *Biochim Biophys Acta (BBA)-Bioenergetics* **1411**:290–309.

Cornelis P, Dingemans J. (2013). *Pseudomonas aeruginosa* adapts its iron uptake strategies in function of the type of infections. *Front Cell Infect Microbiol* **3**:100–106.

Costerton JW, Cheng KJ, Geesey GG, Ladd TI, Nickel JC, Dasgupta M, *et al.* (1987). Bacterial biofilms in nature and disease. *Annu Rev Microbiol* **41**:435–464.

Costerton JW, Geesey GG, Cheng K-J. (1978). How Bacteria Stick. *Sci Am* **238**:86–95.

Costerton JW, Lewandowski Z, DeBeer D, Caldwell D, Korber D, James G. (1994). Biofilms, the customized microniche. *J Bacteriol* **176**:2137.

Cox MJ, Allgaier M, Taylor B, Baek MS, Huang YJ, Daly RA, *et al.* (2010). Airway Microbiota and Pathogen Abundance in Age-Stratified Cystic Fibrosis Patients. *PLoS One* **5**:e11044.

Crane B. (2008). The enzymology of nitric oxide in bacterial pathogenesis and resistance. *Biochem Soc Trans* **36**:1149.

Crossley, J.R., Elliott, R.B. and Smith PA. (1979). Dried-blood spot screening for cystic fibrosis in the newborn. *Lancet* **1**:472–474.

Cruz-López R, Maske H. (2015). A non-amplified FISH protocol to identify simultaneously different bacterial groups attached to eukaryotic phytoplankton. *J Appl Phycol* **27**:797–804.

Cunliffe D, Smart CA, Alexander C, Vulfson EN. (1999). Bacterial adhesion at synthetic surfaces. *Appl Environ Microbiol* **65**:4995–5002.

Cutruzzolà F. (1999). Bacterial nitric oxide synthesis. *Biochim Biophys Acta - Bioenerg* **1411**:231–249.

Daims H, Lücker S, Wagner M. (2006). daime, a novel image analysis program for microbial ecology and biofilm research. *Environ Microbiol* **8**:200–13.

Dalton T, Dowd SE, Wolcott RD, Sun Y, Watters C, Griswold JA, *et al.* (2011). An *in vivo* polymicrobial biofilm wound infection model to study interspecies interactions. *PLoS One* **6**.

Davey ME, Caiazza NC, O'Toole GA. (2003). Rhamnolipid surfactant production affects biofilm architecture in *Pseudomonas aeruginosa* PAO1. *J Bacteriol* **185**:1027–1036.

Davey ME, O'toole GA. (2000). Microbial biofilms: from ecology to molecular genetics. *Microbiol Mol Biol Rev* **64**:847–867.

Davies DG, Parsek MR, Pearson JP, Iglewski BH, Costerton JW, Greenberg EP. (1998). The involvement of cell-to-cell signals in the development of a bacterial biofilm. *Science (80-)* **280**:295–298.

Davies JC. (2007). Cystic fibrosis. *BMJ* **335**:1255–1259.

Davies JC, Bilton D. (2009). Bugs, biofilms, and resistance in cystic fibrosis. *Respir Care* **54**:628–640.

Davis KER, Joseph SJ, Janssen PH. (2005). Effects of growth medium, inoculum size, and incubation time on culturability and isolation of soil bacteria. *Appl Environ Microbiol* **71**:826–834.

Davis SC, Ricotti C, Cazzaniga A, Welsh E, Eaglstein WH, Mertz PM. (2008). Microscopic and physiologic evidence for biofilm-associated wound colonization in vivo. *Wound Repair Regen* **16**:23–9.

Dawson KP, Frossard PM. (2000). The geographic distribution of cystic fibrosis mutations gives clues about population origins. *Eur J Pediatr* **159**:496–499.

Delhaes L, Monchy S, Fréalle E, Hubans C, Salleron J, Leroy S, *et al.* (2012). The airway microbiota in cystic fibrosis: a complex fungal and bacterial community—implications for therapeutic management. *PLoS One* **7**:e36313.

Deligianni E, Pattison S, Berrar D, Ternan NG, Haylock RW, Moore JE, *et al.* (2010). *Pseudomonas aeruginosa* cystic fibrosis isolates of similar RAPD genotype exhibit diversity in biofilm forming ability in vitro. *BMC Microbiol* **10**:38.

DeLong EF, Wickham GS, Pace NR. (1989). Phylogenetic stains: ribosomal RNA-based probes for the identification of single cells. *Science (80-)* **243**:1360–1363.

Denton M, Kerr KG. (1998). Microbiological and clinical aspects of infection associated with *Stenotrophomonas maltophilia. Clin Microbiol Rev* **11**:57–80.

DeSantis TZ, Hugenholtz P, Larsen N, Rojas M, Brodie EL, Keller K, *et al.* (2006). Greengenes, a chimera-checked 16S rRNA gene database and workbench compatible with ARB. *Appl Environ Microbiol* **72**:5069–5072.

Deschaght P, Schelstraete P, Van Simaey L, Vanderkercken M, Raman A, Mahieu L, *et al.* (2013). Is the improvement of CF patients, hospitalized for pulmonary exacerbation, correlated to a decrease in bacterial load? *PLoS One* **8**:e79010.

Dickson, J.S. and Koohmaraie M. (1989). Cell surface charge characteristics and their relationship to bacterial attachment to meat surfaces. *Appl Environ Microbiol* **55**:832–836.

Dige I, Baelum V, Nyvad B, Schlafer S. (2016). Monitoring of extracellular pH in young dental biofilms grown in vivo in the presence and absence of sucrose. *J Oral Microbiol* **8**:30390.

Diggle SP, Cornelis P, Williams P, Cámara M. (2006). 4-quinolone signalling in *Pseudomonas aeruginosa*: old molecules, new perspectives. *Int J Med Microbiol* **296**:83–91.

Sriramulu DD. (2010). Artificial sputum medium. Protocol on webpage: https://protocols.scienceexchange.com/protocols/artificial-sputum-medium.

Dodge JA, Lewis PA, Stanton M, Wilsher J. (2007). Cystic fibrosis mortality and survival in the UK: 1947–2003. *Eur Respir J* **29**:522–526.

Doern G V, Brogden-Torres B. (1992). Optimum use of selective plated media in primary processing of respiratory tract specimens from patients with Cystic Fibrosis. *J Clin Microbiol* **30**:2740–2742.

Doggett RG, Harrison GM, Wallis ES. (1964). Comparison of some properties of *Pseudomonas aeruginosa* Isolated from infections in persons with and without Cystic Fibrosis. *J Bacteriol* **87**:427–431.

Donaldson SH, Bennett WD, Zeman KL, Knowles MR, Tarran R, Boucher RC. (2006). Mucus clearance and lung function in cystic fibrosis with hypertonic saline. *N Engl J Med* **354**:241–250.

Doncaster CP, Davey AJH. (2007). Analysis of variance and covariance: how to choose and construct models for the life sciences. Cambridge University Press.

Donlan RM. (2001). Biofilm formation: a clinically relevant microbiological process. *Clin Infect Dis* **33**:1387–92.

Doroshenko N, Tseng BS, Howlin RP, Deacon J, Wharton JA, Thurner PJ, *et al.* (2014). Extracellular DNA impedes the transport of vancomycin in *Staphylococcus epidermidis* biofilms preexposed to subinhibitory concentrations of vancomycin. *Antimicrob Agents Chemother* **58**:7273–82.

Dörr T, Lewis K, Vulić M. (2009). SOS response induces persistence to fluoroquinolones in *Escherichia coli. PLoS Genet* **5**:e1000760.

Dötsch A, Eckweiler D, Schniederjans M, Zimmermann A, Jensen V, Scharfe M, *et al.* (2012). The *Pseudomonas aeruginosa* transcriptome in planktonic cultures and static biofilms using RNA sequencing. *PLoS One* **7**:e31092.

Dow JM, Crossman L, Findlay K, He Y-Q, Feng J-X, Tang J-L. (2003). Biofilm dispersal in *Xanthomonas campestris* is controlled by cell–cell signaling and is required for full virulence to plants. *Proc Natl Acad Sci* **100**:10995–11000.

Downes KJ, Metlay JP, Bell LM, McGowan KL, Elliott MR, Shah SS. (2008). Polymicrobial bloodstream infections among children and adolescents with central venous catheters evaluated in ambulatory care. *Clin Infect Dis* **46**:387–394.

Doyle J, Doyle JL. (1987). Genomic plant DNA preparation from fresh tissue-CTAB method. *Phytochem Bull* **19**:11–15.

Drapier J-C, Hirling H, Wietzerbin J, Kaldy P, Kühn LC. (1993). Biosynthesis of nitric oxide activates iron regulatory factor in macrophages. *EMBO J* **12**:3643.

Drevinek P, Holden MTG, Ge Z, Jones AM, Ketchell I, Gill RT, *et al.* (2008). Gene expression changes linked to antimicrobial resistance, oxidative stress, iron depletion and retained motility are observed when *Burkholderia cenocepacia* grows in cystic fibrosis sputum. *BMC Infect Dis* **8**:121.

Drew KRP, Sanders LK, Culumber ZW, Zribi O, Wong GCL. (2009). Cationic amphiphiles increase activity of aminoglycoside antibiotic tobramycin in the presence of airway polyelectrolytes. *J Am Chem Soc* **131**:486–493.

Eckburg PB, Bik EM, Bernstein CN, Purdom E, Dethlefsen L, Sargent M, *et al.* (2005). Diversity of the human intestinal microbial flora. *Science (80-)* **308**:1635–1638.

Edwards KJ, Rutenberg AD. (2001). Microbial response to surface microtopography: the role of metabolism in localized mineral dissolution. *Chem Geol* **180**:19–32.

Egland KA, Greenberg EP. (2001). Quorum sensing in *Vibrio fischeri*: analysis of the LuxR DNA binding region by alanine-scanning mutagenesis. *J Bacteriol* **183**:382–386.

Eich RF, Li T, Lemon DD, Doherty DH, Curry SR, Aitken JF, *et al.* (1996). Mechanism of NO-induced oxidation of myoglobin and hemoglobin. *Biochemistry* **35**:6976–6983.

Ellwood D, Keevil CW, Marsh PD, Brown CM, Wardell JN, Le Roux N. (1982). Surface-associated growth. *Philos Trans R Soc London* **297**:517–532.

Ergunay K, Yurdakul P, Sener B, Ozcelik U, Karabulut E, Kiper N. (2008). Comparason of extraction methods for PCR detection of *Burkholderia cepacia* complex (BCC) from cystic fibrosis patients. *Cent Eur J Med* **3**:157–162.

Espinosa-Urgel M. (2003). Resident parking only: rhamnolipids maintain fluid channels in biofilms. *J Bacteriol* **185**:699–700.

Facchetti F, Vermi W, Fiorentini S, Chilosi M, Caruso A, Duse M, *et al.* (1999). Expression of Inducible Nitric Oxide Synthase in Human Granulomas and Histiocytic Reactions. *Am J Pathol* **154**:145–152.

Faden H. (2001). The microbiologic and immunologic basis for recurrent otitis media in children. *Eur J Pediatr* **160**:407–413.

Fanconi G, Uehlinger E, Knauer C. (1936). The coeliac syndrome with congenital cystic pancreatic fibromatosis and bronchiectasis. *Wien Med Wochenschr* **86**:753.

Farrell PM, Rosenstein BJ, White TB, Accurso FJ, Castellani C, Cutting GR, *et al.* (2008). Guidelines for diagnosis of cystic fibrosis in newborns through older adults: Cystic Fibrosis Foundation consensus report. *J Pediatr* **153**:S4–S14.

Farrell PM, Shen G, Splaingard M, Colby CE, Laxova A, Kosorok MR, *et al.* (1997). Acquisition of *Pseudomonas aeruginosa* in Children With Cystic Fibrosis. *Pediatr* **100**:e2–e2.

Farver O, Eady RR, Abraham ZHL, Pecht I. (1998). The intramolecular electron transfer between copper sites of nitrite reductase: a comparison with ascorbate oxidase. *FEBS Lett* **436**:239–242.

Favre-Bonté S, Pache J-C, Robert J, Blanc D, Pechère J-C, van Delden C. (2002). Detection of *Pseudomonas aeruginosa* cell-to-cell signals in lung tissue of Cystic Fibrosis patients. *Microb Pathog* **32**:143–147.

Filkins LM, Graber JA, Olson DG, Dolben EL, Lynd LR, Bhuju S, *et al.* (2015). Coculture of *Staphylococcus aureus* with *Pseudomonas aeruginosa* drives *S. aureus* towards fermentative metabolism and reduced viability in a Cystic Fibrosis model. DiRita, VJ (ed). *J Bacteriol* **197**:2252–2264.

Fleming A. (1929). On the antibacterial action of cultures of a *Penicillium*, with special reference to their use in the isolation of *B. influenzæ. Br J Exp Pathol* **10**:226.

Flemming H-C, Neu TR, Wozniak DJ. (2007). The EPS matrix: the 'house of biofilm cells'. *J Bacteriol* **189**:7945–7947.

Flemming H-C, Wingender J. (2010). The biofilm matrix. *Nat Rev Microbiol* **8**:623–33.

Fletcher M, Loeb GI. (1979). Influence of substratum characteristics on the attachment of a marine Pseudomonad to solid surfaces. *Appl Environ Microbiol* **37**:67–72.

Flores GE, Henley JB, Fierer N. (2012). A Direct PCR Approach to accelerate analyses of human-associated microbial communities. *PLoS One* **7**:e44563.

Fonseca F, Béal C, Corrieu G. (2001). Operating conditions that affect the resistance of lactic acid bacteria to freezing and frozen storage. *Cryobiology* **43**:189–198.

Forrest GN, Mankes K, Jabra-Rizk MA, Weekes E, Johnson JK, Lincalis DP, *et al.* (2006). Peptide nucleic acid fluorescence *in situ* hybridization-based identification of *Candida albicans* and its impact on mortality and antifungal therapy costs. *J Clin Microbiol* **44**:3381–3383.

Förstermann U, Closs EI, Pollock JS, Nakane M, Schwarz P, Gath I, *et al.* (1994). Nitric oxide synthase isozymes. Characterization, purification, molecular cloning, and functions. *Hypertens* **23**:1121–1131.

Förstermann U, Sessa WC. (2012). Nitric oxide synthases: regulation and function. *Eur Heart J* **33**:829–837.

Fox-Robichaud A, Payne D, Hasan SU, Ostrovsky L, Fairhead T, Reinhardt P, *et al.* (1998). Inhaled NO as a viable antiadhesive therapy for ischemia/reperfusion injury of distal microvascular beds. *J Clin Invest* **101**:2497–2505.

Fox S, Wilkinson TS, Wheatley PS, Xiao B, Morris RE, Sutherland A, *et al.* (2010). NO-loaded Zn(2+)-exchanged zeolite materials: a potential bifunctional anti-bacterial strategy. *Acta Biomater* **6**:1515–21.

Friedman A, Blecher K, Sanchez D. (2011). Susceptibility of Gram-positive and-negative bacteria to novel nitric oxide-releasing nanoparticle technology. *Virulence* **2**:217–221.

Frossard PM, Girodon E, Dawson KP, Ghanem N, Plassa F, Lestringant GG, *et al.* (1998). Identification of cystic fibrosis mutations in the United Arab Emirates. *Hum Mutat* **11**:412–413.

Fugère A, Lalonde Séguin D, Mitchell G, Déziel E, Dekimpe V, Cantin AM, *et al.* (2014). Interspecific Small Molecule Interactions between Clinical Isolates of *Pseudomonas aeruginosa* and *Staphylococcus aureus* from Adult Cystic Fibrosis Patients. *PLoS One* **9**:e86705.

Fujita S-I, Senda Y, Nakaguchi S, Hashimoto T. (2001). Multiplex PCR using internal transcribed spacer 1 and 2 regions for rapid detection and identification of yeast strains. *J Clin Microbiol* **39**:3617–3622.

Fung C, Naughton S, Turnbull L, Tingpej P, Rose B, Arthur J, *et al.* (2010). Gene expression of *Pseudomonas aeruginosa* in a mucin-containing synthetic growth medium mimicking cystic fibrosis lung sputum. *J Med Microbiol* **59**:1089–1100.

Fuqua C, Parsek MR, Greenberg EP. (2001). Regulation of gene expression by cell-to-cell communication: acyl-homoserine lactone quorum sensing. *Annu Rev Genet* **35**:439–468.

Furchgott RF, Zawadzki J V. (1980). The obligatory role of endothelial cells in the relaxation of arterial smooth muscle by acetylcholine. *Nature* 373–376.

Gabriel SE, Brigman KN, Koller BH, Boucher RC, Stutts MJ. (1994). Cystic fibrosis heterozygote resistance to cholera toxin in the cystic fibrosis mouse model. *Science (80)* **266**:107–109.

Gall JG, Pardue ML. (1969). Formation and detection of RNA-DNA hybrid molecules in cytological preparations. *Proc Natl Acad Sci U S A* **63**:378–83.

Galperin MY. (2004). Bacterial signal transduction network in a genomic perspective†. *Environ Microbiol* **6**:552–567.

Gammelsrud KW, Sandven P, Høiby EA, Sandvik L, Brandtzaeg P, Gaustad P. (2011). Colonization by Candida in children with cancer, children with cystic fibrosis, and healthy controls. *Clin Microbiol Infect* **17**:1875–1881.

García-Castillo M, Morosini MI, Valverde A, Almaraz F, Baquero F, Cantón R, *et al.* (2007). Differences in biofilm development and antibiotic susceptibility among *Streptococcus pneumoniae* isolates from cystic fibrosis samples and blood cultures. *J Antimicrob Chemother* **59**:301–304.

Gayon V and Dupetit G. (1886). Reduction des nitrates par les infiniments petits. *Mem. Soc. Bordeaux*, Ser. 3,**2**: 201-204.

van der Gast CJ, Walker AW, Stressmann FA, Rogers GB, Scott P, Daniels TW, *et al.* (2011). Partitioning core and satellite taxa from within cystic fibrosis lung bacterial communities. *ISME J* **5**:780–791.

Gerhardt P. (1994). Methods for general and molecular bacteriology. Rev. ed. American Society for Microbiology: Washington, D.C.

Ghaffari A, Jalili R, Ghaffari M, Miller C, Ghahary A. (2007). Efficacy of gaseous nitric oxide in the treatment of skin and soft tissue infections. *Wound Repair Regen* **15**:368–77.

Gião MS, Wilks SA, Azevedo NF, Vieira MJ, Keevil CW. (2009). Validation of SYTO 9/propidium iodide uptake for rapid detection of viable but noncultivable *Legionella pneumophila*. *Microb Ecol* **58**:56–62.

Gibson, L.E. and Cooke RE. (1959). A test for concentration of electrolytes in sweat in cystic fibrosis of the pancreas utilizing pilocarpine by iontophoresis. *Pediatrics* **23**:545–549.

Gibson RL, Burns JL, Ramsey BW. (2003). Pathophysiology and management of pulmonary infections in cystic fibrosis. *Am J Respir Crit Care Med* **168**:918–951.

van der Giessen L. (2009). Does the timing of inhaled dornase alfa matter? *J Cyst Fibros* **8 Suppl 1**:S6-9.

Giovannoni SJ, DeLong EF, Olsen GJ, Pace NR. (1988). Phylogenetic group-specific oligodeoxynucleotide probes for identification of single microbial cells. *J Bacteriol* **170**:720–6.

Girard G, Bloemberg GV. (2008). Central role of quorum sensing in regulating the production of pathogenicity factors in *Pseudomonas aeruginosa*. *Future Microbiol* **3**:97–106.

Gjermansen M, Nilsson M, Yang L, Tolker-Nielsen T. (2010). Characterization of starvation-induced dispersion in *Pseudomonas putida* biofilms: genetic elements and molecular mechanisms. *Mol Microbiol* **75**:815–26.

Goddard AF, Staudinger BJ, Dowd SE, Joshi-Datar A, Wolcott RD, Aitken ML, *et al.* (2012). Direct sampling of cystic fibrosis lungs indicates that DNA-based analyses of upper-airway specimens can misrepresent lung microbiota. *Proc Natl Acad Sci U S A* **109**:13769–74.

Goldstein S, Russo A, Samuni A. (2003). Reactions of PTIO and carboxy-PTIO with NO, NO_2. *J Biol Chem* **278**:50949–50955.

Gomelsky M, Galperin MY. (2013). Bacterial second messengers, cGMP and c-di-GMP, in a quest for regulatory dominance. *EMBO J* **32**:2421–2423.

Gómez-Suárez C, Busscher HJ, van der Mei HC. (2001). Analysis of bacterial detachment from substratum surfaces by the passage of air-liquid interfaces. *Appl Environ Microbiol* **67**:2531–2537.

Gomez M, Alter S, Kumar Mlou, Murphy S, Rathore MH. (1999). Neonatal *Streptococcus pneumoniae* infection: case reports and review of the literature. *Pediatr Infect Dis J* **18**:1014–1018.

Goretski J, Zafiriou OC, Hollocher TC. (1990). Steady-state nitric oxide concentrations during denitrification. *J Biol Chem* **265**:11535–8.

Goss CH, Muhlebach MS. (2011). Review: *Staphylococcus aureus* and MRSA in cystic fibrosis. *J Cyst Fibros* **10**:298–306.

Greenwood D, Slack RCB, Peutherer JF, Barer MR. (1997). Medical Microbiology: A guide to microbial infections: pathogenesis. *Immunity, Lab Diagnosis Control 15th Ed Churchill Livingstne, Edinburgh, United Kingdom* 690.

Greisen K, Loeffelholz M, Purohit A, Leong D. (1994). PCR primers and probes for the 16S rRNA gene of most species of pathogenic bacteria, including bacteria found in cerebrospinal fluid. *J Clin Microbiol* **32**:335–351.

Grigg JC, Ukpabi G, Gaudin CFM, Murphy MEP. (2010). Structural biology of heme binding in the *Staphylococcus aureus* Isd system. *J Inorg Biochem* **104**:341–348.

Gruetter CA, Barry BK, McNamara DB, Gruetter DY, Kadowitz PJ, Ignarro L. (1978). Relaxation of bovine coronary artery and activation of coronary arterial guanylate cyclase by nitric oxide, nitroprusside and a carcinogenic nitrosoamine. *J Cyclic Nucleotide Res* **5**:211–224.

Gunther NW, Nuñez A, Fett W, Solaiman DKY. (2005). Production of Rhamnolipids by *Pseudomonas chlororaphis*, a nonpathogenic bacterium. *Appl Environ Microbiol* **71**:2288–2293.

Guss AM, Roeselers G, Newton ILG, Young CR, Klepac-Ceraj V, Lory S, *et al.* (2011). Phylogenetic and metabolic diversity of bacteria associated with cystic fibrosis. *ISME J* **5**:20–29.

Gutierrez M, Choi MH, Tian B, Xu J, Rho JK, Kim MO, *et al.* (2013). Simultaneous inhibition of rhamnolipid and polyhydroxyalkanoic acid synthesis and biofilm formation in *Pseudomonas aeruginosa* by 2-bromoalkanoic acids: effect of inhibitor alkyl-chain-length. *PLoS One* **8**:e73986.

Haase G, Skopnik H, Groten T, Kusenbach G, Posselt HG. (1991). Long-term fungal cultures from sputum of patients with cystic fibrosis. *Mycoses* **34**:373–376.

Hall-Stoodley L, Stoodley P. (2009). Evolving concepts in biofilm infections. *Cell Microbiol* **11**:1034–43.

Hammond JH, Dolben EF, Smith TJ, Bhuju S, Hogan DA. (2015). Links between Anr and Quorum Sensing in *Pseudomonas aeruginosa* Biofilms. *J Bacteriol* **197**:2810–20.

Han G, Martinez LR, Mihu MR, Friedman AJ, Friedman JM, Nosanchuk JD. (2009a). Nitric oxide releasing nanoparticles are therapeutic for *Staphylococcus aureus* abscesses in a murine model of infection. *PLoS One* **4**:e7804.

Han G, Martinez LR, Mihu MR, Friedman AJ, Friedman JM, Nosanchuk JD. (2009b). Nitric oxide releasing nanoparticles are therapeutic for *Staphylococcus aureus* abscesses in a murine model of infection. *PLoS One* **4**:e7804.

Hancock REW, Speert DP. (2000). Antibiotic resistance in *Pseudomonas aeruginosa*: mechanisms and impact on treatment. *Drug Resist Updat* **3**:247–255.

Handelsman J. (2004). Metagenomics: application of genomics to uncultured microorganisms. *Microbiol Mol Biol Rev* **68**:669–685.

Harris JK, De Groote MA, Sagel SD, Zemanick ET, Kapsner R, Penvari C, *et al.* (2007). Molecular identification of bacteria in bronchoalveolar lavage fluid from children with cystic fibrosis. *Proc Natl Acad Sci* **104**:20529–20533.

Haseloff RF, Zöllner S, Kirilyuk IA, Grigor'ev IA, Reszka R, Bernhardt R, *et al.* (1997). Superoxide-mediated reduction of the nitroxide group can prevent detection of nitric oxide by nitronyl nitroxides. *Free Radic Res* **26**:7–17.

Hasman H, Chakraborty T, Klemm P. (1999). Antigen-43-Mediated Autoaggregation of *Escherichia coli* Is blocked by fimbriation. *J Bacteriol* **181**:4834–4841.

Hataishi R, Rodrigues AC, Neilan TG, Morgan JG, Buys E, Shiva S, *et al.* (2006). Inhaled nitric oxide decreases infarction size and improves left ventricular function in a murine model of myocardial ischemia-reperfusion injury. *Am J Physiol - Hear Circ Physiol* **291**:H379–H384.

Hauser PM, Bernard T, Greub G, Jaton K, Pagni M, Hafen GM. (2014). Microbiota present in cystic fibrosis lungs as revealed by whole genome sequencing. *PLoS One* **9**:e90934.

He X, Ahn J. (2011). Differential gene expression in planktonic and biofilm cells of multiple antibiotic-resistant *Salmonella typhimurium* and *Staphylococcus aureus*. *FEMS Microbiol Lett* **325**:180–188.

Heeb S, Fletcher MP, Chhabra SR, Diggle SP, Williams P, Cámara M. (2011). Quinolones: from antibiotics to autoinducers. *FEMS Microbiol Rev* **35**:247–74.

Hengge R. (2009). Principles of c-di-GMP signalling in bacteria. *Nat Rev Micro* **7**:263–273.

Henry RL, Mellis CM, Petrovic L. (1992). Mucoid *Pseudomonas aeruginosa* is a marker of poor survival in cystic fibrosis. *Pediatr Pulmonol* **12**:158–161.

Hermansson M. (1999). The DLVO theory in microbial adhesion. *Collids Surfaces B Biointerfaces* **14**:105–119.

Hetrick EM, Shin JH, Paul HS, Schoenfisch MH. (2009). Anti-biofilm efficacy of nitric oxide-releasing silica nanoparticles. *Biomaterials* **30**:2782–9.

Heydorn A, Nielsen AT, Hentzer M, Sternberg C, Givskov M, Ersbøll BK, *et al.* (2000). Quantification of biofilm structures by the novel computer program COMSTAT. *Microbiology* **146**:2395–2407.

Hibbs JB, Taintor RR, Vavrin Z. (1987). Macrophage cytotoxicity: role for L-arginine deiminase and imino nitrogen oxidation to nitrite. *Science (80-)* **235**:473–476.

Hibbs JB, Taintor RR, Vavrin Z, Rachlin EM. (1988). Nitric oxide: a cytotoxic activated macrophage effector molecule. *Biochem Biophys Res Commun* **157**:87–94.

Hill D, Rose B, Pajkos A, Robinson M, Bye P, Bell S, *et al.* (2005). Antibiotic susceptibilities of *Pseudomonas aeruginosa* isolates derived from patients with cystic fibrosis under aerobic, anaerobic, and biofilm conditions. *J Clin Microbiol* **43**:5085–5090.

Hiller NL, Ahmed A, Powell E, Martin DP, Eutsey R, Earl J, *et al.* (2010). Generation of genic diversity among *Streptococcus pneumoniae* strains via horizontal gene transfer during a chronic polyclonal pediatric infection. *PLoS Pathog* **6**:e1001108.

Hoffman LR, Deziel E, D'Argenio DA, Lepine F, Emerson J, McNamara S, *et al.* (2006). Selection for *Staphylococcus aureus* small-colony variants due to growth in the presence of *Pseudomonas aeruginosa*. *Proc Natl Acad Sci* **103**:19890–19895.

Hoffman LR, Kulasekara HD, Emerson J, Houston LS, Burns JL, Ramsey BW, *et al.* (2009). *Pseudomonas aeruginosa* lasR mutants are associated with cystic fibrosis lung disease progression. *J Cyst Fibros* **8**:66–70.

Hogardt M, Trebesius K, Geiger AM, Hornef M, Rosenecker J, Heesemann J. (2000). Specific and Rapid Detection by Fluorescent In Situ Hybridization of Bacteria in Clinical Samples Obtained from Cystic Fibrosis Patients. *J Clin Microbiol* **38**:818–825.

Hogardt M, Trebesius K, Geiger AM, Hornef M, Rosenecker J, Heesemann J. (2000). Specific and rapid detection by fluorescent in situ hybridization of bacteria in clinical samples obtained from cystic fibrosis patients. *J Clin Microbiol* **38**:818–25.

Høiby N. (2011). Recent advances in the treatment of *Pseudomonas aeruginosa* infections in cystic fibrosis. *BMC Med* **9**:32.

Høiby N. (1982). Microbiology of lung infections in cystic fibrosis patients. *Acta Paediatr* **71**:33–54.

Høiby N, Ciofu O, Bjarnsholt T. (2010a). *Pseudomonas aeruginosa* biofilms in cystic fibrosis. *Future Microbiol* **5**:1663–1674.

Holden MTG, Seth-Smith HMB, Crossman LC, Sebaihia M, Bentley SD, Cerdeño-Tárraga AM, *et al.* (2009). The genome of *Burkholderia cenocepacia* J2315, an epidemic pathogen of cystic fibrosis patients. *J Bacteriol* **191**:261–277.

Holland LM, O'donnell ST, Ryjenkov DA, Gomelsky L, Slater SR, Fey PD, *et al.* (2008). A staphylococcal GGDEF domain protein regulates biofilm formation independently of cyclic dimeric GMP. *J Bacteriol* **190**:5178–5189.

Howlin R, Cathie K, Sukhtankar P, Duignan C, Pink S, Smith C, *et al.* (2017). Low dose nitric oxide as adjunctive therapy to treat chronic *Pseudomonas aeruginosa* infection in cystic fibrosis. *Mol Ther* (accepted).

Hsu JT, Chen CY, Young CW, Chao WL, Li MH, Liu YH, *et al.* (2014). Prevalence of sulfonamide-resistant bacteria, resistance genes and integron-associated horizontal gene transfer in natural water bodies and soils adjacent to a swine feedlot in northern Taiwan. *J Hazard Mater* **277**:34–43.

Hunter RC, Asfour F, Dingemans J, Osuna BL, Samad T, Malfroot A, *et al.* (2013). Ferrous Iron Is a Significant Component of Bioavailable Iron in Cystic Fibrosis Airways. *MBio* **4**:e00557-13-e00557-13.

Hutchins DA, Witter AE, Butler A, Luther GW. (1999). Competition among marine phytoplankton for different chelated iron species. *Nature* **400**:858–861.

Ichinose F, Roberts JD, Zapol WM. (2004). Inhaled nitric oxide: a selective pulmonary vasodilator: current uses and therapeutic potential. *Circulation* **109**:3106–3111.

Ignarro LJ. (2000). Nitric Oxide: Biology and Pathobiology. Academic Press https://books.google.com/books?id=h5FugARr4bgC&pgis=1 (Accessed April 30, 2016).

Ignarro LJ, Buga GM, Wood KS, Byrns RE, Chaudhuri G. (1987). Endothelium-derived relaxing factor produced and released from artery and vein is nitric oxide. *Proc Natl Acad Sci* **84**:9265–9269.

Ikeda S, Schweiss JF, Frank PA, Homan SM, Miller RD. (1987). In Vitro Cyanide Release from Sodium Nitroprusside. *J Am Soc Anesthesiol* **66**:381–385.

Institute C and LS. (2006). Methods for dilution antimicrobial susceptibility test for bacteria that grow aerobically; approved standard. 7th ed. Wayne, PA.

Iyer L, Anantharaman V, Aravind L. (2003). Ancient conserved domains shared by animal soluble guanylyl cyclases and bacterial signaling proteins. *BMC Genomics* **4**:5.

James G, Korber D, Caldwell D, Costerton J. (1995). Digital image analysis of growth and starvation responses of a surface- colonizing *Acinetobacter* sp. *J Bacteriol* **177**:907–915.

Janda JM, Abbott SL. (2007). 16S rRNA gene sequencing for bacterial identification in the diagnostic laboratory: pluses, perils, and pitfalls. *J Clin Microbiol* **45**:2761–2764.

Jarvis FG, Johnson MJ. (1949). A Glyco-lipide Produced by *Pseudomonas aeruginosa*. *J Am Chem Soc* **71**:4124–4126.

Jenal U. (2004). Cyclic di-guanosine-monophosphate comes of age: a novel secondary messenger involved in modulating cell surface structures in bacteria? *Curr Opin Microbiol* **7**:185–191.

Jennison MW. (1937). The relations between plate counts and direct microscopic counts of Escherichia coli during the logarithmic growth period. *J Bacteriol* **33**:461.

Jensen PØ, Bjarnsholt T, Phipps R, Rasmussen TB, Calum H, Christoffersen L, *et al.* (2007). Rapid necrotic killing of polymorphonuclear leukocytes is caused by quorum-sensing-controlled production of rhamnolipid by *Pseudomonas aeruginosa*. *Microbiology* **153**:1329–1338.

Jermy A. (2013). Bacterial physiology: no rest for the persisters. *Nat Rev Microbiol* **11**:148.

Jesaitis AJ, Franklin MJ, Berglund D, Sasaki M, Lord CI, Bleazard JB, *et al.* (2003). Compromised host defense on *Pseudomonas aeruginosa* biofilms: Characterization of neutrophil and biofilm interactions . *J Immunol* **171**:4329–4339.

Johansen HK. (1996). Potential of preventing *Pseudomonas aeruginosa* lung infections in cystic fibrosis patients: experimental studies in animals. *Apmis* **104**:5–42.

John. H.A., Birnstiel, M.L. and Jones KW. (1969). RNA-DNA hybrids at the cytological level. *Nature* **223**:582–587.

Jones ML, Ganopolsky JG, Labbé A, Prakash S. (2010). A novel nitric oxide producing probiotic patch and its antimicrobial efficacy: preparation and in vitro analysis. *Appl Microbiol Biotechnol* **87**:509–16.

Joyce E, Phull SS, Lorimer JP, Mason TJ. (2003). The development and evaluation of ultrasound for the treatment of bacterial suspensions. A study of frequency, power and sonication time on cultured *Bacillus* species. *Ultrason Sonochem* **10**:315–8.

Jurcisek JA, Bakaletz LO. (2007). Biofilms formed by nontypeable *Haemophilus influenzae* in vivo contain both double-stranded DNA and type IV pilin protein. *J Bacteriol* **189**:3868–75.

Kadurugamuwa JL, Beveridge TJ. (1995). Virulence factors are released from *Pseudomonas aeruginosa* in association with membrane vesicles during normal growth and exposure to gentamicin: a novel mechanism of enzyme secretion. *J Bacteriol* **177**:3998–4008.

Kaeberlein T, Lewis K, Epstein SS. (2002). Isolating 'Uncultivable' Microorganisms in Pure Culture in a Simulated Natural Environment. *Sci* **296**:1127–1129.

Kahl B, Herrmann M, Everding AS, Koch HG, Becker K, Harms E, *et al.* (1998). Persistent infection with small colony variant strains of *Staphylococcus aureus* in patients with cystic fibrosis. *J Infect Dis* **177**:1023–1029.

Karpati F, Jonasson J. (1996). Polymerase chain reaction for the detection of *Pseudomonas aeruginosa*, *Stenotrophomonas maltophilia* and *Burkholderia cepacia* in sputum of patients with cystic fibrosis. *Mol Cell Probes* **10**:397–403.

Keevil, Charles W; Dowsett, A.B. and Rogers J. (1993). Legionella biofilms and their control. In:*Society for Applied Bacteriology Technical Series, Microbial Biofilms*, pp. 201–215.

Keevil CW. (2001). Continuous culture models to study pathogens in biofilms. *Methods Enzymol Microb Growth Biofilms Part B* 104–122.

Keevil CW. (2003). Rapid detection of biofilms and adherent pathogens using scanning confocal laser microscopy and episcopic differential interference contrast microscopy. *Water Sci Technol* **47**:105–116.

Kerem B, Rommens JM, Buchanan JA, Markiewicz D, Cox TK, Chakravarti A, *et al.* (1989). Identification of the cystic fibrosis gene: genetic analysis. *Science (80-)* **245**:1073–1080.

Keren I, Shah D, Spoering A, Kaldalu N, Lewis K. (2004). Specialized persister cells and the mechanism of multidrug tolerance in *Escherichia coli*. *J Bacteriol* **186**:8172–80.

Kharazmi A, Döring G, Høiby N, Valerius NH. (1984). Interaction of *Pseudomonas aeruginosa* alkaline protease and elastase with human polymorphonuclear leukocytes in vitro. *Infect Immun* **43**:161–165.

Kilbourn JP, Campbell RA, Grach JL, Willis MD. (1968). Quantitative bacteriology of sputum. *Am Rev Respir Dis* **98**:810.

Kindaichi T, Tsushima I, Ogasawara Y, Shimokawa M, Ozaki N, Satoh H, *et al.* (2007). In situ activity and spatial organization of anaerobic ammonium-oxidizing (anammox) bacteria in biofilms. *Appl Environ Microbiol* **73**:4931–9.

Kirov SM, Webb JS, O'May CY, Reid DW, Woo JKK, Rice SA, *et al.* (2007). Biofilm differentiation and dispersal in mucoid *Pseudomonas aeruginosa* isolates from patients with cystic fibrosis. *Microbiol* **153**:3264–3274.

Kjærgaard K, Schembri MA, Ramos C, Molin S, Klemm P. (2000). Antigen 43 facilitates formation of multispecies biofilms. *Environ Microbiol* **2**:695–702.

Kleerebezem M, Quadri LEN, Kuipers OP, De Vos WM. (1997). Quorum sensing by peptide pheromones and two-component signal-transduction systems in Gram-positive bacteria. *Mol Microbiol* **24**:895–904.

Kline KA, Fälker S, Dahlberg S, Normark S, Henriques-Normark B. (2009). Bacterial adhesins in host-microbe interactions. *Cell Host Microbe* **5**:580–592.

Kloosterboer M, Hoffman G, Rock M, Gershan W, Laxova A, Li Z, *et al.* (2009). Clarification of laboratory and clinical variables that influence Cystic Fibrosis newborn screening with initial analysis of immunoreactive trypsinogen. *Pediatr* **123**:e338–e346.

Kluyver A.J. and Donker H.J.L. (1926). Die Einheit in der Biochemie. *Chem. Zelle Geweke* **13**: 134-190.

Knowles MR, Boucher RC. (2002). Mucus clearance as a primary innate defense mechanism for mammalian airways. *J Clin Invest* **109**:571–577.

Kobayashi H, Oethinger M, Tuohy MJ, Procop GW, Bauer TW. (2009). Improved detection of biofilm-formative bacteria by vortexing and sonication: a pilot study. *Clin Orthop Relat Res* **467**:1360–4.

Kohanski MA, Dwyer DJ, Collins JJ. (2010). How antibiotics kill bacteria: from targets to networks. *Nat Rev Microbiol* **8**:423–35.

Koshland DE. (1992). The molecule of the year. *Sci* **258**:1861.

Kozioł-Montewka M, Szczepanik A, Baranowicz I, Jóźwiak L, Książek A, Kaczor D. (2006). The investigation of *Staphylococcus aureus* and coagulase-negative staphylococci nasal carriage among patients undergoing haemodialysis. *Microbiol Res* **161**:281–287.

Krsek M, Wellington EMH. (1999). Comparison of different methods for the isolation and purification of total community DNA from soil. *J Microbiol Methods* **39**:1–16.

Lakatošová M, Holečková B. (2007). Fluorescence in situ hybridisation. *Biologia (Bratisl)* **62**:243–250.

Lam J, Chan R, Lam K, Costerton JW. (1980). Production of mucoid microcolonies by *Pseudomonas aeruginosa* within infected lungs in cystic fibrosis. *Infect Immun* **28**:546–556.

Lamont RJ, Jenkinson HF. (2000). Adhesion as an ecological determinant in the oral cavity. *Oral Bact Ecol Mol basis* 131–168.

Lansford R, Bearman G, Fraser SE. (2001). Resolution of multiple green fluorescent protein color variants and dyes using two-photon microscopy and imaging spectroscopy. *J Biomed Opt* **6**:311–318.

Laraya-Cuasay, L.R., Cundy, K.R. and Huang NN. (1976). *Pseudomonas* carrier rates of patients with cystic fibrosis and of members of their families. *J Pediatr* **89**:23–26.

Latifi A, Winson MK, Foglino M, Bycroft BW, Stewart GSAB, Lazdunski A, *et al.* (1995). Multiple homologues of LuxR and LuxI control expression of virulence determinants and secondary metabolites through quorum sensing in *Pseudomonas aeruginosa* PAO1. *Mol Microbiol* **17**:333–343.

Lau GW, Hassett DJ, Ran H, Kong F. (2004). The role of pyocyanin in *Pseudomonas aeruginosa* infection. *Trends Mol Med* **10**:599–606.

Lee B, Haagensen JAJ, Ciofu O, Andersen JB, Høiby N, Molin S. (2005). Heterogeneity of biofilms formed by nonmucoid *Pseudomonas aeruginosa* isolates from patients with cystic fibrosis. *J Clin Microbiol* **43**:5247–5255.

Lee HS, Gu F, Ching SM, Lam Y, Chua KL. (2010). CdpA is a *Burkholderia pseudomallei* cyclic di-GMP phosphodiesterase involved in autoaggregation, flagellum synthesis, motility, biofilm formation, cell invasion, and cytotoxicity. *Infect Immun* **78**:1832–40.

Lee SF, Li YH, Bowden GH. (1996). Detachment of *Streptococcus mutans* biofilm cells by an endogenous enzymatic activity. *Infect Immun* **64**:1035–1038.

Leff LG, Dana JR, McArthur J V, Shimkets LJ. (1995). Comparison of methods of DNA extraction from stream sediments. *Appl Environ Microbiol* **61**:1141–1143.

LeGrys VA. (1996). Sweat testing for the diagnosis of cystic fibrosis: practical considerations. *J Pediatr* **129**:892–897.

Lewis K. (2010). Persister cells. *Annu Rev Microbiol* **64**:357–72.

Li Y, Heine S, Entian M, Sauer K, Frankenberg-Dinkel N. (2013). NO-induced biofilm dispersion in *Pseudomonas aeruginosa* is mediated by an MHYT domain-coupled phosphodiesterase. *J Bacteriol* **195**:3531–42.

LiPuma JJ. (2010). The changing microbial epidemiology in cystic fibrosis. *Clin Microbiol Rev* **23**:299–323.

LiPuma JJ, Mortensen JE, Dasen SE, Edlind TD, Schidlow D V, Burns JL, *et al.* (1988). Ribotype analysis of *Pseudomonas cepacia* from cystic fibrosis treatment centers. *J Pediatr* **113**:859–862.

Liu W-T, Marsh TL, Cheng H, Forney LJ. (1997). Characterization of microbial diversity by determining terminal restriction fragment length polymorphisms of genes encoding 16S rRNA. *Appl Environ Microbiol* **63**:4516–4522.

Liu X, Miller MJS, Joshi MS, Thomas DD, Lancaster JR. (1998). Accelerated reaction of nitric oxide with O2 within the hydrophobic interior of biological membranes. *Proc Natl Acad Sci* **95**:2175–2179.

Loo CY, Mitrakul K, Voss IB, Hughes C V, Ganeshkumar N. (2003). Involvement of an inducible fructose phosphotransferase operon in *Streptococcus gordonii* biofilm formation. *J Bacteriol* **185**:6241–6254.

Van Loosdrecht MC, Lyklema J, Norde W, Zehnder AJ. (1990). Influence of interfaces on microbial activity. *Microbiol Rev* **54**:75–87.

Lopes SP, Azevedo NF, Pereira MO. (2014a). Emergent bacteria in Cystic Fibrosis: In vitro biofilm formation and resilience under variable oxygen conditions. *Biomed Res Int* **2014**.

Lopes SP, Azevedo NF, Pereira MO. (2014b). Microbiome in cystic fibrosis: shaping polymicrobial interactions for advances in antibiotic therapy. *Crit Rev Microbiol* 1–13.

Lopes SP, Ceri H, Azevedo NF, Pereira MO. (2012). Antibiotic resistance of mixed biofilms in cystic fibrosis: impact of emerging microorganisms on treatment of infection. *Int J Antimicrob Agents* **40**:260–263.

Lowenstein CJ, Padalko E. (2004). iNOS (NOS2) at a glance. *J Cell Sci* **117**:2865–2867.

Lynch MJ, Swift S, Kirke DF, Keevil CW, Dodd CER, Williams P. (2002). The regulation of biofilm development by quorum sensing in *Aeromonas hydrophila*. *Environ Microbiol* **4**:18–28.

Lynch S V, Bruce KD. (2013). The cystic fibrosis airway microbiome. *Cold Spring Harb Perspect Med* **3**:a009738.

Ma L, Jackson KD, Landry RM, Parsek MR, Wozniak DJ. (2006). Analysis of *Pseudomonas aeruginosa* conditional Psl variants reveals roles for the Psl polysaccharide in adhesion and maintaining biofilm structure postattachment. *J Bacteriol* **188**:8213–8221.

MacFaddin JF. (2000). Biochemical tests for identification of medical bacteria Third ed. *Philadelphia, Balt Meryl Lippincott Williams &Wilkins* 225–228.

Machan ZA, Pitt TL, White W, Watson D, Taylor GW, Cole PJ, *et al.* (1991). Interaction between *Pseudomonas aeruginosa* and *Staphylococcus aureus*: description of an antistaphylococcal substance. *J Med Microbiol* **34**:213–217.

Maeda Y, Elborn JS, Parkins MD, Reihill J, Goldsmith CE, Coulter WA, *et al.* (2011). Population structure and characterization of viridans group streptococci (VGS) including *Streptococcus pneumoniae* isolated from adult patients with cystic fibrosis (CF). *J Cyst Fibros* **10**:133–139.

Mahenthiralingam E, Coenye T, Chung JW, Speert DP, Govan JRW, Taylor P, *et al.* (2000). Diagnostically and experimentally useful panel of strains from the *Burkholderia cepacia* complex. *J Clin Microbiol* **38**:910–913.

Mannick EE, Bravo LE, Zarama G, Realpe JL, Zhang X-J, Ruiz B, *et al.* (1996). Inducible Nitric Oxide Synthase, Nitrotyrosine, and Apoptosis in *Helicobacter pylori* Gastritis: Effect of Antibiotics and Antioxidants. *Cancer Res* **56**:3238–3243.

Marshall, K.C., Stout, R. and Mitchell R. (1971). Mechanisms of the initial events in the sorption of marine bacteria to surfaces. *J Gen Microbiol* **68**:337–48.

Martinez LR, Han G, Chacko M, Mihu MR, Jacobson M, Gialanella P, *et al.* (2009). Antimicrobial and healing efficacy of sustained release nitric oxide nanoparticles against *Staphylococcus aureus* skin infection. *J Invest Dermatol* **129**:2463–9.

Mashburn LM, Jett AM, Akins DR, Whiteley M. (2005). *Staphylococcus aureus* serves as an iron source for *Pseudomonas aeruginosa* during in vivo coculture. *J Bacteriol* **187**:554–66.

Matar GM, Sidani N, Fayad M, Hadi U. (1998). Two-step PCR-based assay for identification of bacterial etiology of otitis media with effusion in infected Lebanese children. *J Clin Microbiol* **36**:1185–1188.

Matsui H, Grubb BR, Tarran R, Randell SH, Gatzy JT, Davis CW, *et al.* (1998). Evidence for periciliary liquid layer depletion, not abnormal ion composition, in the pathogenesis of cystic fibrosis airways disease. *Cell* **95**:1005–1015.

May JR. (1953). The bacteriology of chronic bronchitis. *Lancet* **265**:534–537.

May JR, Herrick NC, Thompson D. (1972). Bacterial infection in cystic fibrosis. *Arch Dis Child* **47**:908–913.

McDougald D, Rice SA, Barraud N, Steinberg PD, Kjelleberg S. (2012). Should we stay or should we go: mechanisms and ecological consequences for biofilm dispersal. *Nat Rev Microbiol* **10**:39–50.

McKnight SL, Iglewski BH, Pesci EC. (2000). The *Pseudomonas* quinolone signal regulates rhl quorum sensing in *Pseudomonas aeruginosa*. *J Bacteriol* **182**:2702–2708.

Van der Mei HC, Bos R, Busscher HJ. (1998). A reference guide to microbial cell surface hydrophobicity based on contact angles. *Colloids surfaces B Biointerfaces* **11**:213–221.

van der Mei HC, Cowan MM, Busscher HJ. (1991). Physicochemical and structural studies on *Acinetobacter calcoaceticus* RAG-1 and MR-481—Two standard strains in hydrophobicity tests. *Curr Microbiol* **23**:337–341.

Merino S, Gavín R, Altarriba M, Izquierdo L, Maguire ME, Tomás JM. (2001). The MgtE Mg2+ transport protein is involved in *Aeromonas hydrophila* adherence. *FEMS Microbiol Lett* **198**:189–195.

Merod RT, Warren JE, McCaslin H, Wuertz S. (2007). Toward automated analysis of biofilm architecture: bias caused by extraneous confocal laser scanning microscopy images. *Appl Environ Microbiol* **73**:4922–4930.

Metcalf D, Bowler P. (2013). Biofilm delays wound healing: A review of the evidence. *Burn Trauma* **1**:5–12.

Michelsen CF, Christensen A-MJ, Bojer MS, Høiby N, Ingmer H, Jelsbak L. (2014). *Staphylococcus aureus* alters growth activity, autolysis, and antibiotic tolerance in a human host-adapted *Pseudomonas aeruginosa* lineage. *J Bacteriol* **196**:3903–11.

Migiyama Y, Kaneko Y, Yanagihara K, Morohoshi T, Morinaga Y, Nakamura S, *et al.* (2013). Efficacy of AiiM, an N-acylhomoserine lactonase, against *Pseudomonas aeruginosa* in a mouse model of acute pneumonia. *Antimicrob Agents Chemother* **57**:3653–3658.

Miller MB, Bassler BL. (2001). Quorum sensing in bacteria. *Annu Rev Microbiol* **55**:165–199.

Mitik-Dineva N, Wang J, Truong VK, Stoddart P, Malherbe F, Crawford RJ, *et al.* (2009). *Escherichia coli*, *Pseudomonas aeruginosa*, and *Staphylococcus aureus* attachment patterns on glass surfaces with nanoscale roughness. *Curr Microbiol* **58**:268–273.

Miyata, M., Matsubara, T. and Mori T. (1969). Studies on denitrification: XI. some properties of nitric oxide reductase. *J Biochem* **66**:759–765.

Moffett KS. (2010). *Pseudomonas aeruginosa* in Patients with Cystic Fibrosis. *Antimicrob Ther* **1**:1.

Molina-Cabrillana J, Santana-Reyes C, Gonzalez-Garcia A, Bordes-Benítez A, Horcajada I. (2007). Outbreak of *Achromobacter xylosoxidan*s pseudobacteremia in a neonatal care unit related to contaminated chlorhexidine solution. *Eur J Clin Microbiol Infect Dis* **26**:435–437.

Molina A, Del Campo R, Máiz L, Morosini M-I, Lamas A, Baquero F, *et al.* (2008). High prevalence in cystic fibrosis patients of multiresistant hospital-acquired methicillin-resistant *Staphylococcus aureus* ST228-SCCmecI capable of biofilm formation. *J Antimicrob Chemother* **62**:961–967.

Möller L V, Ruijs GJ, Heijerman HG, Dankert J, van Alphen L. (1992). *Haemophilus influenzae* is frequently detected with monoclonal antibody 8BD9 in sputum samples from patients with cystic fibrosis. *J Clin Microbiol* **30**:2495–2497.

Möller LVM, Regelink AG, Grasselier H, Dankert-Roelse JE, Dankert J, van Alphen L. (1995). Multiple Haemophilus influenzae strains and strain variants coexist in the respiratory tract of patients with cystic fibrosis. *J Infect Dis* **172**:1388–1392.

Momozawa Y, Deffontaine V, Louis E, Medrano JF. (2011). Characterization of bacteria in biopsies of colon and stools by high throughput sequencing of the v2 region of bacterial 16s rrna gene in human. Falciani, F (ed). *PLoS One* **6**:e16952.

Monds RD, Silby MW, Mahanty HK. (2001). Expression of the Pho regulon negatively regulates biofilm formation by *Pseudomonas aureofaciens* PA147-2. *Mol Microbiol* **42**:415–426.

Moore JE, Xu J, Millar BC, Crowe M, Elborn JS. (2002). Improved molecular detection of *Burkholderia cepacia* genomovar III and *Burkholderia multivorans* directly from sputum of patients with cystic fibrosis. *J Microbiol Methods* **49**:183–191.

Moore LR, Coe A, Zinser ER, Saito MA, Sullivan MB, Lindell D, *et al.* (2007). Culturing the marine cyanobacterium *Prochlorococcus. Limnol Oceanogr Methods* **5**:353-362.

Morello E, Saussereau E, Maura D, Huerre M, Touqui L, Debarbieux L. (2011). Pulmonary bacteriophage therapy on *Pseudomonas aeruginosa* cystic fibrosis strains: first steps towards treatment and prevention. *PLoS One* **6**:e16963.

Morral N, Bertranpetit J, Estivill X, Nunes V, Casals T, Gimenez J, *et al.* (1994). The origin of the major cystic fibrosis mutation (ΔF508) in European populations. *Nat Genet* **7**:169-175.

Moskowitz SM, Foster JM, Emerson JC, Gibson RL, Burns JL. (2005). Use of *Pseudomonas* biofilm susceptibilities to assign simulated antibiotic regimens for cystic fibrosis airway infection. *J Antimicrob Chemother* **56**:879-886.

Moss RB. (2002). Allergic bronchopulmonary aspergillosis. *Clin Rev Allergy Immunol* **23**:87-104.

Mulcahy H, Charron-Mazenod L, Lewenza S. (2008). Extracellular DNA chelates cations and induces antibiotic resistance in *Pseudomonas aeruginosa* biofilms. *PLoS Pathog* **4**:e1000213.

Mulcahy LR, Burns JL, Lory S, Lewis K. (2010). Emergence of *Pseudomonas aeruginosa* strains producing high levels of persister cells in patients with cystic fibrosis. *J Bacteriol* **192**:6191-9.

Murakami K, Minamide W, Wada K, Nakamura E, Teraoka H, Watanabe S. (1991). Identification of methicillin-resistant strains of staphylococci by polymerase chain reaction. *J Clin Microbiol* **29**:2240-2244.

Muthig M, Hebestreit A, Ziegler U, Seidler M, Müller F-MC. (2010). Persistence of Candida species in the respiratory tract of cystic fibrosis patients. *Med Mycol* **48**:56-63.

Nair B, Stapp J, Stapp L, Bugni L, Van Dalfsen J, Burns JL. (2002). Utility of Gram staining for evaluation of the quality of cystic fibrosis sputum samples. *J Clin Microbiol* **40**:2791-2794.

Nathan C, Cars O. (2014). Antibiotic resistance--problems, progress, and prospects. *N Engl J Med* **371**:1761-3.

Neu TR, Marshall KC. (1991). Microbial 'footprints'—a new approach to adhesive polymers. *Biofouling* **3**:101-112.

Nickel JC, Ruseska I, Wright JB, Costerton JW. (1985). Tobramycin resistance of *Pseudomonas aeruginosa* cells growing as a biofilm on urinary catheter material. *Antimicrob Agents Chemother* **27**:619-624.

Nikolaev YA, Plakunov VK. (2007). Biofilm—'City of microbes' or an analogue of multicellular organisms? *Microbiology* **76**:125-138.

Nistico L, Gieseke A, Stoodley P, Hall-Stoodley L, Kerschner JE, Ehrlich GD. (2009). Fluorescence *in situ* hybridization for the detection of biofilm in the middle ear and upper respiratory tract mucosa. *Methods Mol Biol* **493**:191-213.

Nocker A, Sossa-Fernandez P, Burr MD, Camper AK. (2007). Use of propidium monoazide for live/dead distinction in microbial ecology. *Appl Environ Microbiol* **73**:5111-7.

Novotny LA, Amer AO, Brockson ME, Goodman SD, Bakaletz LO. (2013). Structural stability of *Burkholderia cenocepacia* biofilms is reliant on eDNA structure and presence of a bacterial nucleic acid binding protein. *PLoS One* **8**:e67629.

Nseir S, Di Pompeo C, Brisson H, Dewavrin F, Tissier S, Diarra M, *et al.* (2006). Intensive care unit-acquired *Stenotrophomonas maltophilia*: incidence, risk factors, and outcome. *Crit Care* **10**:R143.

Nunoshiba T, deRojas-Walker T, Wishnok JS, Tannenbaum SR, Demple B. (1993). Activation by nitric oxide of an oxidative-stress response that defends Escherichia coli against activated macrophages. *Proc Natl Acad Sci U S A* **90**:9993–9997.

O'Sullivan BP, Freedman SD. (2009). Cystic fibrosis. *Lancet* **373**:1891–1904.

O'Toole GA, Kolter R. (1998). Flagellar and twitching motility are necessary for *Pseudomonas aeruginosa* biofilm development. *Mol Microbiol* **30**:295–304.

O'Toole G, Kaplan HB, Kolter R. (2000). Biofilm formation as microbial development. *Annu Rev Microbiol* **54**:49–79.

Oliveira MN, Sodini I, Remeuf F, Corrieu G. (2001). Effect of milk supplementation and culture composition on acidification, textural properties and microbiological stability of fermented milks containing probiotic bacteria. *Int Dairy J* **11**:935–942.

Oliver A, Cantón R, Campo P, Baquero F, Blázquez J. (2000). High frequency of hypermutable *Pseudomonas aeruginosa* in cystic fibrosis lung infection. *Science (80-)* **288**:1251–1253.

Oliver JD. (2010). Recent findings on the viable but nonculturable state in pathogenic bacteria. *FEMS Microbiol Rev* **34**:415–425.

Olson ME, Ceri H, Morck DW, Buret AG, Read RR. (2002). Biofilm bacteria: formation and comparative susceptibility to antibiotics. *Can J Vet Res* **66**:86.

Pace NR, Stahl DA, Lane DJ, Olsen GJ. (1986). The analysis of natural microbial populations by ribosomal RNA sequences. In:*Advances in microbial ecology*, Springer, pp. 1–55.

Palmer J, Flint S, Brooks J. (2007). Bacterial cell attachment, the beginning of a biofilm. *J Ind Microbiol Biotechnol* **34**:577–588.

Palmer KL, Mashburn LM, Singh PK, Whiteley M. (2005). Cystic fibrosis sputum supports growth and cues key aspects of *Pseudomonas aeruginosa* physiology. *J Bacteriol* **187**:5267–5277.

Palmer RJ, Kazmerzak K, Hansen MC, Kolenbrander PE. (2001). Mutualism versus independence: strategies of mixed-species oral biofilms in vitro using saliva as the sole nutrient source. *Infect Immun* **69**:5794–5804.

Papagrigorakis MJ, Synodinos PN, Yapijakis C. (2007). Ancient typhoid epidemic reveals possible ancestral strain of *Salmonella enterica* serovar Typhi. *Infect Genet Evol* **7**:126–7.

Papp-Wallace KM, Taracila MA, Gatta JA, Ohuchi N, Bonomo RA, Nukaga M. (2013). Insights into β-lactamases from *Burkholderia* species, two phylogenetically related yet distinct resistance determinants. *J Biol Chem* **288**:19090–19102.

Park JY, Lee YN. (1988). Solubility and decomposition kinetics of nitrous acid in aqueous solution. *J Phys Chem* **92**:6294–6302.

Paul, J.H. and Jeffrey WH. (1985). Evidence for separate adhesion mechanisms for hydrophilic and hydrophobic surfaces in *Vibrio proteolitica*. *Appl Environ Microbiol* **46**:338–343.

Payne GW, Vandamme P, Morgan SH, LiPuma JJ, Coenye T, Weightman AJ, *et al.* (2005). Development of a recA gene-based identification approach for the entire Burkholderia genus. *Appl Environ Microbiol* **71**:3917–3927.

Peeters C, Zlosnik JEA, Spilker T, Hird TJ, LiPuma JJ, Vandamme P. (2013). *Burkholderia pseudomultivorans* sp. nov., a novel *Burkholderia cepacia* complex species from human respiratory samples and the rhizosphere. *Syst Appl Microbiol* **36**:483–9.

Peltroche-Llacsahuanga H, Döhmen H, Haase G. (2002). Recovery of *Candida dubliniensis* from sputum of cystic fibrosis patients. *Mycoses* **45**:15–18.

Pesci EC, Iglewski BH. (1997). The chain of command in *Pseudomonas* quorum sensing. *Trends Microbiol* **5**:132–134.

Pesci EC, Milbank JB, Pearson JP, McKnight S, Kende AS, Greenberg EP, *et al.* (1999). Quinolone signaling in the cell-to-cell communication system of *Pseudomonas aeruginosa. Proc Natl Acad Sci U S A* **96**:11229–34.

Philippsen P, Stotz A, Scherf C. (1991). DNA of *Saccharomyces cerevisiae. Methods Enzymol* **194**:169.

Pier GB. (1985). Pulmonary disease associated with *Pseudomonas aeruginosa* in cystic fibrosis: current status of the host-bacterium interaction. *J Infect Dis* **151**(4): 575–580.

Pier GB, Grout M, Zaidi T, Meluleni G, Mueschenborn SS, Banting G, *et al.* (1998). *Salmonella typhi* uses CFTR to enter intestinal epithelial cells. *Nature* **393**:79–82.

Pitcher DG, Saunders NA, Owen RJ. (1989). Rapid extraction of bacterial genomic DNA with guanidium thiocyanate. *Lett Appl Microbiol* **8**:151–156.

Prigent-Combaret C, Brombacher E, Vidal O, Ambert A, Lejeune P, Landini P, *et al.* (2001). Complex regulatory network controls initial adhesion and biofilm formation in *Escherichia coli* via regulation of thecsgD gene. *J Bacteriol* **183**:7213–7223.

Proia L, Romaní AM, Sabater S. (2012). Nutrients and light effects on stream biofilms: a combined assessment with CLSM, structural and functional parameters. *Hydrobiologia* **695**:281–291.

Purevdorj-Gage, L.B.and Stoodley P. (2004). Hydrodynamic considerations of biofilm structure and behavior. In:*Microbial Biofilms*, Ghannoum, M. and O'Toole, GA (ed) American Society Mic Series, ASM Press: Washington, pp. 160–173.

Quinton PM. (1983). Chloride impermeability in cystic fibrosis. *Nature* **301**:421–422.

Quinton PM. (1999). Physiological basis of cystic fibrosis: a historical perspective. *Physiol Rev* **79**:S3–S22.

Rajan S, Saiman L. (2002). Pulmonary infections in patients with cystic fibrosis. In:*Seminars in respiratory infections*, Vol. 17, pp. 47–56.

Ramanan R, Kim B-H, Cho D-H, Oh H-M, Kim H-S. (2016). Algae–bacteria interactions: Evolution, ecology and emerging applications. *Biotechnol Adv* **34**:14–29.

Rassaf T, Preik M, Kleinbongard P, Lauer T, Heiß C, Strauer BE, *et al.* (2002). Evidence for in vivo transport of bioactive nitric oxide in human plasma. *J Clin Invest* **109**:1241–1248.

Redfield RJ. (1993). Genes for breakfast: the have-your-cake-and-eat-it-too of bacterial transformation. *J Hered* **84**:400–4.

Ren D, Madsen JS, Sørensen SJ, Burmølle M. (2015). High prevalence of biofilm synergy among bacterial soil isolates in cocultures indicates bacterial interspecific cooperation. *ISME J* **9**:81–89.

Renders N, Verbrugh H, Van Belkum A. (2001). Dynamics of bacterial colonisation in the respiratory tract of patients with cystic fibrosis. *Infect Genet Evol* **1**:29–39.

Resch A, Rosenstein R, Nerz C, Götz F. (2005). Differential gene expression profiling of Staphylococcus aureus cultivated under biofilm and planktonic conditions. *Appl Environ Microbiol* **71**:2663–2676.

Riedel K, Hentzer M, Geisenberger O, Huber B, Steidle A, Wu H, *et al.* (2001). N-acylhomoserine-lactone-mediated communication between *Pseudomonas aeruginosa* and *Burkholderia cepacia* in mixed biofilms. *Microbiology* **147**:3249–3262.

Riordan JR, Rommens JM, Kerem B, Alon N, Rozmahel R, Grzelczak Z, *et al.* (1989). Identification of the cystic fibrosis gene: cloning and characterization of complementary DNA. *Science (80-)* **245**:1066–1073.

Rogers, G.B., Carroll, M.P., Serisier, D.J., Hockey, P.M., Jones, G., Kehagia, V., Connett, G.J. and Bruce KD. (2006). Use of 16S rRNA gene profiling by terminal restriction fragment length polymorphism analysis to compare bacterial communities in sputum and mouthwash samples from patients with cystic fibrosis. *J Clin Microbiol* **44**:2601–2604.

Rogers GB, Carroll MP, Serisier DJ, Hockey PM, Jones G, Bruce KD. (2004). Characterization of bacterial community diversity in cystic fibrosis lung infections by use of 16S ribosomal DNA terminal restriction fragment length polymorphism profiling. *J Clin Microbiol* **42**:5176–5183.

Rogers GB, Daniels TW V, Tuck A, Carroll MP, Connett GJ, David GJP, *et al.* (2009). Studying bacteria in respiratory specimens by using conventional and molecular microbiological approaches. *BMC Pulm Med* **9**:14.

Rogers GB, Hart CA, Mason JR, Hughes M, Walshaw MJ, Bruce KD. (2003). Bacterial diversity in cases of lung infection in cystic fibrosis patients: 16S ribosomal DNA (rDNA) length heterogeneity PCR and 16S rDNA terminal restriction fragment length polymorphism profiling. *J Clin Microbiol* **41**:3548–3558.

Rogers GB, Stressmann FA, Koller G, Daniels T, Carroll MP, Bruce KD. (2008). Assessing the diagnostic importance of nonviable bacterial cells in respiratory infections. *Diagn Microbiol Infect Dis* **62**:133–41.

Rogers GB, Stressmann FA, Walker AW, Carroll MP, Bruce KD. (2010). Lung infections in cystic fibrosis: deriving clinical insight from microbial complexity.

Rogers J, Keevil CW. (1992). Immunogold and fluroescein immunolabelling of *Legionella pneumophila* within an aquatic biofilm visualized by using episcopic differential interference contract microscopy. *Appl Environ Microbiol* **58**:2326–2330.

Rolain J-M, François P, Hernandez D, Bittar F, Richet H, Fournous G, *et al.* (2009). Genomic analysis of an emerging multiresistant *Staphylococcus aureus* strain rapidly spreading in cystic fibrosis patients revealed the presence of an antibiotic inducible bacteriophage. *Biol Direct* **4**:1.

Román F, Cantón R, Pérez-Vázquez M, Baquero F, Campos J. (2004). Dynamics of long-term colonization of respiratory tract by *Haemophilus influenzae* in cystic fibrosis patients shows a marked increase in hypermutable strains. *J Clin Microbiol* **42**:1450–1459.

Romeo G, Devoto M, Galietta LJV. (1989). Why is the cystic fibrosis gene so frequent? *Hum Genet* **84**:1–5.

Römling U, Galperin MY, Gomelsky M. (2013). Cyclic di-GMP: the First 25 Years of a Universal Bacterial Second Messenger. *Microbiol Mol Biol Rev* **77**:1–52.

Römling U, Gomelsky M, Galperin MY. (2005). C-di-GMP: the dawning of a novel bacterial signalling system. *Mol Microbiol* **57**:629–639.

Rommens JM, Iannuzzi MC, Kerem B, Drumm ML, Melmer G, Dean M, *et al.* (1989). Identification of the cystic fibrosis gene: chromosome walking and jumping. *Science (80-)* **245**:1059–1065.

Rosenberg M, Gutnick D, Rosenberg E. (1980). Adherence of bacteria to hydrocarbons: a simple method for measuring cell-surface hydrophobicity. *FEMS Microbiol Lett* **9**:29–33.

Ross P, Weinhouse H, Aloni Y, Michaeli D, Weinberger-Ohana P, Mayer R, *et al.* (1987). Regulation of cellulose synthesis in *Acetobacter xylinum* by cyclic diguanylic acid. *Nature* **325**:279–281.

Rost FWD. (1991). Quantitative fluorescence microscopy. Cambridge University Press.

Rutherford ST, Bassler BL. (2012). Bacterial quorum sensing: its role in virulence and possibilities for its control. *Cold Spring Harb Perspect Med* **2**:a012427-.

Ryall B, Davies JC, Wilson R, Shoemark A, Williams HD. (2008a). *Pseudomonas aeruginosa*, cyanide accumulation and lung function in CF and non-CF bronchiectasis patients. *Eur Respir J* **32**:740–7.

Ryall B, Lee X, Zlosnik JEA, Hoshino S, Williams HD. (2008). Bacteria of the *Burkholderia cepacia* complex are cyanogenic under biofilm and colonial growth conditions. *BMC Microbiol* **8**:108.

Ryan RP. (2013). Cyclic di-GMP signalling and the regulation of bacterial virulence. *Microbiology* **159**:1286–1297.

Sadeghi E, Matlow A, MacLusky I, Karmali MA. (1994). Utility of Gram stain in evaluation of sputa from patients with cystic fibrosis. *J Clin Microbiol* **32**:54–58.

Sadekuzzaman M, Yang S, Mizan MFR, Ha SD. (2015). Current and Recent Advanced Strategies for Combating Biofilms. *Compr Rev Food Sci Food Saf* **14**:491–509.

Saiman L, Siegel J. (2004). Infection control in cystic fibrosis. *Clin Microbiol Rev* **17**:57–71.

Salonen A, Nikkilä J, Jalanka-Tuovinen J, Immonen O, Rajilić-Stojanović M, Kekkonen RA, *et al.* (2010). Comparative analysis of fecal DNA extraction methods with phylogenetic microarray: effective recovery of bacterial and archaeal DNA using mechanical cell lysis. *J Microbiol Methods* **81**:127–34.

Santos RS, Guimarães N, Madureira P, Azevedo NF. (2014). Optimization of a peptide nucleic acid fluorescence in situ hybridization (PNA-FISH) method for the detection of bacteria and disclosure of a formamide effect. *J Biotechnol* **187**:16–24.

Sauer K, Camper AK. (2001). Characterization of phenotypic changes in *Pseudomonas putida* in response to surface-associated growth. *J Bacteriol* **183**:6579–6589.

Sauer K, Cullen MC, Rickard AH, Zeef LAH, Davies DG, Gilbert P. (2004). Characterization of nutrient-induced dispersion in *Pseudomonas aeruginosa* PAO1 biofilm. *J Bacteriol* **186**:7312–7326.

Schlag S, Nerz C, Birkenstock TA, Altenberend F, Götz F. (2007). Inhibition of staphylococcal biofilm formation by nitrite. *J Bacteriol* **189**:7911–9.

Schmidt I, Steenbakkers PJM, op den Camp HJM, Schmidt K, Jetten MSM. (2004). physiologic and proteomic evidence for a role of nitric oxide in biofilm formation by *Nitrosomonas europaea* and other ammonia oxidizers. *J Bacteriol* **186**:2781–2788.

Schooling SR, Beveridge TJ. (2006). Membrane vesicles: an overlooked component of the matrices of biofilms. *J Bacteriol* **188**:5945–5957.

Schuster M, Sexton DJ, Diggle SP, Greenberg EP. (2013). Acyl-homoserine lactone quorum sensing: from evolution to application. *Annu Rev Microbiol* **67**:43–63.

Shade A, Hogan CS, Klimowicz AK, Linske M, McManus PS, Handelsman J. (2012). Culturing captures members of the soil rare biosphere. *Environ Microbiol* **14**:2247–2252.

Shak S, Capon DJ, Hellmiss R, Marsters SA, Baker CL. (1990). Recombinant human DNase I reduces the viscosity of cystic fibrosis sputum. *Proc Natl Acad Sci U S A* **87**:9188–92.

Shelly DB, Spilker T, Gracely EJ, Coenye T, Vandamme P, LiPuma JJ. (2000). Utility of commercial systems for identification of *Burkholderia cepacia* complex from cystic fibrosis sputum culture. *J Clin Microbiol* **38**:3112–3115.

Sheppard GJR, Matthews HJ. (1987). Imaging in high-aperture optical systems. *JOSA A* **4**:1354–1360.

Sibley CD, Grinwis ME, Field TR, Eshaghurshan CS, Faria MM, Dowd SE, *et al.* (2011). culture enriched molecular profiling of the cystic fibrosis airway microbiome. *PLoS One* **6**:e22702.

Sibley CD, Parkins MD, Rabin HR, Duan K, Norgaard JC, Surette MG. (2008). A polymicrobial perspective of pulmonary infections exposes an enigmatic pathogen in cystic fibrosis patients. *Proc Natl Acad Sci* **105**:15070–15075.

Sibley CD, Parkins MD, Rabin HR, Surette MG. (2009). The relevance of the polymicrobial nature of airway infection in the acute and chronic management of patients with cystic fibrosis. *Curr Opin Investig drugs (London, Engl 2000)* **10**:787–794.

Sibley CD, Rabin H, Surette MG. (2006). Cystic fibrosis: a polymicrobial infectious disease.

Siebel MA, Characklis WG. (1991). Observations of binary population biofilms. *Biotechnol Bioeng* **37**:778–89.

Simões L, Azevedo N, Pacheco A, Keevil C, Vieira M. (2006). Drinking water biofilm assessment of total and culturable bacteria under different operating conditions. *Biofouling* **22**:91–99.

Singh PK, Schaefer AL, Parsek MR, Moninger TO, Welsh MJ, Greenberg EP. (2000). Quorum-sensing signals indicate that cystic fibrosis lungs are infected with bacterial biofilms. *Nature* **407**:762–764.

Skaar EP. (2010). the battle for iron between bacterial pathogens and their vertebrate hosts. Madhani, HD (ed). *PLoS Pathog* **6**:e1000949.

Skaar EP, Schneewind O. (2004). Iron-regulated surface determinants (Isd) of *Staphylococcus aureus*: stealing iron from heme. *Microbes Infect* **6**:390–397.

Smith A. (1997). Pathogenesis of bacterial bronchitis in cystic fibrosis. *Pediatr Infect Dis J* **16**:91–96.

Smith EE, Buckley DG, Wu Z, Saenphimmachak C, Hoffman LR, D'Argenio DA, *et al.* (2006). Genetic adaptation by *Pseudomonas aeruginosa* to the airways of cystic fibrosis patients. *Proc Natl Acad Sci U S A* **103**:8487–92.

Smith JJ, Travis SM, Greenberg EP, Welsh MJ. (1996). Cystic fibrosis airway epithelia fail to kill bacteria because of abnormal airway surface fluid. *Cell* **85**:229–236.

Smyth CJ, Jonsson P, Olsson E, Soderlind O, Rosengren J, Hjerten S, *et al.* (1978). Differences in hydrophobic surface characteristics of porcine enteropathogenic *Escherichia coli* with or without K88 antigen as revealed by hydrophobic interaction chromatography. *Infect Immun* **22**:462–472.

Sogin ML, Morrison HG, Huber JA, Welch DM, Huse SM, Neal PR, *et al.* (2006). Microbial diversity in the deep sea and the underexplored 'rare biosphere'. *Proc Natl Acad Sci* **103**:12115–12120.

Sousa SA, Ramos CG, Leitao JH. (2010). *Burkholderia cepacia* complex: emerging multihost pathogens equipped with a wide range of virulence factors and determinants. *Int J Microbiol* 2011.

Southern KW. (2012). Determining the optimal newborn screening protocol for cystic fibrosis. *Thorax* **67**. doi:10.1136/thoraxjnl-2012-201589.

Spasenovski T, Carroll MP, Lilley AK, Payne MS, Bruce KD. (2010). Modelling the bacterial communities associated with cystic fibrosis lung infections. *Eur J Clin Microbiol Infect Dis* **29**:319–328.

Speers JGS, Gilmour A. (1985). The influence of milk and milk components on the attachment of bacteria to farm dairy equipment surfaces. *J Appl Bacteriol* **59**:325–332.

Spicuzza L, Sciuto C, Vitaliti G, Di Dio G, Leonardi S, La Rosa M. (2009). Emerging pathogens in cystic fibrosis: ten years of follow-up in a cohort of patients. *Eur J Clin Microbiol Infect Dis* **28**:191–195.

Spinola SM, Peacock J, Denny FW, Smith DL, Cannon JG. (1986). Epidemiology of colonization by nontypeable *Haemophilus influenzae* in children: a longitudinal study. *J Infect Dis* **154**:100–109.

Spiro S. (2007). Regulators of bacterial responses to nitric oxide. *FEMS Microbiol Rev* **31**:193–211.

Sriramulu DD, Lünsdorf H, Lam JS, Römling U. (2005). Microcolony formation: a novel biofilm model of *Pseudomonas aeruginosa* for the cystic fibrosis lung. *J Med Microbiol* **54**:667–676.

Staley JT, Konopka A. (1985). Measurement of in situ activities of nonphotosynthetic microorganisms in aquatic and terrestrial habitats. *Annu Rev Microbiol* **39**:321–346.

Stamler JS, Simon DI, Osborne JA, Mullins ME, Jaraki O, Michel T, *et al.* (1992). S-nitrosylation of proteins with nitric oxide: synthesis and characterization of biologically active compounds. *Proc Natl Acad Sci* **89**:444–448.

Steel KJ. (1961). The oxidase reaction as a taxonomic tool. *J Gen Microbiol* **25**:297–306.

Steinberger RE, Holden PA. (2005). Extracellular DNA in single-and multiple-species unsaturated biofilms. *Appl Environ Microbiol* **71**:5404–5410.

Stoecker K, Dorninger C, Daims H, Wagner M. (2010). Double labeling of oligonucleotide probes for fluorescence in situ hybridization (DOPE-FISH) improves signal intensity and increases rRNA accessibility. *Appl Environ Microbiol* **76**:922–6.

Stoesser G, Tuli MA, Lopez R, Sterk P. (1999). The EMBL nucleotide sequence database. *Nucleic Acids Res* **27**:18–24.

Stone A, Quittell L, Zhou J, Alba L, Bhat M, DeCelie-Germana J, *et al.* (2009). *Staphylococcus aureus* nasal colonization among pediatric cystic fibrosis patients and their household contacts. *Pediatr Infect Dis J* **28**:895–899.

Sudhamsu J, Crane BR. (2015). Bacterial nitric oxide synthases: what are they good for? *Trends Microbiol* **17**:212–218.

Sullivan D, Bennett D, Henman M, Harwood P, Flint S, Mulcahy F, *et al.* (1993). Oligonucleotide fingerprinting of isolates of *Candida* species other than *C. albicans* and of atypical *Candida* species from human immunodeficiency virus-positive and AIDS patients. *J Clin Microbiol* **31**:2124–2133.

Sullivan DJ, Westerneng TJ, Haynes KA, Bennett DE, Coleman DC. (1995). *Candida dubliniensis* sp. nov.: phenotypic and molecular characterization of a novel species associated with oral candidosis in HIV-infected individuals. *Microbiology* **141**:1507–1521.

Szaff M, Høiby N. (1982). Antibiotic Treatment Of *Staphylococcus aureus* Infection In Cystic Fibrosis. *Acta Pædiatrica* **71**:821–826.

Tal R, Wong HC, Calhoon R, Gelfand D, Fear AL, Volman G, *et al.* (1998). Three cdg operons control cellular turnover of cyclic di-GMP in *Acetobacter xylinum*: genetic organization and occurrence of conserved domains in isoenzymes. *J Bacteriol* **180**:4416–4425.

Tam M, Jackson Snipes G, Stevenson MM. (1999). Characterization of chronic bronchopulmonary *Pseudomonas aeruginosa* infection in resistant and susceptible inbred mouse strains. *Am J Respir Cell Mol Biol* **20**:710–719.

Tan K, Conway SP, Brownlee KG, Etherington C, Peckham DG. (2002). *Alcaligenes* infection in cystic fibrosis. *Pediatr Pulmonol* **34**:101–104.

Tanaka T, Kawasaki K, Daimon S, Kitagawa W, Yamamoto K, Tamaki H, *et al.* (2014). A hidden pitfall in the preparation of agar media undermines microorganism cultivability. *Appl Environ Microbiol* **80**:7659–7666.

Tavernier S, Coenye T. (2015). Quantification of *Pseudomonas aeruginosa* in multispecies biofilms using PMA-qPCR. *PeerJ* **3**:e787.

Taylor WI, Achanzar D. (1972). Catalase test as an aid to the identification of Enterobacteriaceae. *Appl Microbiol* **24**:58–61.

Thornton CS, Brown EL, Alcantara J, Rabin HR, Parkins MD. (2015). Prevalence and impact of *Streptococcus pneumoniae* in adult cystic fibrosis patients: a retrospective chart review and capsular serotyping study. *BMC Pulm Med* **15**:49.

Truong VK, Lapovok R, Estrin YS, Rundell S, Wang JY, Fluke CJ, *et al.* (2010). The influence of nano-scale surface roughness on bacterial adhesion to ultrafine-grained titanium. *Biomaterials* **31**:3674–83.

Tseng S-P, Tsai W-C, Liang C-Y, Lin Y-S, Huang J-W, Chang C-Y, *et al.* (2014). The contribution of antibiotic resistance mechanisms in clinical *Burkholderia cepacia* complex isolates: an emphasis on efflux pump activity.

Tsurui H, Nishimura H, Hattori S, Hirose S, Okumura K, Shirai T. (2000). Seven-color fluorescence imaging of tissue samples based on fourier spectroscopy and singular value decomposition. *J Histochem Cytochem* **48**:653–662.

Tunney MM, Klem ER, Fodor AA, Gilpin DF, Moriarty TF, McGrath SJ, *et al.* (2011). Use of culture and molecular analysis to determine the effect of antibiotic treatment on microbial community diversity and abundance during exacerbation in patients with cystic fibrosis. *Thorax* **66**:579–584.

Valm AM, Mark Welch JL, Borisy GG. (2012). CLASI-FISH: principles of combinatorial labeling and spectral imaging. *Syst Appl Microbiol* **35**:496–502.

Valm AM, Welch JLM, Rieken CW, Hasegawa Y, Sogin ML, Oldenbourg R, *et al.* (2011). Systems-level analysis of microbial community organization through combinatorial labeling and spectral imaging. *Proc Natl Acad Sci* **108**:4152–4157.

Vanlaere E, Sergeant K, Dawyndt P, Kallow W, Erhard M, Sutton H, *et al.* (2008). Matrix-assisted laser desorption ionisation-time-of of-flight mass spectrometry of intact cells allows rapid identification of *Burkholderia cepacia* complex. *J Microbiol Methods* **75**:279–286.

Venkataraman S, Martin SM, Buettner G. (2002). Electron Paramagnetic Resonance for Quantitation of Nitric Oxide in Aqueous Solutions. Nitric Oxide, Part D. Nitric Oxide Detection, Mitochondria and Cell Functions and Peroxynitrite Reactions. Academic Press https://books.google.com/books?id=NwJ-y1CuVqMC&pgis=1.

Venter JC, Remington K, Heidelberg JF, Halpern AL, Rusch D, Eisen JA, *et al.* (2004). Environmental genome shotgun sequencing of the Sargasso Sea. *Science (80-)* **304**:66–74.

Verweij PE, Meis JF, Sarfati J, Hoogkamp-Korstanje JA, Latge J-P, Melchers WJ. (1996). Genotypic characterization of sequential *Aspergillus fumigatus* isolates from patients with cystic fibrosis. *J Clin Microbiol* **34**:2595–2597.

Vishnivetskaya TA, Layton AC, Lau MCY, Chauhan A, Cheng KR, Meyers AJ, *et al.* (2013). Commercial DNA extraction kits impact observed microbial community composition in permafrost samples. doi:10.1111/1574-6941.12219.

Vorregaard M. (2008). Comstat2 - a modern 3D image analysis environment for biofilms. http://www2.imm.dtu.dk/pubdb/views/edoc_download.php/5628/pdf/imm5628.pdf (Accessed April 27, 2016).

Wahab AA, Taj-Aldeen SJ, Kolecka A, ElGindi M, Finkel JS, Boekhout T. (2014). High prevalence of *Candida dubliniensis* in lower respiratory tract secretions from cystic fibrosis patients may be related to increased adherence properties. *Int J Infect Dis* **24**:14–19.

Walters MC, Roe F, Bugnicourt A, Franklin MJ, Stewart PS. (2003). Contributions of antibiotic penetration, oxygen limitation, and low metabolic activity to tolerance of *Pseudomonas aeruginosa* biofilms to ciprofloxacin and tobramycin. *Antimicrob Agents Chemother* **47**:317–23.

Wang PG, Xian M, Tang X, Wu X, Wen Z, Cai T, *et al.* (2002). Nitric Oxide Donors: Chemical Activities and Biological Applications. *Chem Rev* **102**:1091–1134.

Wang S, Liu X, Liu H, Zhang L, Guo Y, Yu S, *et al.* (2015). The exopolysaccharide Psl-eDNA interaction enables the formation of a biofilm skeleton in *Pseudomonas aeruginosa*. *Environ Microbiol Rep* **7**:330–40.

Waters V, Atenafu EG, Lu A, Yau Y, Tullis E, Ratjen F. (2013). Chronic *Stenotrophomonas maltophilia* infection and mortality or lung transplantation in cystic fibrosis patients. *J Cyst Fibros* **12**:482–486.

Watt AP, Courtney J, Moore J, Ennis M, Elborn JS. (2005). Neutrophil cell death, activation and bacterial infection in cystic fibrosis. *Thorax* **60**:659–664.

Webb JS, Thompson LS, James S, Charlton T, Tolker-Nielsen T, Koch B, *et al.* (2003). Cell Death in *Pseudomonas aeruginosa* Biofilm Development. *J Bacteriol* **185**:4585–4592.

Wellinghausen N, Köthe J, Wirths B, Sigge A, Poppert S. (2005). Superiority of molecular techniques for identification of Gram-negative, oxidase-positive rods, including morphologically nontypical *Pseudomonas aeruginosa*, from patients with cystic fibrosis. *J Clin Microbiol* **43**:4070–5.

Wertheim HFL, Melles DC, Vos MC, van Leeuwen W, van Belkum A, Verbrugh HA, *et al.* (2005). The role of nasal carriage in *Staphylococcus aureus* infections. *Lancet Infect Dis* **5**:751–762.

Whitby PW, Carter KB, Burns JL, Royall JA, LiPuma JJ, Stull TL. (2000). Identification and Detection of *Stenotrophomonas maltophilia* by rRNA-Directed PCR. *J Clin Microbiol* **38**:4305–4309.

Whitby PW, Dick HLN, Campbell PW, Tullis DE, Matlow A, Stull TL. (1998). Comparison of culture and PCR for detection of *Burkholderia cepacia* in sputum samples of patients with cystic fibrosis. *J Clin Microbiol* **36**:1642–1645.

White TJ, Bruns T, Lee S, Taylor JW. (1990). Amplification and direct sequencing of fungal ribosomal RNA genes for phylogenetics. *PCR Protoc a Guid to methods Appl* **18**:315–322.

Whitehead KA, Verran J. (2006). The Effect of Surface Topography on the Retention of Microorganisms. *Food Bioprod Process* **84**:253–259.

Whiteley M, Bangera MG, Bumgarner RE, Parsek MR, Teitzel GM, Lory S, *et al.* (2001). Gene expression in *Pseudomonas aeruginosa* biofilms. *Nature* **413**:860–864.

Wilking JN, Zaburdaev V, De Volder M, Losick R, Brenner MP, Weitz DA. (2013). Liquid transport facilitated by channels in *Bacillus subtilis* biofilms. *Proc Natl Acad Sci* **110**:848–852.

Williamson KS, Richards LA, Perez-Osorio AC, Pitts B, McInnerney K, Stewart PS, *et al.* (2012). Heterogeneity in *Pseudomonas aeruginosa* biofilms includes expression of ribosome hibernation factors in the antibiotic-tolerant subpopulation and hypoxia-induced stress response in the metabolically active population. *J Bacteriol* **194**:2062–73.

Wilson K. (2001). Preparation of genomic DNA from bacteria. *Curr Protoc Mol Biol* Chapter 2:Unit 2.4.

Wilson R, Sykes DA, Watson D, Rutman A, Taylor GW, Cole PJ. (1988). Measurement of *Pseudomonas aeruginosa* phenazine pigments in sputum and assessment of their contribution to sputum sol toxicity for respiratory epithelium. *Infect Immun* **56**:2515–7.

Wimpenny JWT, Colasanti R. (2006). A unifying hypothesis for the structure of microbial biofilms based on cellular automaton models. *FEMS Microbiol Ecol* **22**:1-16.

Wink DA. (2000). The Chemical Biology of Nitric Oxide. In:*Nitric Oxide: Biology and Pathobiology*, Ignarro, LJ (ed), Elsevier Science, pp. 41–56.

Winstanley C, Fothergill J. (2009). The role of quorum sensing in chronic cystic fibrosis *Pseudomonas aeruginosa* infections. *FEMS Microbiol Lett*. http://femsle.oxfordjournals.org/content/290/1/1.abstract (Accessed April 9, 2016).

Winstanley C, Langille MGI, Fothergill JL, Kukavica-Ibrulj I, Paradis-Bleau C, Sanschagrin F, *et al.* (2009). Newly introduced genomic prophage islands are critical determinants of in vivo competitiveness in the Liverpool Epidemic Strain of *Pseudomonas aeruginosa*. *Genome Res* **19**:12-23.

Woese CR. (2008). Archaea: Evolution, Physiology, and Molecular Biology. In: Garrett, R. and Klenk, HP (ed), pp. 1–16.

Woese CR. (1987). Bacterial evolution. *Microbiol Rev* **51**:221.

Woese CR, Kandler O, Wheelis ML. (1990). Towards a natural system of organisms: proposal for the domains Archaea, Bacteria, and Eucarya. *Proc Natl Acad Sci* **87**:4576–4579.

Wolcott RD, Gontcharova V, Sun Y, Dowd SE. (2009). Evaluation of the bacterial diversity among and within individual venous leg ulcers using bacterial tag-encoded FLX and titanium amplicon pyrosequencing and metagenomic approaches. *BMC Microbiol* **9**:226.

Wood AJJ, Ramsey BW. (1996). Management of pulmonary disease in patients with cystic fibrosis. *N Engl J Med* **335**:179-188.

Wooten OJ, Dulfano MJ. (1978). Improved homogenization techniques for sputum cytology counts. *Ann Allergy* **41**:150-154.

Worlitzsch D, Tarran R, Ulrich M, Schwab U, Cekici A, Meyer KC, *et al.* (2002). Effects of reduced mucus oxygen concentration in airway *Pseudomonas* infections of cystic fibrosis patients. *J Clin Invest* **109**:317-325.

Xiao J, Klein MI, Falsetta ML, Lu B, Delahunty CM, Yates JR, *et al.* (2012). The exopolysaccharide matrix modulates the interaction between 3D architecture and virulence of a mixed-species oral biofilm. *PLoS Pathog* **8**:e1002623.

Xu H-S, Roberts N, Singleton FL, Attwell RW, Grimes DJ, Colwell RR. (1982). Survival and viability of nonculturable *Escherichia coli* and *Vibrio cholerae* in the estuarine and marine environment. *Microb Ecol* **8**:313–323.

Yang L, Jelsbak L, Marvig RL, Damkiær S, Workman CT, Rau MH, *et al.* (2011). Evolutionary dynamics of bacteria in a human host environment. *Proc Natl Acad Sci* **108**:7481–7486.

Yang Y, Zeyer J. (2003). Specific Detection of Dehalococcoides Species by Fluorescence In Situ Hybridization with 16S rRNA-Targeted Oligonucleotide Probes. *Appl Environ Microbiol* **69**:2879–2883.

Yoon SS, Hennigan RF, Hilliard GM, Ochsner UA, Parvatiyar K, Kamani MC, *et al.* (2002). *Pseudomonas aeruginosa* anaerobic respiration in biofilms: relationships to cystic fibrosis pathogenesis. *Dev Cell* **3**:593–603.

Zemanick ET, Wagner BD, Sagel SD, Stevens MJ, Accurso FJ, Harris JK. (2010). Reliability of quantitative real-time PCR for bacterial detection in cystic fibrosis airway specimens. *PLoS One* **5**:e15101.

Zhao J, Carmody LA, Kalikin LM, Li J, Petrosino JF, Schloss PD, *et al.* (2012a). Impact of enhanced *Staphylococcus* DNA extraction on microbial community measures in cystic fibrosis sputum. *PLoS One* **7**:e33127.

Zhao J, Carmody LA, Kalikin LM, Li J, Petrosino JF, Schloss PD, *et al.* (2012b). Impact of enhanced *Staphylococcus* DNA extraction on microbial community measures in cystic fibrosis sputum. *PLoS One* **7**:e33127.

Zhao J, Schloss PD, Kalikin LM, Carmody LA, Foster BK, Petrosino JF, *et al.* (2012). Decade-long bacterial community dynamics in cystic fibrosis airways. *Proc Natl Acad Sci* 201120577.

Zhao K, Tseng BS, Beckerman B, Jin F, Gibiansky ML, Harrison JJ, *et al.* (2013). Psl trails guide exploration and microcolony formation in *Pseudomonas aeruginosa* biofilms. *Nature* **497**:388–391.

Zielenski J, Rozmahel R, Bozon D, Kerem B, Grzelczak Z, Riordan JR, *et al.* (1991). Genomic DNA sequence of the cystic fibrosis transmembrane conductance regulator (CFTR) gene. *Genomics* **10**:214–228.

Zijnge V, van Leeuwen MBM, Degener JE, Abbas F, Thurnheer T, Gmür R, *et al.* (2010). Oral Biofilm Architecture on Natural Teeth. *PLoS One* **5**:e9321.

Zimmermann T, Rietdorf J, Pepperkok R. (2003). Spectral imaging and its applications in live cell microscopy. *FEBS Lett* **546**:87–92.

Zuckerman JB, Seder DB. (2007). Infection control practice in cystic fibrosis centers. *Clin Chest Med* **28**:381–404.

Zuylen J van. (1981). The microscopes of Antoni van Leeuwenhoek. *J Microsc* **121**:309–328.